EPA/600/R-96/149
June 1996

REPORT OF 1995 WORKSHOP ON GEOSYNTHETIC CLAY LINERS

by

David E. Daniel and Heather B. Scranton
University of Texas at Austin
Department of Civil Engineering
Geotechnical Engineering Center
Austin, Texas 78712

Cooperative Agreement No. CR-821448-01-0

Project Officer

David A. Carson
U.S. Environmental Protection Agency
National Risk Management Research Laboratory
Cincinnati, Ohio 45268

NATIONAL RISK MANAGEMENT RESEARCH LABORATORY
OFFICE OF RESEARCH AND DEVELOPMENT
U.S. ENVIRONMENTAL PROTECTION AGENCY
CINCINNATI, OHIO 45268

DISCLAIMER

The information in the document has been funded wholly or in part by the United States Environmental Protection Agency under assistance agreement number CR-815546-01-0. It has been subject to the Agency's peer and administrative review and has been approved for publication as a U.S. EPA document. Mention of trade names or commercial products does not constitute endorsement or recommendation for use.

FOREWORD

The U.S. Environmental Protection Agency is charged by Congress with protecting the Nation's land, air, and water resource. Under a mandate of national environmental laws, the Agency strives to formulate and implement actions leading to a compatible balance between human activities and the ability of natural systems to support and nurture life. To meet this mandate, EPA's research program is providing data and technical support for solving environmental problems today and building a science knowledge base necessary to manage our ecological resources wisely, understand how pollutants affect our health, and prevent or reduce environmental risks in the future.

The National Risk Management Research Laboratory is the Agency's center for investigation of technological and management approaches for reducing risks from threats to human health and the environment. The focus of the Laboratory's research program is on methods for the prevention and control of pollution to air, land, water, and subsurface resources; protection of water quality in public water systems; remediation of contaminated sites and ground water; and prevention and control of indoor air pollution. The goal of this research effort is to catalyze development and implementation of innovative, cost-effective environmental technologies; develop scientific and engineering information needed by EPA to support regulatory and policy decisions; and provide technical support and information transfer to ensure effective implementation of environmental regulations and strategies.

This publication has been produced as part of the Laboratory's strategic long-term research plan. It is published and made available by EPA's Office of Research and Development to assist the user community and to link researchers with their clients.

E. Timothy Oppelt, Director
National Risk Management Research Laboratory

ABSTRACT

A workshop was held at the EPA's National Risk Management Research Laboratory in Cincinnati, Ohio, on August 9 and 10, 1995. On August 9, attendees where shown field plots of GCLs that have been constructed at a site in Cincinnati, and given a detailed account of the test plot layout, instrumentation, and performance to date. Fourteen test plots, with cross-sections that are typical of landfill cover systems, were constructed. Five of the test plots were constructed on 3H:1V slopes, and the remainder were constructed on 2H:1V slopes. All test plots were two GCL roll widths wide (approximately 10 m), and 20 to 30 m long. The thickness of the cover materials over the GCLs was approximately 900 mm. The objective of the project was to verify that the GCLs would remain stable against mid-plane shear on 3H:1V slopes with a factor of safety of at least 1.5 So long as the slopes are stable at 2H:1V, it can be demonstrated that the minimum factor of safety is 1.5 for a 3H:1V slope. Thus far, all slopes have remained stable with respect to mid-plane shear, although two interface failures did occur between the GCL and an overlying textured geomembrane. Both failures occurred at the interface between the woven geotextile component of a GCL and the geomembrane. Interface shear testing performed after the failures demonstrated that the failures could have been predicted, based on the laboratory shear test results. A significant finding from the project is that in landfill cover applications, the internal strength of GCLs may not be the critical strength — interface strengths may be lower than the internal strength of the GCL. Another significant finding has been that bentonite encased between two geomembranes on one test plot has undergone unanticipated hydration, when the expectation was that it would remain dry. The cause of hydration has not been isolated but may be related to water migration through the penetrations made for instrumentation cables.

On August 10, a series of presentations summarized recent research findings for the field test site, as well as other on-going research projects. Significant information was presented concerning laboratory shear testing results and seepage rates through composite geomembrane/GCL liners based on flow rates in the leakage detection layer of double composite liner systems.

This workshop marks the third in a series of workshops. The first two were held in 1990 and in 1992. The breadth and depth of information presented at the 1995 workshop is much greater than in the earlier two workshops, and reflects the maturing of the GCL industry and the efforts of many individuals to develop the technical information that is needed to evaluate and assess GCLs as they are used in waste containment facilities.

Table of Contents

Appendices

List of Figures

List of Tables

ACKNOWLEDGMENTS

This workshop was part of a larger effort on a cooperative agreement CR-815546-01-0 dealing with field performance of waste containment systems. The principal investigators for the project are Robert M. Koerner (Geosynthetic Research Institute, Drexel University), David E. Daniel (University of Texas), and Rudy Bonaparte (GeoSyntec Consultants). Several individuals provided key support for the project, including George M. Koerner (Drexel University), John J. Bowders (University of Texas), and Majdi Othman (GeoSyntec Consultants).

Robert E. Landreth, formerly with the EPA, as well as the EPA project officer, David A. Carson, provided key support for this project and for and input to the workshop. The workshop would not have been possible without the active participation of the many individuals who participated in the workshop.

CHAPTER 1
INTRODUCTION

The first geosynthetic clay liner (GCL) workshop sponsored by the U.S. Environmental Protection Agency (EPA) was held on June 7-8, 1990, in Cincinnati, Ohio, to discuss the use of geosynthetic clay liners (GCLs) in landfill liner and cover systems. One of the primary objectives of the workshop was to identify the most pressing research needs concerning GCLs. The 75 attendees of the workshop identified two key research needs: (1) development of field performance data, and (2) development of better information concerning the shear strength of GCLs (Daniel and Estornell, 1991).

A second GCL workshop was held on June 9-10, 1992, at the same location. The purpose of the second workshop was to present and to discuss new information developed on GCLs. A variety of issues were discussed by the 175 attendees, but the key technical concerns were once again the development of more field performance data and development of more information concerning the shear strength of GCLs (Daniel and Boardman, 1993).

In the period since the first two GCL workshops, much has been learned about GCLs and their use in waste containment facilities. A third GCL workshop was held in Cincinnati, Ohio, at EPA's National Risk Management Research Laboratory on August 9 and 10, 1995. The third Workshop was attended by 170 people (see Appendix A for list of attendees). This report summarizes the proceedings from the workshop.

The 1995 GCL workshop had several objectives. The primary objective was to describe the progress made on a research project in which GCLs were installed on test field plots at a site in Cincinnati, Ohio. The purpose of constructing and monitoring the test plots was to evaluate the mid-plane (internal) shear strength of GCLs in real-world, field-scale situations. A second objective of the workshop was collect and disseminate the latest information that has been developed on GCLs. Significantly more information is currently available on the performance of GCLs compared to the time period of the previous workshops.

The primary presentations at this workshop constitute the major chapters of this report and were as follows:

1. Background on GCLs (presented by David Daniel).
2. History and performance of the GCL field test in Cincinnati, Ohio (presented by David Daniel, John Bowders, and Heather Scranton).
3. Recent research on GCLs (presented by Robert Koerner, Rudy Bonaparte, John Bowders, David Daniel, Jason Kraus, David Carson, and Heather Scranton).

4. Developments by manufacturers (presented by Robert Trauger [Bentomat®], John Fuller [Claymax®], John Siebken [Bentofix®], and Richard Erickson [Gundseal®]).
5. Current Status of the development of ASTM standards for GCL testing (presented by Larry Well).
6. Regulatory Status of GCLs (presented by Kenneth Skahn and Allen Geswein).
7. Panel Discussion of current issues and further research regarding GCLs and comments from conference participants (presented by Rudy Bonaparte, David Daniel, and Robert Koerner).

CHAPTER 2
BACKGROUND ON GCLs

2.1 Types of GCLs

A geosynthetic clay liner (GCL) consists of bentonite sandwiched between two geotextiles or attached to a geomembrane with an adhesive. Figure 2.1 shows cross-sections of the two general types of GCLs. Presently, there are four manufacturers of GCLs in North America and two in Europe. The ownership of geosynthetic manufacturers can change, as can the product lines; therefore, the manufacturer should be consulted concerning specific products. Cross-sections of the current GCLs are shown in Figure 2.2. The GCLs used in the field test plots in Cincinnati include Gundseal®, Bentomat®, Claymax® 500SP, and Bentofix®.

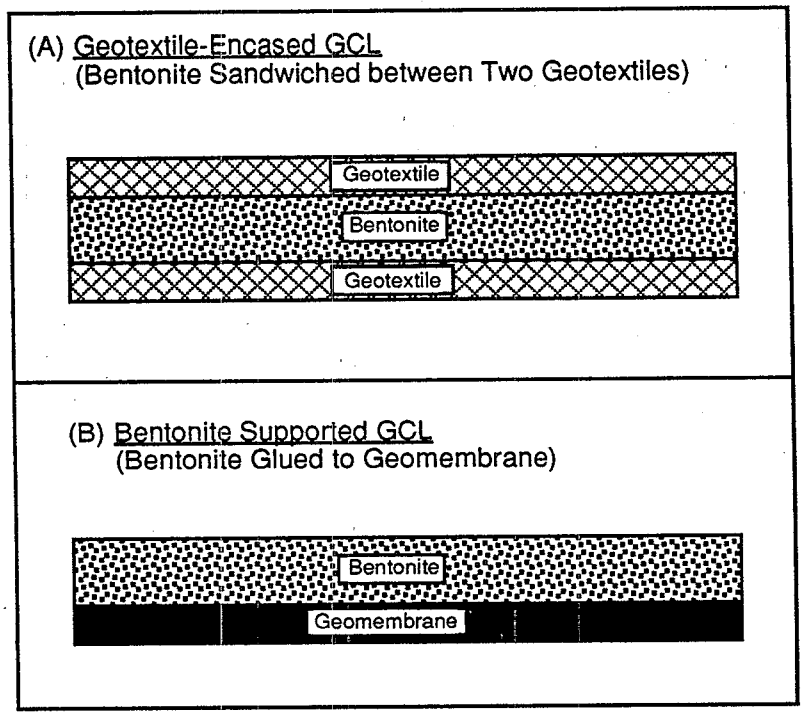

Figure 2.1 General Configuration of Two Principal Types of GCLs.

Bentomat® and Bentofix® consist of dry sodium bentonite sandwiched between two geotextiles. One geotextile is nonwoven while the other geotextile can be either woven or nonwoven. The entire assembly is needle punched together.

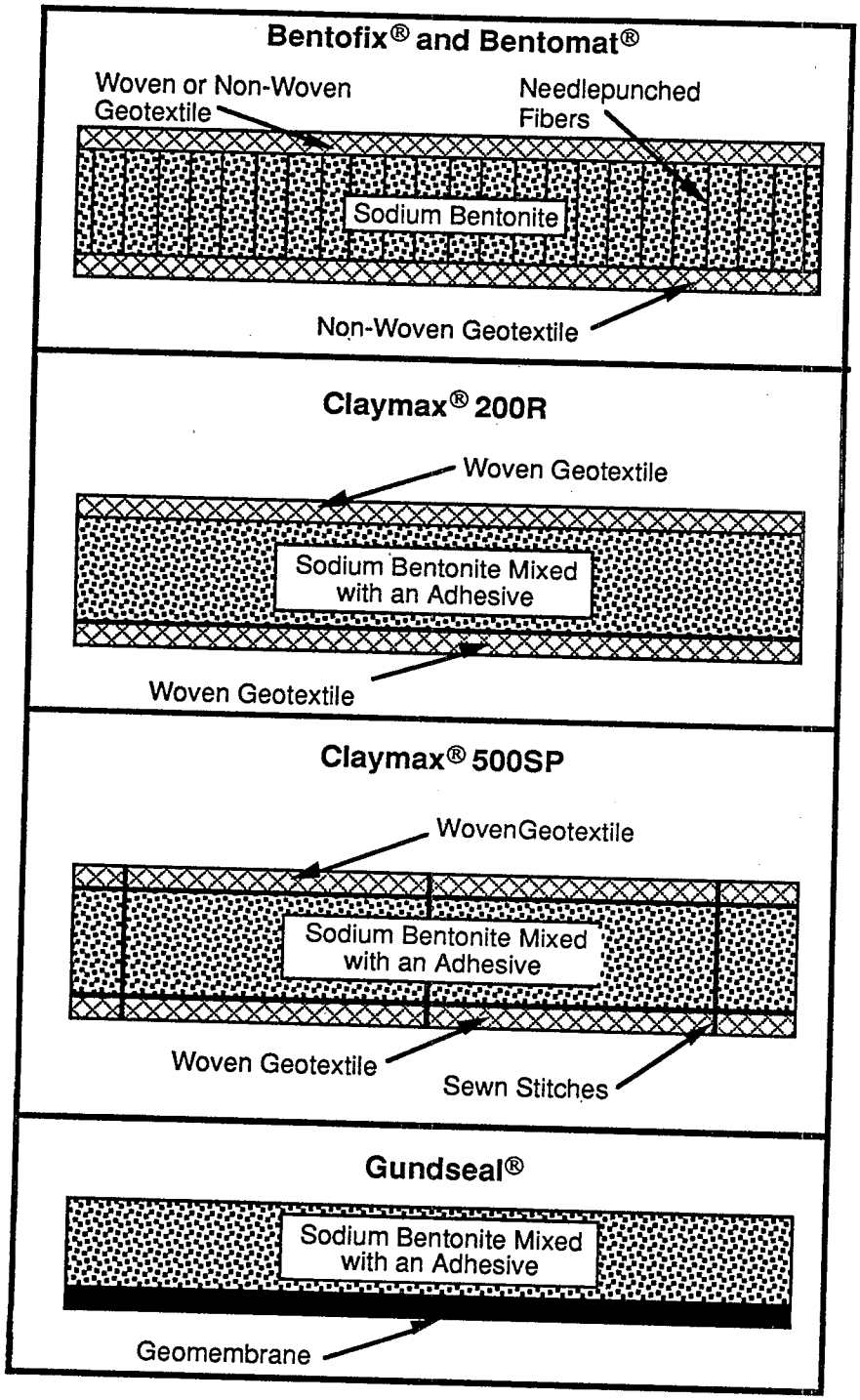

Figure 2.2 Commercial GCLs Produced in North America.

Claymax® employs two woven geotextiles to contain the bentonite, which is mixed with an adhesive. The GCL can either be unstitched (200R) or stitched (500SP). In the stitched material, the rows of stitches are spaced 100 mm apart.

Gundseal® consists of sodium bentonite mixed with an adhesive and bonded to a supporting geomembrane. The geomembrane is normally a 0.3- to 0.5-mm thick high density polyethylene (HDPE) geomembrane, but virtually any geomembrane (smooth or textured) can be used.

2.2 Advantages of GCLs

There are many attractive reasons for using GCLs as a component in a liner system or cover system. First, GCLs typically have a hydraulic conductivity of 1 to 5 x 10^{-9} cm/s or less, which makes them very effective as hydraulic barriers. In addition, the installed cost of GCLs, which is about \$5/m^2, or \$0.50/ft^2, is low compared to compacted clay liners, particularly if clay must be shipped from off site or if bentonite must be blended with soil to form the clay liner material. Under ideal circumstances, with clay readily available on site and little or no processing of the clay required, the cost of a 600-mm thick compacted clay liner can be as little as \$2/m^2 to \$3/m^2 (\$0.20/ft^2 to \$0.30/ft^2) in 1995 dollars. If clay must be hauled great distances, or if bentonite must be blended with on-site soils, the cost of a compacted clay liner is typically \$10/m^2 to \$40/m^2 (\$1/ft^2 to \$4/ft^2). In addition to the material cost savings, the value of airspace must often be factored into the cost analysis. For example, if the airspace that would be occupied by a compacted clay liner becomes available for disposal of waste, additional cost advantages are realized by the GCL. For instance, if the cost of waste disposal is \$55/Mg (\$50 per U.S. ton), and waste has a density of 890 kg/m^3 (1500 lb/yd^3), then the value of airspace associated with a 600-mm thick compacted clay liner is \$28/m^2 (\$2.80/ft^2). Thus, the economic incentives for using GCLs increase greatly when replacement of a compacted clay liner with a GCL generates additional air space that is available for waste disposal.

There are other advantages of GCLs. GCLs are manufactured in rolls that can be shipped anywhere. A local supply of clay is not needed if a GCL is used instead of compacted clay. Installation of GCLs is easy and rapid. GCLs are resistant to freeze-thaw, wet-dry cycles, and differential settlement. There are significant disadvantages of all liner materials, including GCLs. The pros and cons of GCLs are described by Daniel and Boardman (1993).

These advantages are very significant and are the principal reasons why many owners and designers of landfills and impoundments are increasingly selecting GCLs instead of more conventional low-permeability compacted soils.

2.3 Shear Strength of GCLs

One disadvantage of GCLs is the low shear strength of the bentonite contained within the GCL. Shear test data on unreinforced, hydrated GCLs show friction angles of about 10 degrees. In the two previous EPA workshops on GCLs, the shear strength of the bentonite in GCLs, which controls the internal shear strength of unreinforced GCLs, was cited as a primary technical concern in the use of GCLs in waste containment systems. The main factors affecting the internal shear strength of GCLs include the magnitude of normal stress, water content of the bentonite, rate of shearing, response of reinforcement, amount of deformation, and effects of seismic loading. These factors are briefly reviewed in succeeding subsections.

2.3.1 Magnitude of Normal Stress

The classical Mohr-Coulomb failure criterion for the shear strength of soil is:

$$\tau = c + \sigma \tan\phi \qquad (2.1)$$

where τ is the shear stress, c is the cohesion, σ is the normal stress, and ϕ is the angle of internal friction. The concept is illustrated in Fig. 2.3.

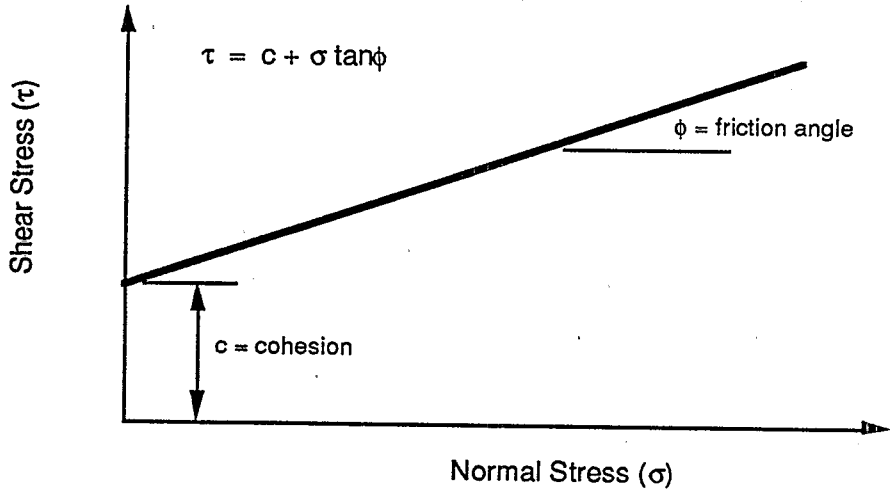

Figure 2.3 Mohr-Coulomb Failure Envelope.

The ideal Mohr-Coulomb failure envelope is linear. However, the relationship between shear stress and normal stress for bentonite is not always linear (Fig. 2.4).

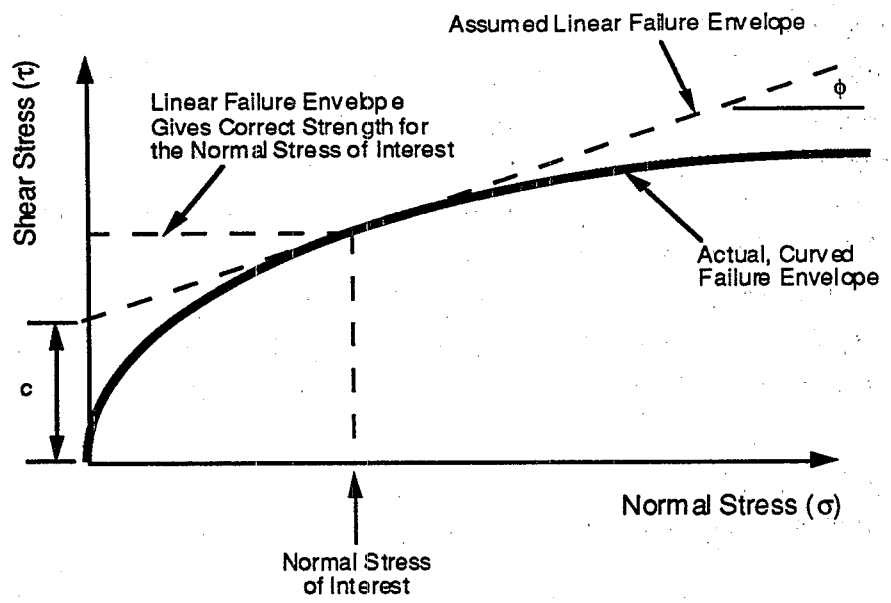

Figure 2.4 Curved Mohr-Coulomb Failure Envelope.

2.3.2 Water Content

The shear strength of bentonite is sensitive to water content. The angle of internal friction decreases with increasing water content. For example, shear tests that were performed on an unreinforced GCL at The University of Texas showed that at a water content of 20%, the angle of internal friction was 22°, but when the water content was increased to 50%, the friction angle of the unreinforced GCL decreased to 7° (Daniel et al., 1993). Hydrated bentonite is significantly weaker than dry bentonite.

2.3.3 Rate of Loading

The rate of loading of GCLs affects the shear strength of the GCL. The general experience with bentonite is the slower the loading, the lower the internal shear strength of the GCL (Daniel et al., 1993). Thus, care should be taken in testing GCLs not to shear the GCL too quickly. The procedure for determining shearing rate that is described in ASTM D3080 for drained direct shear testing of soil is recommended.

2.3.4 Reinforcement

Many commercial GCLs are reinforced to enhance the internal shear strength of the GCL. The reinforced GCLs used in the field test plots included Bentomat®, Claymax® 500SP, and

Bentofix®. When a reinforced GCL is sheared internally, the needlepunched fibers or sewn stitches are put into tension as shearing occurs, which enhances internal shear strength. However, there are limitations on the benefits of this reinforcing, as discussed below.

2.3.5 Amount of Deformation

The peak shear strength is the maximum shear strength measured during shear. Typically, however, many materials "strain soften" after the peak strength is reached. The residual shear strength is the minimum post-peak shear stress, which typically occurs at a very large displacement compared to the displacement at which the peak strength is generated. Figure 2.5 illustrates the difference between peak and residual shear strength.

If a reinforced GCL is loaded to very large shearing displacements (e.g., 50 mm or more), reinforcing fibers may pullout from one or both of the geotextiles, break, or creep. If the reinforcing fibers fail, the strength of the reinforced GCL may be about the same as that of an unreinforced GCL. The key issue is how much deformation will actually occur in the field, and whether there is a risk of residual conditions actually developing.

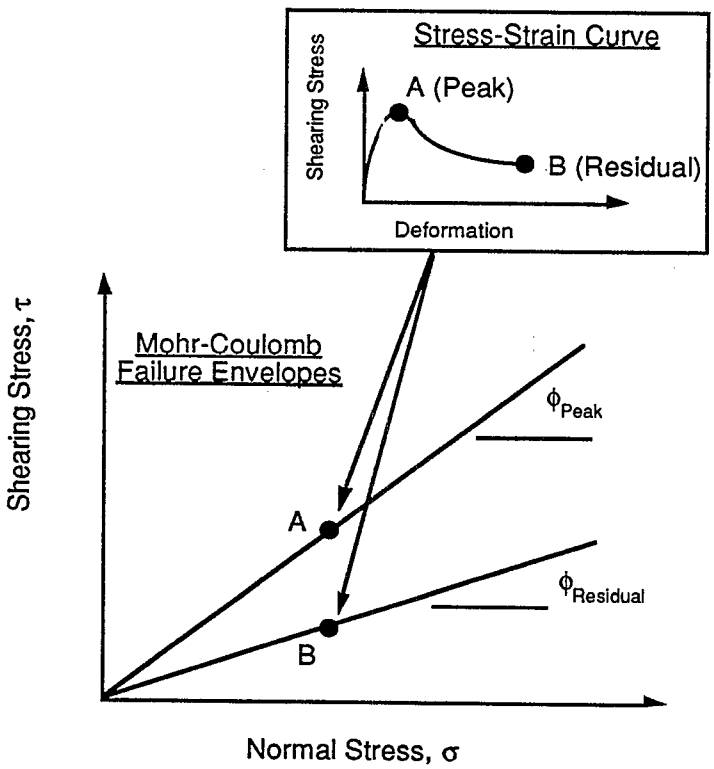

Figure 2.5 Peak and Residual Shear Strength.

2.3.6 Seismic Loading

Data on effects of cyclic loading on the internal shear strength of GCLs is very limited. Several cyclic direct simple shear tests have been performed at The University of Texas. The tests indicate that cyclic loading causes a slight increase in the shear strength of dry GCLs. The increase in strength is the result of a slight densification of the dry bentonite during cyclic loading. However, the tests indicate that saturated bentonite may undergo a slight reduction in strength from cyclic loading. The reduction increases with increasing number of cycles of loading. Results have not yet been described in a written report.

2.4 Interface Shear Strength

The interface shear strength of the GCL with an adjacent material can be the most critical (i.e., lowest) shear strength. The shear strength of GCLs at interfaces can be affected by several factors. One factor is the interfacing materials. For example, the friction angle between a GCL and subsoil will be different from the friction angle between a GCL and a geomembrane. Also, a textured geomembrane will typically have a higher interface friction angle with a GCL than a smooth geomembrane. A second factor affecting the interface shear strength of geotextile-encased GCLs is the different types of geotextiles used in making GCLs. An interface involving a woven geotextile may have a lower shear strength than an interface involving a nonwoven geotextile. A third factor is the degree of hydration of the bentonite and its potential mobility through the geotextile components of the GCL. If hydrated bentonite can swell through the geotextiles, the hydrated bentonite may "lubricate" the interface with an adjacent material. In addition, the level of normal stress and amount of deformation can influence interface shear strengths. Distortion before or during deformation could also be a factor. Finally, the amount of deformation can influence interface shear strength. The large-displacement interface shear strength is generally less than the peak value.

CHAPTER 3
FIELD TEST PLOTS IN CINCINNATI, OHIO

Cooperative Agreement CR-821448-01-0 is a multi-task, multi-year research project entitled, "Field Performance of Waste Containment Systems." The project is being conducted by the U.S. EPA, Drexel University's Geosynthetic Research Institute, The University of Texas, and GeoSyntec Consultants. One of the tasks on this project is to develop more information concerning the shear strength of GCLs. The field test plots that are described in this section of the workshop proceedings constitute the main effort on the GCL shear strength task of the project.

The main objective in constructing the field test plots was to investigate the internal (mid-plane) shear strength of GCLs in carefully controlled, field-scale tests. Other objectives were to verify that GCLs in landfill cover systems will remain stable on 3H:1V slopes with a factor of safety of at least 1.5, to monitor the deformation and creep of GCLs in the field for as long as possible, to develop information on erosion control materials, and to better understand the field performance of GCLs as a component in liner and cover systems.

Fourteen test plots have been constructed at the ELDA Landfill in Cincinnati, Ohio. Nine of the plots were constructed on 2H:1V slopes and five were constructed on 3H:1V slopes. Each plot is about 9 m wide by 20 or 29 m long and is covered by approximately 0.9 m of cover soil. Instrumentation was placed in each test plot (with a few exceptions) in order to monitor the moisture content of the subsoil and deformations of the GCL. An additional plot consisting only of cover soil was constructed on the 2H:1V slope. This plot did not contain geosynthetic materials and was used as a control plot to study the effect of erosion on the cover soil on a plot that did not contain any synthetic erosion control material.

Slope angles of 2H:1V and 3H:1V were selected to test the shear strength limits of the GCLs. The rationale for selecting these slope inclinations was as follows. Many landfill final covers have slopes of approximately 3H:1V. If GCLs are to be widely used in landfill covers, they will have to be stable at a slope angle of 3H:1V. Thus, the 3H:1V slope was selected to be representative of a typical landfill cover. However, it is not sufficient to demonstrate that GCLs are stable on 3H:1V slopes — it must be shown that they are stable with an adequate factor of safety. Many regulators and design engineers require that permanent slopes have a minimum factor of safety for static loading of 1.5.

For an infinite slope in a cohesionless material, with no seepage, the factor of safety (F) is:

$$F = \frac{\tan \phi}{\tan \beta} \qquad (3.1)$$

where ϕ is the friction angle and β is the slope angle. If a GCL remains stable on the 2H:1V slope, the friction angle of the GCL (assuming zero cohesion) must be at least 26.6°, and for this friction angle, the factor of safety on a 3H:1V slope must be at least 1.5. Thus, the logic was to try to demonstrate a minimum factor of safety of 1.5 on 3H:1V slopes, and in order to do this, it was necessary to test the GCLs on 2H:1V slopes. It was recognized that constructing a 2H:1V slope was pushing the test to (and possibly beyond) the limits of stability, not necessarily of the mid-plane of the GCLs but certainly at various interfaces within the system.

3.1 Expectations Concerning Field Performance at the Beginning of the Project

During the conception and design of the field test plots, there were several expectations concerning the performance of the GCLs. First, it was assumed that if the GCLs were placed with the bentonite in contact with the subgrade soils that the bentonite would hydrate by absorbing water from the adjacent soils. However, it was also assumed that if a geomembrane separated the bentonite component of the GCL from the underlying subsoil, and a geomembrane was placed over the bentonite to encase the bentonite between two geomembranes, that the bentonite would be isolated from adjacent soils (except at edges) and would not hydrate.

A key expectation was that none of the GCLs would fail at the mid-plane on either the 3H:1V or 2H:1V slopes. This expectation was based on the results of mid-plane laboratory shearing test on fully-hydrated GCLs. Interface shear slides were viewed as possible, but the greatest concern was with the GCL/subsoil interface. It was predicted that deformations of the GCLs would be downslope with the largest deformations on the 2H:1V slopes. Creep of the GCLs was considered possible. Differential (shear) deformations were expected to be nominal.

3.2 Layout of the Test Plots

The test plots were constructed at the ELDA Landfill in Hamilton County, Cincinnati, Ohio. Fourteen test plots containing a GCL as a component were constructed. The layout of the plots is shown in Figure 3.1. Each plot was assigned a letter. Five plots (plots A-E) were constructed on a 3H:1V slope, and nine plots (plots F to L, N, and P) were built on a 2H:1V slope. An additional plot, plot M, which consisted of only cover soil and no geosynthetics, was an erosion control plot that was installed on a 2H:1V slope to document the degree of erosion that would occur if no synthetic erosion control material was placed over the cover soil. In all

other plots, a synthetic erosion control material covered the surface of the test plot. Plots on the 2H:1V slope were about 20 m long and 9 m wide; plots on the 3H:1V slope were about 29 m long and 9 m wide.

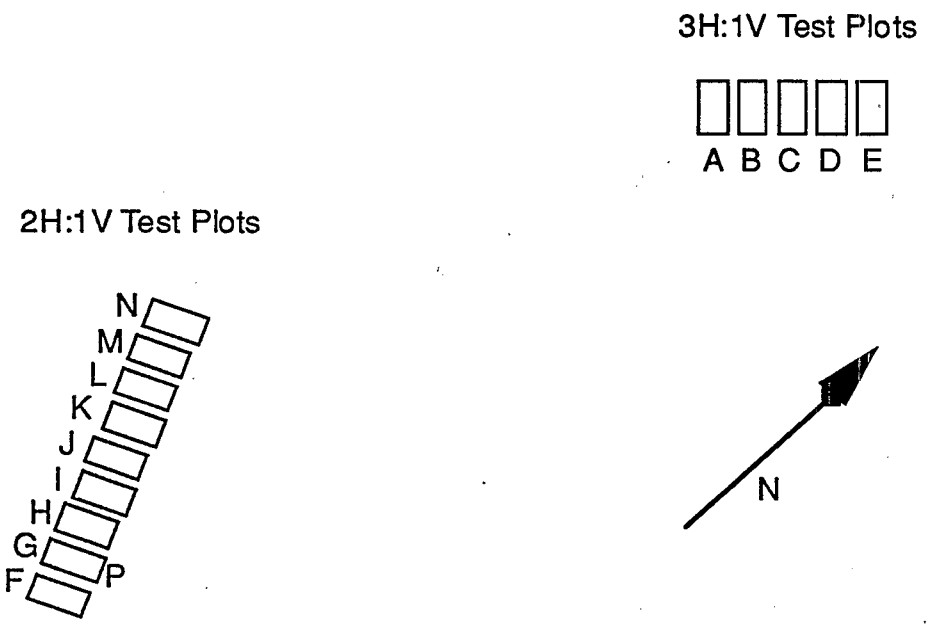

Figure 3.1 Layout of Test Plots.

3.3 Plot Compositions

Four different types of GCLs were placed at the site: Gundseal®, Bentomat®, Claymax® 500SP, and Bentofix®. Two styles of Bentofix® were employed. Bentofix® I contained nonwoven geotextiles on both surfaces. Bentofix® II contained a woven geotextile on the side that faced downward and a nonwoven geotextile on the side that faced upward.

Two general designs were employed. The principal design involved a subgrade overlain by a GCL, textured geomembrane, geotextile/geonet/geotextile drainage layer, and 0.9 m of cover soil. This cross section is typical of many final cover systems for landfills being designed today. The geotextiles were heat-bonded to the geonet. A nonwoven, needlepunched geotextile was used between the textured geomembrane and geonet in an effort to develop a high coefficient of friction between the geomembrane and drainage layer. This type of plot composition (Plot Composition I) is shown in Figure 3.2. Acronyms used are GT (geotextile), GN (geonet), GM (geomembrane), and GCL (geosynthetic clay liner).

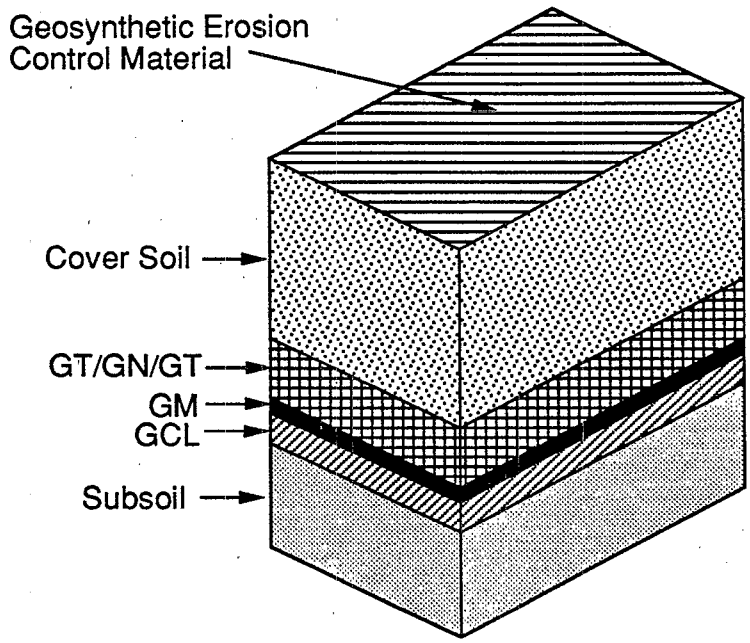

Plot	Slope	GCL
A	3:1	Gundseal
B	3:1	Bentomat
C	3:1	Claymax
D	3:1	Bentofix II

Plot	Slope	GCL
F	2:1	Gundseal
G	2:1	Bentomat
H	2:1	Claymax
I	2:1	Bentofix I
N	2:1	Bentofix II
P	2:1	Gundseal

Notes:
1. Bentomat was installed with woven geotextile facing upward.
2. Bentofix I was Bentofix NW, which has a nonwoven geotextile on both sides.
3. Bentofix II was Bentofix NS, which had a woven geotextile facing downward.

Figure 3.2 Cross Section of Test Plots Containing a Geomembrane (Plot Composition I).

The second design involves a GCL overlain by 0.3 m of drainage soil, a geotextile, and 0.6 m of cover soil. This design is also typical of current GCL designs for final cover systems in which a geomembrane is not used. This design (Plot Composition II) is shown in Figure 3.3.

In Plot E (Figure 3.4), the bentonite part of the Gundseal® GCL is in direct contact with the subsoil, the geomembrane portion of the GCL is facing upward, and a geonet and 0.9 m of cover soil has been placed on top of the GCL. Plots A, F, and P (Figure 3.5) were constructed with the bentonite side of Gundseal® facing upward and the geomembrane portion in contact with the subsoil. The composition of plots with Bentofix I and Bentofix II are shown in Figures 3.6 and 3.7, respectively, and plots with Bentomat are shown in Figure 3.8.

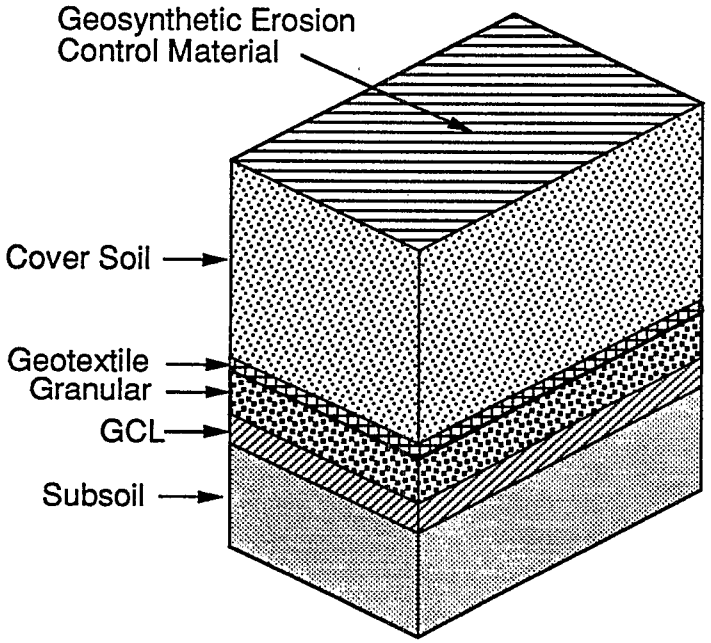

Plot	Slope	GCL
J	2:1	Bentomat (Woven Side Up)
K	2:1	Claymax
L	2:1	Bentofix I (NonWoven on both Sides)

Figure 3.3 Cross Section of Test Plots Not Containing a Geomembrane (Plot Composition II).

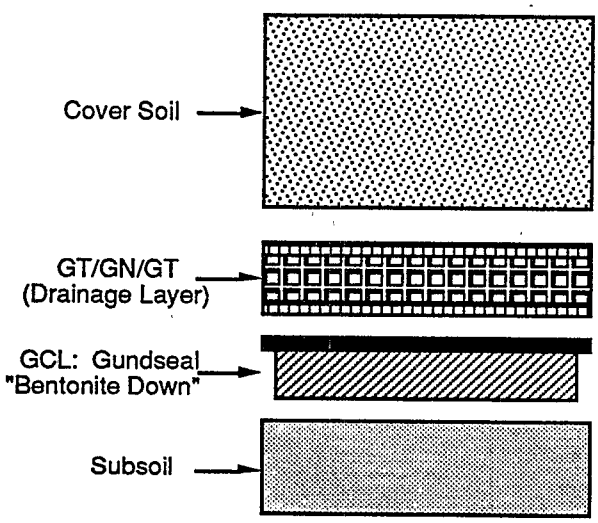

Figure 3.4 Cross Section of Plot E.

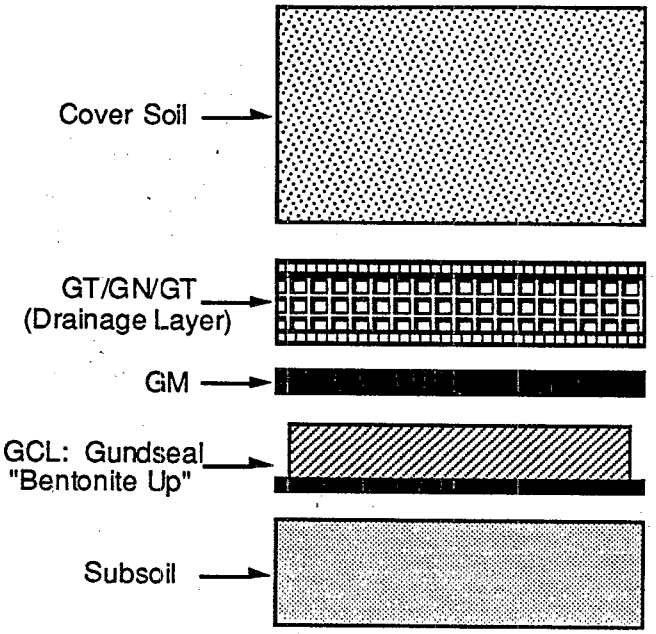

Figure 3.5 Cross Section of Plots A, F, and P.

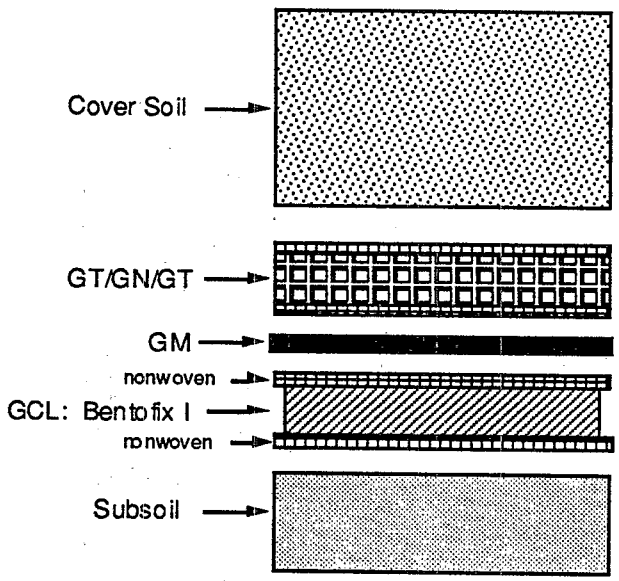

Figure 3.6 Cross Section of Plot I with Bentofix® I.

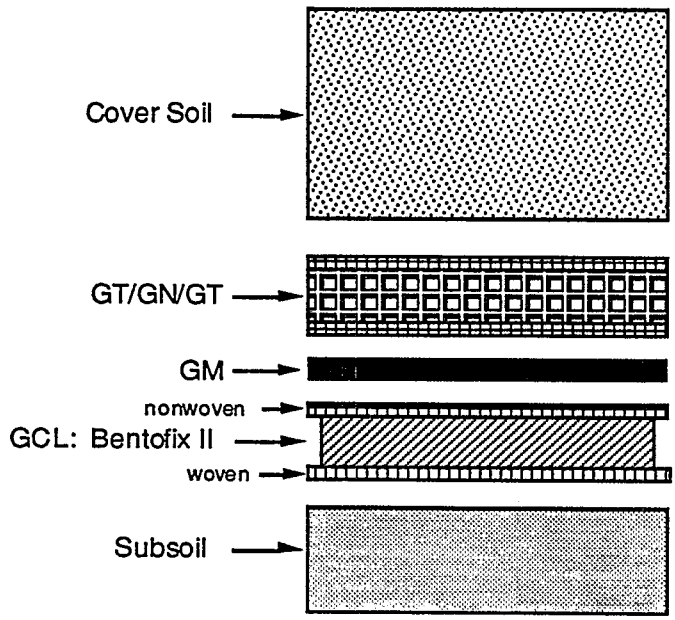

Figure 3.7 Cross Section of Plots D and N with Bentofix® II.

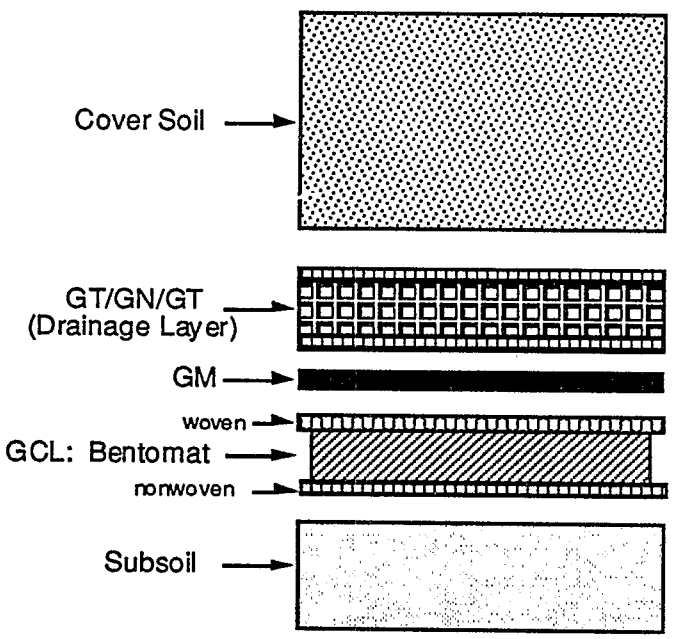

Figure 3.8 Cross Section of Plots B and G with Bentomat.

Plot M is the erosion control section and consists only of 0.9 m of cover soil. There are no geosynthetic materials or instrumentation inside the erosion control section.

General cross sections are shown in Figure 3.9 for plots constructed on the 2H:1V slope and in Figure 3.10 for plots constructed on the 3H:1V slope. A general cross section of a plot's width is shown in Figure 3.11. Each plot width was equal to two GCL panels minus a 150 mm overlap. The spaces between plots on the 2H:1V slope ranged between 0 m and 1.5, and were typically 1.5 m on the 3H:1V slope. There were graded drainage swales only on the 3H:1V slopes. Table 3.1 lists the slope angles, plot, type of GCL, and a description of the plot cross-section from top to bottom. Table 3.2 lists the composition, dimensions, etc., of each plot. Figures 3.12 and 3.13 are schematics of the 2H:1V and 3H:1V slopes, respectively, at the site.

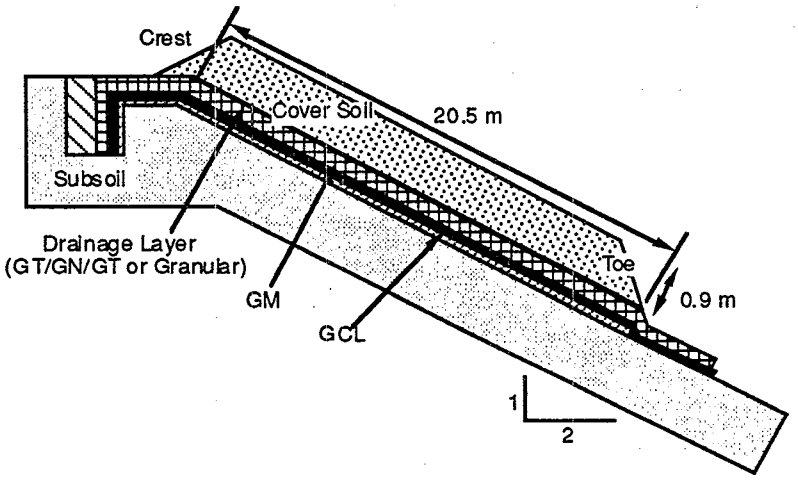

Figure 3.9 General Cross Section of Plots on a 2H:1V Slope.

3.4 Anchor Trenches

Anchor trenches were constructed at the crest of each test plot. On the 3H:1V and 2H:1V slopes all of the geosynthetic materials - GCL, geomembrane, and geonet (if present) - were brought into the anchor trench. A membrane cap strip was placed over the GCL in the anchor trench with the purpose of preventing moisture from entering the GCL from the crest of the plot. A typical anchor trench detail is shown in Figure 3.14.

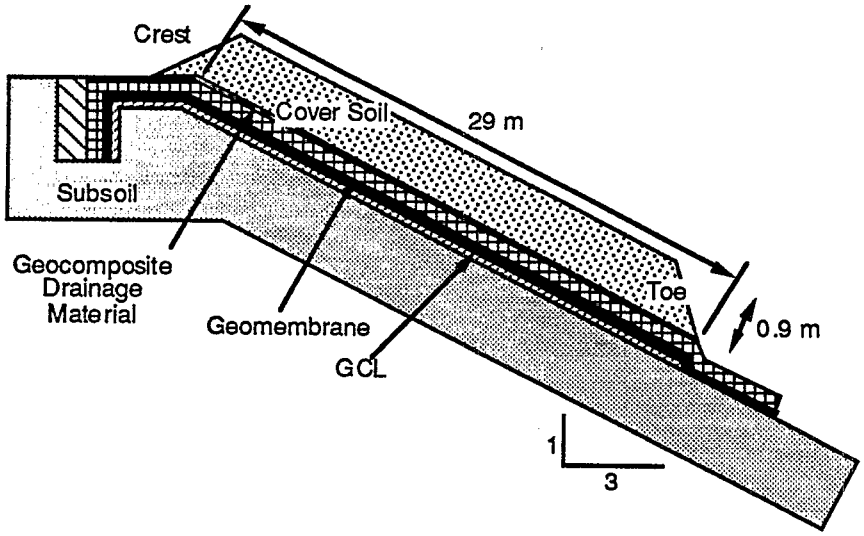

Figure 3.10 General Cross Section of Plots on a 3H:1V Slope.

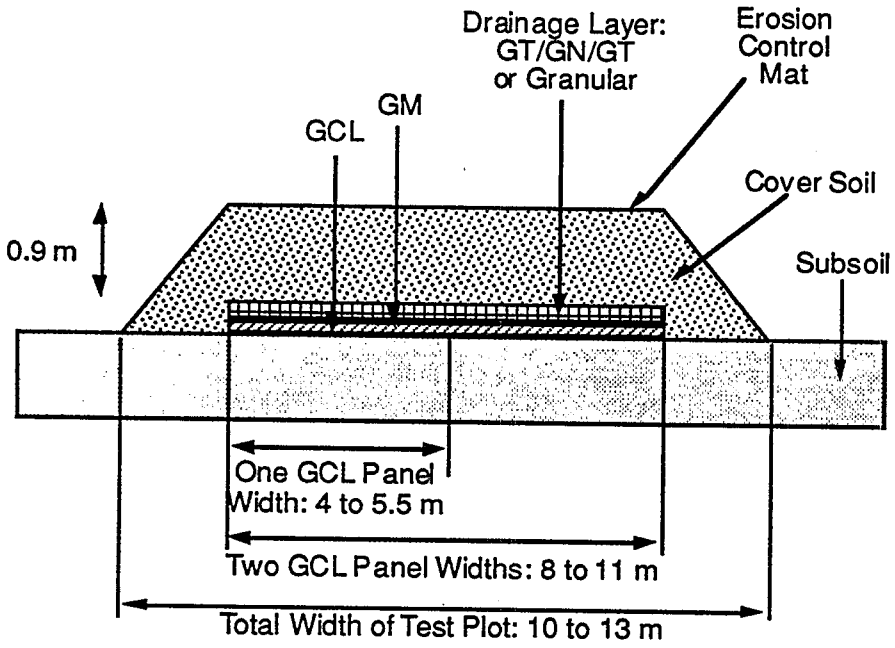

Figure 3.11 General Cross Section of Plots Showing the Width of a Plot.

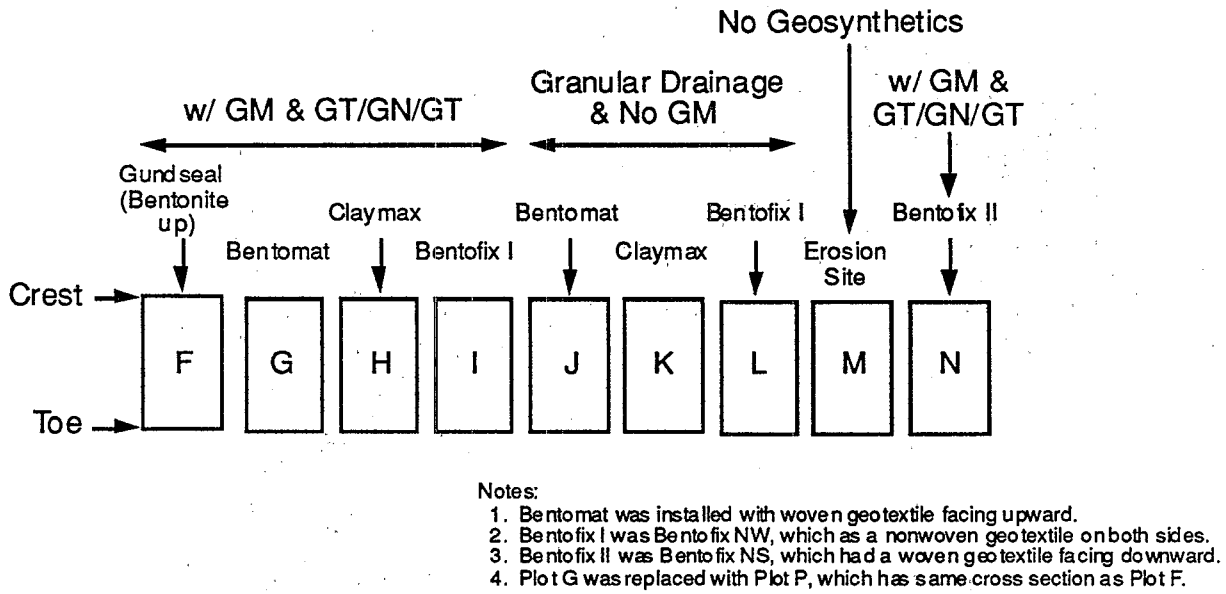

Notes:
1. Bentomat was installed with woven geotextile facing upward.
2. Bentofix I was Bentofix NW, which as a nonwoven geotextile on both sides.
3. Bentofix II was Bentofix NS, which had a woven geotextile facing downward.
4. Plot G was replaced with Plot P, which has same cross section as Plot F.

Figure 3.12 Schematic Diagram of 2H:1V Test Plots.

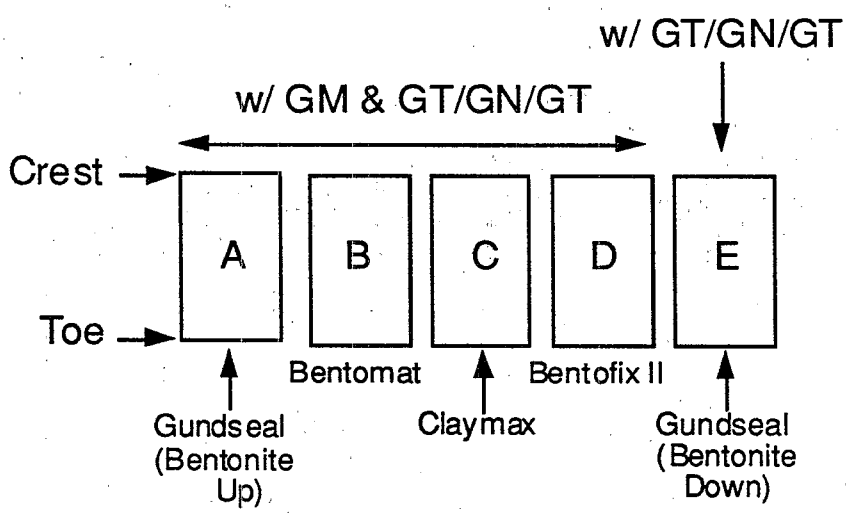

Figure 3.13 Schematic Diagram of 3H:1V Test Plots.

Table 3.1 Components of the GCL Field Test Plots.

Plot	GCL	Target Slope (deg.)	Actual Slope (deg.)	Cross-section (from top to bottom)
A	Gundseal	18.4	16.9	Soil/GN/GM/GCL (Bent. up)
B	Bentomat	18.4	17.8	Soil/GN/GM/GCL (W up)
C	Claymax	18.4	17.6	Soil/GN/GM/GCL
D	Bentofix II	18.4	17.5	Soil/GN/GM/GCL (NW up)
E	Gundseal	18.4	17.7	Soil/GN/GCL (Bent. down)
F	Gundseal	26.6	23.6	Soil/GN/GM/GCL (Bent. up)
G	Bentomat	26.6	23.5	Soil/GN/GM/GCL (W up)
H	Claymax	26.6	24.7	Soil/GN/GM/GCL
I	Bentofix I	26.6	24.8	Soil/GN/GM/GCL (NW-NW)
J	Bentomat	26.6	24.8	Soil/GT/Sand/GCL (W up)
K	Claymax	26.6	25.5	Soil/GT/Sand/GCL
L	Bentofix I	26.6	24.9	Soil/GT/Sand/GCL (NW-NW)
M	Erosion Control	26.6	23.5	Soil
N	Bentofix II	26.6	22.9	Soil/GN/GM/GCL (NW up)
P	Gundseal	26.6	24.7	Soil/GN/GM/GCL (Bent. up)

where:

Soil = cover soil

GN = geonet

GM = textured geomembrane

GT = geotextile

GCL = geosynthetic clay liner

Bent. up = bentonite side of Gundseal facing upward (GM against subgrade)

Bent. down = bentonite side of Gundseal against subgrade

W up = woven geotextile of GCL up, nonwoven side of GCL against subgrade

NW up = nonwoven geotextile of GCL up, woven side of GCL against subgrade

NW-NW = both sides of GCL nonwoven

Bentofix I is Bentofix NW, with a nonwoven geotextile on both sides

Bentofix II is Bentofix NS, with a woven geotextile facing upward.

Table 3.2 Summary of Test Plots.

Plot	GCL Type	Geo-memb. Cap (Y/N)	Drainage Type	Slope	Slope Length (m)	Crest Elev. (m)	Toe Elev. (m)	Test Plot Width (m)
A	Gundseal	Y	GN	3H:1V	28.9	179.2	170.0	10.5
B	Bentomat	Y	GN	3H:1V	28.9	179.2	170.0	9.0
C	Claymax	Y	GN	3H:1V	28.9	179.2	170.0	8.1
D	Bentofix II	Y	GN	3H:1V	28.9	179.2	170.0	9.1
E	Gundseal	Y	GN	3H:1V	28.9	179.2	170.0	10.5
F	Gundseal	Y	GN	2H:1V	20.5	157.9	148.7	10.5
G	Bentomat	Y	GN	2H:1V	20.5	157.9	148.7	9.0
H	Claymax	Y	GN	2H:1V	20.5	157.9	148.7	8.1
I	Bentofix I	Y	GN	2H:1V	20.5	157.9	148.7	9.1
J	Bentomat	N	Sand	2H:1V	20.5	157.9	148.7	9.0
K	Claymax	N	Sand	2H:1V	20.5	157.9	148.7	8.1
L	Bentofix I	N	Sand	2H:1V	20.5	157.9	148.7	9.1
M	Erosion Control	N	Sand	2H:1V	20.5	157.9	148.7	7.6
N	Bentofix II	N	Sand	2H:1V	20.5	157.9	148.7	9.1
P	Gundseal	Y	GN	2H:1V	20.5	157.9	148.3	10.5

Notes:

1. Bentofix I is Bentofix NW, with a nonwoven geotextile on both sides
2. Bentofix II is Bentofix NS, with a woven geotextile facing upward.
3. Bentomat was installed with the woven geotextile facing upward.

3.5 Toe Detail

At the toe of the slope the geomembrane and geonet were extended beyond the GCL in the plots on the 3H:1V and 2H:1V slopes. The geomembrane and geonet were extended (daylighted) approximately 1.5 m past the end of the cover soil as shown in Figure 3.15. The toe was designed to provide no buttressing effect for the cover soil.

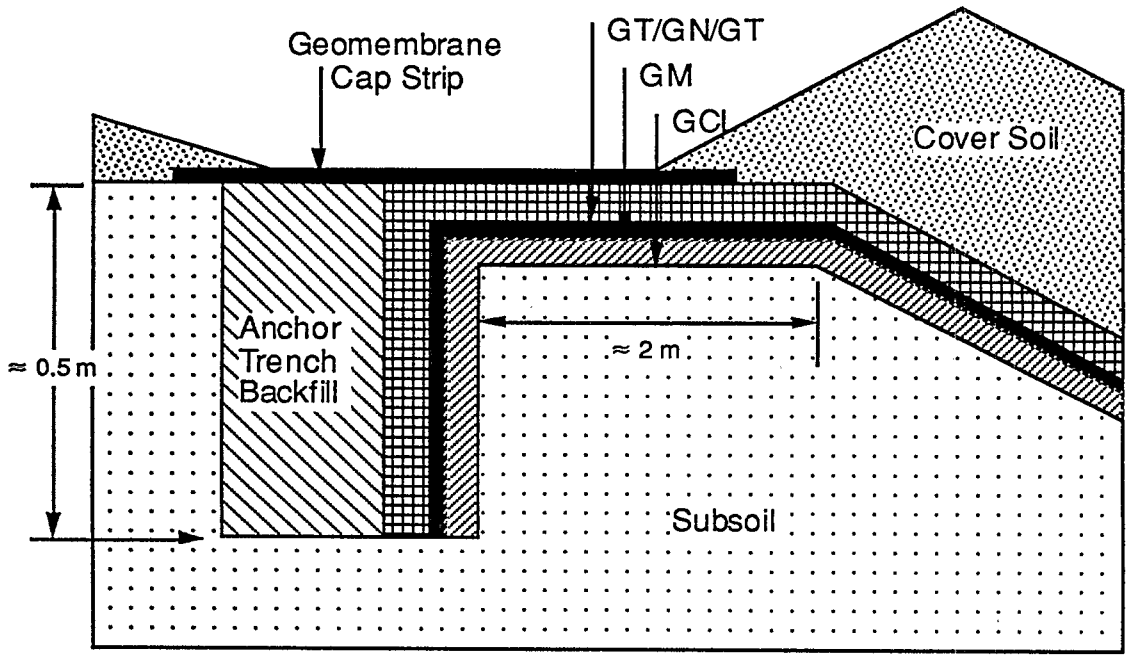

Figure 3.14 Anchor Trench Detail (Not to Scale).

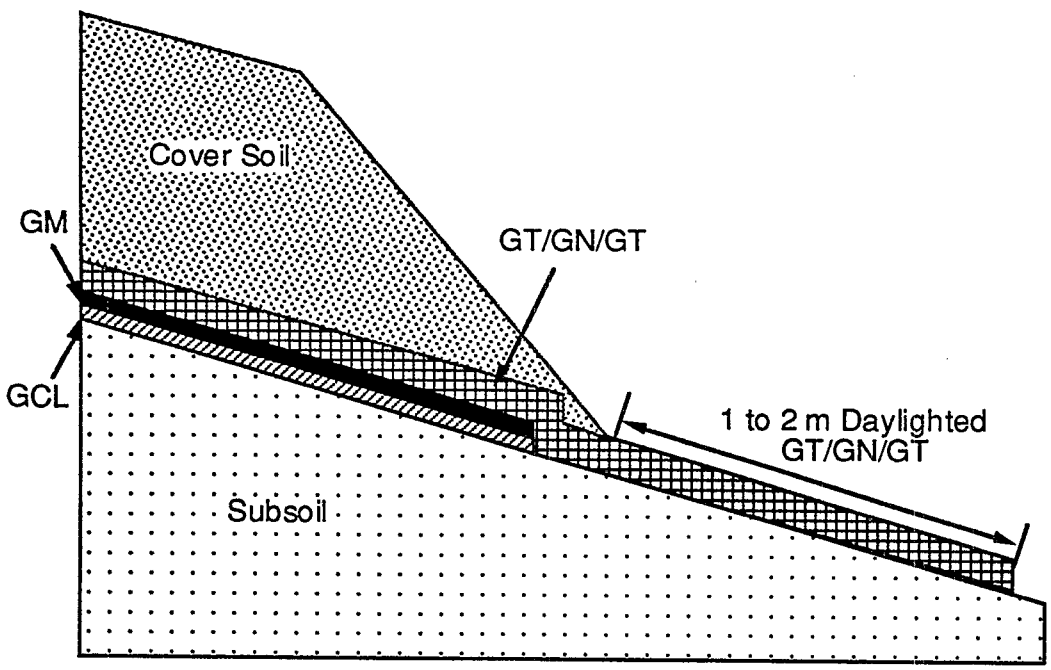

Figure 3.15 Detail of Drainage at Toe for Sections with Geonet Drainage Layer (Not to Scale).

The drainage detail at the toe of the 2H:1V slopes with granular drainage was developed to prevent clogging (Figure 3.16). In order to maintain stability of the drainage material, a 4.2-m wide piece of geonet was placed on top of the last 1.5 m of GCL at the toe of the slope. The geonet extended approximately 1.5 m past the end of the GCL. Sand was placed on the geonet above the GCL to ensure hydraulic continuity between the sand and geonet. The sand extended on the geonet about 0.5 m past the end of the GCL. Cover soil was then placed on the sand and geonet. At the toe of the slope, the geonet was excavated and exposed to permit drainage of the encapsulated sand layer.

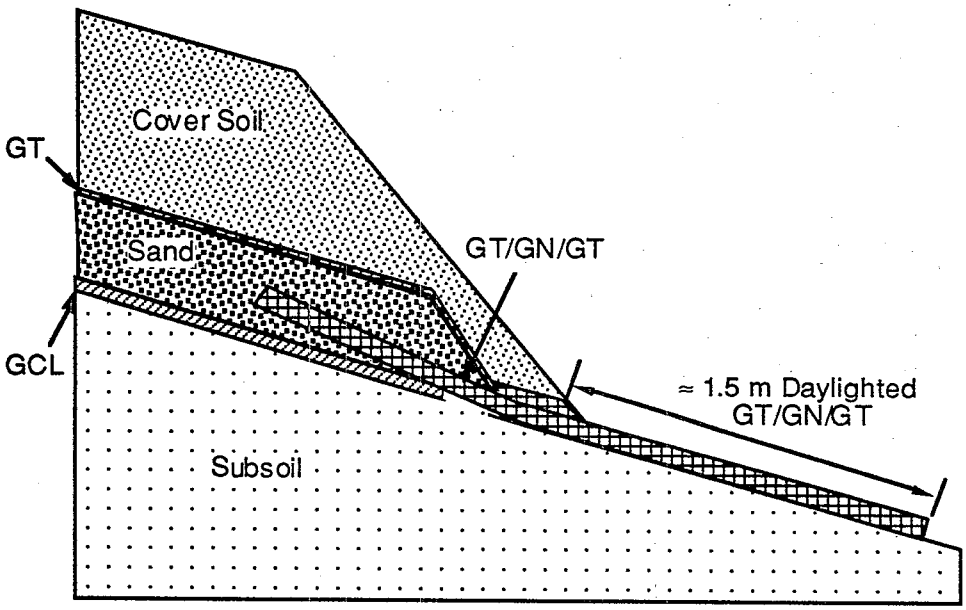

Figure 3.16 Detail of Drainage at Toe for Sections with Granular Drainage Material (Not to Scale).

3.6 Instrumentation

The objectives of the instrumentation for the field test plots were to monitor the wetting of the subsoil and the bentonite in the GCLs, and to monitor deformations of the GCLs. Moisture sensors were installed to verify that the bentonite was hydrated, or in the case of plots A, F, and P, to verify that the bentonite was dry. Extensometers were installed to document the

mid-plane shear and creep of the GCLs in each plot. As there was a limited budget, the instrumentation was selected based on simplicity, low cost, and redundancy.

3.6.1 Moisture Sensors

Moisture sensors were installed in each test plot in order to assess the moisture conditions impacting the bentonite within the GCLs. Two types of sensors were used in the project: a gypsum block sensor and a fiberglass mesh sensor (Figure 3.17). The gypsum block sensors were placed in the subsoil beneath the GCLs; the fiberglass sensors were placed within the bentonite of the GCLs. Both sensors operate on a resistance basis. The fiberglass sensors contain a porous fiberglass mesh embedded in two wire screens . The resistance to flow of electric current between the two screens is dependent on the moisture present in the fiberglass mesh. The resistance is measured and converted to moisture content by comparison with a calibration chart. The calibration is a function of soil type and the constituents of the soil moisture. The gypsum block sensors have two concentric spirals of wire between which resistance of gypsum is determined. The electrical resistance of the gypsum is a function of the moisture content of the gypsum. The resistance is measured using a digital meter manufactured specifically to measure resistance for these sensors.

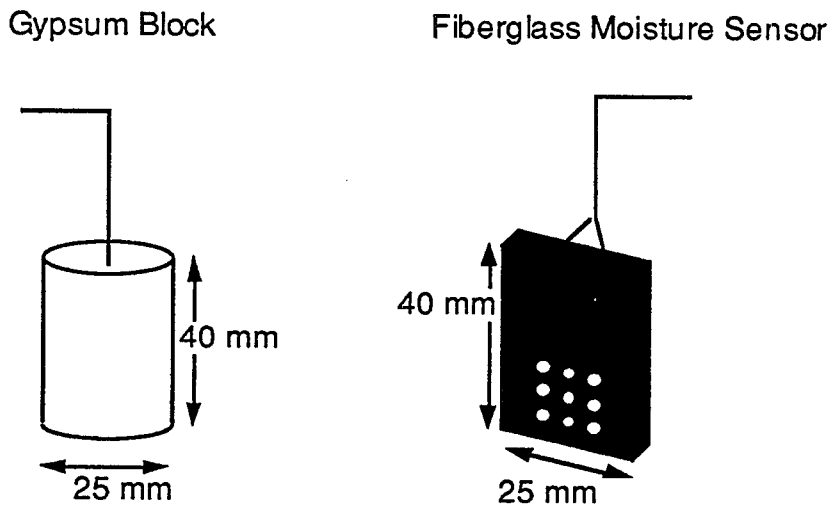

Figure 3.17 Schematic Diagrams of Moisture Sensors.

The sensors were placed on the centerline of one of the two GCL panels at three locations - top , middle, and bottom - of each plot as shown in Figure 3.18. The sensors were installed 5.2

m, 10.7 m, and 16.8 m from the crest on the 2H:1V slope and 6.1 m, 15.2 m, and 24.4 m from the crest on the 3H:1V slope. At each location two, and in some cases three, moisture sensors were placed in the subsoil, at the subsoil-GCL interface, and in a few instances, above the GCL. The purpose of the sensors was to monitor the moisture content of the bentonite and soil adjacent to the bentonite. Because most plots contained a geomembrane above the GCL, placing sensors in the cover soil would not provide information on moisture conditions within or near the GCLs. Therefore, moisture sensors were generally placed adjacent to or beneath the GCLs. A cross section of the moisture sensor installation in all plots except for plots A and F, is shown in Figure 3.19. Figure 3.20 shows how the moisture sensors were installed in plots A and F.

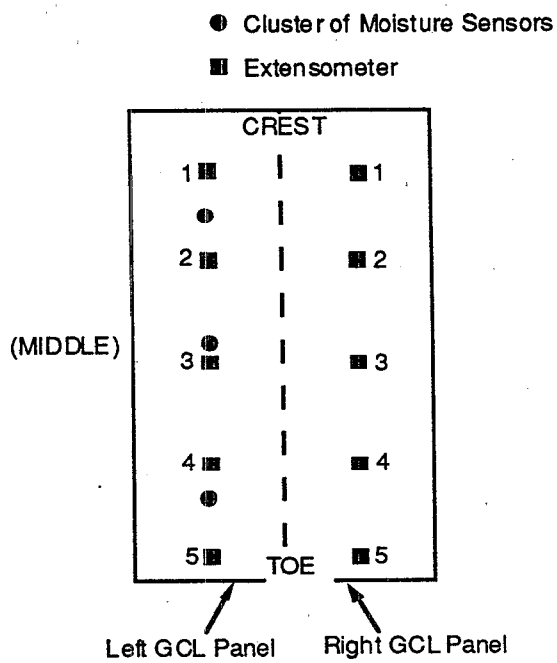

Figure 3.18 Locations of Moisture Sensors and Extensiometers.

The moisture sensors in Plot P were installed differently than the other plots. Only fiberglass moisture sensors were installed in Plot P. Sixteen moisture sensors were placed in a 4 x 4 grid on the upper side of the bentonite of the GCL but underneath the overlying geomembrane.

The gypsum blocks and digital meter were obtained from Soil Moisture Equipment Corporation of Santa Barbara, CA. The fiberglass sensors were obtained from Techsas, Inc. of Houston, TX.

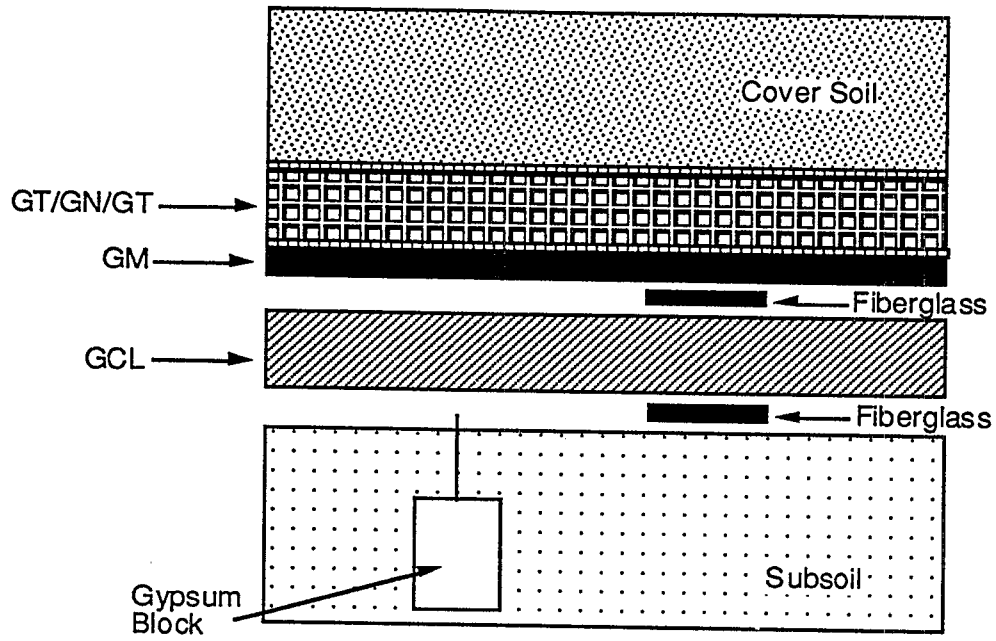

Figure 3.19 Location of Moisture Sensors in All Plots Except A and F.

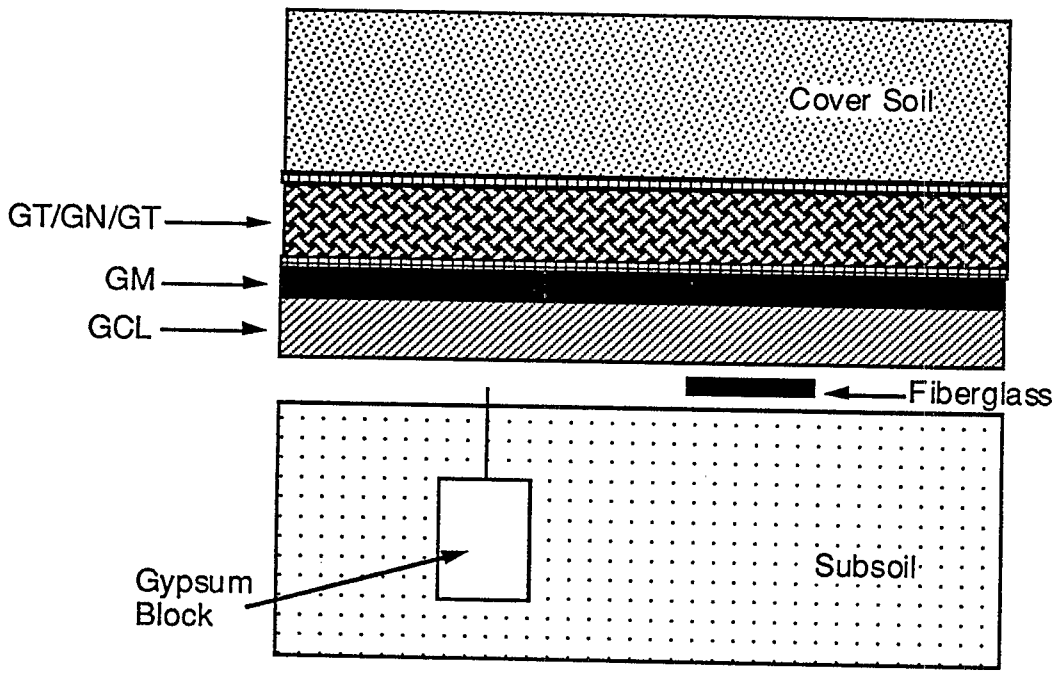

Figure 3.20 Location of Moisture Sensors in Plots A and F.

As mentioned above, the electrical resistance of a moisture sensor is measured and converted to moisture content by comparison with a calibration chart. The moisture sensor readout device used on this project reads from 0 to 100, with 0 corresponding to no soil moisture and 100 corresponding to a very wet soil. However, the calibration is a function of soil type.

There are generally four different soil types at the site. The different subsoils on the 2H:1V slope are shown in Figure 3.21. Soil A is a gray fat clay, soil B is a clayey silt, and soil C is a silty clay (field classifications). The subsoil on the 3H:1V slope is primarily a clayey silt (soil D).

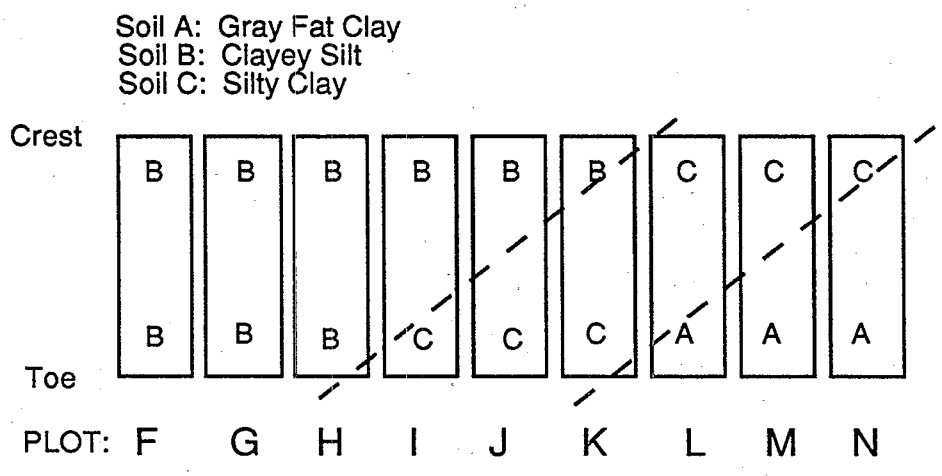

Figure 3.21 Soil Types at 2H:1V Test Plots.

Calibration tests were performed for both the gypsum block and fiberglass moisture sensors for soils A, B, C, and D. A 1000 ml beaker was filled with soil, and a circular piece of Gundseal® was placed above the soil with the bentonite portion of the GCL in contact with the soil. A small layer of sand was placed over the GCL and a pressure of 18 kPa was applied to the specimen. A gypsum block was inserted within the subsoil, and a fiberglass moisture sensor was placed at the interface of the GCL and the subsoil. The subsoil was incrementally wetted, and after the moisture gauge reading had equilibrated, the resistance reading was recorded and a sample of the soil was obtained for measurement of water content. A typical calibration curve for the gypsum block in the subsoil and the fiberglass moisture gauge at the soil/GCL interface is shown for soil A in Fig. 3.22.

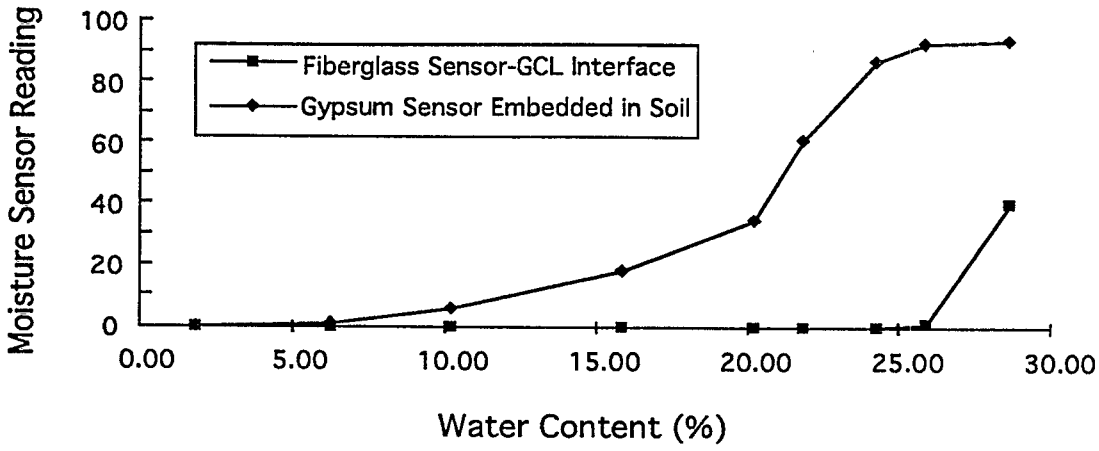

Figure 3.22 Calibration of Moisture Sensors for Soil A (Typical Calibration).

The calibration of the fiberglass moisture sensor with bentonite was performed as follows. A fiberglass sensor was sandwiched between two prewetted pieces of Gundseal® so that the sensor was surrounded by bentonite. Sand was placed below and above the GCLs, and a pressure of 18 kPa was applied. After the moisture gauge reading had stabilized, the moisture gauge reading was recorded. The calibration curve for the fiberglass moisture sensor with bentonite is shown in Fig. 3.23. The scatter is due to the use of 15 different sensors in the development of the calibration curve (each moisture sensor should ideally have its own individual calibration curve). This calibration curve can clearly be used to qualitatively distinguish whether the bentonite is relatively dry or saturated. Beyond that, however, statistical scatter limits resolution. For example, a moisture gauge reading of 20 indicates that the water content of the bentonite could range between 40 and 150%, and for a gauge reading of 80 the water content of the bentonite could range between 190 and 290%. However, a gauge reading of close to 0 clearly indicates that the bentonite is dry, and a reading close to 100 clearly indicates that it is wet.

3.6.2 Deformation Gauges

Deformation gauges, or extensometers, were installed in each plot to measure deformations and to assess shear strains in the GCL at multiple locations. Twenty deformation gauges were installed in each plot (10 pairs on each panel). Five gauges in each panel were attached to the upper side of the GCL along the centerline. Five gauges of each panel were attached to the lower portion of the GCL directly opposite the gauge attached to the upper surface of the GCL. The layout of the deformation gauges on the upper side of a GCL is shown

in plan view in Fig. 3.24. With gauges on the upper and lower side of the GCL, the difference in total deformation between the upper and lower gauges provides a measure of shearing deformation. Figure 3.25 shows the measurement of the differential movement (ΔL) of the upper and lower geotextile of the GCL.

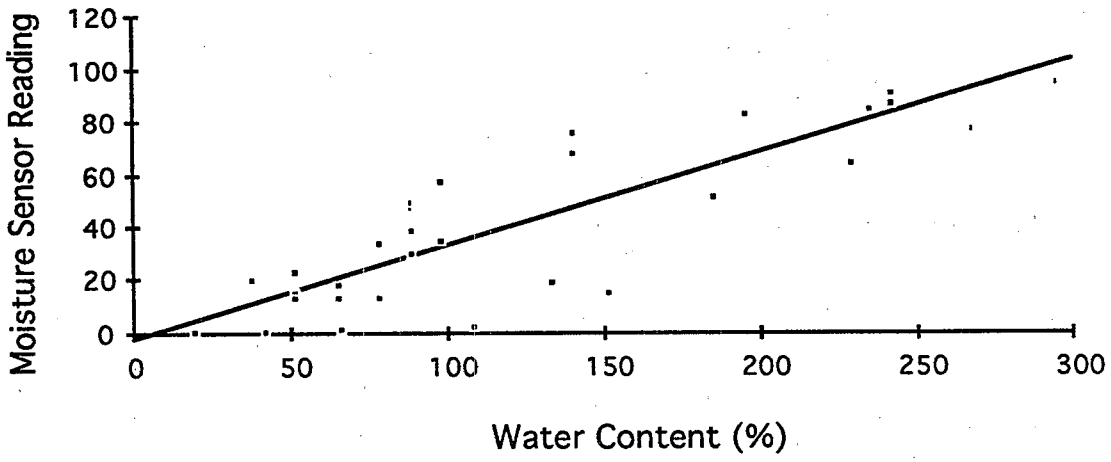

Figure 3.23 Calibration of Fiberglass Moisture Sensors with Bentonite.

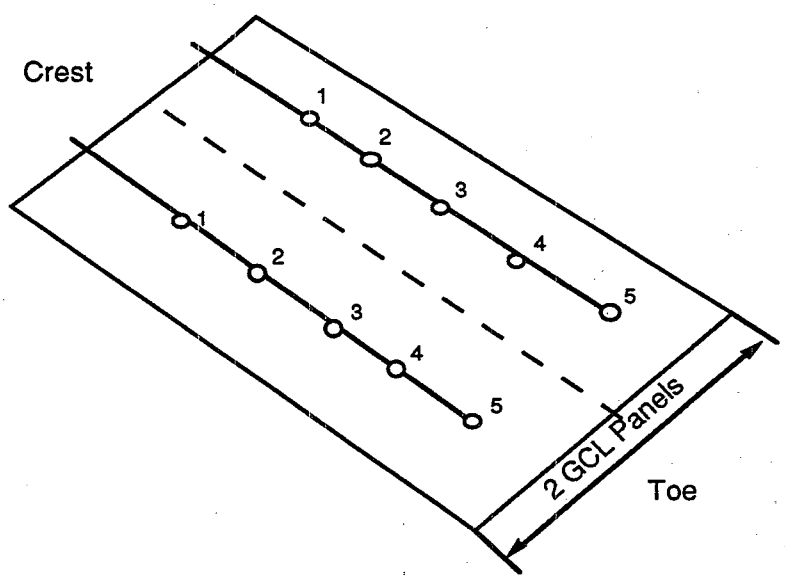

Figure 3.24 Locations of Deformation Sensors.

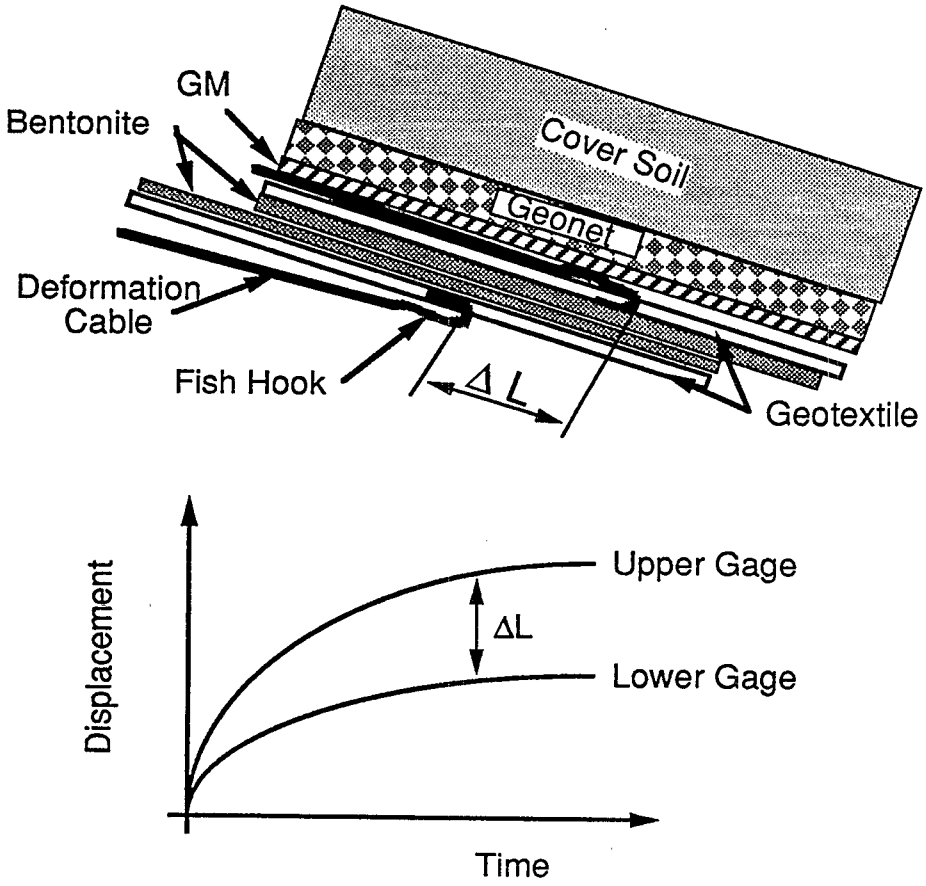

Figure 3.25 Measurement of Shearing Displacement.

Each extensometer consisted of a wire running from its point of attachment to above the crest of the slope. The wire was contained within a 6.4-mm OD (outside diameter) plastic tubing, and was connected to a fish hook at the end of the wire (Figure 3.26). The fish hook was attached by epoxy to the surface of the geotextile component of the GCL. Each wire extended from the fish hook to a monitoring station, or deformation table, at the crest of the slope. A deformation table is shown in Figure 3.27.

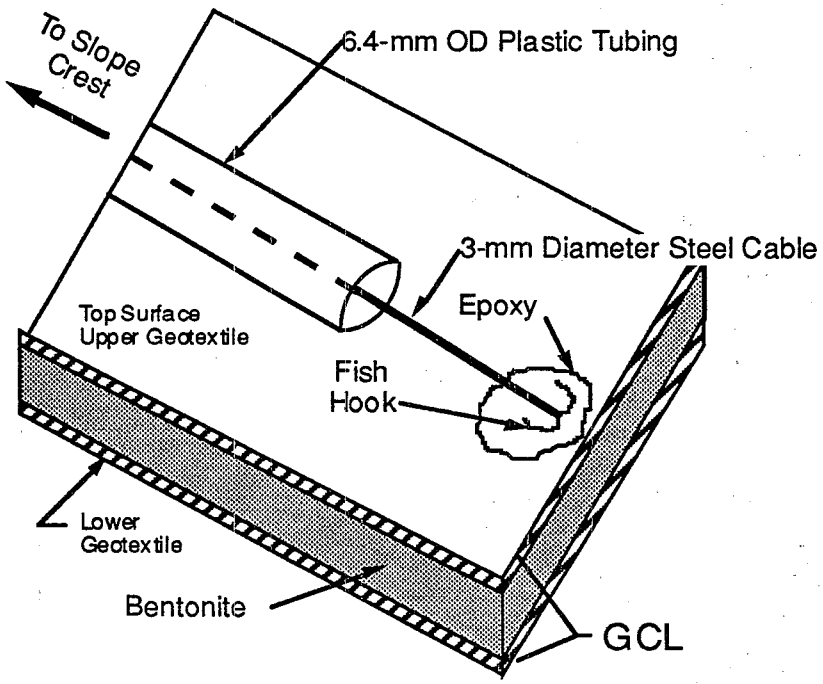

Figure 3.26 Attachment of Deformation Sensor to GCL.

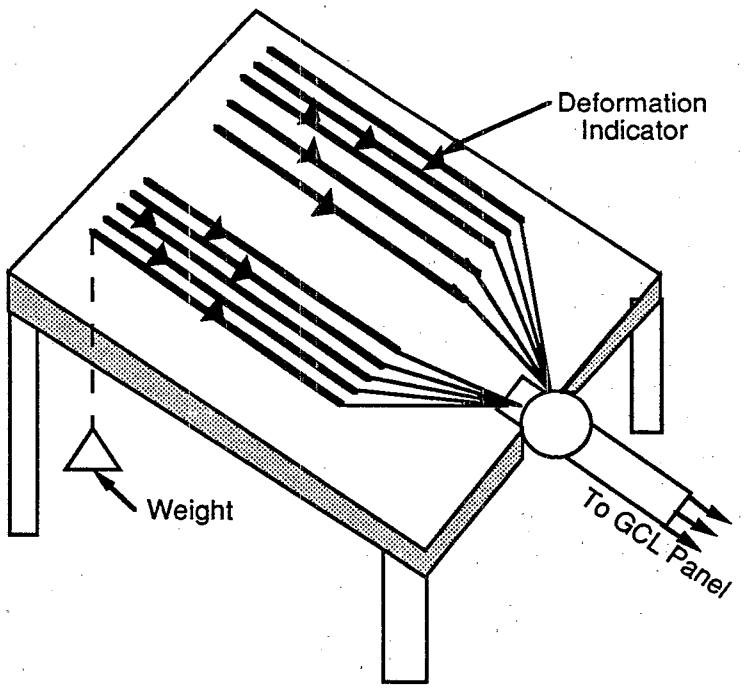

Figure 3.27 Deformation Table at Crest of Slope.

3.7 Construction

Construction of the plots began on November 15, 1994, and was completed on November 23, 1994. The construction sequence was as follows:

1. Subgrade preparation.
2. Installation of moisture sensors in the subgrade and at the surface of the subgrade.
3. Placement of GCL.
4. Installation of the extensometers and deformation cables.
5. Installation of moisture gauges within the GCL (plots A, F, P).
6. Placement of geomembrane (not applicable to plots J, K, L, and M).
7. Placement of geonet or granular drainage layer (plots J, K, L, M).
8. Placement of geotextile (plots J, K, L, M only).
9. Placement of cover soil.
10. Construction of deformation tables.

3.8 Cutting of the Geosynthetics

With other geosynthetic material besides the GCL leading into the anchor trench, part of the down-slope component of force created by the cover soil is carried by tension in the geosynthetic materials. To concentrate all of the shear stress within the mid-plane of the GCL, the geosynthetic materials above the mid-plane of the GCL were severed. The geosynthetics above the mid-plane of the GCLs in plots A through D (3H:1V slope) were cut on April 13, 1995, and the geosynthetics above the mid-plane of the GCLs on the 2H:1V slopes and plot E (3H:1V slope) were cut on May 2, 1995.

In plots with geotextile-encased GCLs, the geonet, geomembrane, and the upper geotextile of the GCL were cut at the crest of the slope down to the mid-plane of the GCL as shown in Fig. 3.28. The geosynthetic materials in plots constructed with a granular drainage layer were cut down to the mid-plane of the GCL as shown in Fig. 3.29. The granular drainage material did not extend into the anchor trench, so the geotextile separating the cover soil and drainage soil was cut as well as the upper geotextile in the GCL.

The cutting of anchor trench materials in plots with Gundseal® is shown in Figures 3.30 and 3.31. In the case with the bentonite side of the GCL facing up (Figure 3.30), the geonet and geomembrane were cut leaving the entire GCL intact. In the case with the bentonite side of the GCL facing downward (Figure 3.31), the geonet and the geomembrane of the GCL were cut.

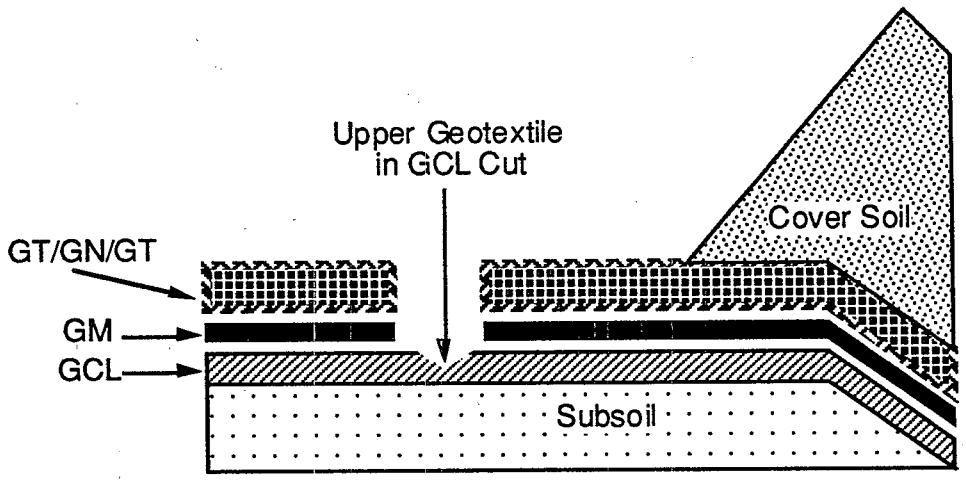

Figure 3.28 Cross-Section at Crest of Slope Showing Cutting of Geosynthetics Down to Mid-Plane of GCL on Test Plots with a Geomembrane.

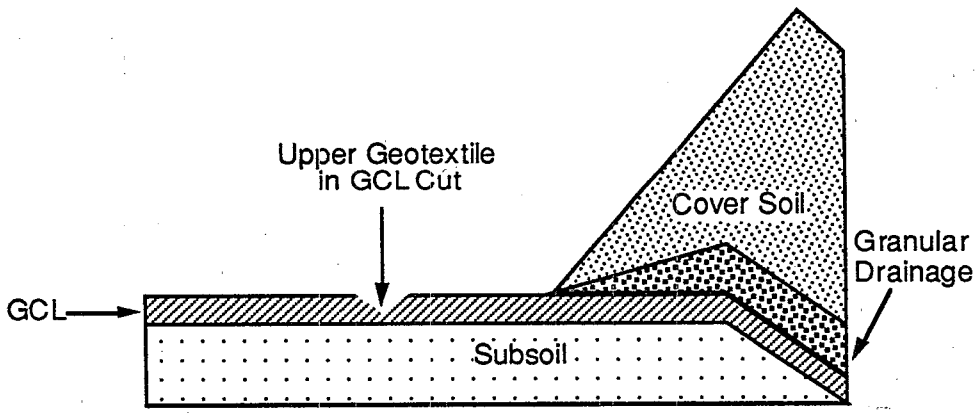

Figure 3.29 Cross-Section at Crest of Slope Showing Cutting of Geosynthetics Down to Mid-Plane of GCL on Test Plots without a Geomembrane.

3.9 Field Performance

Deformation and moisture data have been collected once every two to three weeks since the plots were installed. The data have been combined into three different types of plots. Two different graphs are associated with deformation movements: 1) total displacement versus time,

and 2) relative deformation versus time. The third type of graph is associated with the wetting of the GCL and subgrade soils and shows the moisture gauge readings versus time.

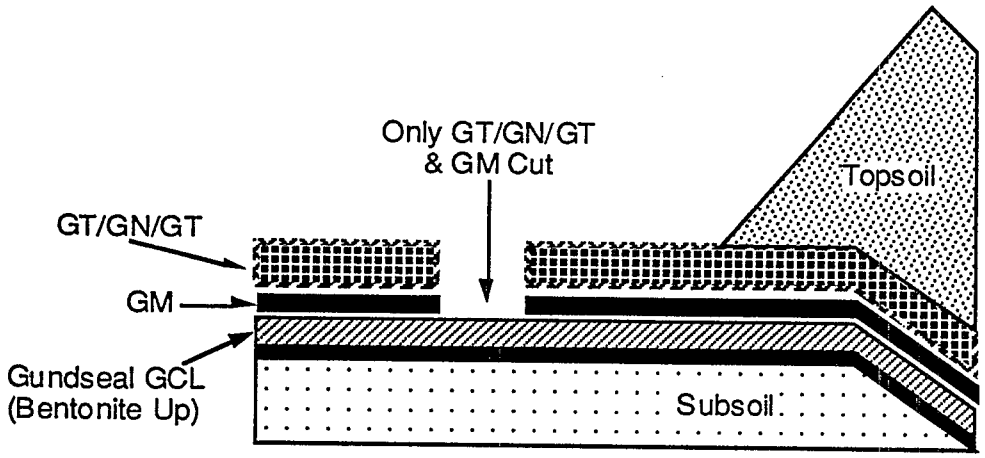

Figure 3.30 Cutting of Slope with Gundseal®, Bentonite Side Facing Upward.

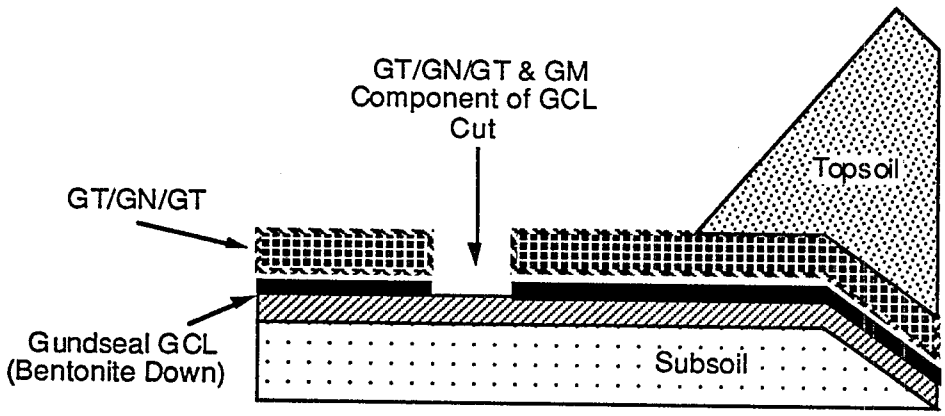

Figure 3.31 Cutting of Slope with Gundseal®, Bentonite Side Facing Downward.

3.9.1 Deformation Data

3.9.1.1 Total Displacement Data

Total displacement graphs for all plots are presented in Appendix B. Total displacement is the displacement of the gauge after the construction period. The total displacement is referred

to as "steady state" displacement in Appendix B. Each total displacement vs. time figure involves four plots. The two upper graphs show total displacement for the upper and lower deformation gauges at the crest of the slope (gauge 1); while the two lower are for the upper and lower deformation gauges for the toe (gauge 5) of the slope. Each graph includes data points for both the left and right GCL panels of the plot. The vertical axis on the graphs show values of increasing displacement down the axis (to simulate downslope movement). The accuracy of the deformation gauges is thought to be approximately ± 25 mm. With this accuracy, the deformation gauges can only be used to distinguish larger deformations or general trends in the movement of the GCL. For plot A, the total deformations associated with plot A are less than 25 mm.

3.9.1.2 Relative Displacement

The relative displacement, or the displacement of the upper gauge minus the displacement of the lower gauge, has been plotted versus time in Appendix C for each test plot. A positive value of relative displacement indicates that the GCL is experiencing shear in the downslope direction. The vertical axis on the graphs in Appendix C shows values of increasing displacement down the axis (to simulate downslope shear). The relative displacement versus time graphs include pre-cutting as well as post-cutting deformations.

3.9.1.3 Displacements after Materials in the Anchor Trench were Cut

In both the graphs of total displacement versus time (Appendix B) and relative displacement versus time (Appendix C), the times when the anchor trench materials were cut is noted. There was no sudden movement after the cutting of the geosynthetics in any test plot.

3.9.1.4 Moisture Gauge Readings

The readings from the moisture sensors are plotted versus time in Appendix D. These figures provide a general indication of how the soil is wetting and to what extent the soil has become saturated. The moisture reading is the instrument reading, not the actual water content.

3.9.1.5 Summary of Moisture and Deformation Data for all Plots

Moisture and deformation data for all test plots are summarized in Table 3.3. Only the readings from the fiberglass moisture sensors are included in Table 3.3.

Plots A through E on the 3H:1V slope have all deformed less than 25 mm. The moisture reading of the fiberglass gauges sandwiched between the bentonite of the GCL and the overlying

geomembrane has remained zero for plot A (Gundseal® with the bentonite side facing upward) and has ranged from 0 to 90 for most of the other plots on the 3H:1V slope.

Table 3.3 Moisture and Deformation Data.

Plot	Slope	GCL®*	Fiberglass Moisture Sensor Reading**	Total Movement (mm)
A	3H:1V	Gundseal (Bent. up)	0 (B)	<25
B	3H:1V	Bentomat	0 - 10	<25
C	3H:1V	Claymax	0 - 90	<25
D	3H:1V	Bentofix II	0 - 70	<25
E	3H:1V	Gundseal (Bent. down)	0 - 70	<25
F	2H:1V	Gundseal (Bent. up)	0 - 100 (B)	<375
G	2H:1V	Bentomat	0 -90	sliding***
H	2H:1V	Claymax	0 - 60	sliding***
I	2H:1V	Bentofix I	0 - 90	<100
J	2H:1V	Bentomat	0 - 90	<50
K	2H:1V	Claymax	0 -90	<25
L	2H:1V	Bentofix I	0 -100	<50
N	2H:1V	Bentofix II	0 -90	<25
P	2H:1V	Gundseal (Bent. up)	0 -10 (B)	NA

where:

*Bent. up = bentonite side of Gundseal® facing upward (GM against subgrade)
Bent. down = bentonite side of Gundseal® against subgrade

**readout value (not water content); sensor placed at the interface of the GCL and subsoil
B = sensor placed within the GCL

*** interface slide occurred -- see section 3.9.2

The plots on the 2H:1V slope have deformed more than the plots on the 3H:1V slope. Plot F (Gundseal® with the bentonite side facing upward) has experienced deformations close to 375 mm. Plots G and H have slid at the geomembrane/GCL interfaces, and a discussion of the interface slides will follow in the next subsection. The largest displacement of the other plots is less than 100 mm. Deformations in plot P are not being monitored (no deformation gauges were

installed). The moisture gauge readings show that all of the plots (with the exception of plot P) have experienced wetting of the bentonite within the GCL, with a general trend of increased wetting near the toe and crest of the slope. The wetting of plot F (Gundseal® with the bentonite side facing upward) is discussed in section 3.10.

3.9.2 Interface Slides

There have been two slides at the interface between the GCLs and the overlying geomembrane. Interface sliding occurred in plot H (Claymax® 500SP) on December 10, 1994 (21 days after the cover soil was placed), and plot G (Bentomat®) on January 12, 1995 (52 days after the cover soil was placed). Both interface slides were associated with slippage at the geomembrane-GCL interface (between a textured geomembrane and a woven geotextile), and in both cases no mid-plane distress was noted. In both plots G and H, all of the material except the GCL pulled out of the anchor trench (both slides occurred before the geosynthetics above the mid-plane of the GCL were cut) and slid as one block down the slope leaving the GCL intact on the slope. Both slides were sudden and rapid.

Analysis of the deformation data collected before the slides provided no indication that sliding was imminent; the deformation readings were very small (< 25 mm of movement) prior to sliding. The relative displacements, both construction and post-construction, in plot G do not indicate that a significant amount of shear had developed within the GCL before the interface slides occurred. Only construction deformations were collected for plot H prior to sliding. Analysis of the readings of moisture sensors suggests that the crest and toe of plot G were undergoing some hydration while the middle of the slope was still relatively dry. Moisture readings from plot H show slight drying at the crest and middle of the slope, but the small number of data points make drawing any conclusions difficult.

The objective of the test plots was to evaluate the internal, mid-plane shear strength of the GCLs, not the interface strength of the various components. Although interface slides occurred at these two test plots, the plots were viewed as successfully demonstrating the short-term, internal, mid-plane stability of the GCLs, since there was no indication of internal distress or deformation in the GCLs.

3.10 Plot F (Gundseal® with the Bentonite Side Facing Upward)

Plot F was constructed using Gundseal® with the bentonite sandwiched between two geomembranes. Theoretically, the bentonite should remain dry because significant moisture through the underlying and overlying geomembranes should be negligible and because wetting along the edges and around any small holes in the geomembrane should be limited to a distance

of a few millimeters or tens of millimeters from the source of the water. However, Plot F has experienced wetting of the bentonite within the GCL.

When moisture sensors indicated wetting of the bentonite in the GCLs in early 1995, holes were drilled through the cover soil, and core samples of the GCL were obtained to confirm the moisture sensor readings and to investigate the cause(s) of the wetting. The results of the water content tests are shown in Figure 3.31. The water content was found to be variable; some areas were dry, and others were wet. The initial water content of the GCL in this test plot was about 20%. Moisture contents of the samples ranged from 27 to 188%.

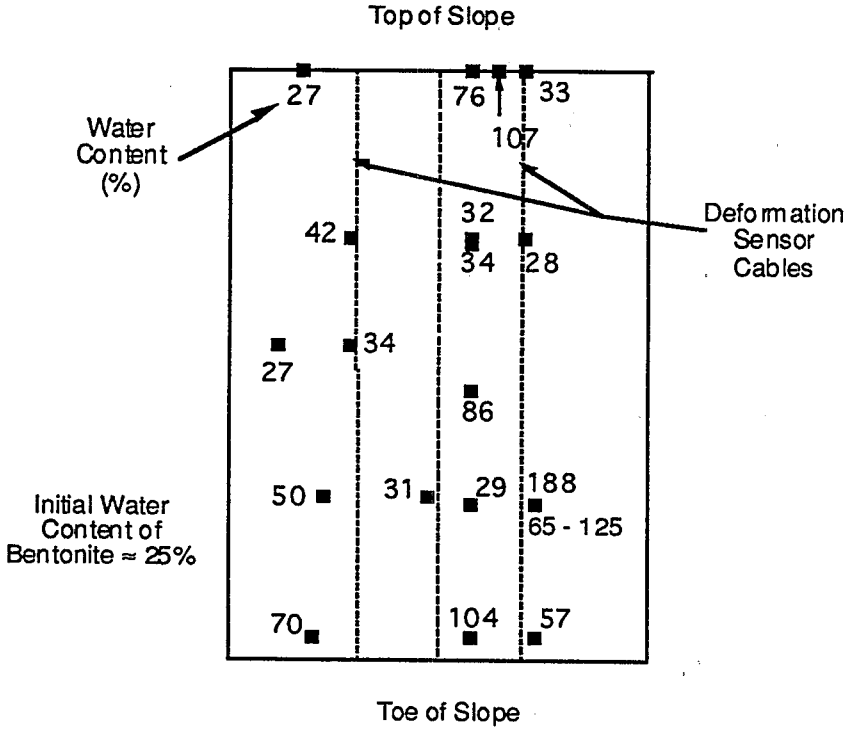

Figure 3.32 Measured Water Contents in the Bentonite in Plot F.

Different pathways in which water could have hydrated the bentonite and the likelihood of those pathways having occurred are listed in Table 3.4. There are three mechanisms that are considered to be the most likely ones. One possible mechanism is through a surface leak at the crest of the slope in which water traveled along the deformation cables that extended down the entire slope length. Another possible pathway involves the "spider web" (a thin geotextile placed over the bentonite in the GCL to keep excess bentonite from falling off the GCL) providing a

wick for lateral water migration. A third possible pathway is lateral water movement from the edges of the GCL through wrinkles in the geomembrane at the geomembrane/bentonite interface.

In addition to the unexpected hydration of the bentonite, Plot F has also undergone large deformations in one of the GCL panels. The deformation gauges above the GCL have registered large deformations (up to 375 mm) along the length of the slope in the right panel. The large deformations could be due to disconnection of the gauges or to the wetting of the bentonite in the GCL. Deformations in the left panel are comparatively small (generally < 1 mm). The highest moisture contents were measured in the right panel (Figure 3.32).

Table 3.4 Possible Pathways of Hydration of Plot F.

Source of Water	Comments	Likelihood that this Source Caused Hydration of Bentonite
Surface leak @ crest	Path through slots cut in upper GM for deformation instrumentation cables	Probable based on crest conditions and surface water drainage.
Leak from edges along slope face	Water must travel ≈ 2.1 m laterally to wet moisture gauge and sampled area	Tests on GCL without geotextile indicate that this mechanism is impossible; but actual GCL has not been tested
Leak from below through overlap seam	Water must travel ≈ 2.1 m laterally to wet moisture gauge and sampled area	Tests on GCL without geotextile indicate that this mechanism is impossible; but actual GCL has not been tested
GCL was folded longitudinally during placement	Folding GM could have cracked or impaired the GM	Unlikely
Vapor transmission through geomembrane	Some vapor transmission is expected	Rate of vapor transmission is expected to be negligible
Installation damage - holes & tears	Cover soil on Plot F was placed with a D-4 dozer. No damage observed during installation	Unlikely
Effect of the thin geotextile used to secure bentonite	Could GT provide lateral flow path, increasing transmissivity?	Possible that the geotextile wicked water laterally
Wrinkles in geomembrane provided seepage pathway	Any wrinkles between the geomembrane and bentonite would provide a pathway for spreading of water	Some wrinkles are likely.

3.11 Additional Test Plot P (Gundseal® with the Bentonite Side Facing Upward)

An additional test plot, plot P, was constructed (construction completed on June 13, 1995) in the same location that plot G (Bentomat®) had been located until the plot G slide. Plot P was installed to verify that bentonite sandwiched between the geomembrane component of the Gundseal® GCL and the overlying geomembrane could remain dry throughout the monitoring of the test when placed on the 2H:1V. Plot P was installed similarly to plot F except that a spider web was not used and deformation gauges were not installed. Sixteen moisture gauges were installed in a 4x4 grid pattern to monitor the wetting of the bentonite. The moisture gauge readings for Plot P have all been less than 10, indicating that the bentonite is relatively dry.

3.12 Erosion Control Materials

Erosion control materials were placed on the surfaces of all the test plots, except Plot M, which was intentionally not covered with any erosion control material as a control plot. The purpose of the erosion control materials was to stabilize the slopes rapidly and to maintain each slope's surface integrity. Erosion control materials provide for the rapid growth of seeded grass by retaining heat from the sun and limiting erosion due to overland runoff. The erosion control materials give shelter to the seeds from flowing water and winds.

Table 3.5 summarizes the erosion control products that were placed on the various test plots. Three plots (E, K, and N) had a sacrificial, biodegradable woody material applied to the surface. All erosion control materials were installed according to manufacturer's specifications. The erosion control materials were installed in an overlapping manner and stapled together and to the soil at spacings of approximately 1 m. Some plots were seeded prior to placement of the erosion control material, and others were seeded after the erosion control placement (depending on the manufacturer's recommendation). The site owner provided for the seeding of the plots in December, 1994.

Only visual information was available at the time of the workshop about the performance of the various materials. It was noted that (1) all of the erosion control materials seemed to be working well, and (2) there were significant erosion gullies in the control Plot M that did not contain any erosion control material. As of August, 1995, the erosion control materials appeared to be functioning as designed and have maintained the slopes' integrity.

3.13 Summary/Future Plans

The project so far has illustrated several important points about the use of GCLs as a component in a waste containment system:

1. GCLs have been stable on 2H:1V slopes with a factor of safety greater than or equal to 1.0 for mid-plane shear.
2. This indicates that GCLs on 3H:1V slopes have maintained a factor of safety greater than or equal to 1.5 for mid-plane shear.
3. Reinforced GCLs have greater internal, mid-plane shear strength than the interface strength between the woven geotextile component of the GCL and the textured geomembrane that was used in constructing the test plots.
4. The weakest interface has been between a woven geotextile in the GCL and a textured geomembrane.
5. In one plot the bentonite sandwiched between two geomembranes has become partly hydrated, but the mechanisms of wetting remain uncertain.

Future work for this project will include continued monitoring of the instrumentation for an additional 12 months, testing at the end of the project to determine water contents, etc., and additional work on determining how the bentonite between two geomembranes can hydrate. A final report will be issued in a little over a year.

Table 3.5 Geosynthetic Erosion Control Products.

Plot	Manufacturer	Product	Color	Material
A	Tensar	TB 1000	Green	Polyolefin
B	Synthetic Industries	Polyjute	Beige	Degradable Polypropylene
C	Synthetic Industries	Polyjute	Beige	Degradable Polypropylene
D	Akzo	Enkamat 7010	Black	Nylon
E	Akzo	Enkamat 7010	Black	Nylon (with Excelsior)
F	Tensar	TM 3000	Black	Polyethylene
G	Tensar	TM 3000	Black	Polyethylene
H	Tensar	TM 3000	Black	Polyethylene
I	Synthetic Industries	Landlok 450	Green	Polyolefin
J	Synthetic Industries	Landlok 450	Green	Polyolefin
K	Akzo	Enkamat 7010	Black	Nylon (with Excelsior)
L	Akzo	Enkamat 7010	Black	Nylon
M	None	Control Plot	-	-
N	Akzo	Enkamat 7010	Black	Nylon (with Excelsior)
P	Akzo	Enkamat 7220	Black	Nylon

CHAPTER 4
RESEARCH ON GCLs

4.1 Shear Behavior of GCL Interfaces at the EPA Test Plots in Cincinnati, Ohio

As discussed in Chapter 3, two test plots at the EPA GCL test facility in Cincinnati, Ohio, have slid at the interface between the geotextile component of the GCL and the overlying textured geomembrane. After these interface slides occurred, there was concern about potential interface slides at similar interfaces in other test plots. To assist in evaluating if the interfaces between materials at the test site would be stable, Drexel University's Geosynthetic Research Institute (GRI) performed shear tests on critical interfaces.

At the time the shear testing was performed, thirteen plots had been constructed. Five plots were constructed on a 3H:1V slope, and eight plots were constructed on a 2H:1V slope. The shear testing focused on the plots and interfaces installed on the 2H:1V slope because these were the more critical slopes. The interfaces of concern were:

1. The interface between the top of the GCL and the overlying textured geomembrane (T-GM).
2. The interface between the top of the GCL and the overlying sand.
3. The interface between the bottom of the GCL and the underlying subgrade (particularly the clayey subgrade soils identified as Soil A and Soil C in Fig. 3.21).

In addition, the internal shear strengths at the midplane of the GCLs were also evaluated through direct shear testing, although no results were available at the time of the workshop.

The shear tests were performed according to ASTM D5321 in a 300 mm (12 in.) square shear box. The specimens were hydrated for 2 to 10 days in the shear device under a normal stress of 18 kPa. This stress is the approximate normal stress acting on the GCLs in the 2H:1V test plots. The specimens were sheared at a strain rate of 1 mm/min. For each test, the peak and large-displacement strengths were reported. Single point failure envelopes were created by fitting a straight line through the origin and the failure point.

The interface between the top of the GCL and the textured geomembrane was the main focus of the program of laboratory shear testing because of the two interface slides at the test site. To simulate the field conditions as best as possible, site-specific products were used in the tests. In order to obtain the large-displacement strengths, the specimens were sheared to displacements of 35 mm.

The results of the direct shear tests are presented in Appendix E. The testing results are summarized in Table 4.1. Table 4.1 also summarizes the calculated factor of safety of the plots, based in Equation 3.1.

The testing of the Bentofix® - HDPE (textured) geomembrane interface for plot N was performed with the slit film woven geotextile at the interface. In reality, plot N was constructed with the nonwoven geotextile of Bentofix® at the interface with the textured geomembrane (facing upward). Therefore, the shear test on Bentofix® is not representative of the actual conditions at the site. Another note of importance is that the shear test on the interface between the bentonite portion of Gundseal® and the overlying textured geomembrane (plot F) was performed with the bentonite at the "as-received" water content. As discussed in Section 3.10, the bentonite component of the GCL has become hydrated in some locations. Thus, the direct shear tests on dry bentonite are not representative of the actual conditions in Plot F.

The direct shear tests that simulated interfaces on plots G and H produced friction angles lower than the actual angle of the slope. Therefore, if the interface shear tests had been performed before construction, e.g., as would be the case for a typical landfill design project, the interface slides on plots G and H would have been designed, and the slope would have been designed differently (e.g., different materials, flatter slopes, or internal reinforcement in the slope). The interface shear tests on all the other interfaces indicate that the peak interfacial friction angles are greater than the slope angles, indicating stable interfaces, which correlates well with field observations.

Plots J, K, and L were installed with sand as a drainage layer directly overlying the GCL. Placed above the sand was a nonwoven geotextile overlain by cover soil that was protected with an erosion control geosynthetic. A geomembrane was not installed. The concern in plots J, K, and L was the shear strength of the interfaces between the geotextile component of the GCL and the overlying sand. Direct shear tests were performed on this interface. The results are presented in Appendix E and are summarized in Table 4.1. The sand-GCL interfaces appear to be stable at the 2H:1V slopes, but just barely.

The stability of the subsoil at the 2H:1V test plots was of concern because of clayey nature and high water content of the soil. Direct shear tests were performed by GeoSyntec Consultants on the interfaces between the different GCL materials and the subsoil. These tests showed that the interfaces should be stable, but just barely. During construction the goal was to spread sand over the top of the prepared subgrade to provide additional resistance at the interface of the subsoil and the GCL. However, due to scheduling problems and weather delays, no sand was spread over the prepared subgrade. Instead, the GCLs were placed directly on the subgrade, which, on the 2H:1V slopes, frequently consisted of wet, clayey soil.

Table 4.1 Summary of Single-Point Direct Shear Tests.

Test Plot	GCL Type	GCL Interface	Other Interface	Peak Friction Angle (deg.)	Large-Displ. Friction Angle (deg.)	Actual Slope Angle (deg.)	Field Performance	Factor of Safety (Peak Strength)	Factor of Safety (Large-Displ. Strength)
Tests on Interfaces Above the GCL									
F	Gundseal®	Dry Clay**	T-GM	36.9	34.7	23.6	Stable	1.72	1.58
G	Bentomat®	SF-GT	T-GM	22.9	16.8	23.5	Slid (Interface)	0.97	0.69
H	Claymax®	SF-GT	T-GM	20	20	24.7	Slid (Interface)	0.79	0.79
I	Bentofix® TL-NW	NW-GT	T-GM	37.1	24.1	24.8	Stable	1.64	0.97
K	Claymax®	SF-GT	Sand	31	31	25.5	Stable	1.26	1.26
J,K,L	n/a	Sand	Sand	27.3	27.3	≈ 25	Stable	1.11	1.11
1/N*	Bentofix® TL-NS	SF-GT	T-GM	29.2	22.4	23.0	Stable	1.32	0.97
Tests on Interfaces Below the GCL									
All	All	Lower	Lower Subgrade	--	--	--	All Are Stable		

Notes:

*Plot N actually installed with NW/T-GM interface

**shear test on Gundseal® at "as-received" water content

TL = Thermal Lock

NW = nonwoven geotextile on both sides of GCL

NS = nonwoven and woven geotextiles

SF = slit film (woven)

GT = geotextile

T-GM = textured geomembrane

4.2 Aspects of GCL Performance of Composite Liners Containing GCLs

GeoSyntec Consultants has studied several aspects of GCL performance as a component in a liner system. The studies they have performed include:

1. The field hydraulic performance of composite liners containing GCLs
2. The hydration of GCLs adjacent to subgrade soil layers
3. The causes of failure of a landfill cover system containing a GCL
4. Direct shear strength of hydrated GCLs at high normal stress
5. Interface shear strength between unhydrated GCLs and textured geomembranes at high normal stress.

A detailed report of the these studies is presented in Appendix F. Key aspects of the work are summarized in the succeeding subsections.

4.2.1 Field Hydraulic Performance of Composite Liners Containing GCLs

The performance of a GCL as a liner in the field can be evaluated from several points of view. For example, a GCL can be evaluated based on its ability to limit advective transport (leakage), to restrict diffusive transport, or to attenuate the movement of chemicals. The focus of this study was to evaluate how well a GCL performs as part of a composite top liner. The work involved monitoring flow from leakage detection systems (LDS) below top liners at 26 waste management units.

Flow through the top liner is not the only source of LDS flow. Other sources include construction water, compression water, consolidation water, and infiltration water. Construction water is the drainage of water (mostly rainwater) that infiltrates the leakage detection layer during construction but does not drain to the LDS sump until after the facility starts to operate. Compression water is water that is expelled from the LDS layer as a result of compression under the weight of the waste. Consolidation water is water expelled from any clay component of the top liner as a result of consolidation under the weight of the waste. Infiltration water is groundwater that infiltrates through the bottom liner under an inward hydraulic gradient.

The methodology for evaluating the LDS flow sources in this study was as follows:

1. Identify the potential sources of flow based on design, climatic and hydrogeologic setting, and operating history.
2. Estimate the flow rates from each potential source.
3. Estimate the time frame for flow from each potential source.

4. Evaluate the potential sources of flow by comparing measured flow rates to calculated flow rates at specific times.
5. Compare leachate collection and removal system (LCRS) and LDS chemical constituent data to further establish the likely source(s) of liquid.

Results from the study are summarized in Appendix F. The average LDS flow rate in the 26 waste management units attributable to top liner leakage ranged from 0 to 50 liters/hectare/day (lphd), with most values being less than about 2 lphd. The average flow rate in the primary leachate collection and removal system was much higher: 5,350 lphd.

It was convenient, in analyzing the data, to define an "apparent" hydraulic efficiency of the top liner. The apparent hydraulic efficiency, AE, is defined as:

$$AE(\%) = (1 - \frac{\text{LDS Flow Rate}}{\text{LCRS Flow Rate}}) \times 100 \qquad (4.1)$$

The range and mean of apparent efficiencies of the composite liner during the initial, active, and post-closure periods were calculated for the cells with a sand LDS. During the initial period the AE_{mean} = 98.60% and AE_{range} = 91.84 to 100.00%; during the active period the AE_{mean} = 99.58% and AE_{range} = 97.50 to 100.00%; during the post closure period the AE_{mean} = 99.89% and the AE_{range} = 99.55 to 100.00%. The AEs in the initial period are lower than in the active and post closure periods because the flow in the initial period is affected to a large extent by construction water. During post closure, all of the flow is assumed to be from leakage through the top liner, and the AE is highest in this period. The range and mean of apparent efficiencies of the cells with top liners and geonet LDSs during the initial period of operation are: AE_{mean} = 99.96% and AE_{range} = 99.90 to 100.00%. Based on the data collected in this study, a composite geomembrane-GCL liner provides excellent hydraulic containment.

The field performance of composite liners containing GCLs in 26 waste management units has been evaluated. The study has found that LDS flow rates attributable to top liner leakage range from 0 to 50 liter/hectare/day (lphd), or 0 to 5 gallons per acre per day (gpad), with most values being less than 2 lphd. The "true" hydraulic efficiency of the top liner is greater than or equal to 99.9%. Composite top liners containing GCLs, when appropriately used as part of an overall liner system, can provide a very high degree of liquid containment capability.

4.2.2 Hydration of GCLs Adjacent to Subgrade Soil Layers

GeoSyntec Consultants measured the rate of hydration of three GCLs used at the GCL test site in Cincinnati, Ohio. The GCLs were placed in direct contact with the subgrade soils from the test site and were expected to fully hydrate.

The GCLs included in the hydration tests were Claymax®, Bentomat®, and Bentofix®. The soil used in the study was the subgrade soil from the western side of the 2H:1V slope at the GCL field test site (Soil C in Figure 3.21). The soil was classified as a low plasticity clay (CL) with a liquid limit equal to 41% and a plasticity index equal to 19%. A standard proctor compaction test was performed; the optimum moisture content (OMC) was found to be equal to 20%, and the corresponding maximum dry unit weight was equal to 16.7 kN/m^3 (106 pcf).

The soil was tamped into 75-mm-diameter molds to a relative compaction of 90% and at water contents ranging from -4% OMC to +4% OMC. The range in water contents were selected as the driest and wettest conditions that the GCLs might encounter at the GCL test site. The GCL was placed against the soil, covered with a geomembrane, and loaded to 10 kPa with a loading platen.

Plots for each GCL of the water content of the GCLs versus hydration time for subsoil water contents equal to OMC - 4%, OMC, and OMC + 4% are shown in Appendix F. The results are consistent for each GCL. The water contents of GCL specimens placed against subgrades with a moisture content equal to OMC - 4% were all close to 40% after 25 days. GCL specimens placed against subsoils with moisture contents equal to OMC had water contents ranging from about 55% to 65% after 70 days, and GCL specimens placed against soils with water contents equal to OMC + 4% had water contents ranging from 70% to 100% after 70 days.

The effect of overburden pressure was evaluated for one GCL (Bentofix®) by varying the overburden pressure from 5 kPa to 400 kPa. The water contents varied randomly over a small range (46% to 52%), and there was no trend. Therefore, overburden stress does not appear to have an effect on the hydration of a GCL when placed in contact with subsoil.

Tests were performed varying the height of the soil column in contact with the GCL from 50 to 200 mm thickness. GCL specimens had slightly lower water contents (≈ 40%)when in contact with thinner (≈ 50 mm thickness) subsoils. Water contents of GCL specimens increased to about 54% when in contact with thicker subsoils, but for subsoil specimens with 100 mm or greater thickness, the water contents did not vary with the thickness of the soil. This indicates that a subsoil specimen length greater than 100 mm will provide representative results.

Several conclusions can be drawn from the rate of hydration study:

for reinforced GCLs. The major conclusions are that internal shear strengths of GCLs must be measured at the appropriate normal stress, displacement rate, and total displacement to obtain representative results, and that GCL shear strengths should be described in terms of the corresponding range of normal stress for which the values were determined.

4.2.5 Shear Strength of GCL-Geomembrane Interfaces

For a project located in southern California, GeoSyntec Consultants performed 14 interface direct shear tests on the interface between an unhydrated GCL and a textured HDPE geomembrane. The tests were performed in a 300 mm by 300 mm direct shear box following procedures in general accordance with ASTM D5321. Three GCLs were tested using a range of normal stress of 350 to 1,920 kPa. Two shearing rates were used (0.016 mm/s and 0.0007 mm/s), and it was found that the slower shearing rate yielded interface friction angles that were 1 to 2 degrees lower. It was also found that the normal stress had a significant effect on the interface friction angles, which were 5 to 10 degrees lower at a normal stress of 1,920 kPa than at 350 kPa. It was also observed that there are relatively wide variances in the degree of texturing of geomembranes, even from a given manufacturer. Further details are provided in Appendix F.

4.3 University of Texas Research

4.3.1 Direct Shear Tests of GCL Bentonite

The internal shear strength of the bentonite within the GCL determined from laboratory tests are dependent on different preparation conditions and shearing methods. The University of Texas is performing direct shear tests on the bentonite within samples of Claymax® 200R to help develop appropriate direct shear testing procedures for GCLs. Two variables of shear testing of GCLs that are being studied are the hydration time and the shear rate.

Shear tests have been performed on GCLs after they have hydrated for various lengths of time - 24 hours, 48 hours and 72 hours - while holding all other variables constant (shear rate, normal stress, etc.). Figure 4.1 is a typical plot of shear stress vs. displacement for three shear tests performed after 24 hours of hydration under a normal stress of 17 kPa and at a shear rate of 1 mm/min. Similar tests were performed on specimens hydrated for 48 hours and 72 hours. A graph of the shear stress vs. normal stress plots for the 24, 48, and 72 hour hydration series is shown in Figure 4.2. Regression was performed for each hydration series (24, 48, and 72 hours of hydration) with the cohesion assumed to be equal to zero, and the friction angles are listed in Table 4.3. The friction angles from the three different hydration periods were similar, indicating that the period of hydration does not significantly affect the shear strength of the bentonite within a GCL.

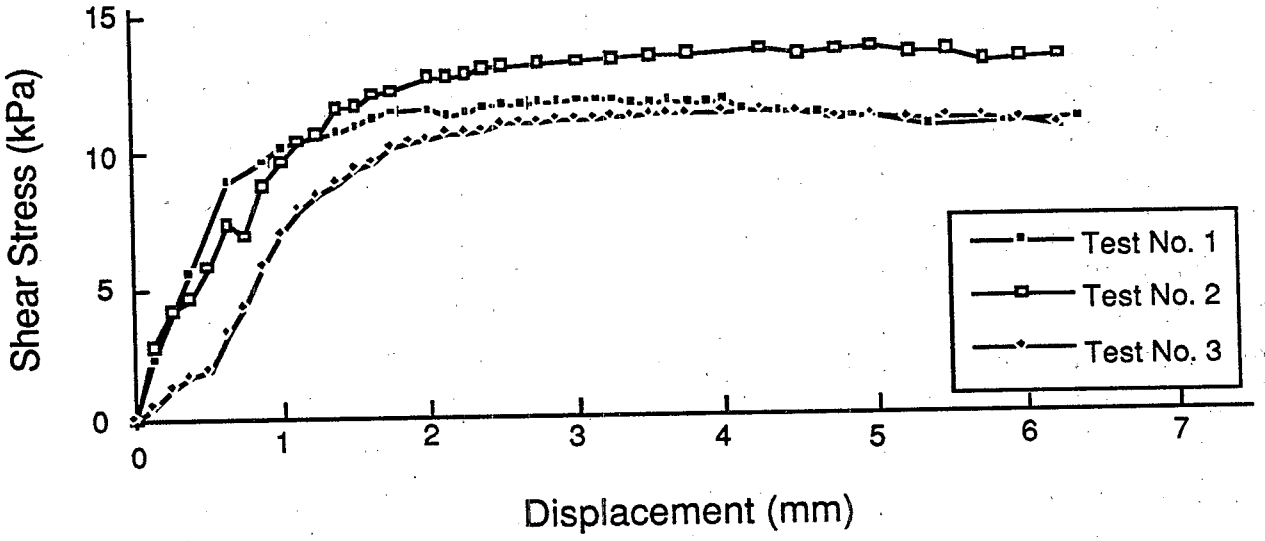

Figure 4.1 Typical Plot of Shear Stress Vs. Displacement at a Normal Stress of 17 kPa.

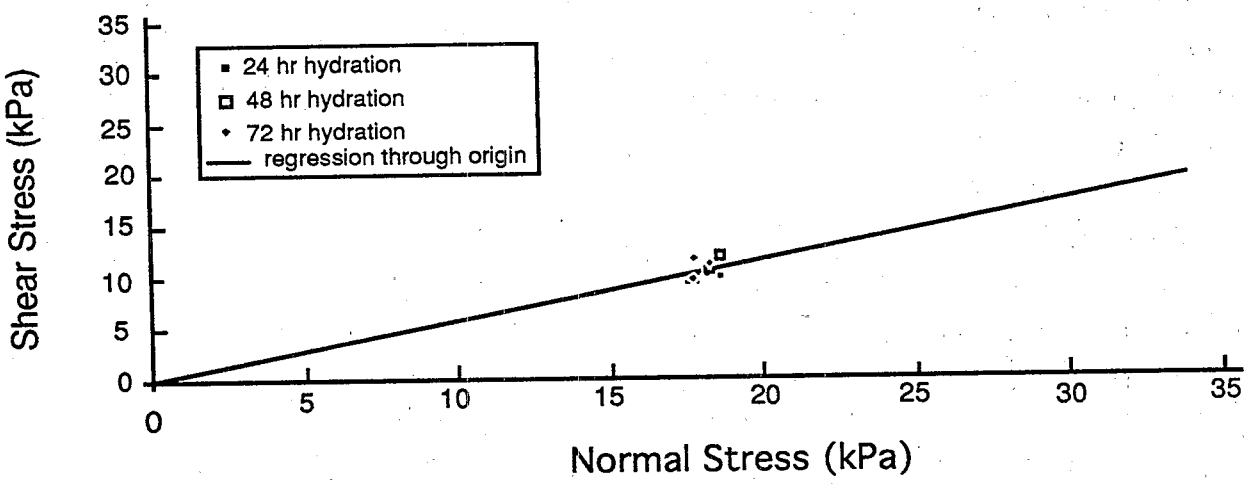

Figure 4.2 Results of Internal Shear Strength Tests on a GCL Hydrated for Various Periods.

Table 4.3 Strength Parameters from Shear Testing.

Test Series (Hydration Time)	Angle of Internal Friction (deg)	Cohesion* (kPa)	Average Final Water Content (%)
24 hour hydration	29.5	0	166
48 hour hydration	30.0	0	182
72 hour hydration	30.5	0	171

Note: * assumed c = 0
Shear rate = 1 mm/min
64 mm diameter shear box

Tests will be performed on hydrated specimens of GCLs where the only variable is the shear rate. All of the testing will be performed in 64 mm diameter shear boxes.

4.3.2 Hydration Tests

At low water contents, bentonite has a very large suction potential. At a water content of 20%, a common water content for manufactured GCLs, bentonite can have a suction greater than 80 bars (Daniel et al., 1993). This means that bentonite will hydrate when placed in contact with a material that is even slightly wet. To study how fast the bentonite in a GCL hydrates when in contact with another material, hydration tests have been performed on several GCL specimens.

Three tests have been performed where the water content of the bentonite is monitored over time. The first test involves placing Gundseal® in contact with moist fine sand and monitoring the water content of Gundseal® over time. This test is repeated for different water contents of the fine sand, and the results are shown in Figure 4.3. The second test is similar to the first test except that coarse sand was used instead of fine sand. The results of the second test are shown in Figure 4.4. The third test involves placing sealed "coupons" of Gundseal® in contact with moist sand and monitoring the water content of the sealed coupons over a long period of time. The "coupons" are 450-mm square sections of the GCL with a geomembrane placed over the bentonite portion of the GCL (Figure 4.5). The edges are sealed by welding along the edges. The variation of the water content of the bentonite within the sealed coupons is shown in Figure 4.6.

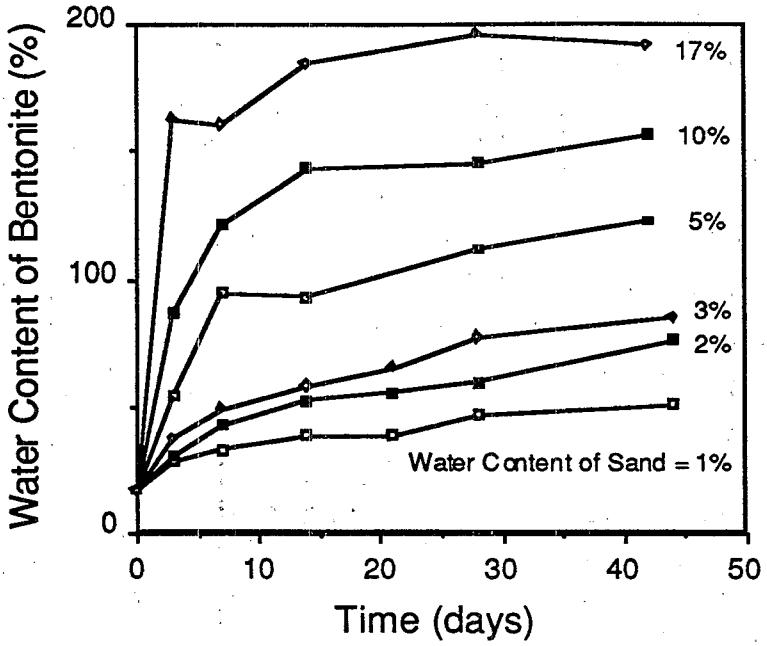

Figure 4.3 Rate of Wetting of Bentonite Component of Geomembrane-Supported GCL Placed in Contact with Fine Sand at Different Water Contents (from Daniel et al., 1993).

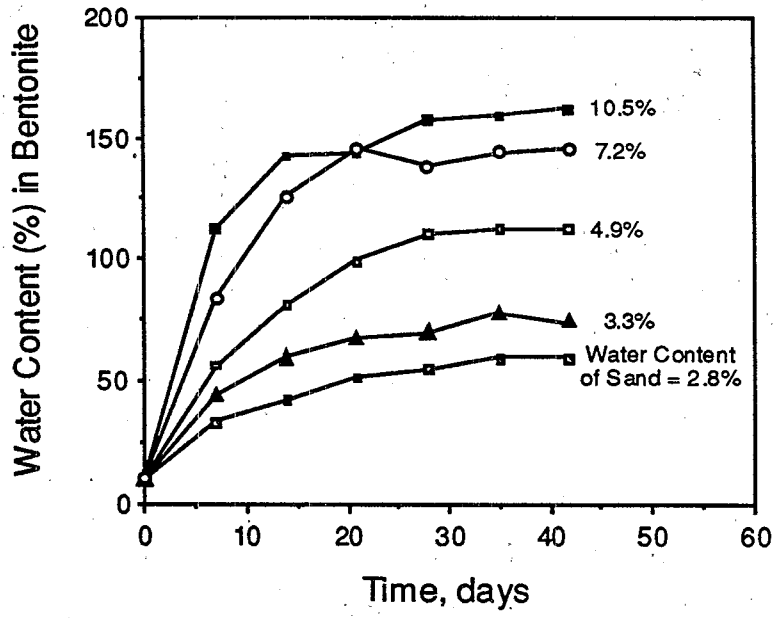

Figure 4.4 Rate of Wetting of Bentonite Component of Geomembrane-Supported GCL Placed in Contact with Coarse Sand at Different Water Contents (from Daniel et al., 1993).

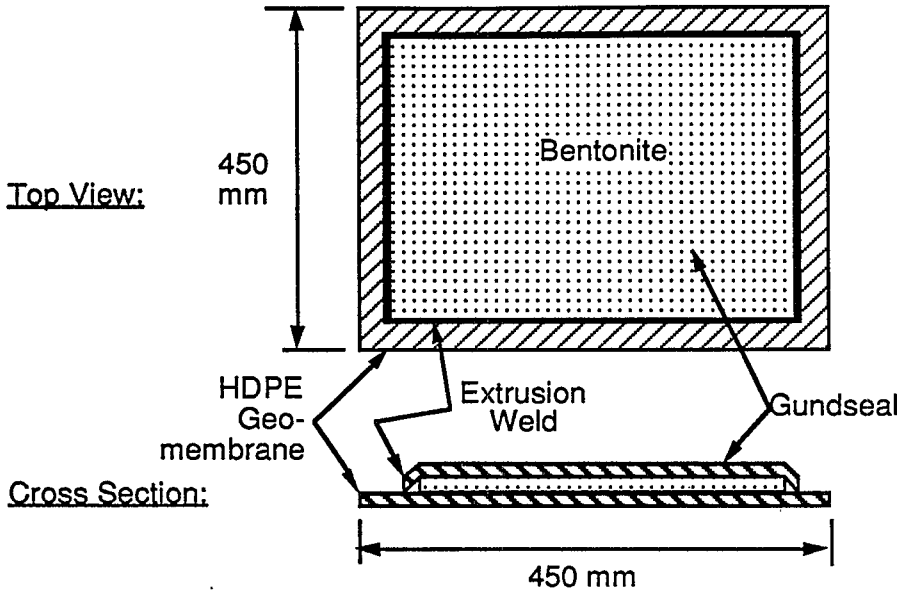

Figure 4.5 Bentonite Sealed between Two HDPE Sheets in "Coupons."

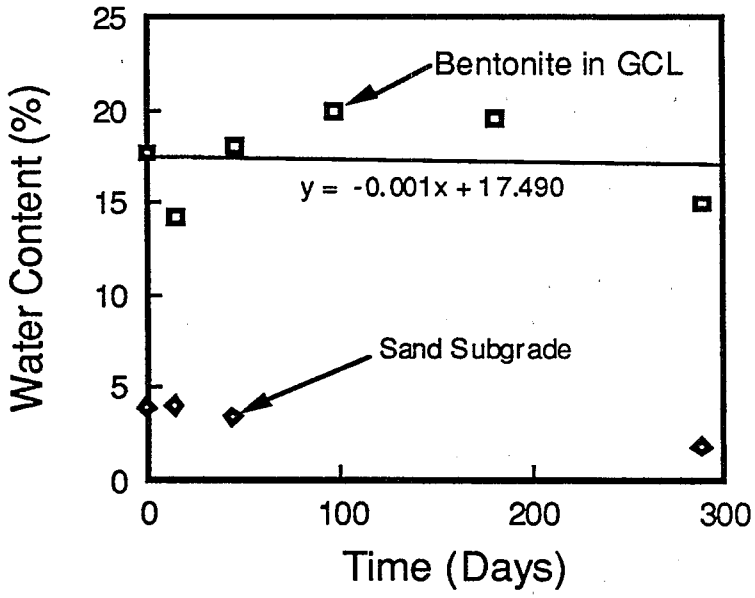

Figure 4.6 Results of Hydration Tests on Bentonite Sealed in Coupons.

The water content of the bentonite in the sealed coupons changed by less than 5 percentage points. The results indicate that vapor transmission is not significant, and that a GCL sandwiched between two geomembranes should not hydrate, unless there is a source of water such as water infiltration through a defect in the geomembrane.

4.3.3 Leachate Compatibility

Research has been conducted by Ruhl (1994) to study the effect of various permeant liquids on the hydraulic conductivity of GCLs. Seven permeant liquids were used in tests: simulated municipal solid waste (MSW) leachate, simulated hazardous waste (HW) leachate, actual MSW leachate, fly ash leachate, a strong acid (HCl), a strong base (NaOH), and tap water. Characteristics of the permeant liquids are listed in Table 4.4.

The GCLs were tested in a flexible-wall permeameter. In the initial phase of the testing program, some GCL specimens were hydrated with tap water prior to the introduction of the permeant liquid ("prehydrated" GCLs), while other GCL specimens were permeated directly with the chemical solution or leachate without any water hydration prior to permeation ("non-prehydrated" GCLs). Under field conditions, a GCL could be hydrated by water prior to contact with the chemical or leachate, e.g., by absorbing water from the adjacent soil. Alternatively, in other situations the first wetting liquid could be the chemical or leachate. Results from the initial tests that were performed for this study were consistent with findings reported by Daniel et al. (1993), who found that the critical (highest) hydraulic conductivity occurs when the GCL is not hydrated with water prior to permeation with chemicals. Therefore, in an effort to concentrate the research on the critical condition, attention was focused on testing non-prehydrated samples. However, when the dry GCLs were permeated directly with the chemical solutions or leachates, the permeant liquid typically flowed rapidly through the GCL, and dozens of pore volumes flowed through the test specimens in a few minutes or hours. The investigators were concerned that this was insufficient time for full reaction and swelling to occur in the bentonite. In response to this concern, a third condition of hydration was used in place of the "non-prehydrated" condition for the remainder of the testing program. For the third condition of hydration, GCLs were given an opportunity to "hydrate" with the specific permeant liquid for a 48 hour period of exposure prior to initiating the permeation process. The 48 hour "hydration" with permeant liquid was accomplished by introducing the permeant liquid directly into the dry GCL test specimen that was set up inside the permeameter, but closing the outflow valve from the permeameter for 48 hours to prevent permeation and to allow time for reactions to occur.

Table 4.5 summarizes the results of the tests. Further detail is provided by Ruhl (1994).

Table 4.4 Composition and Characteristics of the Permeant Liquids.

Permeant Liquid	Reason Liquid Was Used	Composition/Characteristics
Simulated Municipal Solid Waste (MSW) Leachate	Designed to represent an aggressive "worst case" MSW leachate, with a high concentration of calcium (which is a chemical known to increase the hydraulic conductivity of bentonite).	0.15 M acetic acid 0.15 M sodium acetate 0.007 M salicylic acid 1000 mg/L calcium pH = 4.4 (Based on the formulation for synthetic MSW leachate by Stanforth et al., 1979)
Simulated Hazardous Waste (HW) Leachate	Designed to represent an aggressive HW leachate with relatively high concentrations of organics in an aqueous-phase leachate.	4000 mg/L acetone 2000 mg/L benzoic acid 3000 mg/L phenol 1000 mg/L methyl chloride 100-200 mg/L cadmium (Formulation based on data published by Bramlett, 1987; McNabb et al., 1987; and Sai and Anderson, 1991)
Simulated Flyash Leachate	Designed to simulate leachate from Type C coal combustion fly ash.	Constituents not measured. pH = 11.5 - 12 (Leachate developed following procedure of Texas Water Commission, 1985)
Actual MSW leachate	Selected as a typical, real-world MSW leachate.	Key constituent concentrations are: 112 mg/L calcium 520 mg/L chloride 368 mg/L sodium 100 mg/L potassium 50 mg/L magnesium 4,340 mg/L sulfate 2.5 mg/L phenol 116 mg/L acetone 9 mg/L benzene 11 mg/L toluene 41 mg/L ethylbenzene 130 mg/L xylene 87 mg/L chlorobenzene 1,800 mg/L dissolved solids 60 mg/L suspended solids 687 mg/L COD 254 mg/L BOD (5-day) 312 mg/L total organic carbon pH = 7 (Obtained from a midwestern US municipal landfill, which had been in operation for several years)
Tap Water	Designed to comply with recommendations of ASTM D5084 for permeation with tap water.	Key constituent concentrations are: 18 mg/L calcium 54 mg/L chloride 15 mg/L magnesium 25 mg/L sodium
Hydrochloric Acid (HCl)	Designed to represent a strong, acidic leachate.	0.1 M solution of reagent grade HCl in distilled water; pH = 1
Sodium Hydroxide (NaOH)	Designed to represent a strong, basic leachate.	0.1 M solution of reagent grade NaOH in distilled water; pH = 13

Table 4.5 Summary of Results of Hydraulic Conductivity Tests with Different Permeant Liquids (from Ruhl, 1994).

Permeant Liquid	Condition of Hydration	Type of GCL	Hydraulic Conductivity (cm/s)	Pore Volumes of Flow	Final Water Content (%)	Final Thickness/Initial Thickness	Final pH of Effluent Liquid
Simulated MSW Leachate	Non-prehydrated	Bentofix	5E-05	6.2	94	1.24	4.6
		Claymax 200R	5E-06	5.9	80	1.17	4.4
		Contaminant Resisistant Gundseal	8E-06	17.2	82	1.44	4.4
		Regular Gundseal	2E-05	10.4	---	1.00	4.0
	Non-prehydrated/ 48 hour exposure	Bentofix	2E-06	9.9	98	1.18	4.5
		Bentomat	1E-07	8.4	---	1.44	4.5
		Claymax 200R	3E-08	10.6	---	1.18	4.6
		Contaminant Resisistant Gundseal	2E-05	9.7	74	1.14	4.6
		Regular Gundseal	4E-05	10.7	63	1.00	4.6
	Prehydrated	Contaminant Resisistant Gundseal	3E-10	3.0	131	2.09	8.9
		Regular Gundseal	2E-09	5.6	---	0.92	5.0
Simulated HW Leachate	Non-prehydrated	Contaminant Resisistant Gundseal	3E-10	8.8	150	1.43	8.9
		Regular Gundseal	2E-09	7.7	---	1.00	8.8
	Non-prehydrated/ 48 hour exposure	Bentofix	1E-09	3.2	147	1.00	9.0
		Bentomat	8E-10	2.2	146	1.26	8.4
		Claymax 200R	1E-08	7.4	128	1.23	8.0
	Prehydrated	Contaminant Resisistant Gundseal	8E-10	0.7	262	3.33	8.0
		Regular Gundseal	2E-09	4.7	---	1.23	7.7
Real MSW Leachate	Non-prehydrated/48 hour exposure	Bentofix	< 1E10-10	1.1	137	1.14	---
		Bentomat	2E-08	9.1	88	1.08	---
		Claymax 200R	7E-10	7.4	117	1.64	---
		Contaminant Resisistant Gundseal	6E-10	5.3	118	1.65	---
		Regular Gundseal	3E-10	5.6	108	1.34	---
HCl (pH = 1)	Non-prehydrated	Contaminant Resisistant Gundseal	5E-06	15.4	72	1.19	1.6
		Regular Gundseal	2E-07	4.0	---	1.00	1.0
	Prehydrated	Contaminant Resisistant Gundseal	2E-09	8.2	144	1.74	3.3
		Regular Gundseal	3E-10	2.5	---	1.02	8.6
NaOH (pH = 13)	Non-prehydrated	Contaminant Resisistant Gundseal	2E-06	21.7	76	1.00	12.9
		Regular Gundseal	1E-06	8.2	---	0.83	13.0
	Prehydrated	Contaminant Resisistant Gundseal	5E-10	4.8	243	2.19	10.0
		Regular Gundseal	1E-06	15.7	---	1.00	12.5

Table 4.5 Summary of Results of Tests with Different Permeant Liquids (Continued).

Permeant Liquid	Condition of Hydration	Type of GCL	Hydraulic Conductivity (cm/s)	Pore Volumes of Flow	Final Water Content (%)	Final Thickness/Initial Thickness	Final pH of Effluent Liquid
Tap Water	Non-prehydrated/48 hour exposure	Bentofix	7E-10	2.9	195	0.93	---
		Bentomat	9E-10	1.3	119	1.50	---
		Claymax 200R	1E-09	3.8	169	1.41	---
		Contaminant Resisistant Gundseal	1E-09	12.9	143	2.10	---
		Regular Gundseal	1E-09	12.2	116	1.79	---
Simulated Fly Ash Leachate	Non-prehydrated/48 hour exposure	Bentomat	6E-10	2.5	146	1.03	9.5
		Claymax 200R	2E-9	10.3	208	1.70	9.0
		Contaminant Resisistant Gundseal	2E-9	10.81	273	1.59	8.8
		Regular Gundseal	1E-9	15.3	147	1.43	8.9

The significant findings from the work may be summarized as follows:

1. The hydraulic conductivity to tap water was 3×10^{-10} to 2×10^{-9} cm/s, which is typical of other measurements that have been reported on GCLs.
2. The GCLs were permeated with a simulated MSW leachate that was rich in calcium (1,000 mg/L Ca^{+2}). When dry GCLs were permeated directly with the simulated MSW leachate, the hydraulic conductivity was typically 10^{-6} to 10^{-5} cm/s, which is about 4 orders magnitude higher than the hydraulic conductivity to water. Replacement of sodium by calcium is the obvious cause of the high hydraulic conductivity. The GCLs were much less permeable to the simulated MSW leachate when they were hydrated with water prior to permeation with leachate: the prehydrated GCLs had about the same hydraulic conductivity to leachate as to water.
3. Very different results were obtained when the GCLs were permeated with a real MSW leachate, which did not tend to increase the hydraulic conductivity of the GCLs. The real MSW leachate appeared to be less aggressive than the simulated MSW leachate because the real MSW leachate: (1) contained roughly equal amounts of monovalent and polyvalent cations; (2) contained suspended solids and microorganisms that tended to plug the pores of the bentonite; and (3) produced gases of decomposition that tended to block flow paths.
4. Permeation of dry GCLs with a strong acid or base resulted in high hydraulic conductivity (10^{-6} to 10^{-7} cm/s). In nearly all cases, prehydration with water, followed by permeation with the acid or base, resulted in hydraulic conductivities that were several orders of magnitude lower than the same GCLs that were directly permeated with the acid or base. Non-water-hydrated bentonite had no significant capacity to buffer the pH of the acid or base, but for pre-hydrated GCLs, about 15 pore volumes of flow were required before the pH of the effluent liquid became similar to that of the influent liquid.
5. When the GCLs were permeated with simulated hazardous waste leachate, the hydraulic conductivity was in the range of 10^{-9} to 10^{-10} cm/s (similar to and in some cases less than the values for tap water). The simulated hazardous waste leachate contained 10,000 mg/L of several organics, but this concentration was not high enough to significantly alter the dielectric constant of the simulated leachate and, hence, there was little impact on hydraulic conductivity.
6. Tests on simulated fly ash leachate showed little difference between the hydraulic conductivity to water and the hydraulic conductivity to the fly ash leachate.

7. In addition to these specific findings, several practical conclusions were reached that should be considered by engineers or scientists who are evaluating the potential for a chemical solution or waste liquid to increase the hydraulic conductivity of a GCL:
   A. Small concentrations or organic liquids do not appear to be damaging;
   B. Perhaps the most aggressive liquid is one that is free of suspended solids or microorganisms, but which contains a high concentration of multivalent cations such as Ca^{+2};
   C. Simulated and real leachates may react very differently with GCLs — whenever possible, real leachate should be used;
   D. The first wetting liquid (water or leachate) is a critical testing variable — the worst case is always direct exposure of a dry GCL to the chemical solution or waste liquid;
   E. The period of time that the GCL is exposed to the chemical solution or waste liquid prior to permeation can affect the test results significantly — laboratory tests should simulate field conditions as closely as possible;
   F. Laboratory tests, particularly on GCLs that have first been hydrated in water, may have to continue to a large number of pore volumes of flow (e.g., 15 for strong acids or bases) in order to achieve full breakthrough of key chemical constituents; and
   G. Not all contaminant-resistant bentonites are as resistant to attack as regular bentonites for certain chemicals — great care should be exercised when selecting a contaminant-resistant bentonite to make sure that it is resistant to the specific chemical solution or leachate that is of interest.

4.3.4 In-Plane Hydraulic Conductivity of a GCL

Testing has been performed to study the in-plane hydraulic conductivity and transmissivity of GCLs in contact with geomembranes (Amble, 1994). To study the in-plane hydraulic conductivity of a GCL, the GCL and geomembrane specimens were placed between two acrylic half cylinders. The geomembrane was bonded to the face of one acrylic half cylinder. The GCL and acrylic half-cylinders were oriented vertically in a flexible wall permeameter. Therefore permeation of the GCL took place through the plane of the bentonite. In tests with GCLs having geotextiles on both sides, one or both geotextiles were smeared with a thin layer of bentonite. This was to study the effects that each geotextile had on the in-plane hydraulic conductivity of the GCL.

Hydraulic conductivity tests were performed on Bentomat® Regular, Bentomat® HS (a product with adhesive added to one of the geotextiles to bond the needlepunched fibers to the geotextile), Bentofix® (the version with a woven geotextile on one side and a nonwoven geotextile on the other side), Claymax® 200R, Claymax® 500SP, Gundseal® with contaminant-resistant bentonite, regular Gundseal®, and Gundseal® with a very light-weight fabric backing on the bentonite. In some cases bentonite was placed on one or both of the geotextiles of the GCL. Some of the GCLs have different geotextiles on either side of the GCL. Side A of a GCL denotes the woven geotextile while side B denotes the nonwoven geotextile of the GCL. For Claymax® 500SP only, side A indicates the cream-colored woven geotextile while side B indicates the gray woven geotextile.

Results are provided by Amble (1994). It was generally found that the presence of a geotextile increased the in-plane transmissivity of a GCL, and that the transmissivity decreased with increasing confining stress. Table 4.6 summarizes the results and compares the findings with those published by Harpur, Wilson-Fahmy, and Koerner (1993).

In general, geotextile-encased GCLs with bentonite smeared on the woven geotextile (side A) had a higher in-plane transmissivity than when bentonite was smeared on the nonwoven geotextile (side B). In other words, the nonwoven geotextile (side B) is more transmissive than the woven geotextile (side A). Exceptions include regular Bentomat® and Bentomat® HS, where side A was more transmissive than side B. The cream-colored, woven geotextile (side A) in Claymax® 500SP appeared to be slightly more transmissive than the gray, woven geotextile (side B).

The three different samples of Gundseal® were found to have in-plane transmissivities that varied by less than one order of magnitude. The lowest hydraulic conductivity was found for the sample of Gundseal® with a light-weight fabric, indicating that the fabric component of this GCL does not significantly affect its in-plane transmissivity. Amble (1994) provides further detail.

Samples of Gundseal® typically had lower in-plane transmissivities than the geotextile-encased GCL samples. In some cases, the differences were almost insignificant. However, in other cases, the differences were as large as four orders of magnitude, indicating that the geotextiles formed flow paths.

Table 4.6 Comparison of Transmissivity Values Found in the Study by Harpur, Wilson-Fahmy, and Koerner (1993) and the In-Plane Hydraulic Conductivity Tests.

Description of GCL	Transmissivity (m^2/s) at a compressive stress of 69 kPa (from Harpur, Wilson-Fahmy, and Koerner, 1993)	Transmissivity (m^2/s) at a compressive stress of 69 kPa (from Amble, 1994)
Bentofix® with bentonite on Side A (leaving the nonwoven geotextile to provide most of the in-plane transmissivity) (GCL "E" from Harpur et al.)	$8x10^{-11}$	$4x10^{-9}$
Bentofix® with bentonite on Side B (leaving the woven geotextile to provide most of the in-plane transmissivity) (GCL "B" from Harpur et al.)	$9x10^{-12}$	$2x10^{-11}$
Bentomat® with bentonite on Side B (leaving the woven geotextile to provide most of the in-plane transmissivity) (GCL "D")	$1x10^{-10}$	$3x10^{-9}$
Claymax® 200R with bentonite on Side A (leaving the woven geotextile on the other side to provide most of the in-plane transmissivity) (GCL "C")	$6x10^{-12}$	$1x10^{-11}$
Gundseal® (GCL "A")	$3x10^{-12}$	$2x10^{-12}$

4.3.5 Differential Settlement

Research has been performed at the University of Texas to study the effect of differential settlement on the hydraulic conductivity of GCLs. More information about differential settlements of GCLs is provided by LaGatta (1992). In the research, large sections of GCL were bolted to a frame that was fitted to the inside of tanks measuring 2.4 m in length, 1.2 m in width, and 0.9 m in height (Figure 4.7). The sections of GCL were placed over a large water-filled bladder (Figure 4.8). The GCLs were buried beneath 600 mm of gravel, and a head of water of 300 mm above the top of the GCL was maintained. The deformations were created by slowly deflating the bladder. The GCLs were tested with and without an overlap.

Four GCLs were tested. Bentomat® was tested with the nonwoven geotextile facing downward. Gundseal® was tested with the geomembrane portion of the GCL facing upward. Two versions of Claymax were tested: the original version of Claymax® and Claymax® 500SP. In the cases where overlaps were tested, the overlaps were created 225 mm wide.

The GCLs were subjected to differential settlement in either a dry or saturated state. The water-filled bladder was deflated in four stages for GCLs that were initially hydrated with water, and in one stage for GCLs that were deformed in a dry state. Differential settlement may be characterized by the distortion, D/L, which is defined as the settlement, D, over a horizontal distance, L (Figure 4.9). The average tensile strain caused by distortion can be computed by integrating over the deflected shape to determine the arc length of the deformed section from simple mechanics. If tensile strains are large enough, the GCL may crack and undergo an increase in hydraulic conductivity.

Outflow was collected from a line leading out from the base of the tank. Hydraulic conductivity was calculated using Darcy's law. The thicknesses of the GCLs were determined from separate tests performed in the laboratory using the appropriate vertical compressive stress. The hydraulic gradient ranged from 20 to 30. Typical test lengths were about 4 months each.

The results of the tests are summarized in Table 4.7. Most of the GCLs maintained a hydraulic conductivity $\leq 1 \times 10^{-7}$ cm/s (a common regulatory limit) while subjected to a tensile strain of 1% to 10% or more, depending on the material and conditions of testing. Some GCLs were able to bridge over the underlying subsidence because of the tensile strength of the geosynthetics of the GCL. Overlapped and non-overlapped materials performed about the same mostly due to the swelling and self-healing capability of the bentonite. Further information is provided by LaGatta (1992) and Boardman (1993).

In general, GCLs can undergo large settlements without experiencing a significant increase in hydraulic conductivity. It appears that GCLs can withstand more differential settlement than compacted clay, but less than very flexible geomembranes.

Table 4.7 Results of Settlement Tests on Geosynthetic Clay Liners.

Type of GCL	Specimen	Hydrated Prior to Settlement?	Settlement Increment	Differential Settlement (Δ, mm)	Δ/L	Tensile Strain (%)	Hydraulic Conductivity (cm/s)		
							Minimum	Maximum	Final
Bentomat® (Intact)	1	Yes	0	0	0	0	6×10^{-10}	1×10^{-8}	7×10^{-10}
			1	19	0.084	0.4	7×10^{-10}	7×10^{-9}	7×10^{-9}
			2	46	0.204	2.1	3×10^{-9}	7×10^{-9}	3×10^{-9}
			3	61	0.271	3.6	2×10^{-9}	9×10^{-9}	3×10^{-9}
			4	74	0.325	5.0	1×10^{-9}	8×10^{-9}	5×10^{-9}
	2	Yes	0	0	0	0	1×10^{-10}	2×10^{-9}	1×10^{-9}
			1	17	0.076	0.3	8×10^{-10}	2×10^{-9}	2×10^{-9}
			2	40	0.178	1.6	1×10^{-9}	2×10^{-9}	1×10^{-9}
			3	84	0.347	6.0	8×10^{-10}	1×10^{-9}	8×10^{-10}
	3	No	1	75	0.333	5.4	6×10^{-10}	3×10^{-9}	3×10^{-9}
Bentomat® (Overlapped)	1	Yes	0	0	0	0	2×10^{-9}	4×10^{-9}	3×10^{-9}
			1	17	0.076	0.3	1×10^{-9}	3×10^{-9}	2×10^{-9}
			2	43	0.191	1.8	8×10^{-10}	5×10^{-9}	1×10^{-9}
			3	81	0.360	6.2	2×10^{-9}	3×10^{-9}	2×10^{-9}
			4	86	0.504	12.0	9×10^{-10}	6×10^{-9}	2×10^{-9}
	2	Yes	0	0	0	0	2×10^{-10}	8×10^{-10}	3×10^{-10}
			1	8	0.037	0.1	4×10^{-10}	8×10^{-10}	7×10^{-10}
			2	30	0.133	0.9	6×10^{-10}	8×10^{-10}	8×10^{-10}
			3	86	0.383	7.1	8×10^{-10}	7×10^{-7}	2×10^{-9}
			4	110	0.573	15.0	2×10^{-9}	2×10^{-5}	3×10^{-7}
	3	No	0	75	0.333	5.4	2×10^{-8}	2×10^{-6}	7×10^{-8}

Table 4.7 Results of Settlement Tests on Geosynthetic Clay Liners. (Continued - Page 2)

Type of GCL	Specimen	Hydrated Prior to Settlement?	Settlement Increment	Differential Settlement (Δ, mm)	Δ/L	Tensile Strain (%)	Hydraulic Conductivity (cm/s)		
							Minimum	Maximum	Final
Discontinued Claymax® (Intact)	1	Yes	0	0	0	0	4×10^{-9}	7×10^{-9}	5×10^{-9}
			1	16	0.071	0.3	4×10^{-9}	9×10^{-9}	9×10^{-9}
			2	25	0.111	0.6	2×10^{-8}	8×10^{-7}	2×10^{-8}
			3	69	0.391	9.1	3×10^{-7}	1×10^{-5}	3×10^{-7}
	2	Yes	0	0	0	0	2×10^{-9}	1×10^{-8}	1×10^{-8}
			1	10	0.131	0.8	1×10^{-8}	2×10^{-5}	2×10^{-6}
	3	No	1	75	0.333	5.4	8×10^{-8}	2×10^{-4}	3×10^{-6}
Claymax 500®SP (Intact)	1	Yes	0	0	0	0	8×10^{-10}	3×10^{-9}	3×10^{-9}
			1	16	0.067	0.3	4×10^{-9}	7×10^{-9}	6×10^{-9}
			2	31	0.133	0.9	1×10^{-7}	2×10^{-6}	3×10^{-7}
			3	46	0.204	2.1	5×10^{-8}	6×10^{-7}	6×10^{-8}
			4	84	0.373	6.7	9×10^{-7}	2×10^{-5}	2×10^{-5}
	2	No	1	75	0.333	5.4	4×10^{-10}	9×10^{-9}	7×10^{-9}
Discontinued Claymax® (Overlapped)	1	Yes	0	0	0	0	6×10^{-9}	9×10^{-9}	9×10^{-9}
			1	12	0.053	0.1	8×10^{-9}	9×10^{-9}	9×10^{-9}
			2	22	0.200	2.0	9×10^{-9}	4×10^{-5}	1×10^{-5}
	2	Yes	0	0	0	0	4×10^{-9}	1×10^{-8}	7×10^{-9}
			1	11	0.049	0.1	2×10^{-9}	1×10^{-8}	1×10^{-8}
			2	22	0.179	1.6	8×10^{-9}	3×10^{-6}	6×10^{-7}
	3	No	1	75	0.333	5.4	2×10^{-8}	3×10^{-8}	2×10^{-8}

Table 4.7 Results of Settlement Tests on Geosynthetic Clay Liners. (Continued - Page 3)

Type of GCL	Specimen	Hydrated Prior to Settlement?	Settlement Increment	Differential Settlement (Δ, mm)	Δ/L	Tensile Strain (%)	Hydraulic Conductivity (cm/s)		
							Minimum	Maximum	Final
Claymax 500®SP (Overlapped)	1	Yes	0	0	0	0	2×10^{-9}	4×10^{-9}	3×10^{-9}
			1	14	0.067	0.2	4×10^{-9}	9×10^{-9}	5×10^{-9}
			2	30	0.133	0.9	1×10^{-7}	2×10^{-6}	2×10^{-7}
			3	45	0.204	2.1	1×10^{-8}	3×10^{-7}	2×10^{-8}
			4	119	0.528	13.1	9×10^{-7}	3×10^{-6}	2×10^{-6}
	2	No	1	75	0.333	5.4	5×10^{-9}	1×10^{-8}	9×10^{-9}
Gundseal® (Intact)	1	Yes	4	54	0.266	3.5	No Flow	No Flow	No Flow
Gundseal® (Overlapped)	1	Yes	4	124	0.813	29	No Flow	No Flow	No Flow
	2	No	1	75	0.333	5.4	9×10^{-11}	3×10^{-9}	3×10^{-10}

4.3.6 Desiccation Tests

Research has been performed by Boardman (1993) to study the effect of cyclic wetting and drying on the hydraulic conductivity of GCLs. Three GCLs were tested: Bentomat®, Gundseal®, and Claymax®. Large sections of each type of GCL were bolted to a frame (preventing contraction) that was fitted to the inside of tanks measuring 2.4 m in length, 1.2 m in width, and 0.9 m in height. The overburden soil was 0.6-m thick. As indicated in Figure 4.10, eight PVC pipes were installed vertically above the GCL; six of the pipes were used for the injection of hot air, while two were used for extraction of air. A water head of 300 mm was maintained throughout the permeation portion of the tests. The GCLs were not subjected to multiple stresses (e.g., differential settlement and desiccation).

The GCL was first allowed to hydrate, then water was drained out of the tank. The heating system was turned on and the GCL was dried for 2 to 3 weeks. The GCL became cracked and desiccated. The GCL was then rehydrated by applying water to the surface of the GCL at a rate of 40 mm per hour. When outflow through the GCL sample stopped after the initial rehydration, the water head was raised in increments of 100 mm to 300 mm over several days. The tests were carried out until steady-state flow was reached.

The variation of hydraulic conductivity with time for a typical GCL is shown in Figure 4.11. The geotextile-encased GCLs (Bentomat® and Claymax® 200R) swelled and self-sealed upon re-hydration, after one cycle of wetting and drying. When the desiccated GCLs were re-hydrated, water initially flowed rapidly through most of the desiccated samples, but the bentonite quickly expanded and the hydraulic conductivity decreased as the cracked bentonite began to adsorb water and swell. The long term, steady value of hydraulic conductivity was essentially the same before and after the desiccation cycle. In tests performed on a GCL containing bentonite attached to a geomembrane (Gundseal®), there was no outflow of water either before or after the wetting and drying cycle. Due to the presence of the geomembrane, very little of the GCL actually became hydrated, but the bentonite in the overlapped area did self seal. The initial hydraulic conductivity after rehydration was high. If the GCLs are slowly wetted, unlike the tests where 40 mm of water was added to the surface of the GCL per hour, the GCL would have time to adsorb water and to swell without allowing seepage through the GCL.

4.3.7 Freeze Thaw

Research has been performed by Hewitt (1994) to study the effect of freeze-thaw on the hydraulic conductivity of GCLs. The tests were performed using the same tanks described earlier. The GCLs were covered with 25 mm of gravel, and a cooling manifold was placed on the gravel. Figures 4.12, 4.13, and 4.14 show the testing equipment and set-up.

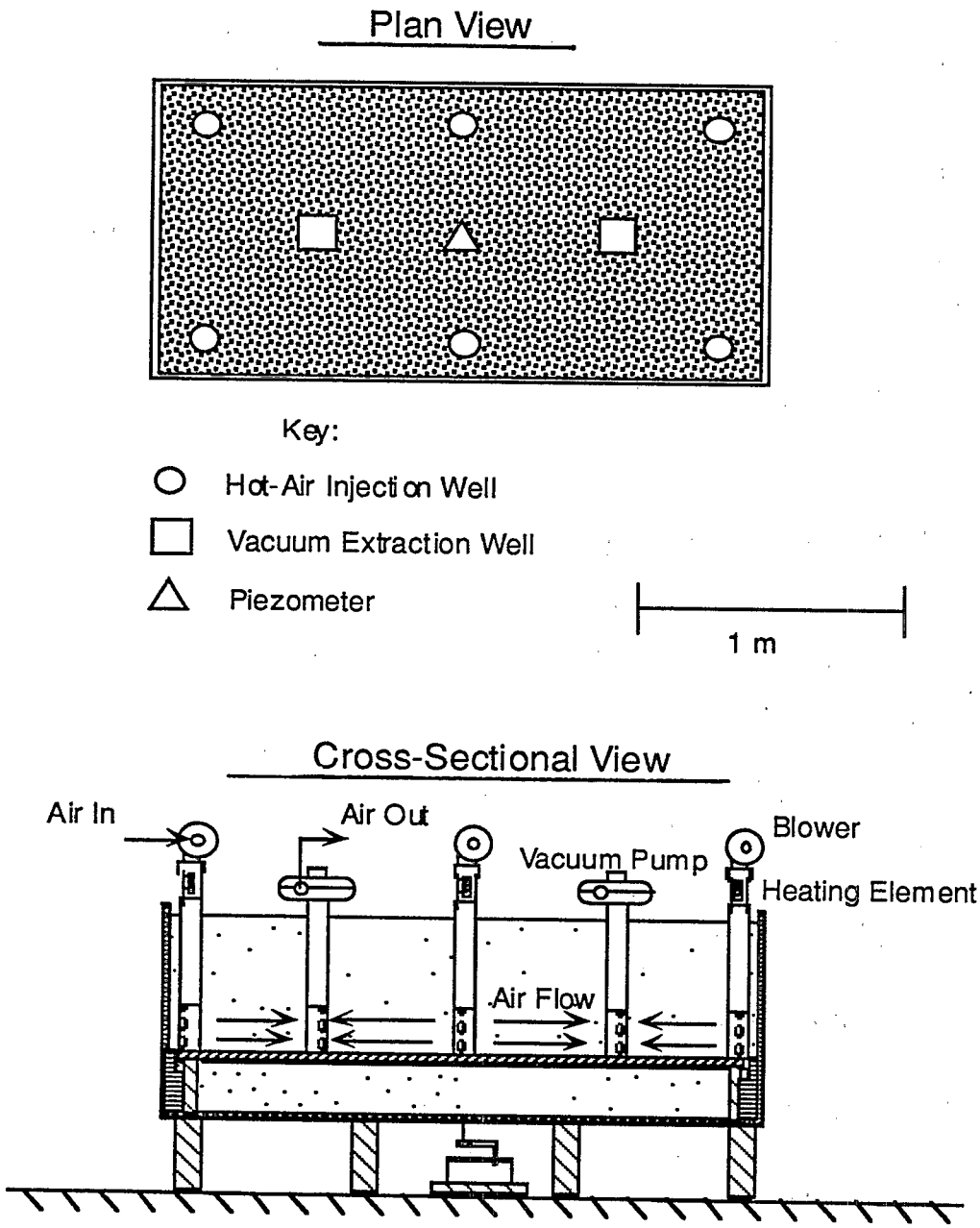

Figure 4.10 Tanks Used to Study Desiccation of GCLs (from Boardman, 1993).

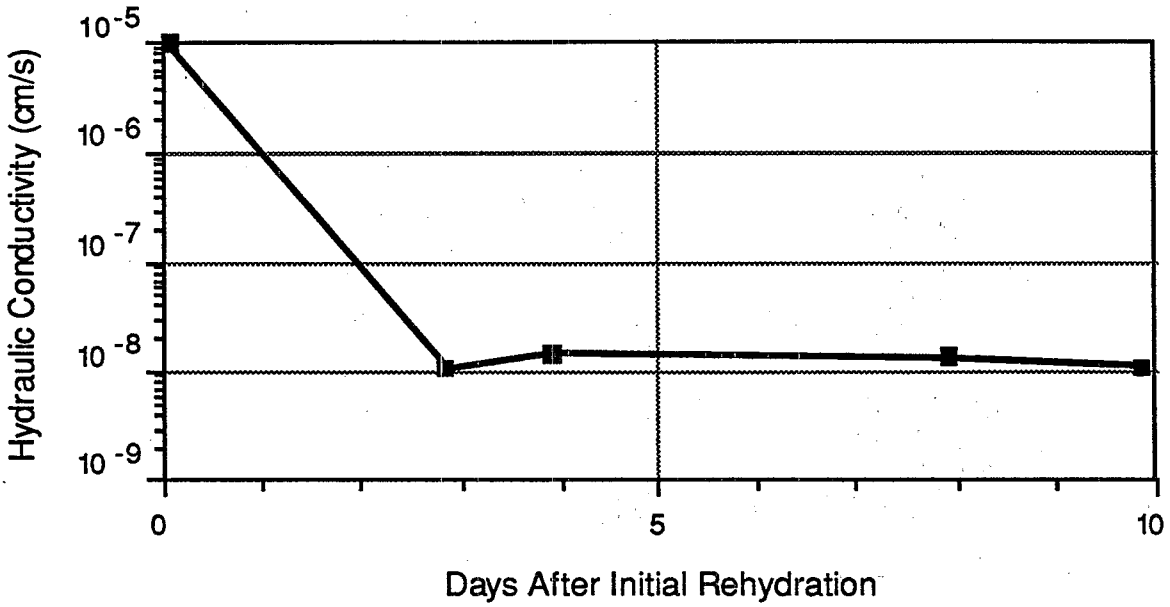

Figure 4.11 Typical Results after Desiccated GCLs Were Permeated (from Boardman, 1993).

The GCLs were allowed to hydrate with a water level in the tank of 300 mm. When the flow of water through the GCLs became steady, the water depth was lowered to 25 to 50 mm. The GCLs were then frozen by circulating chilled fluid at -17° C through the cooling manifold. Thermisters installed above and below the GCL in the gravel were used to monitor temperature. The GCLs were chilled until the thermisters registered less than -1° C. This usually took 4 to 5 days. The fluid circulation was stopped, and the GCL was allowed to thaw under ambient conditions. Thawing of the GCLs to 10° C usually took 3 to 4 days. Each GCL sample was subjected to three cycles of freeze-thaw.

Flexible wall hydraulic conductivity tests were performed on each type of GCL to determine the hydraulic conductivity. The hydraulic conductivity of the GCLs (in the large tanks) after three freeze-thaw cycles can then be compared to the flexible wall hydraulic conductivity. The tests performed in the large tanks are called bench-scale tests. Results from the bench-scale and flexible wall tests are presented in Table 4.8.

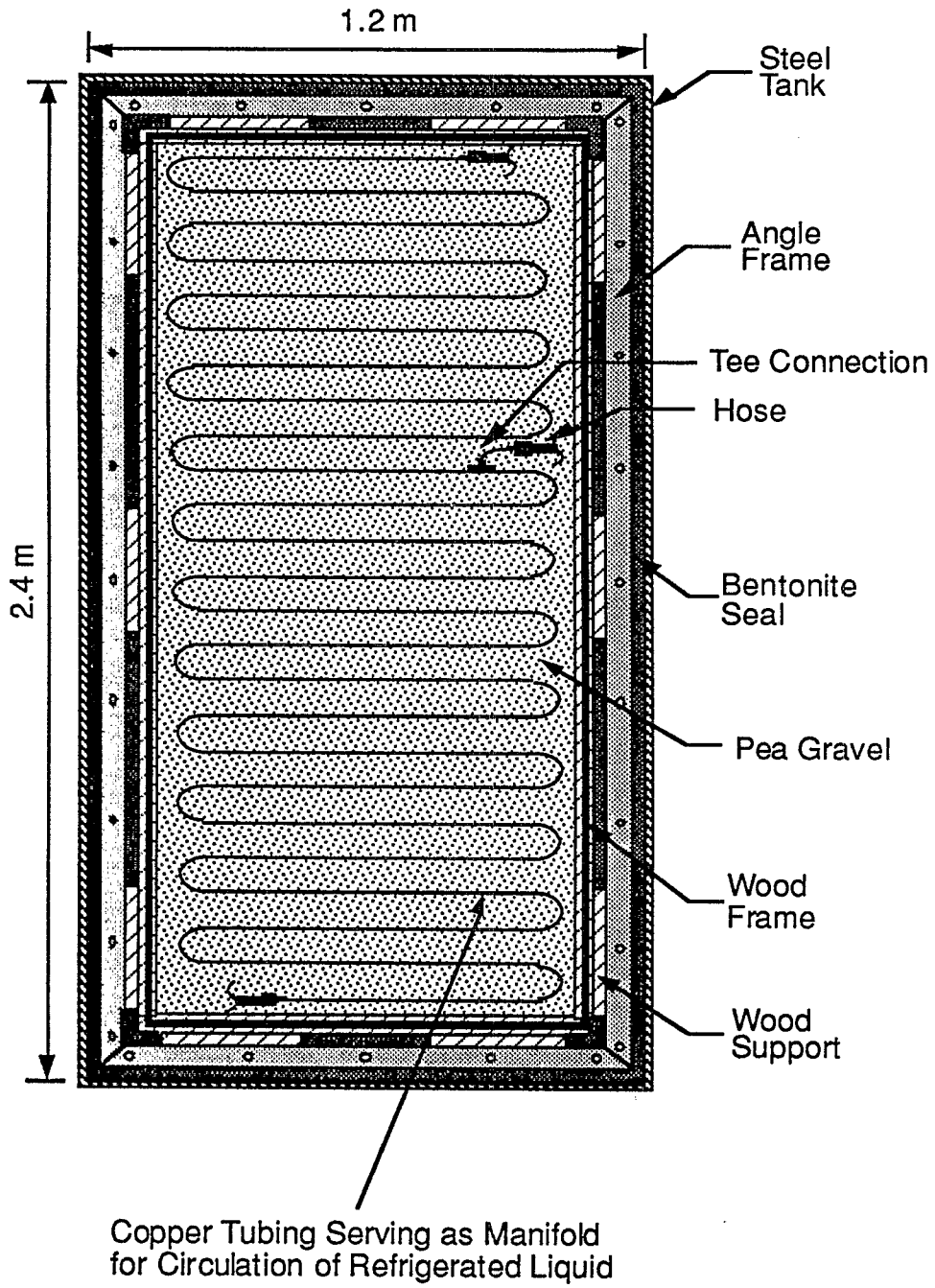

Figure 4.12 Plan View of Cooling Coil Used for Freeze-Thaw Tests (from Hewitt, 1994).

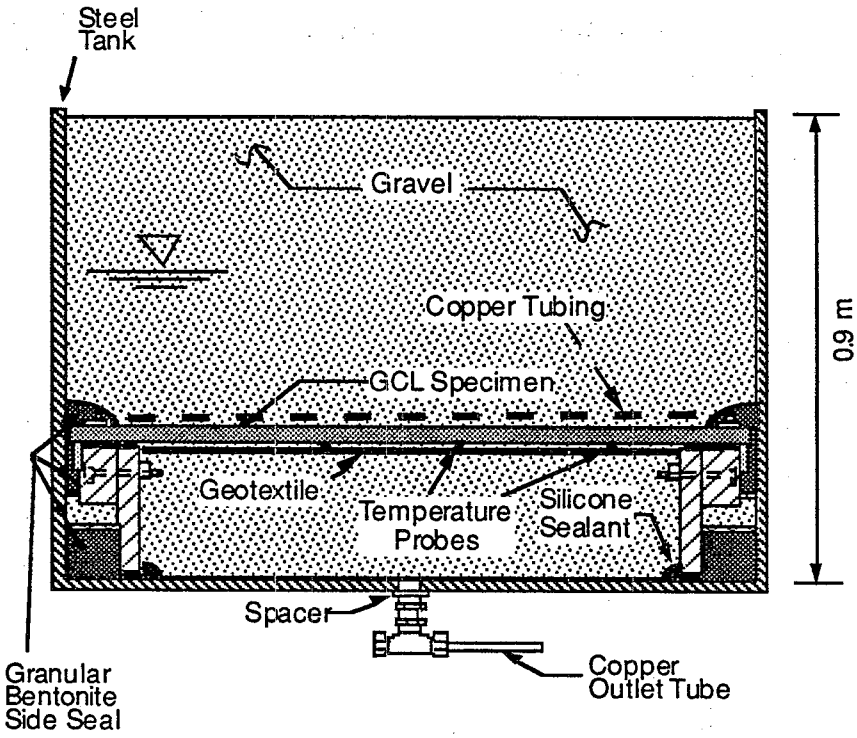

Figure 4.13 Cross Section of Tank Used for Freeze-Thaw Tests (from Hewitt, 1994).

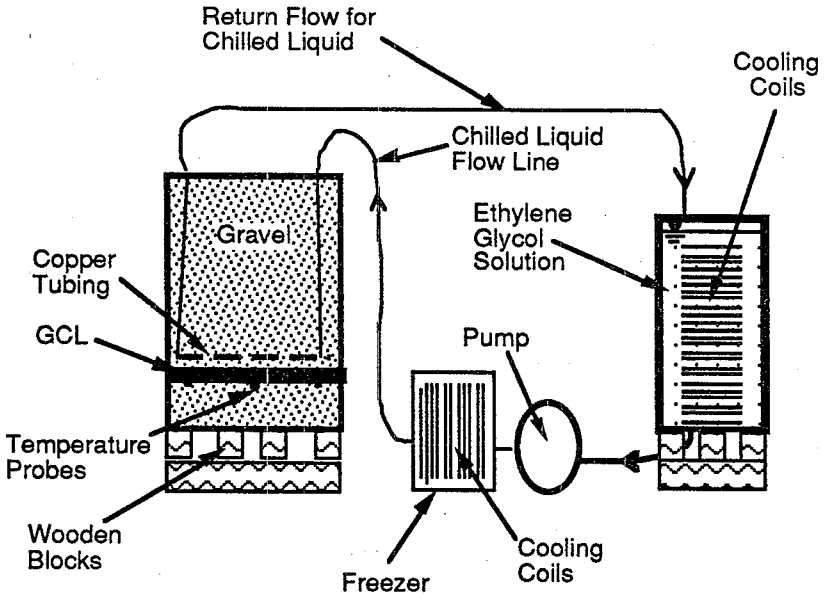

Figure 4.14 Cross Section of Tank Used for Freeze-Thaw Tests (from Hewitt, 1994).

Table 4.8 Summary of Experimental Results for 0, 1, and 3 Freeze-thaw Cycles.

GCL	Type of Test	$\overline{\sigma}$ (kPa)	Hydraulic Conductivity (cm/s)		
			0 Freeze-Thaw Cycles	1 Freeze-Thaw Cycle	3 Freeze-Thaw Cycles
Geotextile-Encased, Needle-Punched GCL	Bench-scale (Intact)	7.6	2×10^{-9}	3×10^{-9}	2×10^{-9}
	Bench-scale (Overlap)	7.6	4×10^{-9}	7×10^{-9}	3×10^{-9}
	Flexible-wall	12.4	2×10^{-9}	3×10^{-9}	3×10^{-9}
Geotextile-Encased, Stitch-Bonded GCL	Bench-scale (Intact)	7.6	3×10^{-9}	5×10^{-9}	7×10^{-9}
	Bench-scale (Overlap)	7.6	1×10^{-8}	1×10^{-5}	7×10^{-6}
	Flexible-wall (No Stitching)	10.3	2×10^{-9}	4×10^{-10}	3×10^{-9}
	Flexible-wall (With Stitching)	10.3	2×10^{-9}	2×10^{-9}	2×10^{-9}
Geomembrane-Supported GCL	Bench-scale (Overlap)	7.6	No flow(*)	-	No Flow(**)
	Flexible-wall (Bentonite Only)	12.4	3×10^{-9}	2×10^{-9}	2×10^{-9}

Note: $\overline{\sigma}$ = effective stress (kPa)
- Not available
(*) No flow occurred during 25 days of permeation
(**) No flow occurred during 52 days of permeation

It is concluded that under the conditions of these tests, most GCLs (intact and overlapped panels) can withstand at least 3 freeze-thaw cycles without undergoing a significant increase in hydraulic conductivity. However, the tests were performed under carefully controlled conditions in laboratory devices at a compressive stress of about 8 kPa. The GCLs were only subjected to 3 freeze-thaw cycles, and the conditions of freeze-thaw were not superimposed with other environmental stresses (e.g., differential settlement and desiccation). Ultimately, field data are needed to understand how GCLs perform in the field.

4.4 Effect of Freeze-Thaw in the Laboratory and Field

The University of Wisconsin studied the effect of freeze-thaw on GCLs at laboratory and field scale. Three GCLs were studied in the laboratory portion of the research: Claymax® 200R, Bentomat® CS, and Bentofix®. Three GCLs were used in the field portion of the research: Claymax® 500SP, Bentomat® CS, and Gundseal® (results of Gundseal® are discussed in Erickson et al., 1994).

In the laboratory tests, GCL specimens with a diameter of 150 mm were placed in flexible-wall permeameters for saturation and hydraulic conductivity measurement (GRI test method GCL-2 with an average effective stress of 14 kPa and hydraulic gradient of 75). After permeation the specimens were removed from the permeameters and sealed in plastic freezer bags to prevent desiccation and placed in a freezer. After freezing, the specimens were removed and allowed to thaw at room temperature. If the specimen was to be permeated after thawing, the specimen was placed in the permeameter and then allowed to thaw. The hydraulic conductivity of each specimen was measured after 1, 3, 5, and 20 freeze-thaw cycles.

The field scale tests were performed first in lagoons. The lagoons were 8 m wide by 10 m long by 0.6 m deep. One lagoon was built for each type of GCL in 1992. The GCL was placed in the lagoon and overlain by 0.25 m of gravel. A sump was used to measure outflow, and thermisters were used to determine when the GCLs froze. The GCLs in the lagoons were exposed to two freeze-thaw cycles (two winters of exposure with one freeze-thaw cycle per winter). The field tests in lagoons developed problems with the seepage collection and measurement system, and the tests within the lagoons were abandoned.

Smaller specimens (1 m x 1 m) were cut from the GCLs in the abandoned lagoon field tests. Even smaller specimens were cut from the 1 m x 1 m sections and placed in flexible wall permeameters for evaluation of hydraulic conductivity. In these tests, sidewall leakage tended to be a problem and resulted in high measured flow rates.

Another field test was then constructed in 1993. Each type of GCL was placed in three separate pans, 1 larger pan (1.34 m x 1.34 m) and 2 smaller pans (0.84 m x 0.84 m). The large pans were constructed on welded HDPE, and the small pans were constructed on molded HDPE. Thermisters were placed below the GCLs and were used to determine when freezing had taken place. Gravel was placed over the GCL specimens. The large pans and one of the smaller pans contained GCLs seamed per manufacturers' specifications. The second smaller pan in each group contained a seamless GCL specimen. The GCLs in the pan field tests were allowed to hydrate under 30 mm of water for one week. The water level was then raised to 250 mm, and the GCLs were allowed to hydrate for one month. Tests were performed with the water level at 250

mm. The hydraulic gradient ranged from 5 to 15 and averaged 10. Measurements of hydraulic conductivity were made by measuring outflow, and the hydraulic conductivity was measured before winter up to December 1993 and after winter starting April, 1993.

The laboratory freeze-thaw tests were performed on GCL specimens that were permeated to a steady-state hydraulic conductivity. The results are listed in Table 4.9. All initial hydraulic conductivities are less than 4.9×10^{-9} cm/s and all of the final hydraulic conductivities are less than 3.3×10^{-9} m/s. The k_{20}/k_0 ratio is equal to the ratio of the hydraulic conductivity after exposure to twenty freeze-thaw cycles to the initial hydraulic conductivity. All but one specimen had a k_{20}/k_0 ratio less than one, and the one value that is greater than one is only slightly greater (1.1). A t-test confirmed that the decrease in hydraulic conductivity is statistically significant.

Table 4.9 Results of Laboratory Freeze-Thaw Tests (n = Number of Freeze-Thaw Cycles).

Sample Number	Initial Hydraulic. Conductivity $k_0 \times 10^{-9}$ (cm/s)	Hydraulic Conductivity after n Freeze-Thaw Cycles, $k_n \times 10^{-9}$ (cm/s)				
		k_1	k_3	k_5	k_{20}	k_{20}/k_0
Bentofix®-1	2.9	3.0	2.8	NP	3.2	1.10
Bentofix®-2	4.9	1.6	2.3	2.7	2.2	0.45
Bentofix®-3	5.6	1.7	3.5	3.6	2.5	0.45
Bentomat®-1	3.1	2.9	2.8	1.3	1.7	0.55
Bentomat®-2	3.1	1.7	2.4	2.5	1.9	0.61
Bentomat®-3	2.9	1.8	1.4	1.5	1.9	0.66
Claymax®-1	3.8	2.9	4.8	4.2	3.4	0.89
Claymax®-2	2.9	2.4	2.7	3.6	2.1	0.72
Claymax®-3	4.2	3.5	3.4	3.2	2.4	0.57
Claymax®-4	4.9	4.1	3.2	4.4	3.3	0.67

note: NP = not performed

The field freeze-thaw tests were performed in nine test pans with three pans per GCL type. The three pans for each type of GCL included one large pan and two smaller pans. The results of the field tests are listed in Table 4.10. The results for Gundseal® are reported by Erickson et al. (1994). There was essentially no increase in hydraulic conductivity for four of the

six Bentomat® and Claymax® specimens. One specimen had no seepage before winter so no comparison could be made between the before- and after-winter hydraulic conductivities. The large, overlapped Claymax specimen exhibited an increase in hydraulic conductivity by a factor of 25 after exposure to one winter (one freeze-thaw cycle).

Table 4.10 Results from the Field Freeze-Thaw Tests in Pans.

Specimen	Seam?	Before-Winter Hydraulic Conductivity (cm/s)	After-Winter Hydraulic Conductivity (cm/s)	Ratio of Value After Freeze-thaw to Value Before Freeze Thaw
Bentomat®, 1.8 m^2	Yes	1.5×10^{-8}	1.9×10^{-8}	1.3
Bentomat®, 0.7 m^2	Yes	1.0×10^{-8}	1.4×10^{-8}	1.4
Bentomat®, 0.7 m^2	No	no outflow	1.0×10^{-8}	-
Claymax®, 1.8 m^2	Yes	2.8×10^{-8}	7.0×10^{-8}	25.0
Claymax®, 0.7 m^2	Yes	2.0×10^{-8}	3.0×10^{-8}	1.5
Claymax®, 0.7 m^2	No	2.4×10^{-8}	2.8×10^{-8}	1.2

Laboratory hydraulic conductivity tests were performed on specimens taken from the field, where the GCLs had been subjected to two freeze-thaw cycles. The results from the hydraulic conductivity tests are summarized in Table 4.11. Low hydraulic conductivities were measured for two 0.45 m diameter Claymax® specimens. Sidewall leakage occurred in two 0.45 diameter Bentomat® specimens. The Bentomat specimens were retrimmed to a diameter of 0.30 m and retested. One Bentomat specimen had a low hydraulic conductivity. The other continued to exhibit sidewall leakage and was not tested.

Table 4.11 Hydraulic Conductivities of Large Specimens Removed from Lagoons.

Specimen	Diameter (m)	Hydraulic Conductivity (cm/s)
Bentomat®	0.30	not measured*
Bentomat®	0.30	1.7×10^{-8}
Claymax®	0.45	3.5×10^{-8}
Claymax®	0.45	6.3×10^{-8}

The laboratory and field freeze-thaw tests produced similar results. Freeze-thaw had essentially no effect on the hydraulic conductivity of the GCLs. The only exception was the large, overlapped Claymax® GCL tested in the field in a test pan. The hydraulic conductivity of the overlapped Claymax® specimen was significantly more permeable after winter. The other overlapped Claymax® specimen did not exhibit an increase in hydraulic conductivity. The hydraulic conductivities of laboratory specimens exposed to freeze-thaw were approximately one order of magnitude lower than the hydraulic conductivities of the field specimens exposed to winter weather. This may be a result of testing conditions (higher effective stresses and hydraulic gradients used in the laboratory).

The structure of the frozen and thawed GCL specimens was examined. Vertical and horizontal sections were cut through the frozen GCL specimens. Small, randomly oriented lenses of segregated ice were observed in both sections. The thawed specimens revealed no cracking commonly seen in compacted clays exposed to freeze-thaw. The structure of the thawed specimens appeared similar to the hydrated specimens that had not been exposed to freeze-thaw. The specimens removed from the lagoons were also devoid of cracks induced by freeze-thaw.

CHAPTER 5
MANUFACTURE AND DEPLOYMENT OF GCLs

5.1 Perspective of CETCO with Respect to Bentomat ®

Mr. Robert Trauger of Colloid Environmental Technology Co. (CETCO) presented an overview of past and present needs in the GCL industry, a summary of the technical data collected for Bentomat®, and a list of the future needs for GCLs in general.

5.1.1 Overview

Mr. Trauger identified the principal concerns for GCLs in 1992 as:

1. Intimate contact
2. Freeze/thaw
3. Seam performance
4. Shear strength
5. Puncture resistance
6. Conformance testing
7. Subtitle D equivalency

Many of the concerns from 1992 have been resolved or researched to a significantly further degree than in 1992. According to Mr. Trauger, the concerns for GCLs in 1995 are shear strength, chemical compatibility, and manufacturing quality control (QC). Shear strength has emerged as the major technical concern, and the issues associated with shear strength are:

1. Testing techniques
2. High normal stress
3. Interface strength
4. Long term behavior (creep)
5. Seismic effects

5.1.2 Summary of Technical Data

Shear tests have performed on Bentomat® to examine some of the issues concerning the shear strength of GCLs. The results of some of the shear testing were presented and a general description of the conclusions from each test is provided. A summary of Bentomat® direct shear results and the data from the direct shear and creep shear tests are located in Appendix G.

compare test results and products. More workshops on GCLs would be helpful to everyone involved, because everyone benefits from shared information.

5.2 Perspective of CETCO with Respect to Claymax®

Mr. John Fuller of CETCO discussed the manufacturing process, internal shear behavior, creep shear testing, and interface friction testing of the Claymax® 500SP (Shearpro®) product. He also described some new products, namely the high tensile strength GCL.

5.2.1 Manufacture

During manufacture of Shearpro®, bentonite is spread on top of the bottom geotextile. The bentonite is covered with a water-soluble adhesive (to keep the bentonite in place), and the cover geotextile is placed over bentonite. The stitch-bonding process is the next step for stitch-bonded GCLs. In the stitch-bonding process, parallel rows of stitches are made connecting the bottom and top geotextiles. The stitches are created in the machine direction the entire length of the roll 100 mm between rows. The thread used in the stitch-bonding process is polypropylene. Polypropylene is used because of its durability and its inert characteristics with respect to chemicals. There is some flexibility in designing the reinforcing components of the stitch-bonded GCLs. The stitch-bonding process can be changed by modifying the type of yarn, the stitch bonding process, and the type of textiles used.

5.2.2 Internal Shear Strength

Mr. Fuller reported that the internal shear strength of Shearpro® includes a friction angle of 5 degrees and a cohesion of 26 kPa, although the normal stress and shearing rate for which these values apply were not specified. The cohesion is due to the interaction of the reinforcing stitches and the fabric. The shear strength of the stitch-bonded GCLs is a function of the yarn strength, fabric strength, and the stitch spacing. Therefore, the shear strength can be changed by changing the yarn and fabric strength or stitch spacing.

5.2.3 Creep Shear Tests

Creep internal shear testing is being researched. Large-scale creep shear tests will be performed at Purdue University. The speaker suggests that the reinforcing method used in Shearpro® is not prone to creep. The reinforcing fibers in the GCL are not likely to "pull-out" of the GCL when subjected to creep, because the stitch-bonding process ties the thread into knots in the bottom geotextile. However, there is the potential for the reinforcing fibers to break or for the polypropylene to creep. Interface shear testing of the GCL against different textured

geomembranes will be pursued. The interface shear testing will help to see if the different texturing processes (calendering, hot air, and HDPE spray) result in different shear strengths with the GCLs.

5.2.4 New Products

New stitch-bonded products are being created including a high tensile strength GCL that has been used already in a California "canyon" landfill. An advantage of the stitch-bonding process is its flexibility in using a wide variety of textiles. Also, the stitch-bonded GCL with a nonwoven fabric provides a high interface shear strength. The interface shear strength can be modified by altering the weights of the nonwoven fabric.

5.3 Perspective of National Seal Co. with Respect to Bentofix®

Bentofix® is manufactured in North America by Albarrie Naue Ltd., and is distributed in the United States by National Seal Company. The factory is located in Barrier, Ontario, Canada, which is located near Toronto.

5.3.1 Manufacture

The product is created on a continuous production line by dispersing dry sodium bentonite onto a carrier geotextile at a minimum rate of approximately 5 kg/m^2. The carrier geotextile can be either woven or nonwoven (although the nonwoven is actually a woven/nonwoven composite, with the woven side facing inward toward the bentonite and the nonwoven component facing outward). The version of Bentofix® with a nonwoven geotextile on one side and a woven on the other is Bentofix® NS, which is referred to as Bentofix II in Chapter 3 and which was installed in the test plots with the woven geotextile facing downward. The version of Bentofix® with a nonwoven geotextile on both sides is Bentofix® NW, which is referred to as Bentofix® I in Chapter 3. A nonwoven geotextile is then placed over the bentonite layer. The materials then pass through a series of needle boards where thousands of barbed needles are punched through the composite. The needles carry fibers from the nonwoven upper geotextile through the bentonite layer and entangle them in the carrier layer. The entangling clumps are then thermally locked to the carrier layer by passing over a heat source. This process encapsulates and stabilizes the bentonite layer in the product. The thermal-locking of the needlepunched fibers to the geotextile gives the GCL internal strength and resistance to deformation in a creep mode.

5.3.2 Shear Tests

Short-term internal shear and long-term creep shear tests were performed to determine the strength of the GCL and the results are included in the following paragraphs. Results of the short term shear and long term creep tests are located in Appendix H.

The laboratory shear devices used in the creep and internal shear tests were large direct shear boxes having dimensions 300 mm by 300 mm. The lower half of the shear box was larger than the upper to allow for translation over a constant area. The normal load was applied to the top by either an air bladder for large loads or by weights for lighter loads. The shear load was applied by moving the lower half of the shear box for the short-term internal tests and by applying a constant shear load to the lower box for the long-term creep tests.

Two internal shear tests series were performed on Bentofix® NS Thermal Lock. One series of tests was performed at low normal stresses (34 kPa, 69 kPa, and 138 kPa), and the other series at high normal stresses (965 kPa, 1170 kPa, and 1380 kPa). In each test the specimen was placed in the test device dry, and then the target stress was applied. The test device was then flooded, and the GCL was allowed to hydrated for 24 hours. After the hydration period, the specimens were sheared at a displacement rate of 1 mm/min. The specimen area, in the tests at higher normal stresses, was reduced to 200 mm by 200 mm in order to apply such a large stress to the GCL.

When sheared under low normal stresses, the test specimens developed a peak shear resistance during the first 12 mm of displacement, and then the shear stress decreased rapidly after the internal connections were forced to fail. The peak apparent friction angle and cohesion were 29 degrees and 33 kPa, respectively. The large-displacement apparent friction angle and cohesion after 50 mm of displacement were 4 degrees and 6 kPa, respectively.

When sheared under high normal stresses, the specimens developed a peak shear resistance, and then, with further deformation, the shear resistance dropped off as the specimen was forced to fail internally. The peak friction angle under high stresses was 23 degrees, and the peak cohesion was essentially zero. The large-displacement friction angle was 2 degrees after 50 mm of displacement, and the cohesion was 90 kPa.

5.3.3 Creep Tests

To evaluate how the GCL behaves during long-term shear (creep), two types of shear tests were performed. The tests were performed to simulate conditions at the EPA field site, with the normal and shearing stresses selected to be representative of the 2H:1V slopes. One type of test was performed on both Bentofix® NS and Bentofix® NW at a normal stress of 20 kPa and a shear stress of 10 kPa. The other type of test was performed on Bentofix® NS and Bentofix®

NW at a normal stress of 413 kPa and a shear stress of 207 kPa. The shear devices for both types of tests were 300 mm by 300 mm. In both types of tests the specimens were allowed to hydrate and consolidate for 5 days prior to the application of the shear load.

When the shear load was applied to the specimens under lower normal stresses, there was an initial segment of movement. This adjustment to the application of the shear load rapidly fell to effectively zero displacement versus time for both the NS and NW products. The specimens were allowed to remain under the test conditions for nearly four thousand hours before the tests were terminated.

In the long-term creep shear tests under higher normal stresses, there was an initial segment of movement in response to the application of shear stress. The movement slowed and the stresses were increased to a normal stress of 516 kPa and a shear stress of 241 kPa. There was another initial response to the increased load, but it was smaller in magnitude than the first response. As of August, 1995, the long-term creep shear tests at higher normal stresses are currently at 500 hours of elapsed time.

After extrapolations of the results of these shear tests, the effective displacement rate was determined to be 5×10^{-8} mm/min. It is believed that these date provide a good indication that internal failure by creep is not a significant issue for the conditions examined so far.

5.4 Perspective of GSE Lining Technology with Respect to Gundseal®

Mr. Richard Erickson presented a brief description of Gundseal®, the GCL product manufactured by GSE, and described two ongoing projects with GCLs. The two projects include the GCL field test site in Cincinnati, Ohio, and a bentonite hydration monitoring test in the Coffin Butte landfill in Corvallis, Oregon.

5.4.1 GCL Product

The Gundseal® GCL product consists of approximately 5 kg/m^2 sodium bentonite with a geomembrane backing. GSE manufactures several different polymer geomembranes that can be used as the geomembrane portion of the GCL. The polymers include HDPE, ultraflex, polypropylene, or any combination of the listed polymers given GSE's coextrusion process. The geomembrane can be either smooth or textured, and its thickness can range from 0.3 mm to 2 mm. The length of the GCL product ranges from 46 m to 61 m depending on the thickness and flexibility of the geomembrane. Gundseal® can be placed in the field with the bentonite facing "up" or "down". Gundseal® is placed facing down in situations where the GCL replaces a CCL in a composite liner. In these instances the bentonite is usually in contact with the subgrade. The bentonite will hydrate, and therefore the strength of the bentonite becomes a concern in the

design. More typically, especially in slope applications, is for Gundseal® to be placed where the bentonite is facing upward. The geomembrane portion of the GCL is usually in contact with the subgrade. A textured 0.76 mm to 2 mm geomembrane is used to increase the frictional resistance between the subgrade and the geomembrane. In this case an additional geomembrane is placed above the bentonite to create a "seal" so that the bentonite remains dry. The additional geomembrane can be either a single or double-sided textured geomembrane.

5.4.2 GCL Field Test in Cincinnati, Ohio

The Gundseal® product has been installed in four of the plots at the GCL field test site in Cincinnati, Ohio. Gundseal® has been installed in Plot A, F, and P with the bentonite side facing up and covered by an additional geomembrane. Plot E was constructed with the bentonite facing down and in contact with the subgrade. Plots F and P were constructed on the 2H:1V slopes while plots A and E have been constructed on the 3H:1V slopes.

The bentonite in Plot F is encased by two geomembranes and should have remained at the manufactured water content. Instead, Plot F experienced wetting of the bentonite. Sampling was performed to determine the extent of hydration of the bentonite within the plot. An area of elevated hydration was found on the right panel of plot F near the entrance of the extensometer cables. Also, the hydration seemed to "fan" out near the toe of the panel. It is not very clear how the bentonite became hydrated, but it appears that the extensometer cables provided an avenue for water to hydrate the bentonite. Because the causes of hydration were hard to identify, GSE decided to construct another test plot, plot P, with the same configuration as plot F except without the extensometer cables. Plot P was constructed in June, 1995, and the only instrumentation placed in plot P was a 4 x 4 grid of moisture sensors. The moisture sensors in Plot P indicate that the bentonite has not become hydrated.

At the same time that plot F was sampled to determine the water content of the bentonite, plot A and E on the 3H:1V slopes were also sampled to make sure the moisture instruments were functioning properly. The bentonite samples taken from plot A, which is encased by two geomembranes, were still relatively dry. The one sample of bentonite taken from plot E, where the bentonite is in direct contact with the subgrade, was at a water content of 50%. These water contents were consistent with the moisture sensor readings.

5.4.3 Field Instrumentation of GCL/Bentonite Moisture Monitoring Program

The purpose of this project was to demonstrate the performance of Gundseal® with respect to hydration and stability in a canyon landfill. The landfill is the Coffin Butte landfill in

Corvallis, Oregon, and the instrumented cell is Cell 2C, which is a 5.6 ha cell with a double composite bottom liner system. The lining system consists, from top to bottom, of a 0.3 m operations layer, a 0.3 m drainage layer, a 1.5 mm textured HDPE geomembrane, Gundseal® GCL (1.0 mm textured HDPE geomembrane with the bentonite side facing up), a 0.3 m leak detection layer, a 1.5 mm textured HDPE geomembrane, and a compacted subgrade. The lining system has an underdrain system because of a high water table.

The moisture instrumentation was installed for the long-term collection and processing of moisture data for the bentonite within Gundseal®. Three distinct locations on the cell floor were targeted: two locations with high potential for bentonite hydration, and one location for average conditions. A total of eighty-eight fiberglass resistance block moisture sensors were installed. They were placed in six transducer group arrays and in three pairs for redundancy. All moisture sensors were covered with powdered bentonite so there would be no damage to the overlying geomembrane. The moisture sensors were calibrated before installation. The data will be used to extrapolate the behavior for the remainder of the cell.

CHAPTER 6
REPORT OF ASTM D 35.04 SUBCOMMITTEE ACTIVITIES

Mr. Larry Well, the Chairman of ASTM Subcommittee D-35.04 on Geosynthetic Clay Liners, provided a status report on standards development activities concerning GCLs with ASTM. At the June, 1992, meeting of the ASTM D-35 Committee, a special session was held to discuss the development of a standard practice for testing GCLs. A scope of work for a GCL task group was developed. On the basis of discussions with Committee D-18 on Soil and Rock, it was decided that Committee D-35 should manage the task group. During the June, 1993, ASTM meetings, the task group was made into a new Subcommittee D-35.04.

As of last May there were 48 members on the subcommittee composed of 16 producers, 11 users, and 21 general interest members. The subcommittee is working closely with ASTM Committee D 18.04 for Hydraulic Properties as related to the clay component of GCLs.

The new subcommittee comprises six task groups for physical properties, manufacturing quality control/quality assurance (QA/QC), logistics, endurance, hydraulic properties, and mechanical properties. Their task and activities are described as follows:

6.1 Physical Properties

Robert Mackey is the task group chairman leading the development of a standard test method to determine the mass per unit area of the clay component of a GCL. The task group has balloted a draft at subcommittee and main committee level. Comments received will be incorporated to revise the draft for re-balloting. A round-robin testing program is being developed to test the proposed method. The results of the ballot will be reviewed at the January meeting and the standard moved forward.

6.2 Manufacturing QC/QA

Kent von Maubeuge is the task group chairman for developing a standard of practice for manufacturing quality control and quality assurance of GCLs and a method for determining a swell index value for clay and the fluid loss of clays. The first draft of the standard of practice for QC/QA will be ready subcommittee ballot this fall. Draft ballots for standard method of test for swell index value and for fluid loss of clays will be prepared if Committee D-18 agrees that D-35 should do it. The results of the ballot will be reviewed at the January meeting and the standard moved forward.

6.3 Logistics

Robert Trauger leads as task group chairman in developing three draft standards. This group is developing standards of practice for GCL installations, standards of practice for GCL storage and handling, and standards of practice for GCL sampling. The first two items have had one subcommittee ballot. Comments will be used to modify the draft for re-balloting at subcommittee level. The scope of the procedure for GCL sampling was revised to remove specimen preparation procedures and will be balloted this fall. The results of the ballot will be reviewed at the January meeting and the standards moved forward.

6.4 Endurance

John Siebken is the task group chairman for developing index tests to evaluate the chemical resistance or compatibility of the clay component of a GCL to liquids in soils. Tests being evaluated for this use at this time include free-swell and fluid loss. These index tests may serve to indicate further hydraulic conductivity testing is needed.

6.5 Hydraulic Properties

Scott Luettich is task group chairman. This task group is developing an index test for measuring the flux or flow of liquids through GCLs. A subcommittee ballot was reviewed and all issues were addressed and resolved. Plans are to co-ballot the re-draft at subcommittee level with both D-35.04 GCLs and D18.04, and if possible get it to main committee ballot by October, 1995. The results to the ballot will be reviewed at the January meeting and the standard moved forward.

6.6 Mechanical Properties

Alan Marr is the task group chairman for development of a standard for determining the internal and interface shear strength of GCLs. At the task group meetings the details of the test have been discussed and a draft of the standard will be balloted this fall. The results to the ballot will be reviewed at the January meeting and the standard moved forward.

CHAPTER 7
REGULATORY STATUS OF GCLs

7.1 Perspective of U.S. EPA Superfund Headquarters

Mr. Kenneth Skahn discussed the Superfund program's perspectives concerning GCLs, the reasons why GCLs are not incorporated into waste containment designs more frequently, and how EPA documents might be modified to provide more information on GCLs and more flexibility in landfill design.

The use of GCLs varies from region to region. The northeastern regions in the U.S. have used GCLs in waste containment applications with success. However, the designs have been very conservative; GCLs have been used on slopes less than 6H:1V. In Region 4, potentially responsible parties (PRPs) have suggested the use of GCLs in landfills, but the communities are skeptical about the equivalency between GCLs and compacted clay liners. The scattered use of GCLs comes mostly from regulators' unwillingness to accept designs that differ from the technical guidance document (U.S. EPA, 1989).

The EPA is involved in a research project with Sandia National Laboratory in which test pads containing GCLs have been constructed (not on slopes) to monitor their performance with respect to infiltration. One type of test pad has the configuration of a standard Resource Conservation and Recovery Act (RCRA) Subtitle C cover, another test pad type is constructed like the standard RCRA Subtitle D cover, and a third test pad has been constructed like the standard RCRA Subtitle C cover except that a GCL has been incorporated in the design. In phase one of the project, water will be sprayed on half of the test pads, while the other half will be subjected to actual precipitation occurring at the site. The performance of the different test pads will be compared. This project was constructed with the purpose of helping develop designs for landfills in arid climates.

There has been some discussion with the RCRA program to amend the guidance document (U.S. EPA, 1989) in order to provide alternative designs. These amendments are considered desirable by the Superfund program.

7.2 Perspective of U.S. EPA Office of Solid Waste

Mr. Al Geswein discussed how three areas of EPA regulations and documents concerning RCRA Subtitle D landfills interacted with GCLs. The three areas include the basic regulation promulgated on October 9, 1991, the guidance document issued in October, 1993 explaining how EPA suggests states comply with regulations, and an upcoming EPA publication, or "issue paper", which will provide information on GCLs.

There are two places in the basic regulations where GCLs may be incorporated. These include the bottom liner and final cover of landfills. A liner must be a composite liner described in the regulations. If a designer desires to use an alternative liner instead of the prescribed composite liner in a Subtitle D landfill, it must be demonstrated that the alternative liner will not allow the concentration of certain chemicals to exceed specified concentrations at a point of compliance, and the alternative must be approved by the Direction of an approved state. Therefore, there is no restriction to the use of GCLs, and a GCL may be chosen for design as a component in the liner, provided the required demonstration concerning impact to ground water is made and the Director of an approved state concurs with the use of the proposed alternative.

A final cover in a Subtitle D landfill is required to not let more fluid into the top of the landfill than the amount which exits the bottom of the landfill. There is no restriction on the type of materials; therefore, a GCL may be used in a final cover. There is no formal restriction of the use of GCLs in the regulations.

The second area which EPA Office of Solid Waste is involved with GCLs is the supporting technical manual issued in 1993 (U.S. EPA, 1993). The technical manual includes three sections: a regulations section, an applicability section stating who must comply with the regulations, and a technical section which addresses technical concerns and gives suggestions on how to comply with regulations. GCLs are mentioned once in the technical portion of the guidance document. At the time of development of the technical document there was little published information about GCLs, and therefore there was little included in the technical guidance document.

The third area where the EPA's Office of Solid Waste interacts with GCLs is in an upcoming publication called a fact sheet. The fact sheet is a one-page summary which will discuss how GCLs might be used in Subtitle D landfills. The fact sheet will describe the technology, summarize case studies where GCLs have been used, discuss how GCLs fit into the regulations, and provide a list of references on GCLs.

CHAPTER 8
PANEL DISCUSSION

8.1 Critical Issues Concerning GCLs - EPA Project Team

8.1.1 Intimate Hydraulic Contact vs. Shear Strength

David Daniel pointed out that, based on the slides that have occurred at the EPA test site where sliding occurred at the interface between a woven geotextile and a textured geomembrane, and based on the discussion during the conference, designers might consider placing the thick nonwoven geotextile of a GCL next to a textured geomembrane. However, this would reduce the quality of the hydraulic contact between the geomembrane and GCL, since a thick, nonwoven geotextile would separate the bentonite from the geomembrane. Placing a thick, nonwoven geotextile next to a geomembrane on steep slopes may not matter as much as on flatter slopes. Designers should be cautioned to not forget about hydraulic properties of GCLs in efforts to increase the shear strength of liner systems and interfaces.

8.1.2 Internal Shear Strength of GCLs under High Normal Stresses

Rudy Bonaparte discussed an issue of growing concern, especially in the design of canyon landfills. The issue is the internal shear strength of GCLs under high normal stresses and long-term loading conditions. There is not much available in the literature that describes the limits of GCLs under these conditions. All that is available is the knowledge that mostly all of the GCL products have large-displacement shear strengths of about 3 to 5 degrees under very high normal stresses. More information about the behavior of GCLs at high normal stresses must be obtained. The GCL manufacturers are challenged to continue their effort to produce new or modified GCLs with higher internal shear strengths and decreased strain-softening behavior under high normal stresses. Possibly this can be accomplished by using different types of bentonite, adding granular admixtures such as sand in GCLs, or through other methods.

8.1.3 Long Term Effects

Robert Koerner touched on the issue of long-term effects. Since GCLs have the potential to be included in many long-term projects, the ability of GCLs to perform after long periods of time should be determined. One factor that seems to limiting the more widespread use of GCLs is the uncertainty of its performance in the long term. Long-term tests are not performed often because of the difficulty in testing.

8.2 Questions by the Audience

8.2.1 Do Bid Projects vs. Designs Need to be Sole-Sourced?

David Daniel commented that construction specifications can be developed to allow for alternatives so that bid projects and designs do not need to be sole-sourced. Rudy Bonaparte noted that if a designer desires to include a GCL as a component in a waste containment facility he or she must, for example, perform project specific testing to establish the shear strength. The designer has an option to proceed in two different ways. The first option is to test all of the products and prequalify them all during the design stage. The second option is to limit the testing program to determine the validity of the design, then write the specifications that require the successful contractor, as part of initial activities, to carry out further testing. The additional testing will prove that the specific product the contractor is going to buy and install for the project will be stable in the design. The second option eliminates the sole-sourced problem.

8.2.2 What is the Suitability of Replacing a Compacted Clay Liner (CCL) in a Composite Liner with a GCL?

Rudy Bonaparte commented that most research indicates that substitution for a CCL with a GCL would be favorable, but the substitution must be made on a project-specific basis. The ultimate goal in constructing a liner is to protect ground water, and for double liners, a GCL in the primary liner would be an adequate component in the attempt to achieve that goal.

Robert Koerner remarked that this topic has been the subject of several papers authored by Koerner and Daniel. In the discussion of technical equivalency between a CCL and GCL there are 25 issues. Some of these issues include hydraulic properties, shear strength, constructability, and performance. Only in the issues of adsorption and subgrade conditions is the GCL not equivalent to a CCL. However, these two issues can be bypassed with proper construction quality control and assurance.

David Daniel offered several observations. To begin, Subtitle D regulations do not allow for a direct comparison between CCLs and GCLs. The regulations do not require it to be shown that a GCL is superior to a CCL when replacing a CCL with a GCL. If a CCL is to be replaced, it must be demonstrated that the replacement material will not allow unacceptable impact to ground water at a point of compliance. It is curious that the regulations do not require that a CCL be demonstrated as having no impact to ground water with a prescriptive design. It is Mr. Daniel's belief that if all of the 0.6-m-thick CCLs in Subtitle D landfills in the U.S. were replaced with GCLs, and assuming all GCLs were stable on the slopes, the GCLs would generally outperform the CCLs. This is mostly a result of the incorrect construction of CCLs and the desiccation/cracking of CCLs. As smaller landfills with less technical capability for

building and construction, the advantages to GCLs increase, because it is easier to install a GCL than compacted clay. The largest concern in the discussion of equivalency is the resistance to puncture. A GCL is never going to be equivalent to a thick layer of compacted clay in regards to resistance to puncture. Therefore, it is a fair and appropriate question to ask what will happen if the GCL is punctured, especially in a hydrogeologically sensitive area.

8.2.3 Should Designs for Waste Containment Structures Be Based on Peak or Residual Shear Strengths?

Rudy Bonaparte commented that designs should be project-specific. More generally, designs may be based on slope stability evaluations using peak strength, while checking the design for stability using residual strengths. David Daniel noted that if the factor of safety calculated for slope stability using the residual strength is greater than one, then the design is generally acceptable. If the factor of safety with residual strengths is less than one, then it must be determined if residual conditions will develop and how critical those conditions will be. Robert Koerner noted that the design should include residual strengths because of the long-term question.

CHAPTER 9
REFERENCES

Amble, T. (1994), "In-Plane Hydraulic Conductivity and Rate of Wetting of Geosynthetic Clay Liners," M.S. Thesis, University of Texas at Austin, 136 p.

Boardman, B.T. (1993), "The Potential Use of Geosynthetic Clay Liners as Final Covers in Arid Regions," M.S. Thesis, University of Texas at Austin,109 p.

Bramlett, J.A., Furman, C. Johnson, A., Ellis, W.D., Nelson, H., and Vick, W.H. (1987), "Composition of Leachates from Actual Hazardous Waste Sites," United States Environmental Protection Agency, Cincinnati, Ohio, 113 p.

Daniel, D.E., and Estornell, P.M. (1991), "Compilation of Information on Alternative Barriers for Liner and Cover Systems," U.S. Environmental Protection Agency, Risk Reduction Engineering Laboratory, Cincinnati, Ohio, EPA 600/2-91/002.

Daniel, D.E., and Boardman, B.T. (1993), "Report of Workshop on Geosynthetic Clay Liners," U.S. Environmental Protection Agency, Risk Reduction Engineering Laboratory, Cincinnati, Ohio, EPA 600/2-93/171.

Daniel, D.E., Shan, H.Y., and Anderson, J.D. (1993), "Effects of Partial Wetting on the Performance of the Bentonite Component of a Geosynthetic Clay Liner," *Geosynthetics '93*, Industrial Fabrics Association International, St. Paul, Minnesota, 3: 1483-1496.

Erickson, A.E., Chamberlain, E.J., and Benson, C.H. (1994), "Effects of Frost Action on Covers and Liners Constructed in Cold Environments," *Proceedings*, Seventeenth Madison Waste Conference, University of Wisconsin, Madison, Wisconsin, 198-220.

Harpur, W. A., R. F. Wilson-Fahmy, and Koerner, R.M. (1993), "Evaluation of the Contact Between Geosynthetic Clay Liners and Geomembranes in Terms of Transmissivity," *Proceedings of the 7th GRI Seminar*, Geosynthetic Research Institute, Drexel University, Philadelphia, 138-149.

Hewitt, R.D. (1994), "Hydraulic Conductivity of Geosynthetic Clay Liners Subjected to Freeze/Thaw," M.S. Thesis, University of Texas at Austin, 103 p.

LaGatta, M.D. (1992), "Hydraulic Conductivity Tests on Geosynthetic Clay Liners Subjected to Differential Settlement," M.S. Thesis, University of Texas at Austin, 120 p.

McNabb, G.D., Payne, J.R., Harkins, P.C., Ellis, W.D., and Bramlett, J.A. (1987), "Composition of Leachates From Actual Hazardous Waste Sites," Land Disposal, Remedial Action, Incineration and Treatment of Hazardous Waste, Proceedings of the Thirteenth Annual Research Symposium at Cincinnati, Ohio, EPA/600/9-87/015, 130-138.

Ruhl, J.L. (1994), "Effects of Leachates on the Hydraulic Conductivity of Geosynthetic Clay Liners (GCLs)," M.S. thesis, University of Texas at Austin, 101 p.

Sai, J.O., and Anderson, D.C. (1991), " Long-Term Effect of an Aqueous Landfill Leachate on the Permeability of a Compacted Clay Liner," *Hazardous Waste & Hazardous Materials*, 8(4): 303-312.

Stanforth, R., Ham, R. Anderson, M., and Stegmann, R. (1979), "Development of a Synthetic Municipal Leachate," *Journal of the Water Pollution Control Federation*, 51(7): 1965-1975.

Texas Water Commission (1985), Technical Guideline No. 1, "Waste Evaluation/Classification," Austin, Texas.

U.S. Environmental Protection Agency (1989), "Technical Guidance Document: Final Covers on Hazardous Waste Landfills and Surface Impoundments," EPA/530-SW-89-047, Washington, D.C., 39 p.

U.S. Environmental Protection Agench (1993), "Solid Waste Disposal Facility Criteria, Technical Manual," EPA 530-R-93-017, Washington, D.C., 349 p.

Appendix A

List of Attendees

SPEAKERS FOR WORKSHOP

Bonaparte, Rudolph	GeoSyntec Consultants	5775 Peachtree Dunwood Rd., Suite 200F, Altanta, GA 30342
Bowders, John	The Univ. of Texas at Austin	Cockrell Hall, Austin, TX 78712
Carson, David A.	U.S. EPA	26 W. Martin Luther King Dr., Cincinnati, OH 45268
Cowland, John W.	Hong Kong Government	101 Princess Margaret Rd., Ho Man Tin, Kowloon, Hong Kong
Daniel, David E.	The Univ. of Texas at Austin	Cockrell Hall, Room 9.102,Austin, TX 78712
Fuller, John	Claymax Corp.	P.O. Box 88, 234 Gordon St., Fairmount, GA 30139
Geswein, Allen J.	U.S. EPA	401 M St. S.W.,MS-5306W, Washington, DC 20460
Koerner, Robert M.	Drexel University	33rd & Lancaster, Bldg. 10 West Wing, Philadelphia, PA 19104
Kraus, Jason F.	CH2M HILL	8501 West Higgins Rd., Suite 300, Chicago, IL 60631-2801
Landreth, Robert E.	U.S. EPA	26 W. Martin Luther King Dr., Cincinnati, OH 45268
Scranton, Heather	The Univ. of Texas at Austin	Cockrell Hall, Austin, TX 78712
Siebken, John R.	National Seal Company	1255 Monmouth Blvd., Galesburg, IL 61401
Skahn, Kenneth R.	U.S. EPA	401 M St. S.W.,MS-5203G, Washington, DC 20460
Trauger, Robert	CETCO	1350 W. Shure Drive, Arlington Heights, IL 60004
Well, Larry W.	CH2M HILL	825 NE Multnon, Portland, OR 97232-2146

Adams, Matthew W.	SLT North America, Inc.	200 S. Trade Center Pkwy.,Conroe, TX 77385
Afiffi, Sherif	NTH Consultants	38955 Hill Tech Drive, Farmington Hills, MI 48331
Al-Saleem, Zaidoon	Indiana Dept. of Env. Mgmt.	100 N. Senate, POBox 6015,Indianapolis, IN 46206-6015
Alexander, Rodney	DSWA	P.O. Box 455, Dover, DE 19903
Allred, Jerry D.	TNRCC/MSW	P.O. Box 13087/MC-124, Austin, TX 78711-3087
Alshammaa, Bassam	Indiana Dept. Of Env. Mgmt.	100 N. Senate, POBox 6015,Indianapolis, IN 46206-6015
Alshunnar, Ibraheem	NTH Consultants	38955 Hills Tech Dr., Farmington Hills, MI 48331
Anderson, Robert	CA Integrated Waste Mgmt. Board	8800 Cal Center Drive, Sacremento, CA 85826
Anderson, P.E., James D.	JANCO Engineers	23526 Canyon Lake, Spring, TX 77373
Arunachalam, Selvan	WV DEP	1356 Hansford Street, Charleston, WV 25301
Asgari, CHMM, EIT, Said	Indiana Dept. of Env. Mgmt.	100 N. Senate, POBox 6015,Indianapolis, IN 46206-6015
Asser, Joerg-Dieter	Gerbruder Friedrich GmbH	MuseumstraBe 69, D-38229 Salzgitter, Germany
Bakanas, Carol J.	WV DEP	1356 Hansford Street, Charleston, WV 25301
Baker, Gale L.	TNRCC	P.O. Box 13087,MC-124, Austin, TX 78711-3087
Bandi, Sanjeev	Rust E&I	17250 Newburgh Road, Livonia, MI 48167
Baron, P.E., James W.	Indiana Dept. of Env. Mgmt.	100 N. Senate, POBox 6015,Indianapolis, IN 46206-6015
Barry, Celeste	Bechtel Environmental, Inc.	151 Lafayette Drive, Oak Ridge, TN 37831-0350
Batt, Douglas R.	FMSM Engineers	10018 International Blvd., Cincinnati, OH 45246-4839
Baxter-Potter, Wanada	E/S Environmental Engineers, Inc.	1701 North Ironwood, South Bend, IN 46635
Belanger, Ronald E.	Precision Laboratories	1742 W. Katella Ave., Ste. 4, Orange, CA 92667
Bell, Wiley D.	RUST E&I	11785 Highway Drive, Cincinnati, OH 45241
Benedum, Paul	WV DEP	1356 Hansford Street, Charleston, WV 25301
Benson, Craig H.	Univ. of Wisconsin	1415 Engineering Drive, Madison, WI 52706
Bhattacharja, Sankar	Construction Technology Laboratories, Inc.	5420 Old Orchard Road, Skokie, IL 60077
Bingham, Randy	Trivaco	4460 Lake Forest Dr., Suite 214, Cincinnati, OH 45242
Booth, Mike	Sevee & Maher Engineers	P.O. Box 85A, Cumberland, ME 04021
Bravo A. Ph. D., Humberto	Circuito Exterior, Cd. Universitaria	Centro de Cienciad de la Atmosfera, C.L.,Mexico 04510
Brown, Craig	U.S. EPA	345 Courtland Street, Atlanta, GA 30306
Bukhari, Muhammad	Bechtel National, Inc.	151 Lafayette Drive, Oak Ridge, TN 37831
Bush, Sandra	Ohio EPA	347 N. Dunbridge Rd., Bowling Green, OH 43402
Chen, D.K.	MKES	180 Howard Street, San Francisco, CA 94105
Christopher, Barry		210 Box Elder Lane, Roswell, GA 30076
Conner, Jack	Claymax	6013 Tulip Hill Road, Columbus, OH 43235
Corcoran, Greg	Roy F. Weston, Inc.	1 Weston Way, West Chester, PA 19380
Cox, Mike	Indiana Dept. of Env. Mgmt	100 N. Senate, Indianapolis, IN 460206-6015
Czajkowski, Ron	TNRCC	P.O. Box 13087,Austin, TX 78711-3087
Daugherty, PE, Tom	Indiana Dept. of Env. Mgmt.	100 N. Senate Ave., POBox 6015,Indianapolis, IN 46206-6015
Davis, S.	Indiana Dept. of Env. Mgmt.	P.O. Box 6015,Indianapolis, IN 46206-6015
DeHavilland, Annette	Ohio EPA	P.O. Box 1049,Columbus, OH 43216-1049
Dugan, Patrick	EO-The Environmental Co.	5011 Lilley Road, Canton, MI 48188
Dzierzbicki, Ted	National Seal Company	1245 Corporate Blvd., Ste. 30, Aurora, IL 60504
Ebelhar, P.E., Ronald J.	Rust Environment & Infrastructure	11785 Highway Dr., Suite 100, Cincinnati, OH 45241
Eckman, Scott	Bryan-Stirrat & Assoc.	3662 Mission Mesa Way, San Diego, CA 92120
Englander, Linda	Fluid Systems	1245 Corporate Blvd., Suite 300, Aurora, IL 60504
Evans, Doug	Ohio EPA	P.O. Box 1049,Columbus, OH 43216-1049
Filshill, Archie	Claymax Corp.	2105 Ashwood Avenue, Philadelphia, PA 19154

Fox, Patrick J.	Purdue University	School of Civil Engineering, West Lafayette, IN 47907
Fox, Richard J.	Ohio EPA	P.O. Box 1049, Columbus, OH 43216-1049
Foxwell, Russell	Scott Wilson Kirkpatrick (Hong Kong) Ltd.	38th Floor Metroplaza Tower 1, 223 Hing Fong Road, Kwai Fong, Hong Kong,
French, Rick	Granger Companies	16980 Wood Road, Lansing, MI 48906
Fruendt, Joel L.	Fluid Systems	1245 Corporate Blvd., Aurora, IL 60504
Gerard, Ken	Parsons	6120 S. Gilmore Road, Fairfield, OH 45014
Gerdeman, Angela M.	Hull & Associates, Inc.	2726 Monroe Street, Toledo, OH 43606
Gerdeman, David A.	North Point Environmental	P.O. Box 36688, Canton, OH 44735-6688
Germain, Anne	DSWA	P.O. Box 455, Dover, DE 19903-0455
Gibson, P.E., Gerald N.	Nebraska Dept. of Env. Quality	Suite 400, The Atrium, 1200 N. St., Lincoln, NE 68509-8922
Gilbert, P.E., Ph.D., Robert B.	The University of Texas at Austin	Cockrell Hall 9.227, Austin, TX 78712
Goldstein, Jay	Land & Lakes Co.	123 N. Northwest Highway, Parkridge, IL 60068
Grahlheer, Don	GAI Consultants, Inc.	570 Realty Road, Pittsburgh, PA 15146
Guglielmetti, John L.	DuPont Environmental	P.O. Box 80027, Barley Mill Plaza #27, Wilmington, DE 19880-0027
Hall, PE, James A.	Burgess & Niple Engineers Architects	5085 Reed Road, Columbus, OH 43220
Hamel, Timothy W.	Pennsylvania Electric Co.	1001 Broad Street, Johnstown, PA 15907
Harris, Jeffrey M.	Browning-Ferris Ind.	757 N. Eldridge, Houston, TX 77079
Heath, P.E., Richard E.	FERMCO	25 Merchant Street, Cincinnati, OH 45246
Heidenreich, R.S., Scott D.	Ohio EPA	347 N. Dunbridge Rd, Northwest District Office, Bowling Green, OH 43402-0466
Held, William M.	Kelchner Environmental	6834 Loop Road, Centerville, OH 45459
Hester, Scott	Ohio EPA	2305 Westbrooke, Bldg. C, Columbus, OH 43228-9644
Hewitt, Robert D.	Haley & Aldrich Inc.	58 Charles Street, Cambridge, MA 02141-2147
Hirshberg, Ralph	Hull & Associates, Inc.	4700 Duke Dr., Suite 172, Mason, OH 45040
Hullings, Donald	EMCON	1921 Ringwood Ave., San Jose, CA 95131
Hyer, Charles	Jacob Engineering	125 Broadway, Oak Ridge, TN 37830
Jaros, David L.	Corps. of Engineers	12565 West Center Road, Omaha, NE 68157
Johnson, Ralph	Colloid Environmental Technologies Co.	1350 West Shure Drive, Arlington Heights, IL 60004-1440
Klesmith, Daniela J.	Indiana Dept. of Env. Mgmt.	100 N. Senate, Indianapolis, IN 46206-6015
Korkzan, Mohammad H.	Indiana Dept. of Env. Mgmt.	100 N. Senate, Indianapolis, IN 46206-6015
Kraus, Jason F.	CH2M HILL	8501 West Higgins Rd., Suite 300, Chicago, IL 60631-2801
Kreipe, Kevin	ViroGroup of SC	1445 Pisgah Church Road, Lexington, SC 29072
Kubrix, Ed	Parsons	6120 S. Gilmore Road, Fairfield, OH 45014
Kumthedar, P.E., Uday A.	FERMCO	P.O. Box 538704, Cincinnati, OH 45253-8704
Lemaster, Herbert R.	Commonwealth Technology	2526 Regency Road, Lexington, KY 40503
Lockhart, Scott	Hull & Associates, Inc.	2726 Monroe Street, Toledo, OH 43606
Lothspeich, P.E., Steven E.	Huesder Inc.	1107a So. Commerce Blvd., Charlotte, NC 28241
Lyang, Jenghwa	NTH Consultants	38955 Hills Tech Drive, Farmington, MI 48331
Lydick, Larry	National Seal Co.	1245 Corporate Blvd., Suite 300, Aurora, IL 60504
Magel, Steve	Synthetic Industries	4019 Industry Drive, Chattanooga, TN 37416
Martin, Cherrie	Ohio EPA	401 E. 5th St., Southwest District Office, Dayton, OH 45402-2911
Martin-Hayden, E.I.T., Dana	Ohio EPA	347 N. Dunbridge Rd., Northwest District Office, Bowling Green, OH 43402
Massey-Norton, John T.	American Electric Power	1 Riverside Plaza, Columbus, OH 43215-2273
Mazanec, Paul	Wayne Disposal	5011 S. Lilley Road, Canton, MI 48188
McAughan, Charles H.	Bentonite Corporation	1999 Broadway, 43rd Floor, Denver, CO 80202
McKelvey, III, P.E., James A.	Roy F. Weston, Inc.	1 Weston Way, West Chester, PA 19380-1499
McManis, Ph.D., Kenneth L.	University of New Orleans	810 Engineering Bldg., New Orleans, LA 70148

Mills, Clive	NSC	1245 Corporate Blvd., Suite 300, Aurora, IL 60504
Mlynarek, Ph.D., Jacek	SAGEOS	300, rue Boulle, Saint-Hyacinthe, Quebec, Canada J2S 1H9
Moore, Harry	Joyce Engineering Inc.	4808 Radford Avenue, Richmond, VA 23230
Murphy, P.E., David	MA DEP	1 Winter Street, Boston, MA 02108
Nagda, P.E., Durga S.	KY D.E.P., Div. of Waste Mgmt.	14 Reilly Road, Frankfort, KY 40601
Nelson, Steve	Parsons	6120 S. Gilmore Road, Fairfield, OH 45014
Nikorak, P.E., Forrest	Texas Natural Resource Conservation Commission	MC-124, P.O. Box 13087, Austin, TX 78711-3087
Norton, Ken	Sevee & Mahey Eng.	P.O. Box 85A, Cumberland, ME 04021
Oliver, Charles D.	Dow Chemical Company	P.O. Box 3387, Houston, TX 77253-3387
Ossivand, Bahman	Indiana Dept. of Env. Mgmt.	100 N. Senate, Indianapolis, IN 46206-6015
Othman, Majdi	GeoSyntec Consultants	7700 Lake Hearn Dr., Ste. 200, Atlanta, GA 30342
Ottarson, Jim	Ohio EPA	347 Dunbridge Road, Bowling Green, OH 43402
Parkinson, Laura	Ohio EPA	3232 Alum Creek Dr., Columbus, OH 43207-3417
Parsons, James J.	NTH Consultants, Ltd.	38955 Hill Tech Drive, Farmington Hills, MI 48331
Pasquarette, John	Ohio EPA	347 N. Dunbridge Road, Bowling Green, OH 43402
Patterson, P.E., Craig L.	International Technology Corp.	11499 Chester Road, Cincinnati, OH 45246-4012
Peggs, Dr. Ian D.	I-Corp International Inc.	1250 S. Federal Highway, Boynton Beach, FL 33435
Perzia, Phil	TerraFix Geosynthetic	425 Attwell Dr., Rexdale, Ontario, Canada M9W 5C4
Pickett, Shannon L.	Commonwealth Technology	2526 Regency Road, Lexington, KY 40503
Pollard, David	OK Dept. of Env. Quality	1000 NE 10th Street, Oklahoma City, OK 73117-1212
Poulnott, Elisa	Ohio EPA -DS/WM	P.O. Box 1049, Columbus, OH 43216-1049
Provost, Terry G.	DDE-SRS	P.O. Box A, Azken, SC 29803
Quaranta, John	West Virginia University	645 ESB, Morgantown, WV 26506-6101
Raman, Shyamala C.	Indiana Dept. of Env. Mgmt.	100 N. Senate, Indianapolis, IN 46206-6015
Ravlik, Kevin	U.S. Army Corps of Engineers	215 N. 17th Street, Omaha, NE 68102-4978
Rector, Dean	Golder Associates	200 Union Blvd., Ste. 500, Lakewood, CO 80228
Rocca, Earl	RMT, Inc.	3928 Varsity Drive, Ann Arbor, MI 48108
Roemerman, Paul W.	U.S. EPA	726 Minnesota Avenue, Kansas City, KS 66101
Rogers, Robert	Illinois EPA	2200 Churchill Rd., Box 19276, Springfield, IL 62794-9276
Rome, Bruce E.	Rust Environment & Infrastructure	11785 Highway Drive., Suite 100, Cincinnati, OH 45241
Rowe, Dr. R. Kerry	Univ. of Western Ontario, Dept. of Civ. Eng.	London, Ontario, Canada N6A 5B9
Russell, P.E., Randall W.	Kenvirons, Inc.	452 Versailles Road, Farnkfort, KY 40601
Ryan, Maryann	Texas Natural Resource Conservation Commission	P.O. Box 13087, Austin, TX 78711-3087
Schrader, John	WV DEP	1356 Hansford Street, Charleston, WV 25301
Schumm, Tim	Ohio EPA	347 N. Dunbridge Rd., Bowling Green, OH 43402
Shack, Pete	Phoenix Env. Engrs.	P.O. Box 12155, Nashville, IN 37212
Shafer, P.E., Andrew L.	Browning-Ferris Industries	P.O. Box 3151, Houston, TX 77253
Sheehan, Kimerly A.	Ohio EPA	401 E. 5th St., Southwest District Office, Dayton, OH 45402-2911
Sheridan, Terry	Tensar Environmental Systems, Inc.	1405 Third Ave., Suite 8, Spring Lake, NJ 07762
Sides, D.	Indiana Dept. of Env. Mgmt.	P.O. Box 6015, Indianapolis, IN 46206-6015
Slivka, Donal C.	Ohio EPA	P.O. Box 1049, Columbus, OH 43216-1049
Sonnefeld, Michael	Indiana Dept. of Env. Mgmt.	100 N. Senate, Indianapolis, IN 46206-6015
Soydemir, P.E., Cetin "Chet"	Haley & Aldrich Inc.	58 Charles Street, Cambridge, MA 02141
Spikula, P.E., Daniel R.	Browning-Ferris Industries	757 N. Eldridge, Houston, TX 77253
Staab, Fred A.	National Seal Company	1245 Corporate Blvd., Suite 300, Aurora, IL 60504
Stafford, Richard	New Mexico Environment	P.O. Box 26110, Santa Fe, NM 87502

Stark, Timothy D.	Univ. of IL, Dept. of Civil Eng.	205 N. Mathews Ave., Urbana, IL 61801
Stewart, Don	Terrafix Geosynthetics Inc.	425 Attwell Drive, Toronto, Canada M6G 3J7
Strassburger, PE, Eric A.	Bechtel Environmental, Inc.	151 Lafayette Drive, Oak Ridge , TN 37831-0350
Struve, Fred	Gundle	19103 Gundle Road, Houston, TX 77073
Stulgis, Richard P.	Haley & Aldrich Inc.	10 Harvey Road, Bedford, NH 03110
Suryasamita, Vince	ViroGroup, Inc.	5301 Office Park Dr., #420, Bakersfield, CA 93309
Swyka, P.E., Mark A.	EMCON	666 East Main Street, Middletown, NY 10940-0858
Taylor, Mark	Joyce Engineering Inc.	436 Spring Garden St., Greensboro, NC 27401
Tedder, Richard B.	Dept. of Env. Protection	2600 Blair Stone Rd., MS #4565, Tallahassee, FL 32399-2400
Terry, Jeff	Ohio EPA	3232 Alum Creek Drive, Colubmus, OH 43207-3417
Twardock, Rob	STS Consultants, Ltd.	1415 Lake Look Road, Deerfield, IL 60015
Van Arsdale, Charles	Rust E&I	11785 Highway Dr., Suite 100, Cincinnati, OH 45241
Vargas, PE, Juan C.	Browning-Ferris Industries	9188 Glenoaks Blvd., Ste. 300, Sun Valley, CA 91352
von Maubenge, Kent	Nane Fasertechnik	Alter Bahndamm 12, Lemfoede, Germany 49448
Vonderembse, Glen	CINergy	139 E. 4th St., Room 552, Cincinnati, OH 45202
Wadsack, PE, Patricia	Burgess & Niple, Ltd.	5085 Reed Road, Columbus, OH 43220
Walkenhorst, Victor L.	US EPA (SEE Program)	726 Minnesota Ave. WSTM/SPFD, Kansas City, KS 6KS 66101
Walling, W.W.	SLT North America Inc.	200 S. Trade Center Parkway, Conroe, TX 77385
Walsh, David	Black & Veatch	601 Walnut Street, Philadelphia, PA 19106
Watson, Richard	DSWA	P.O. Box 455, Dover, DE 19903
Webber, Tom	Pyramid Environmental	357 Riverland Drive, Crested Butte, CO 81224
Well, Larry W.	CH2M Hill	825 N.E. Multnomah, Suite 1300, Portland, OR 97232-2146
White, David F.	Texas Natural Resource Conservation Commission	12015 Park 35 Circle, Bldg. F, Austin, TX 78711-3087
Williams, Mick	IT Corporation	5754 Pacific Center Blvd., Ste. 203, San Diego, CA 92121
Winslett, Brian A.	C G&E CO.	P.O. Box 960, Rm 552A, Cincinnati, OH 45201
Workman, John	Laidlaw Waste Systems	9001 Airport Freeway, N. Richaland Hills, TX 76180

Appendix B

Total Down-Slope Displacement in Test Plots

STEADY-STATE DISPLACEMENT VS. TIME
Plot A: Gundseal - Bentonite Side Up - 3:1 Slope

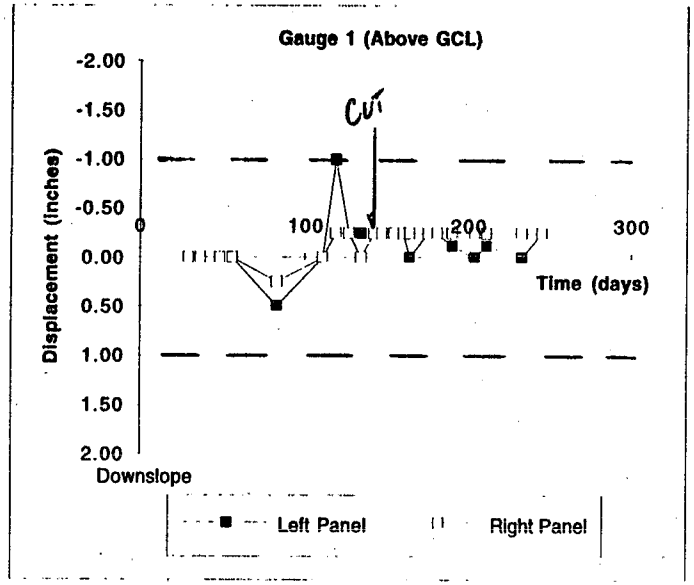

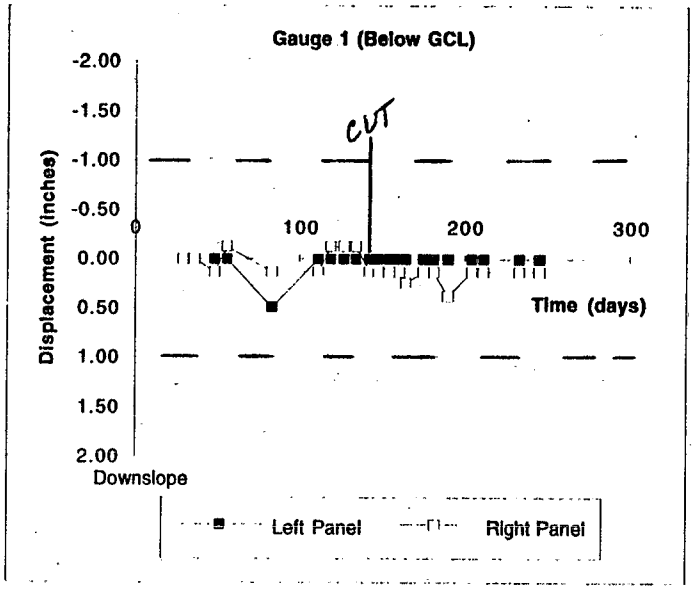

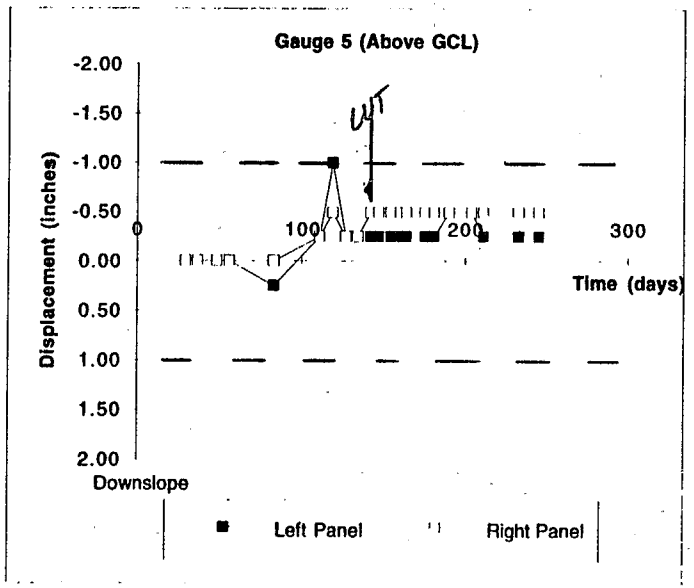

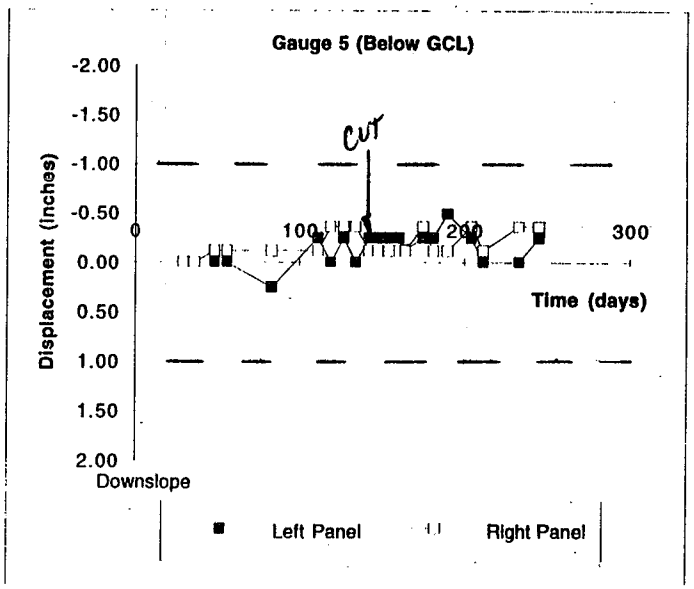

STEADY-STATE DISPLACEMENT VS. TIME
Plot B: Bentomat - 3:1 Slope

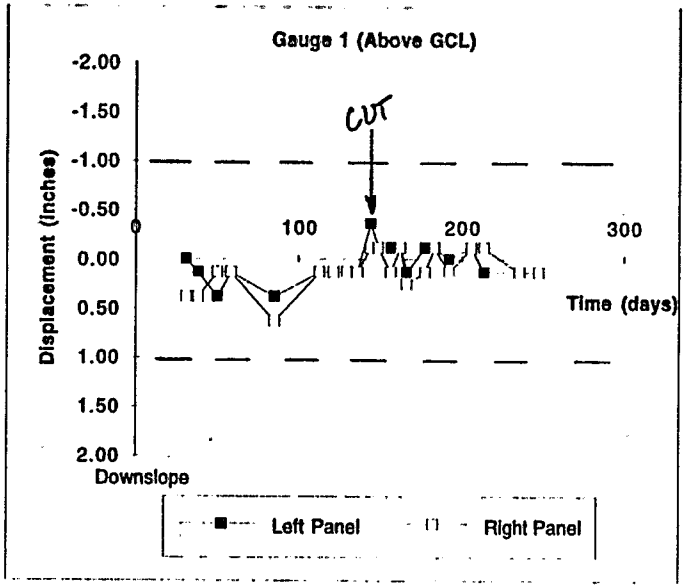

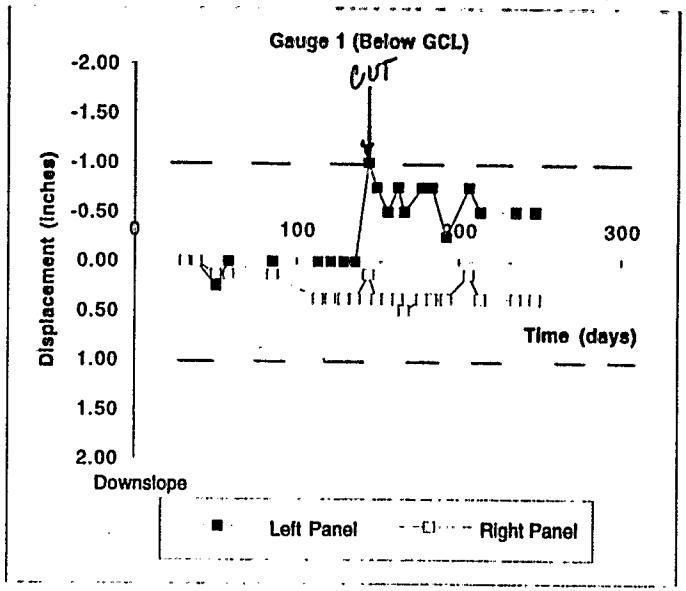

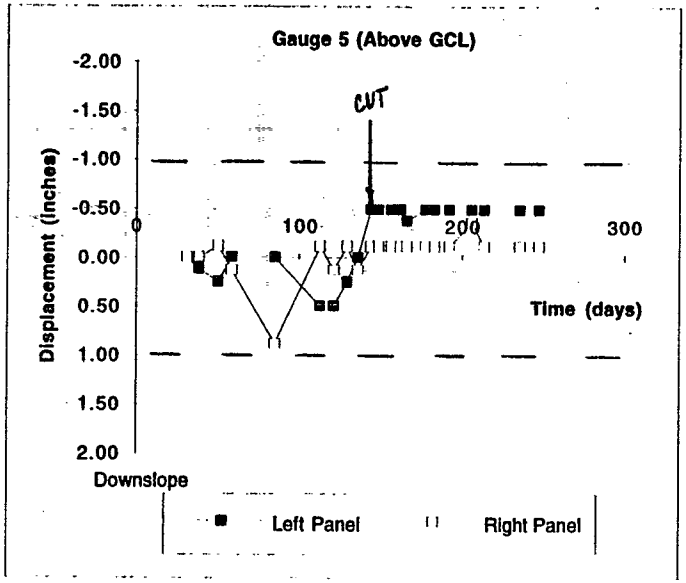

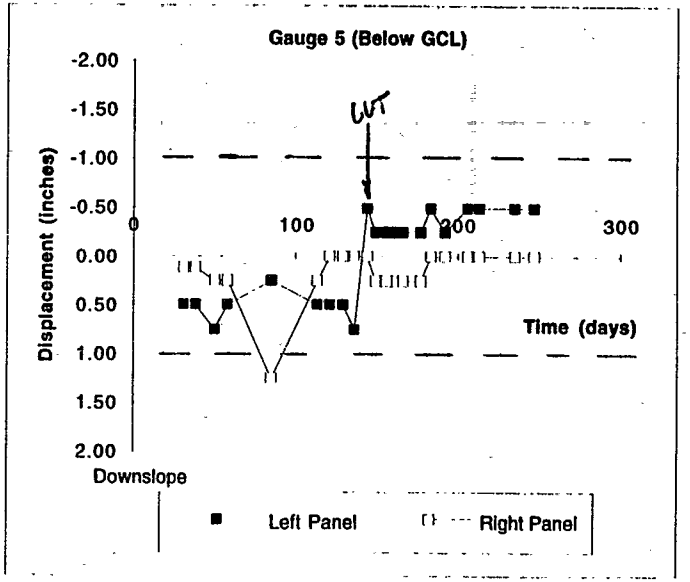

STEADY-STATE DISPLACEMENT VS. TIME
Plot C: Claymax - 3:1 Slope

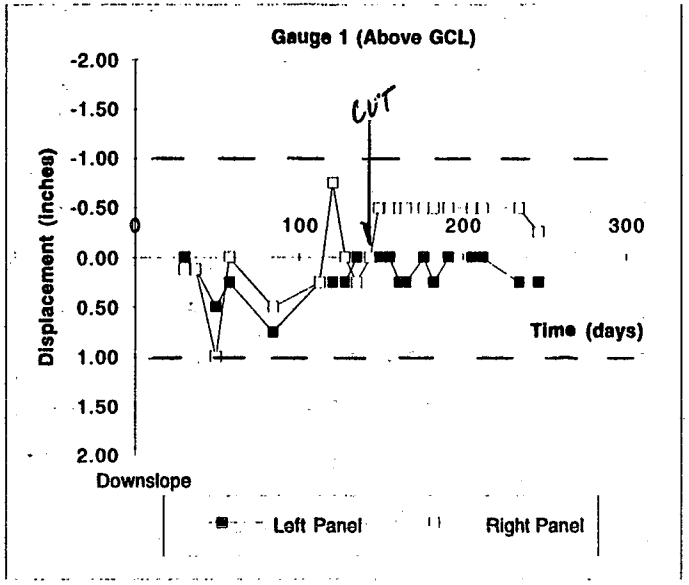

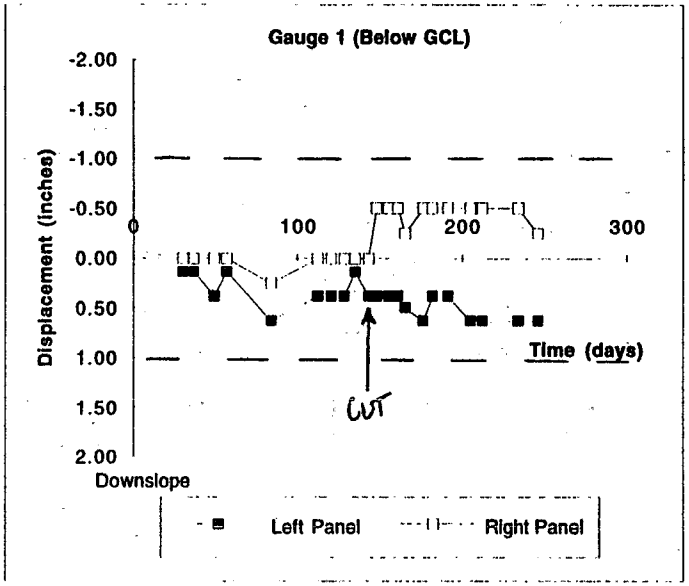

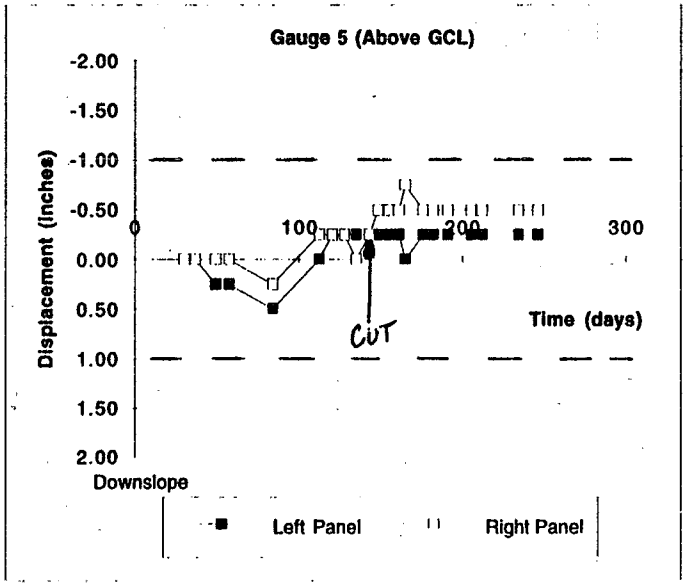

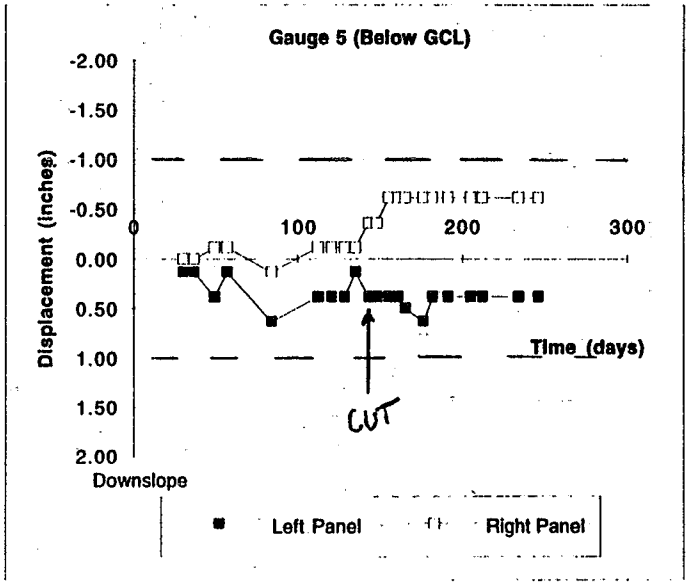

STEADY-STATE DISPLACEMENT VS. TIME
Plot D: Bentofix II (NW up) - 3:1 Slope

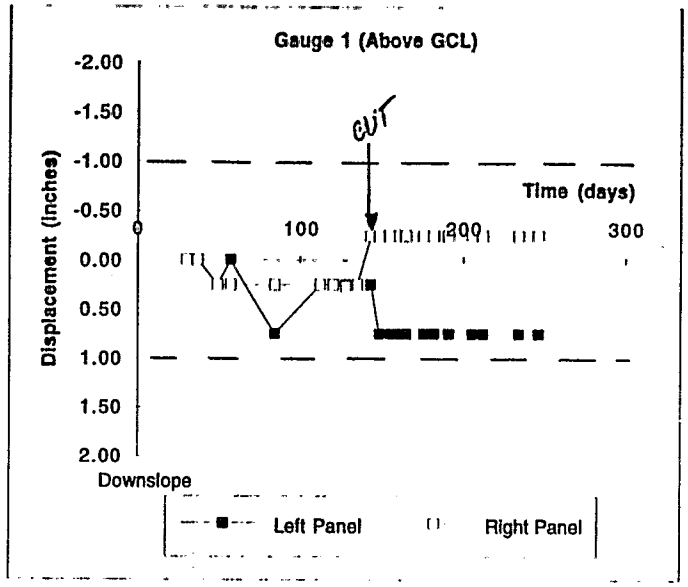

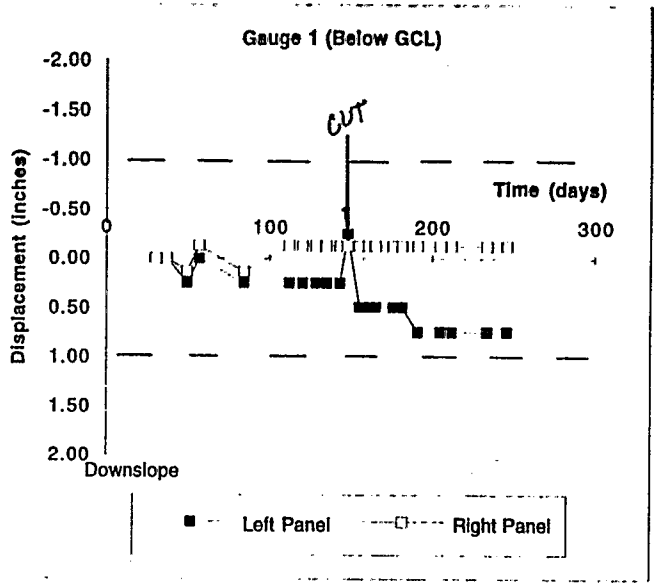

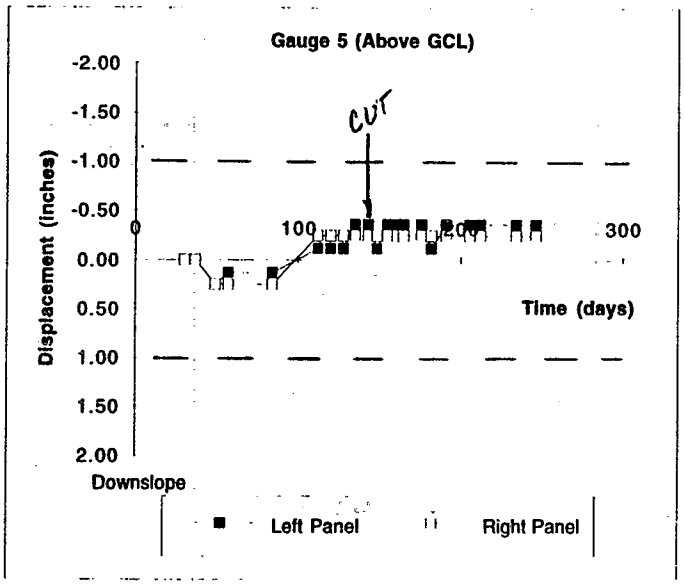

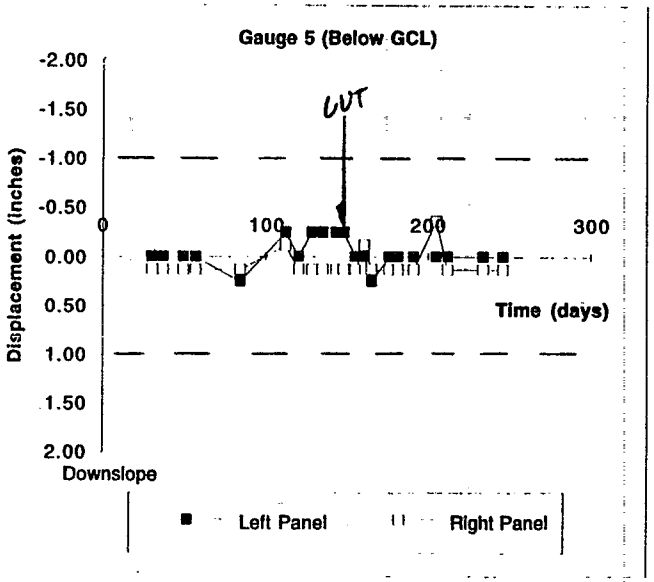

STEADY-STATE DISPLACEMENT VS. TIME
Plot E: Gundseal - Bentonite Side Down - 3:1 Slope

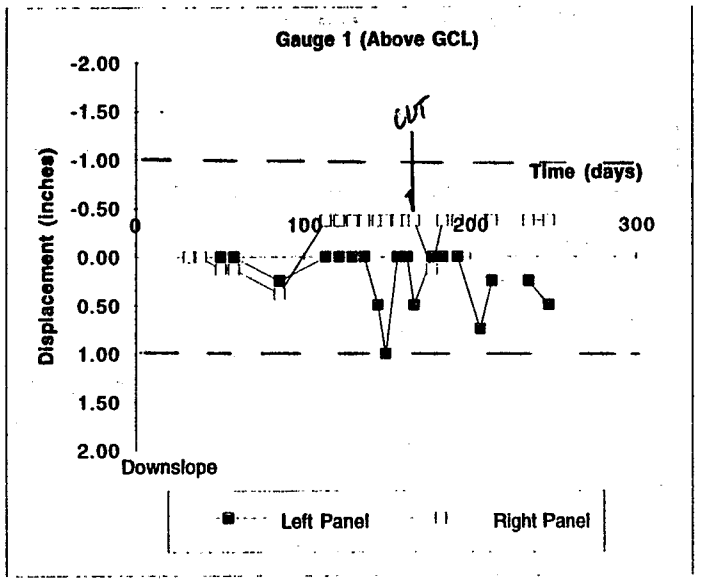

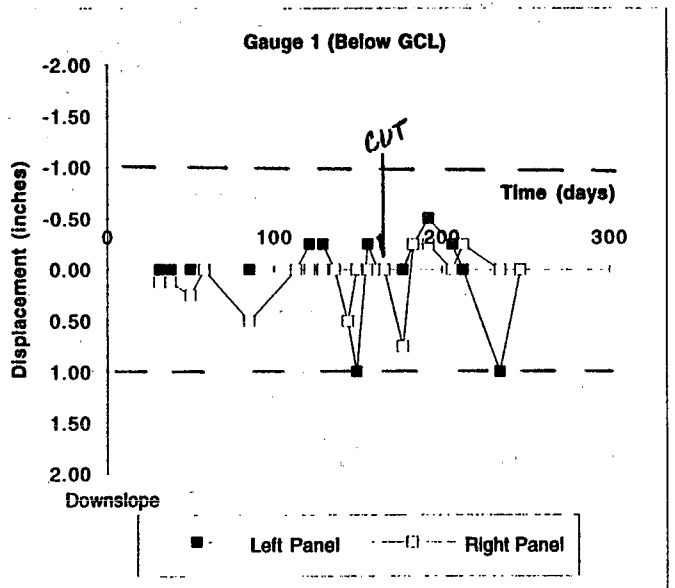

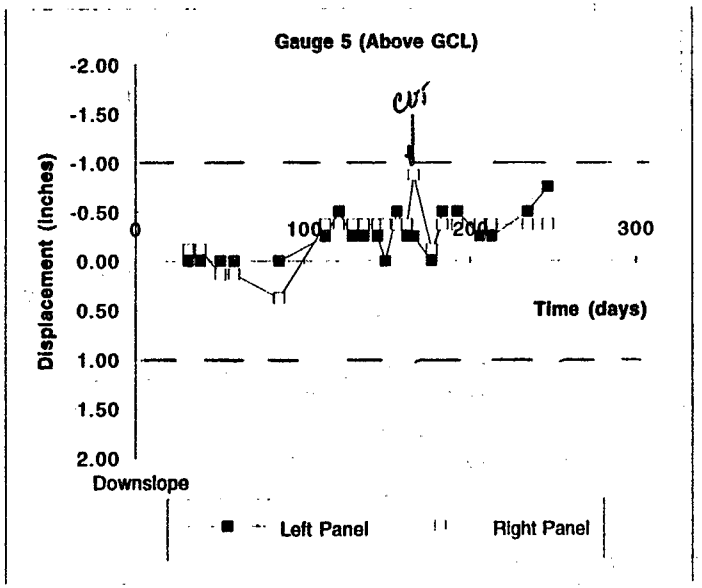

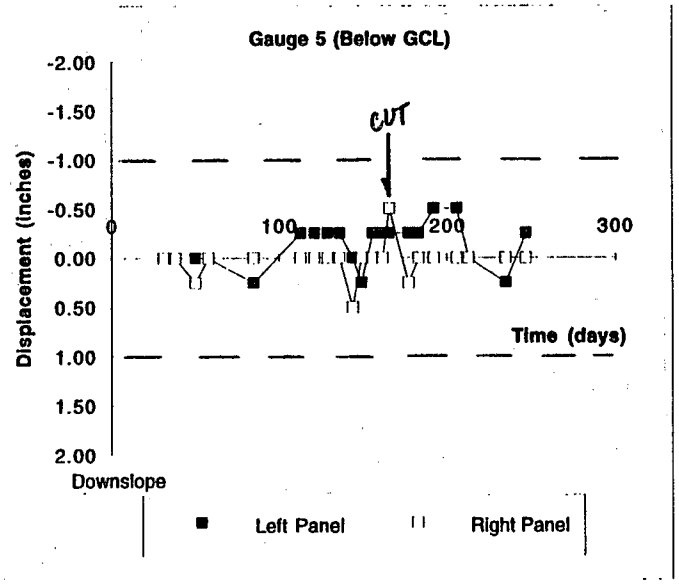

STEADY-STATE DISPLACEMENT VS. TIME
Plot H: Claymax - 2:1 Slope

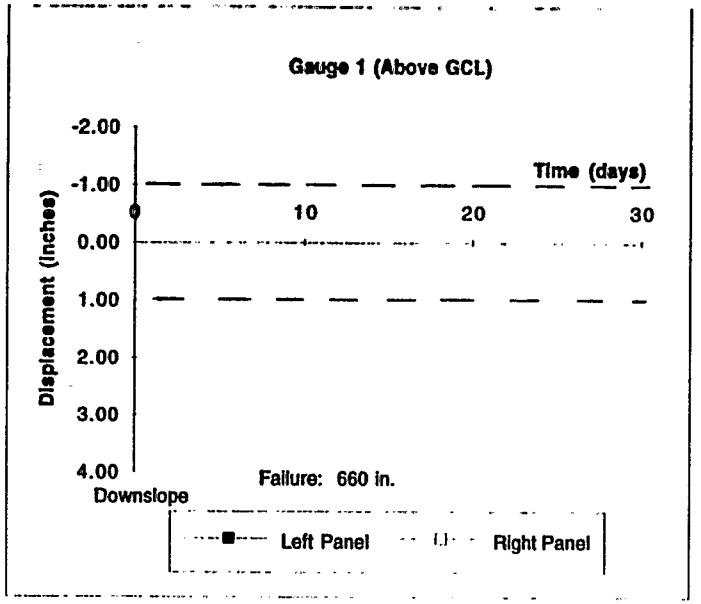

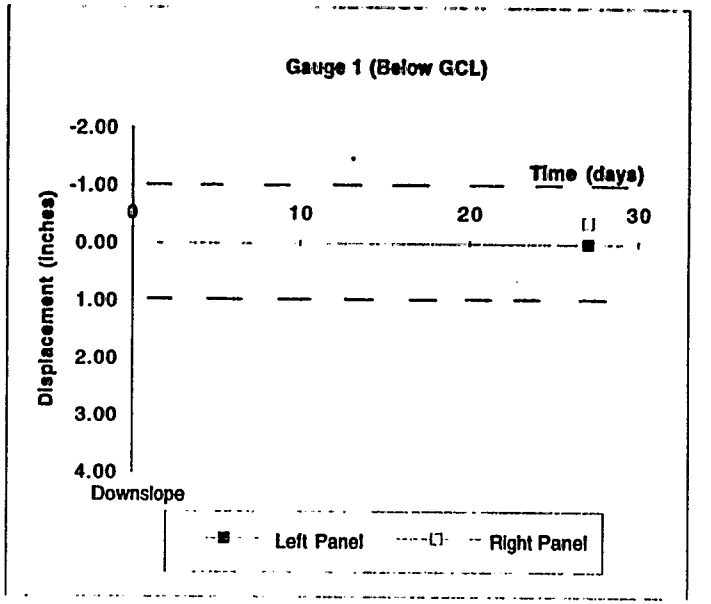

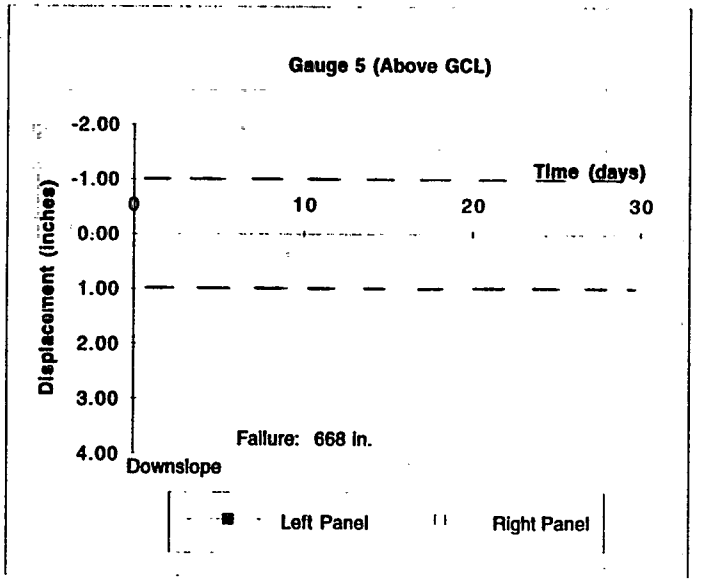

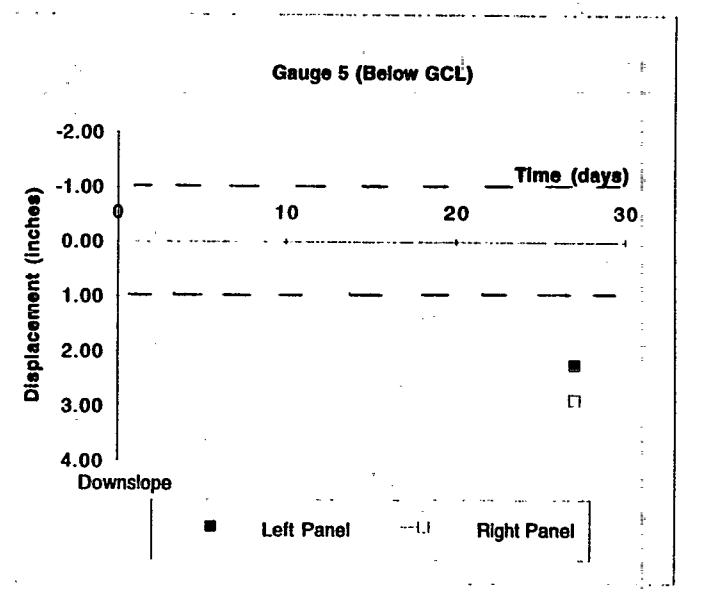

STEADY-STATE DISPLACEMENT VS. TIME
Plot I: Bentofix I - 2:1 Slope

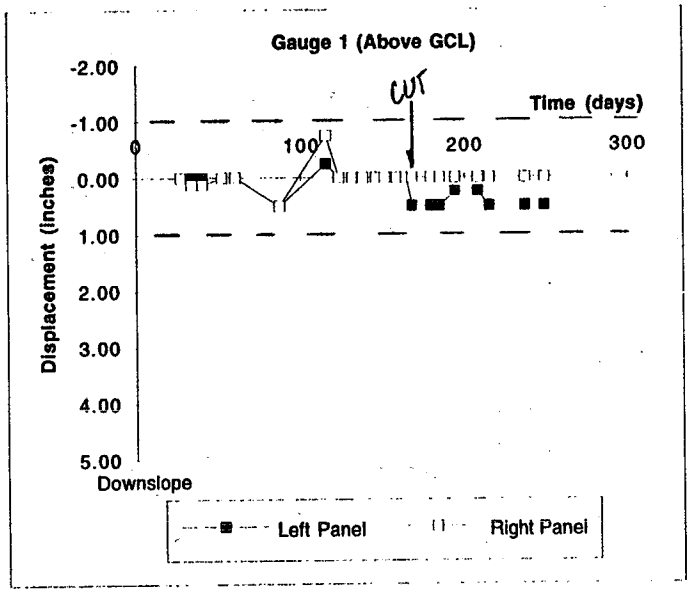

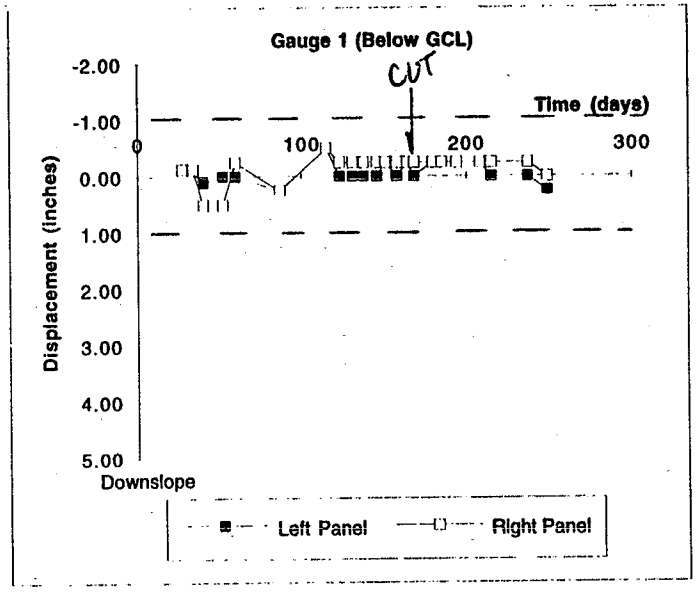

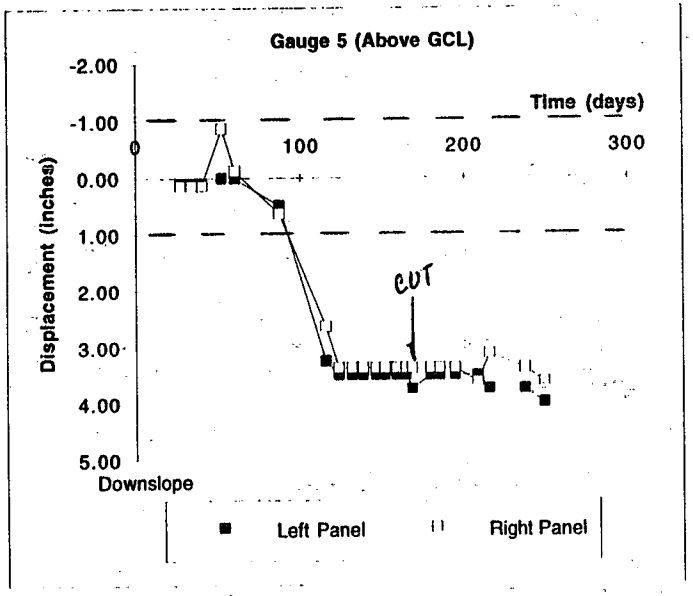

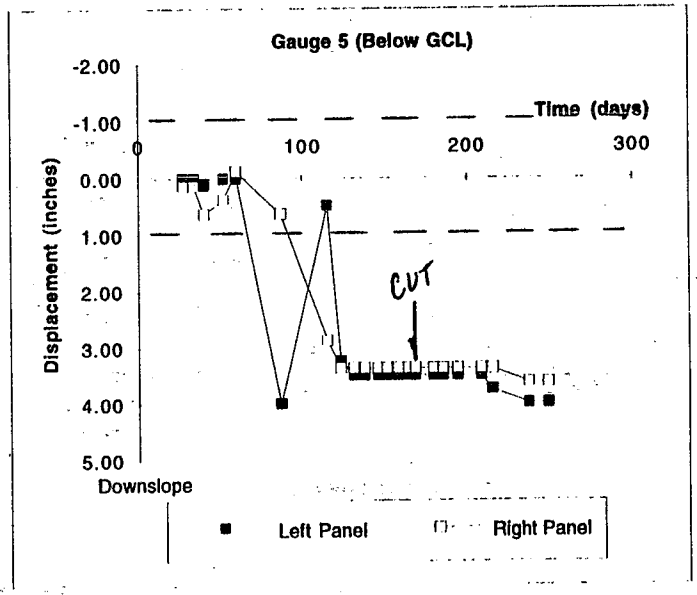

STEADY-STATE DISPLACEMENT VS. TIME
Plot J: Bentomat - Granular Drainage - 2:1 Slope

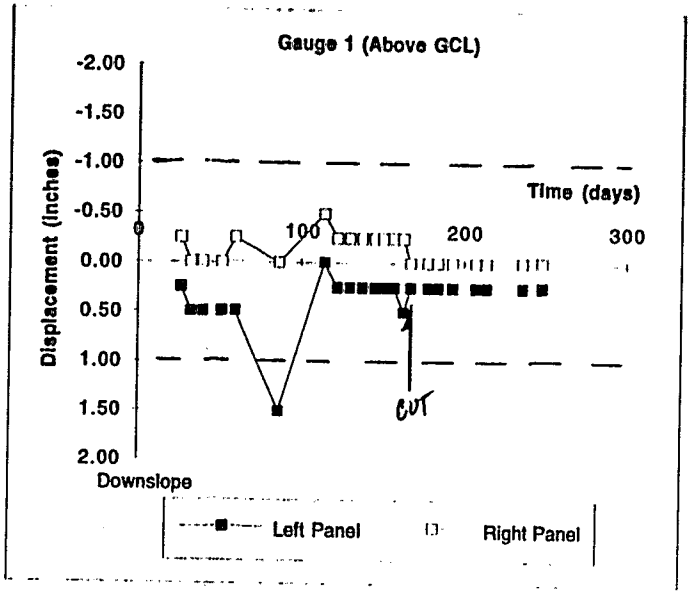

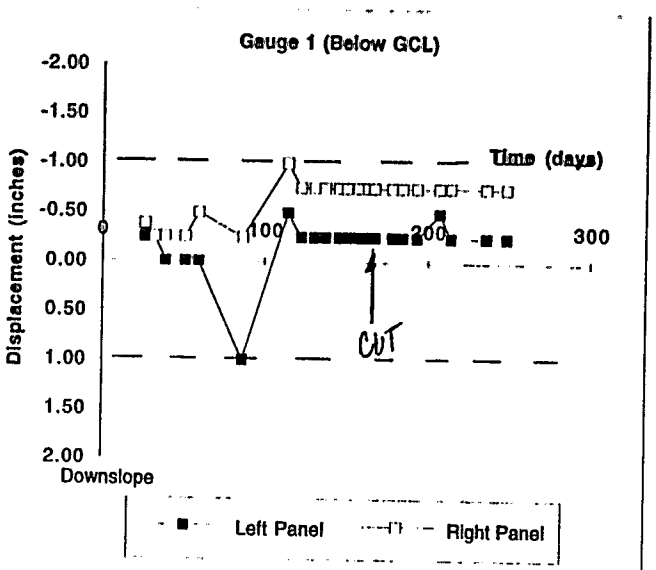

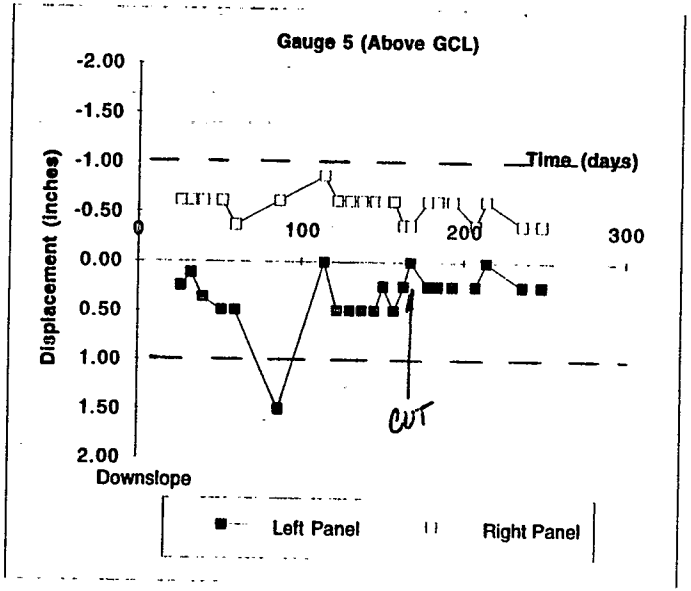

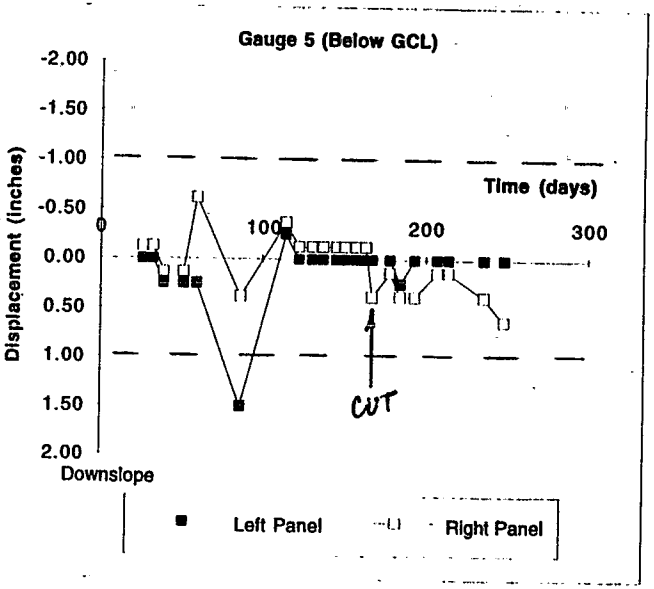

STEADY-STATE DISPLACEMENT VS. TIME
Plot K: Claymax - Granular Drainage - 2:1 Slope

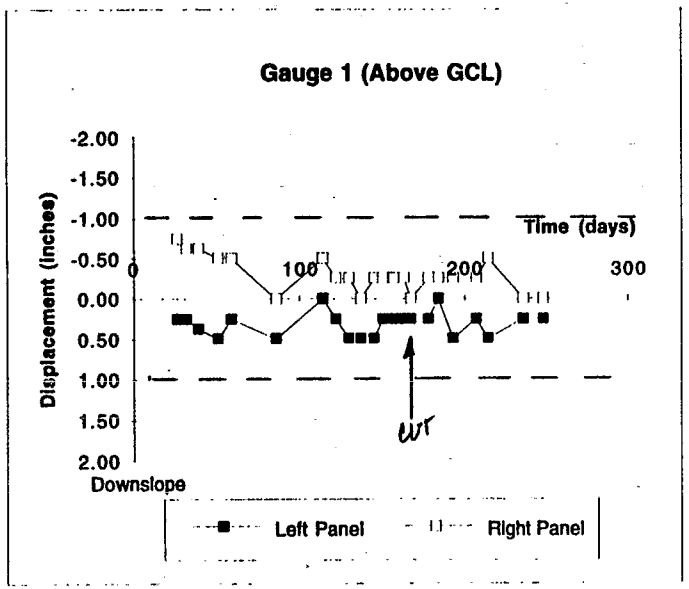

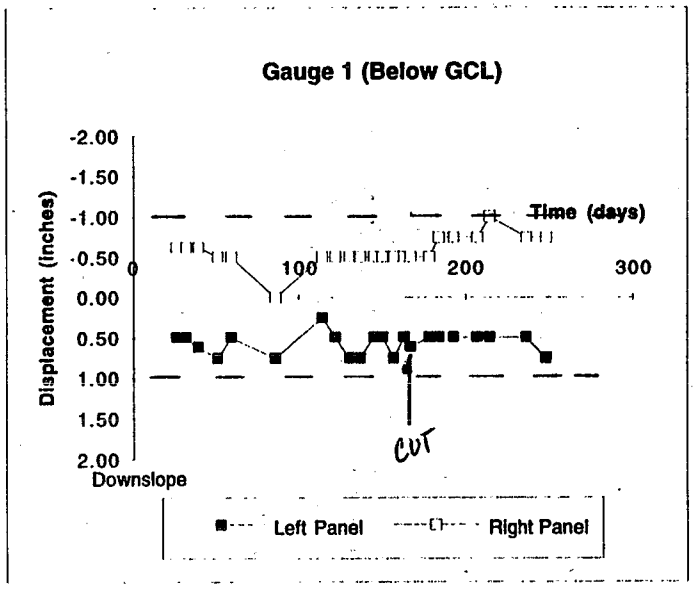

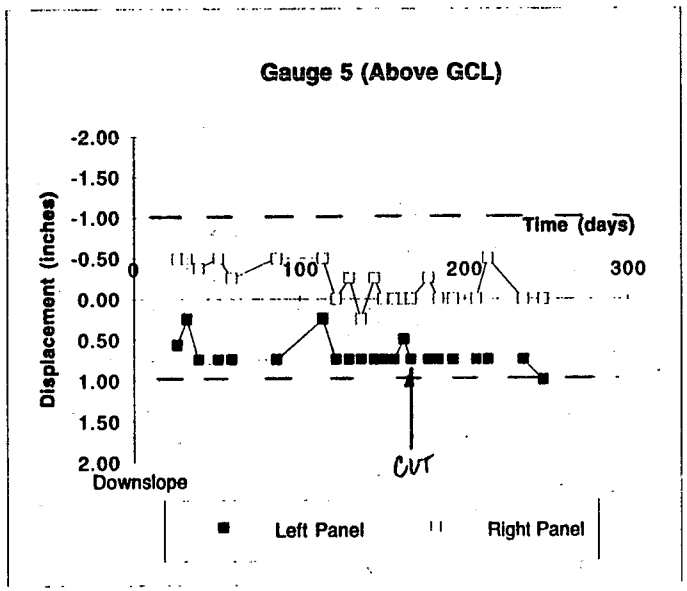

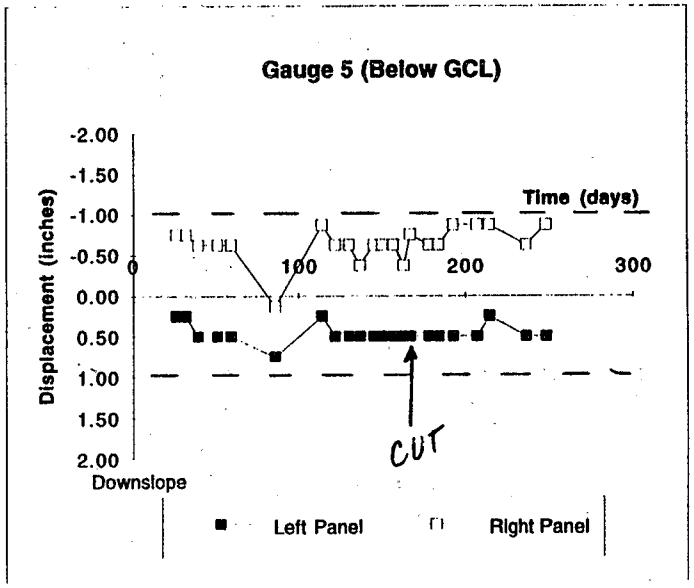

STEADY-STATE DISPLACEMENT VS. TIME
Plot L: Bentofix - Granular Drainage I - 2:1 Slope

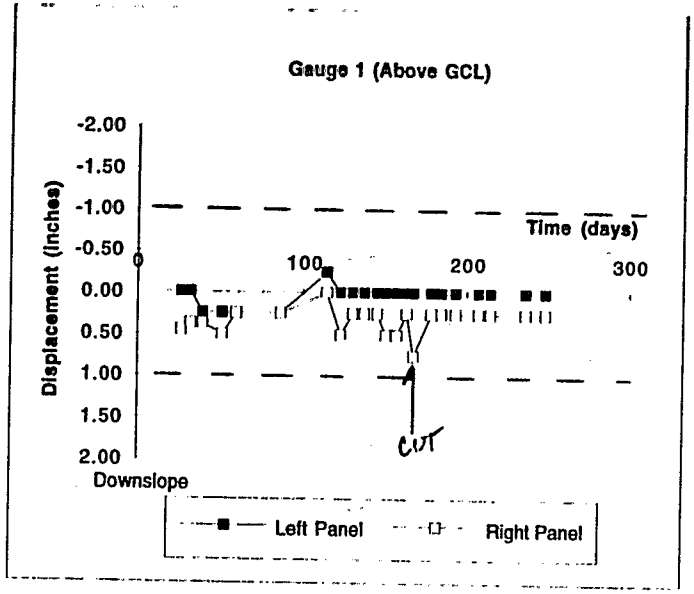

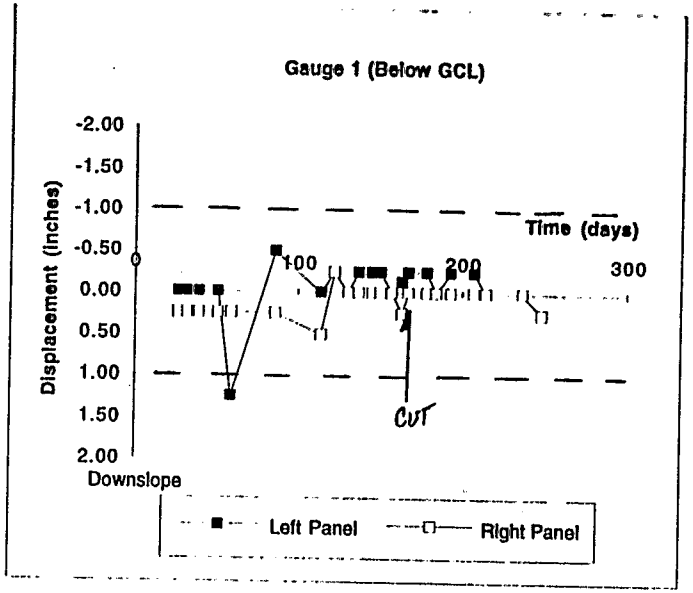

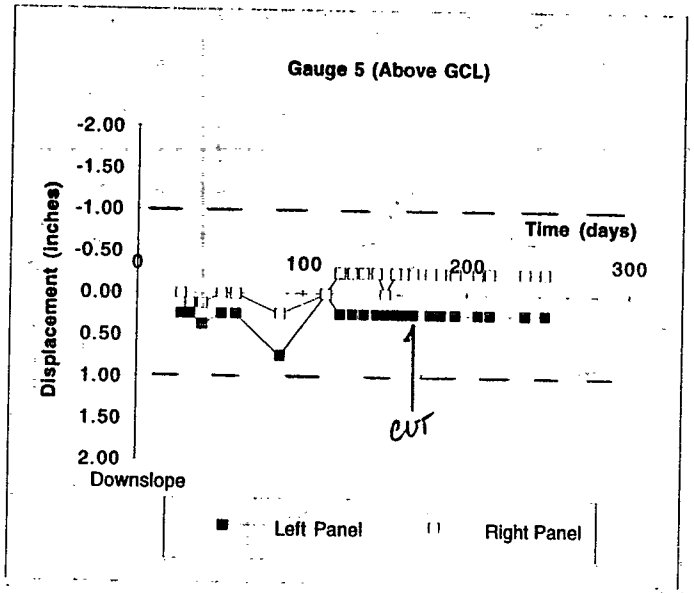

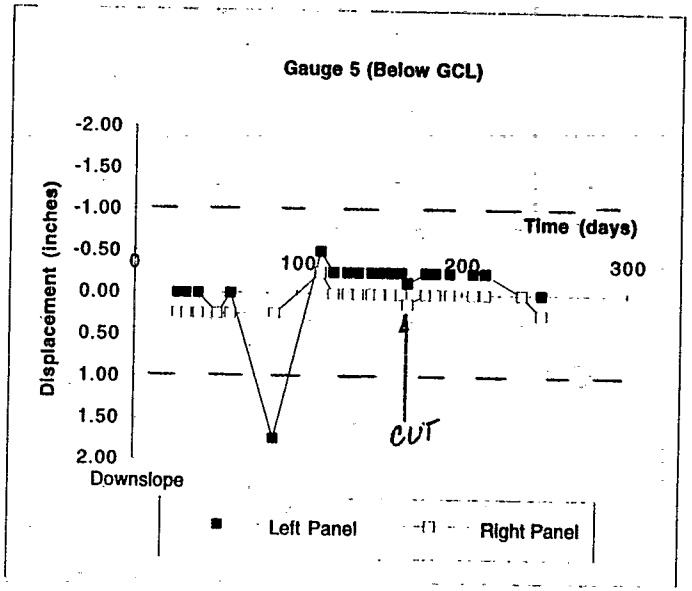

STEADY-STATE DISPLACEMENT VS. TIME
Plot N: Bentofix II (NW up) - 2:1 Slope

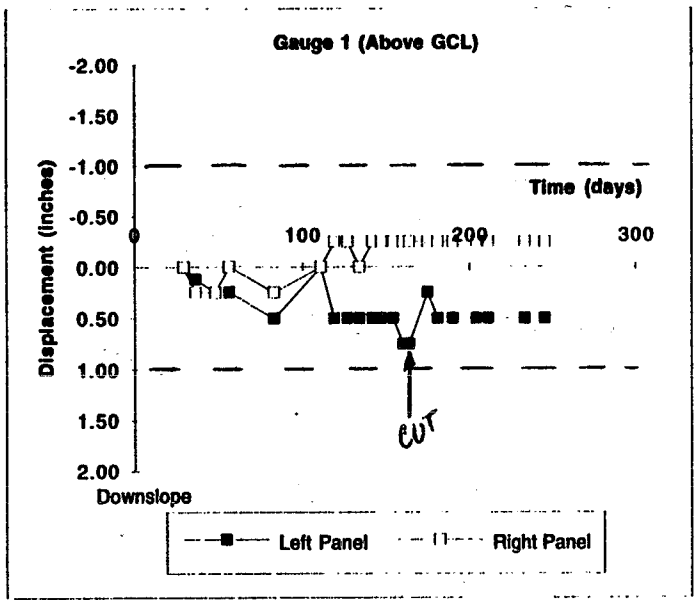

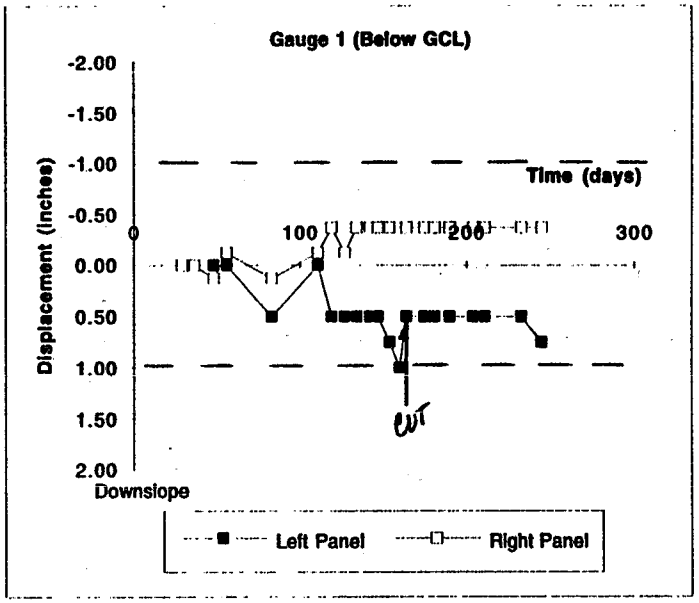

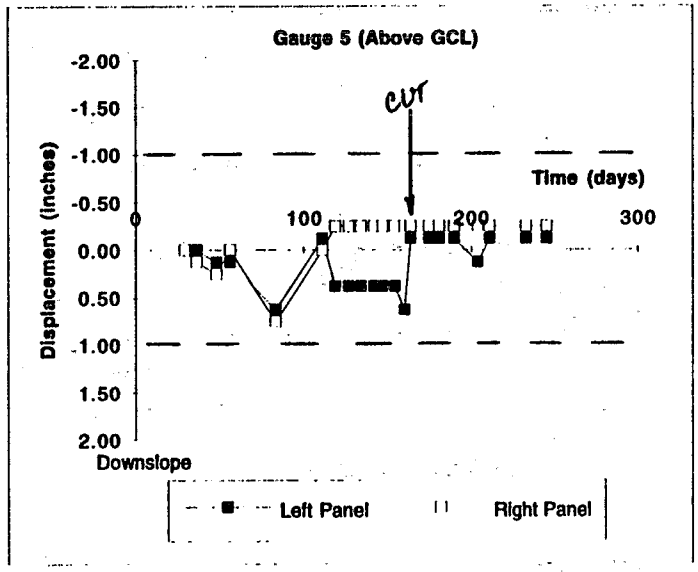

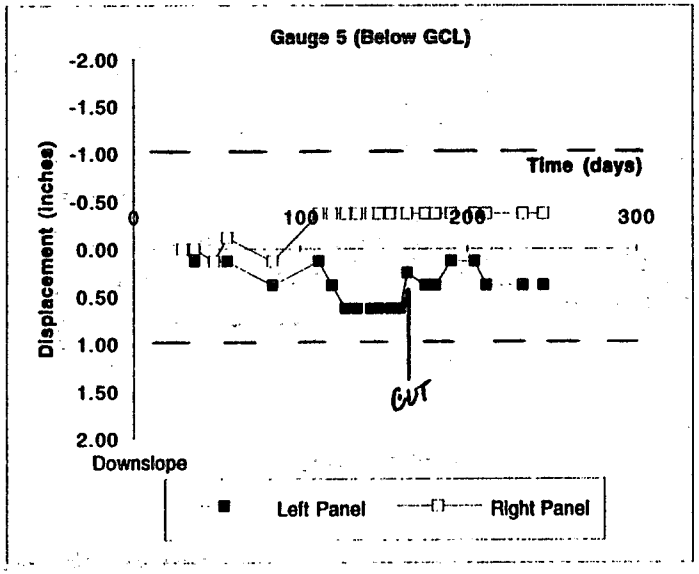

PLOT P Gundseal (bentonite up) - 2:1 Slope

Moisture Readings vs. Time

Plot Location: Crest

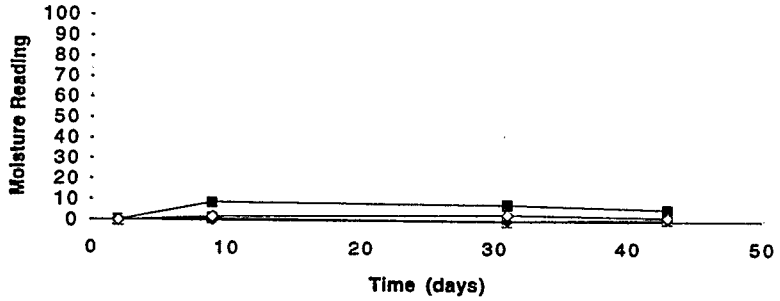

Plot Location: Upper Middle

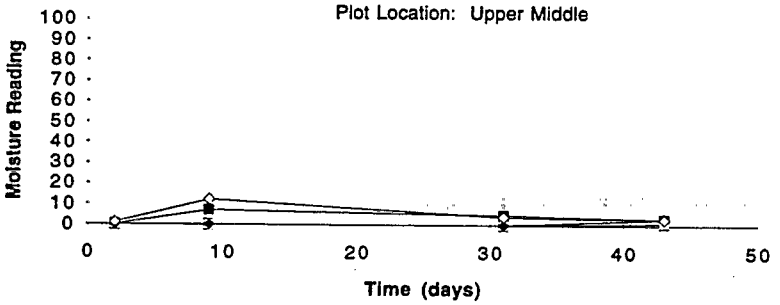

Plot Location: Lower Middle

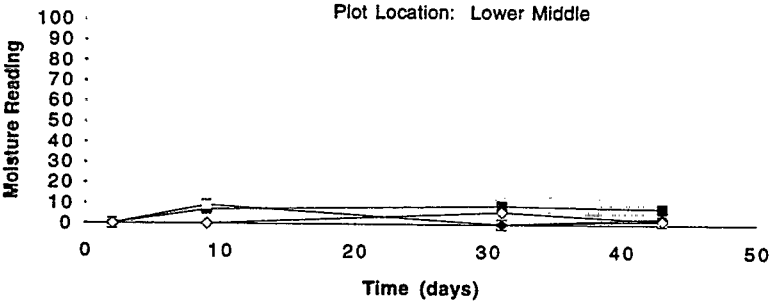

Plot Location: Toe

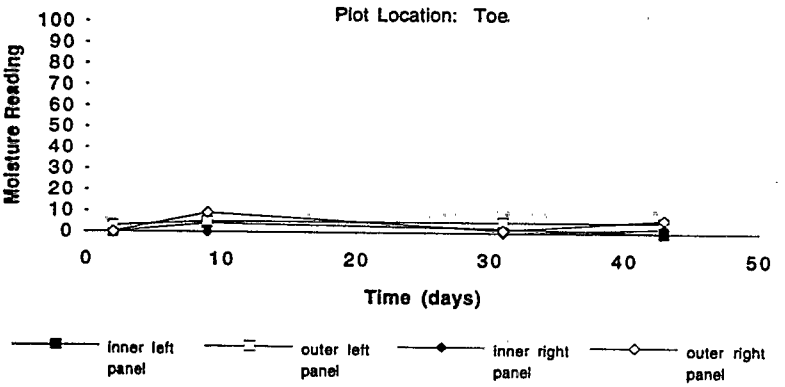

Appendix C

Differential Displacement in Test Plots

Displacement Above GCL - Displacement Below GCL

PLOT A — Gundseal - Bentonite Side Up - 3:1 Slope

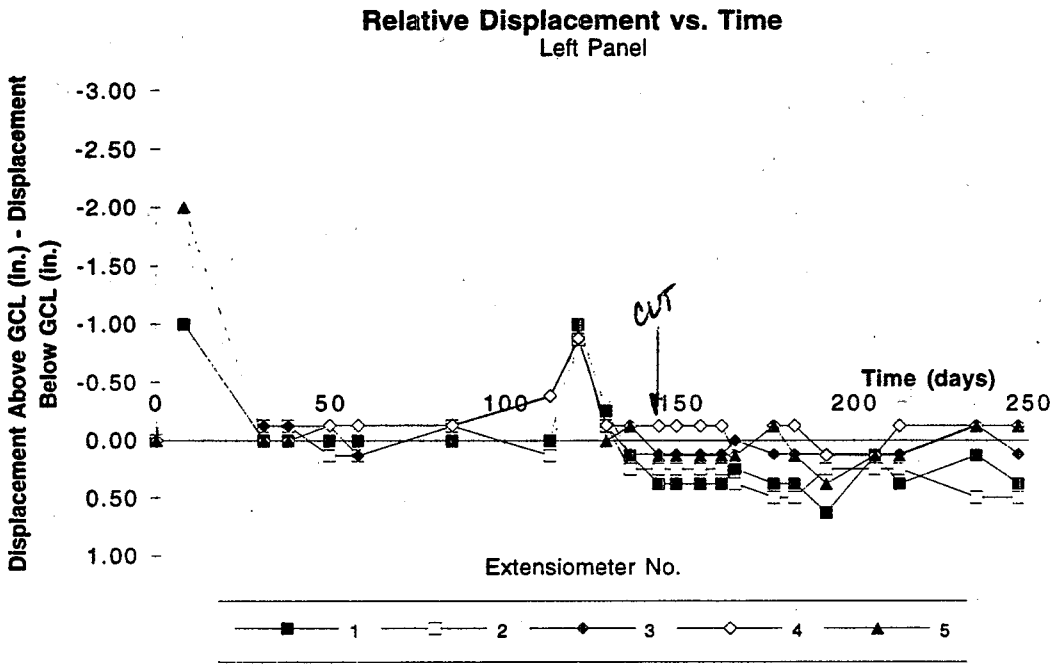

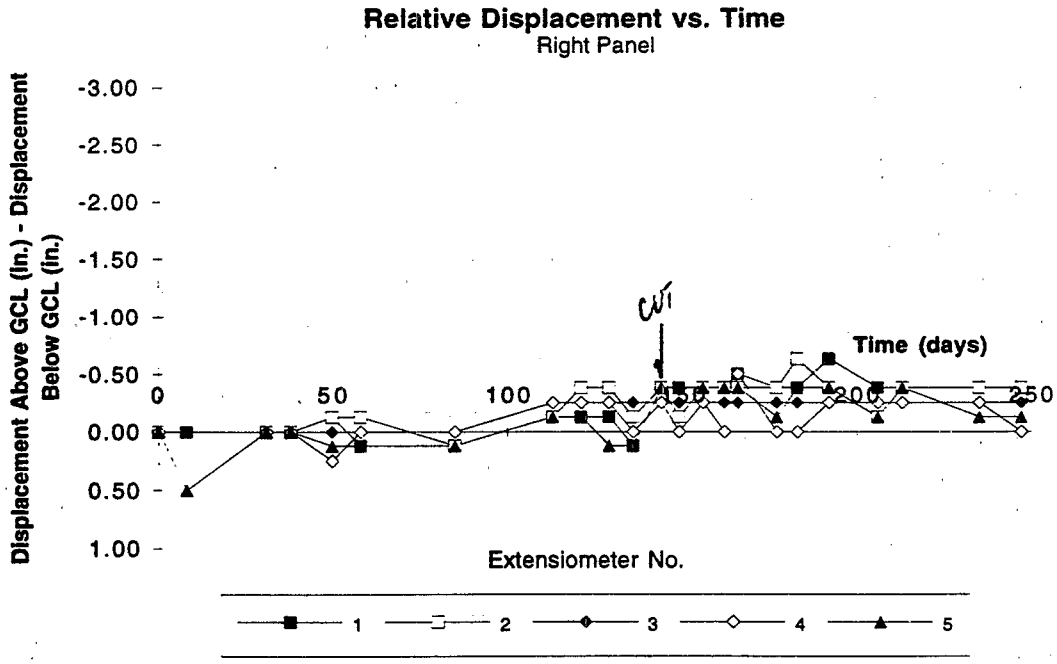

Displacement Above GCL - Displacement Below GCL

PLOT B Bentomat - 3:1 Slope

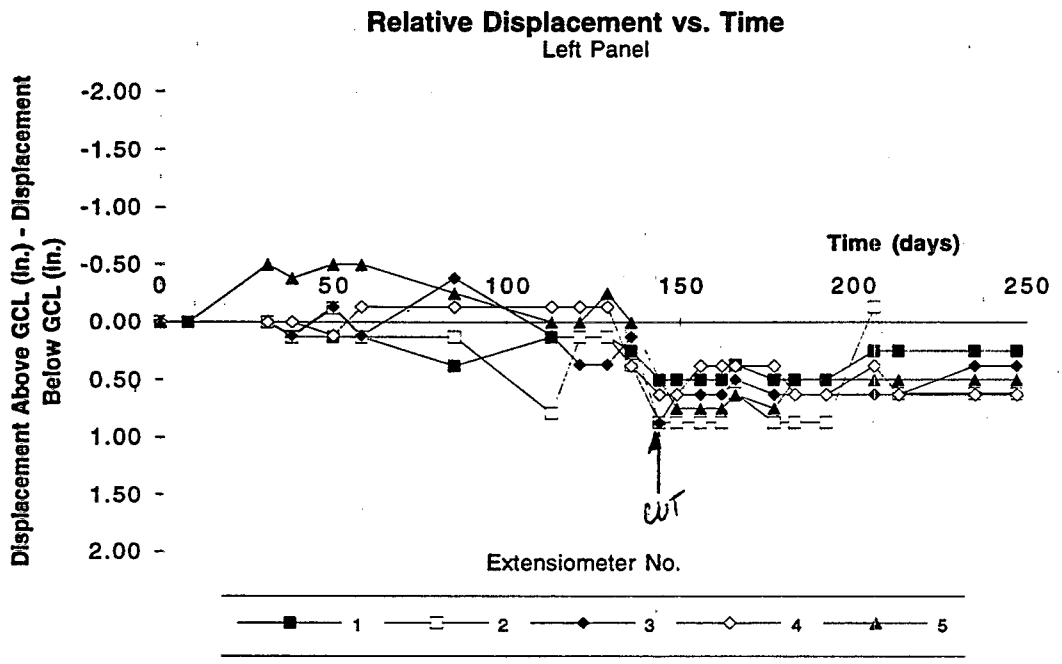

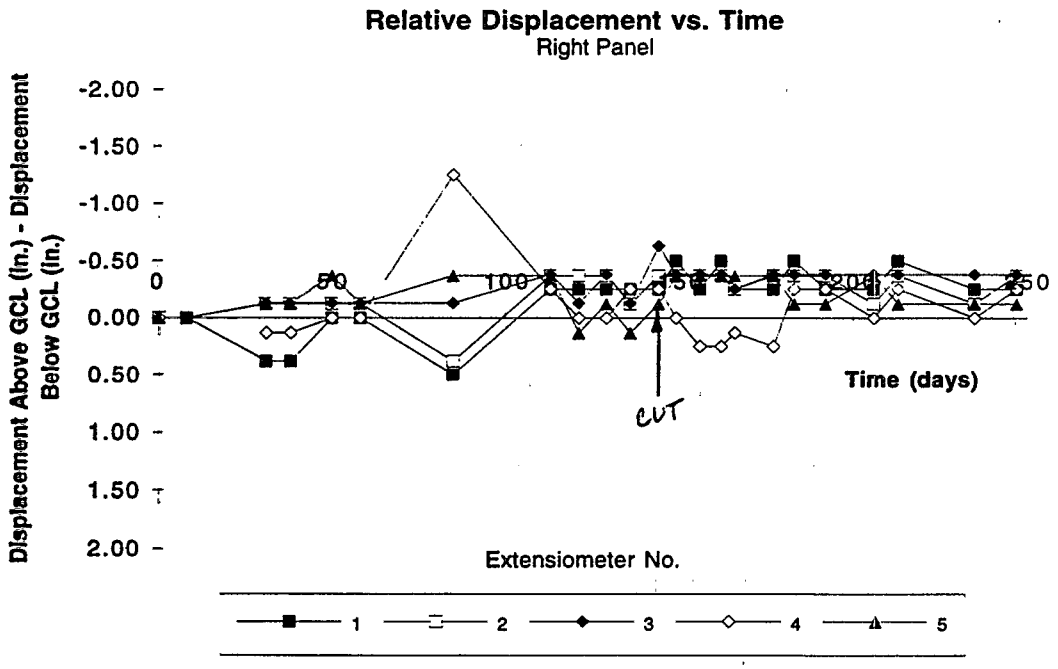

Displacement Above GCL - Displacement Below GCL

PLOT C Claymax - 3:1 Slope

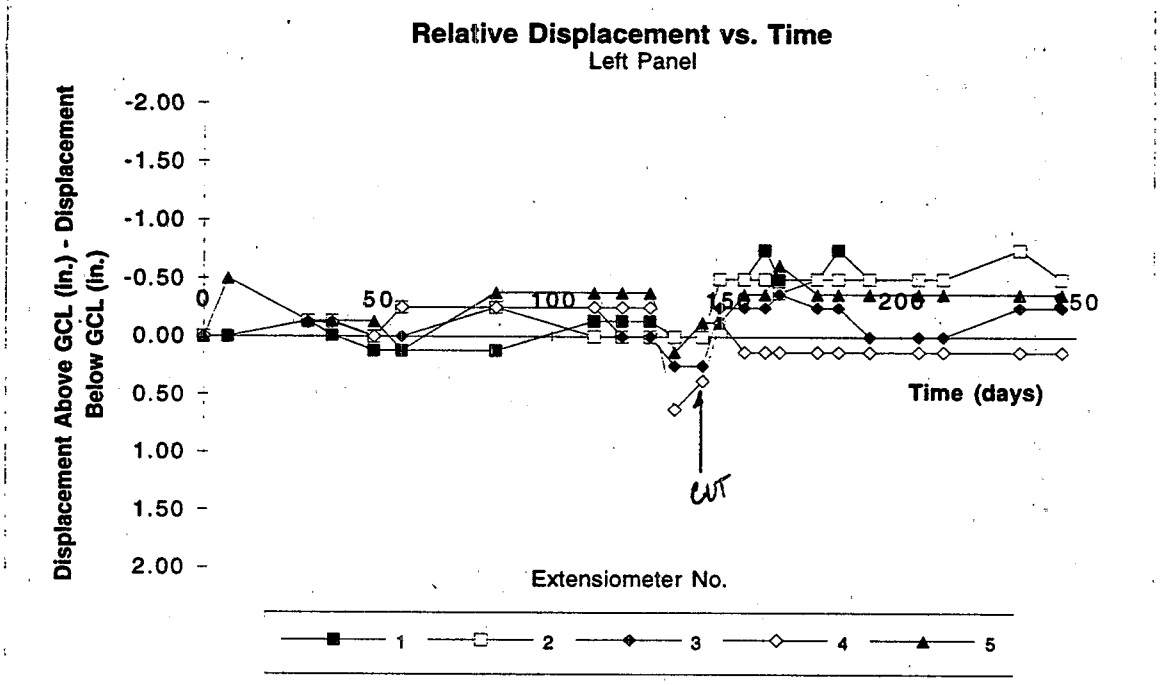

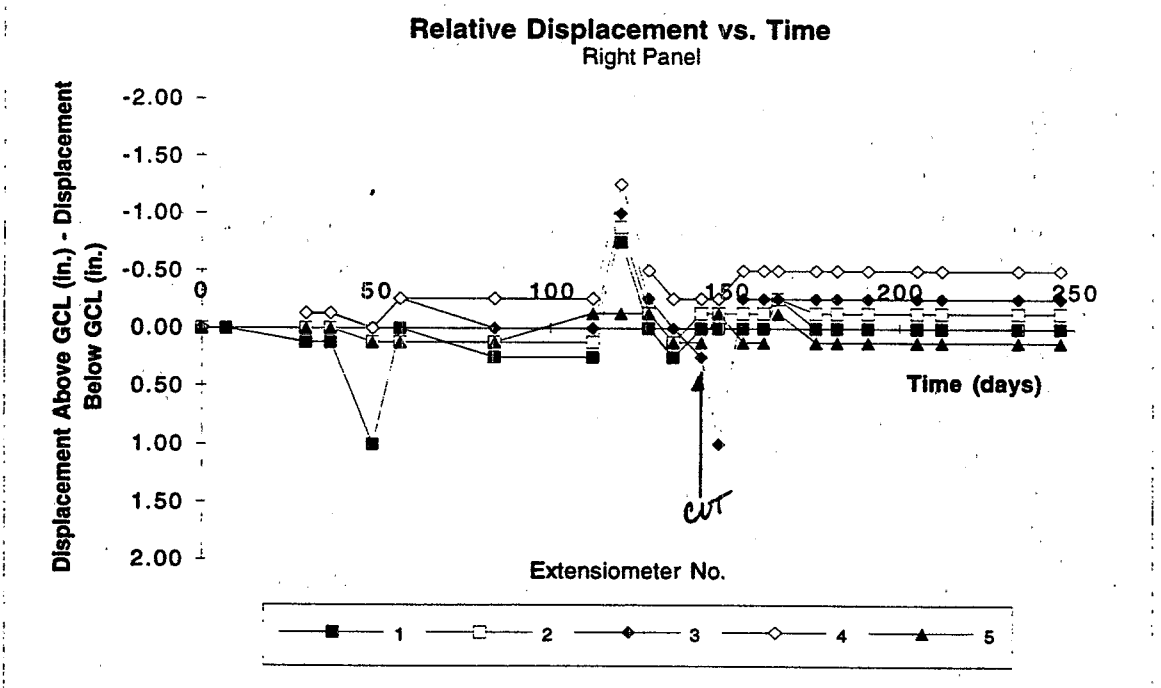

Displacement Above GCL - Displacement Below GCL

PLOT D — Bentofix II (NW up) - 3:1 Slope

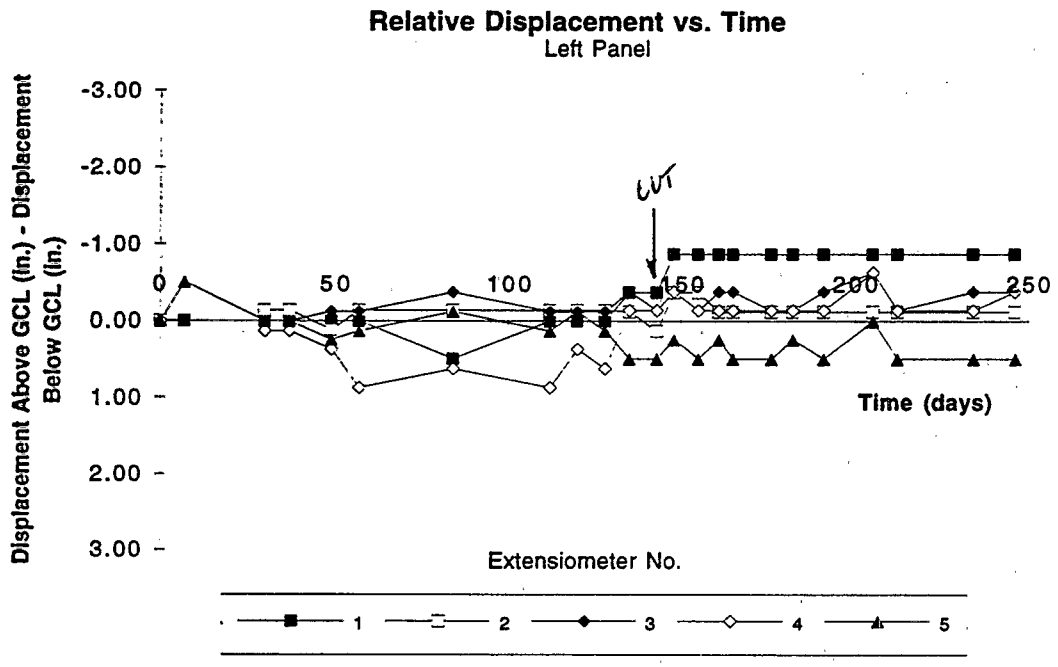

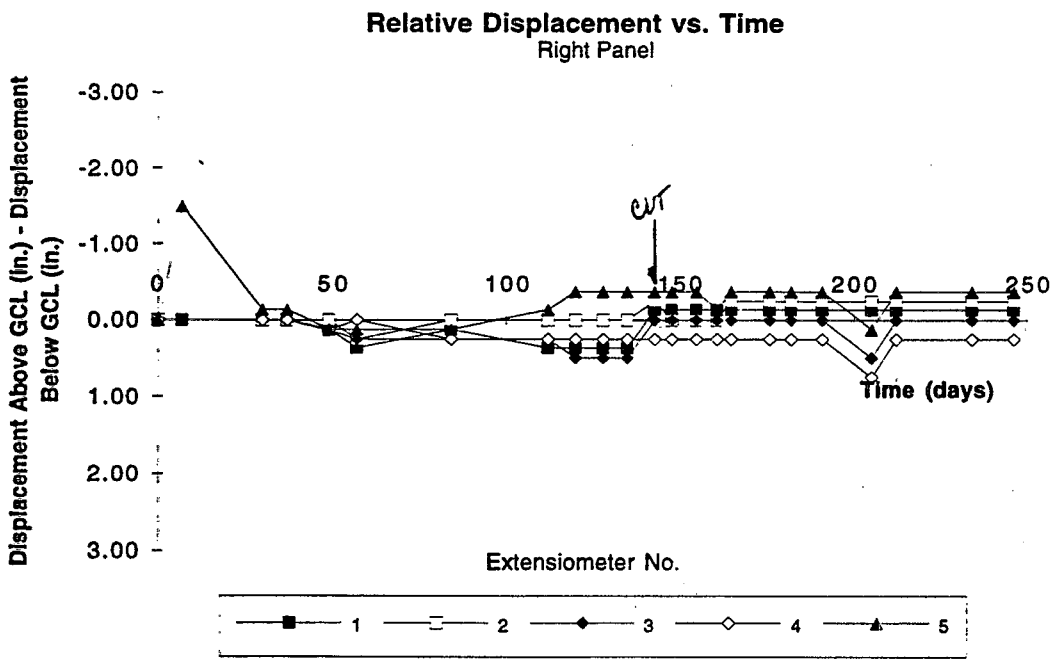

Displacement Above GCL - Displacement Below GCL

PLOT E Gundseal - Bentonite Down - 3:1 Slope

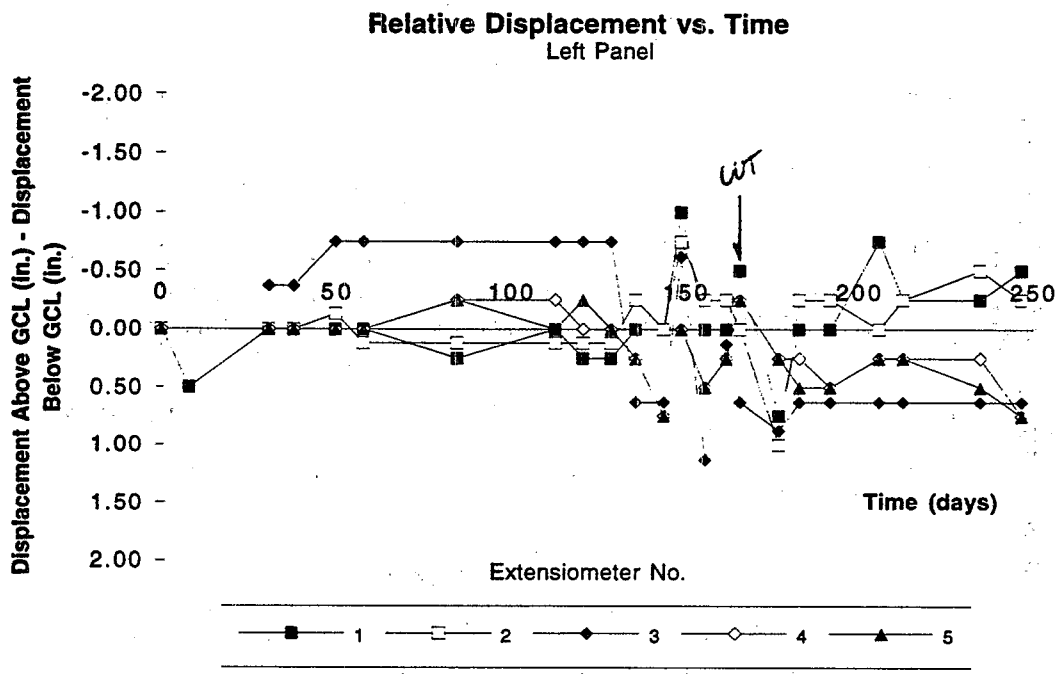

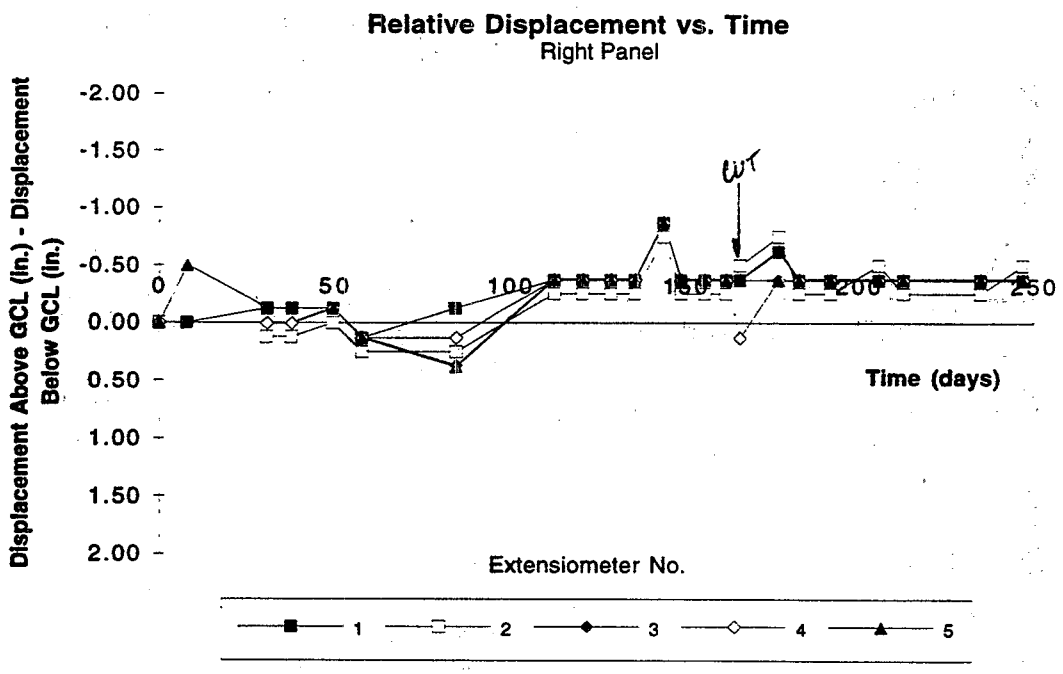

Displacement Above GCL - Displacement Below GCL

PLOT F — Gundseal - Bentonite Up - 2:1 Slope

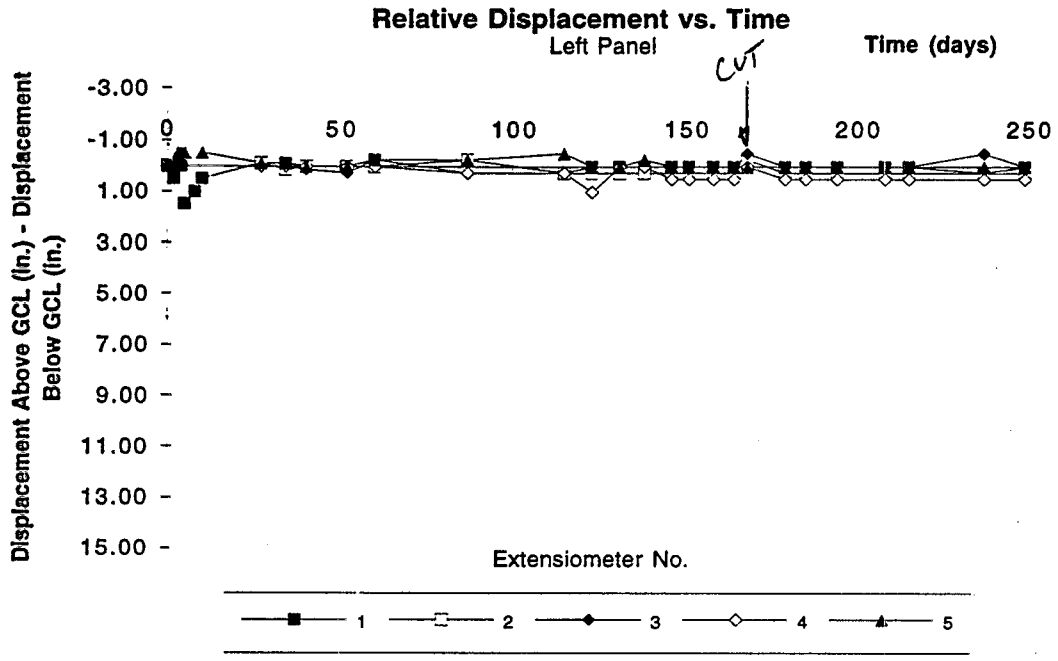

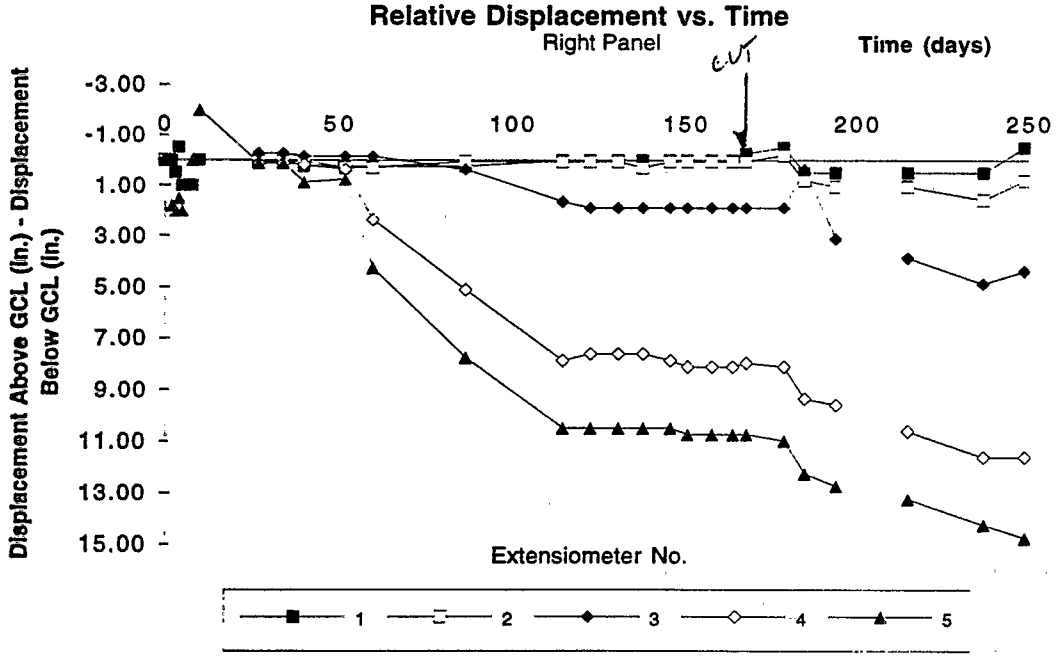

Displacement Above GCL - Displacement Below GCL

PLOT G Bentomat - 2:1 Slope

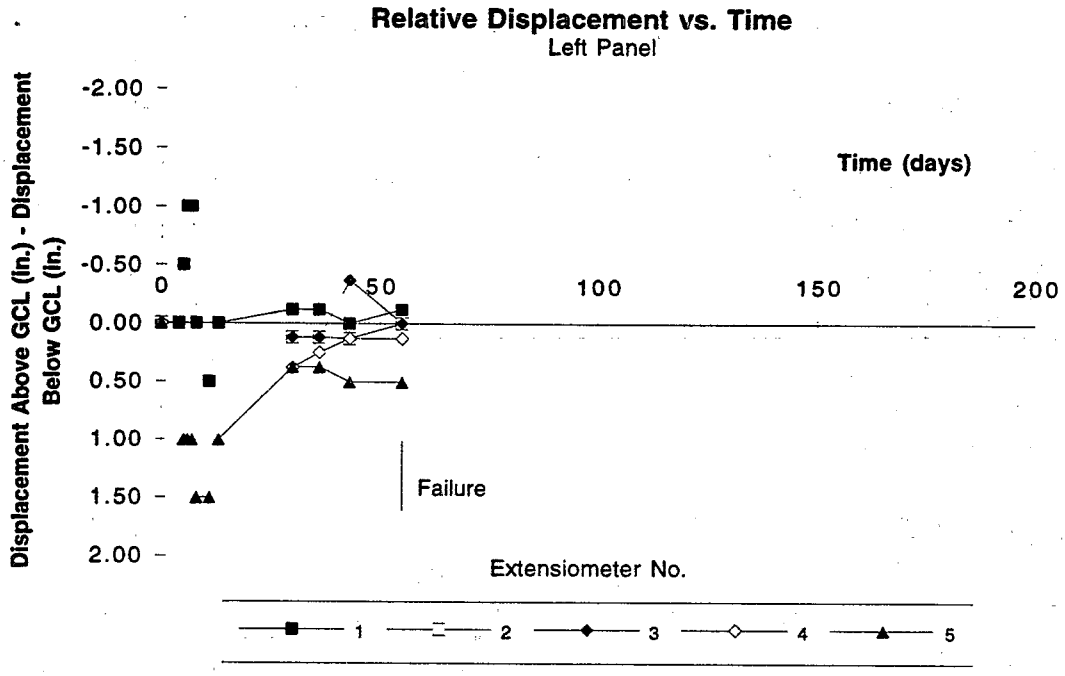

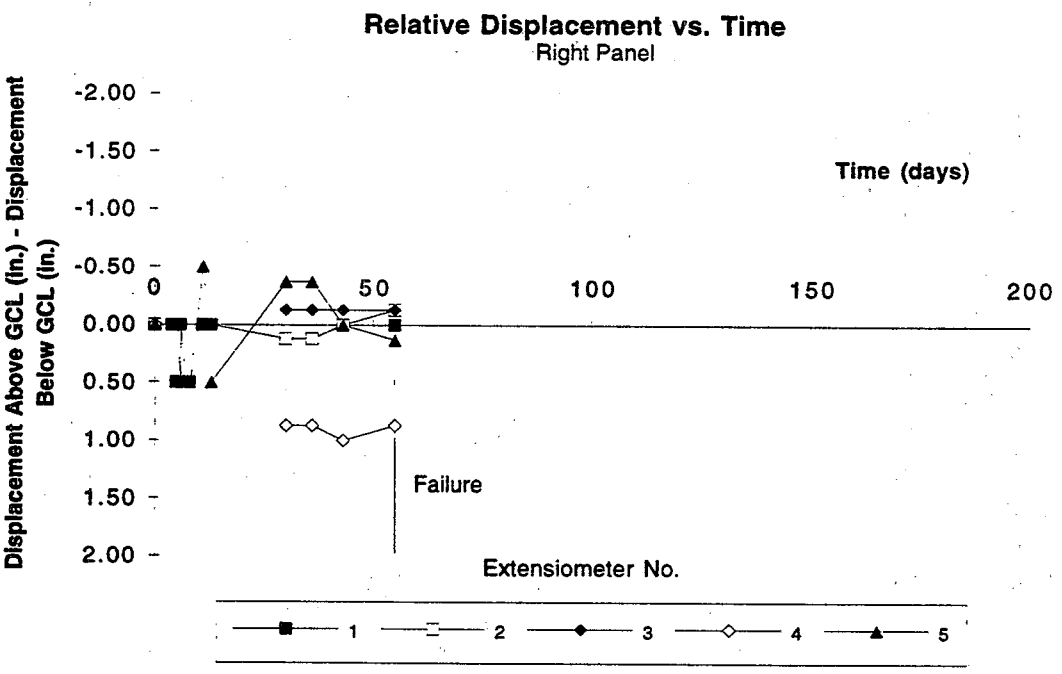

Displacement Above GCL - Displacement Below GCL

PLOT H Claymax - 2:1 Slope

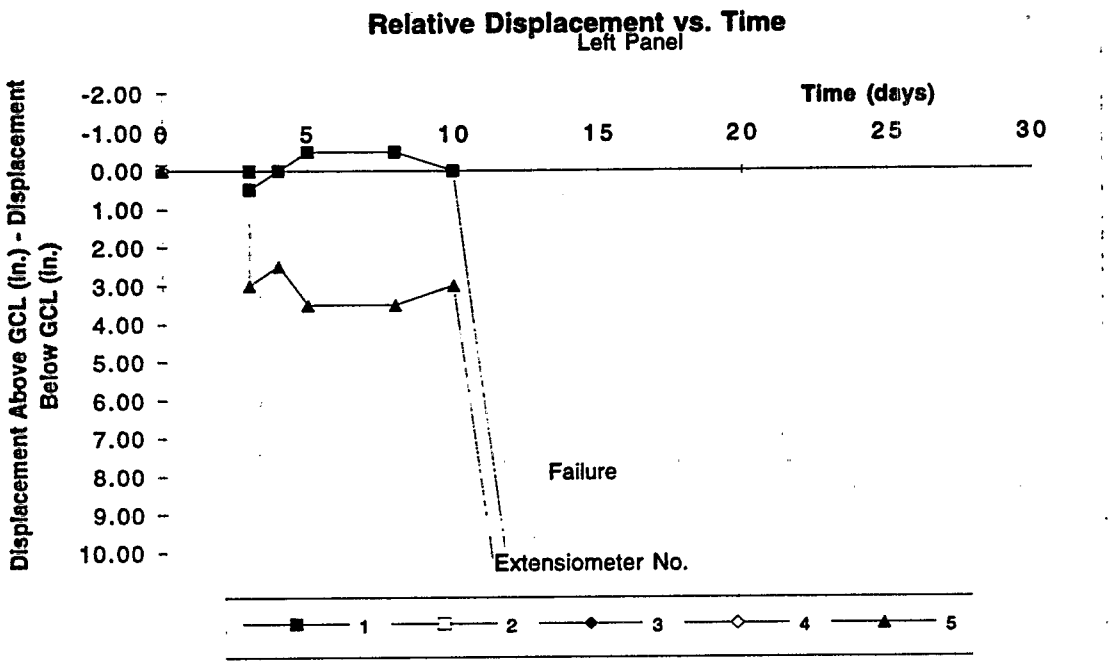

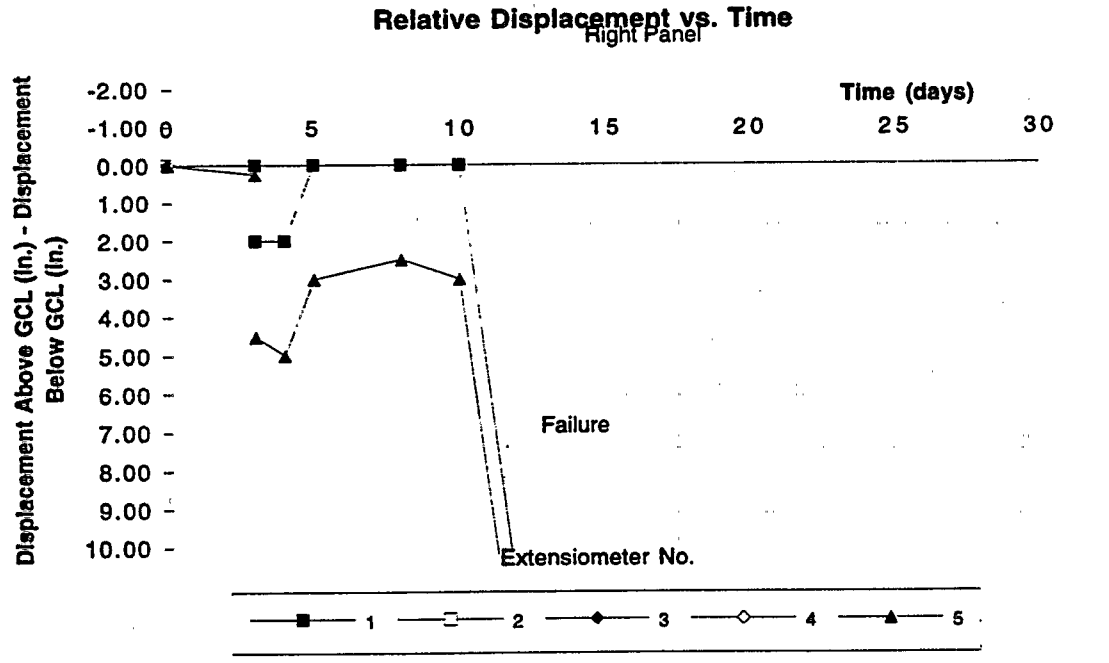

Displacement Above GCL - Displacement Below GCL

PLOT I Bentofix I - 2:1 Slope

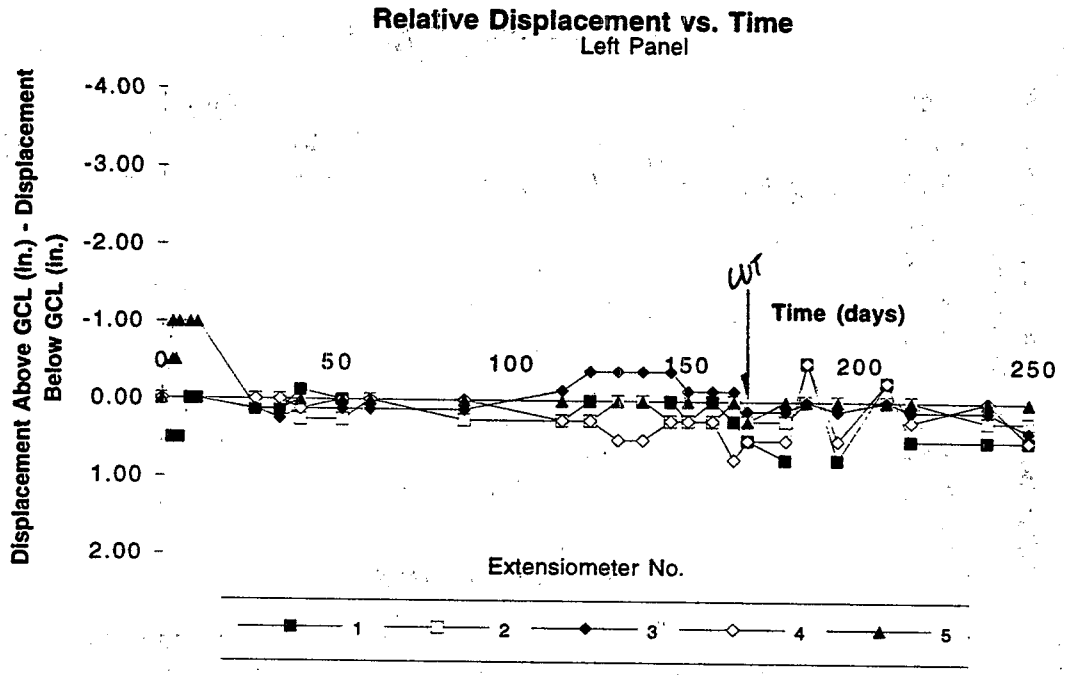

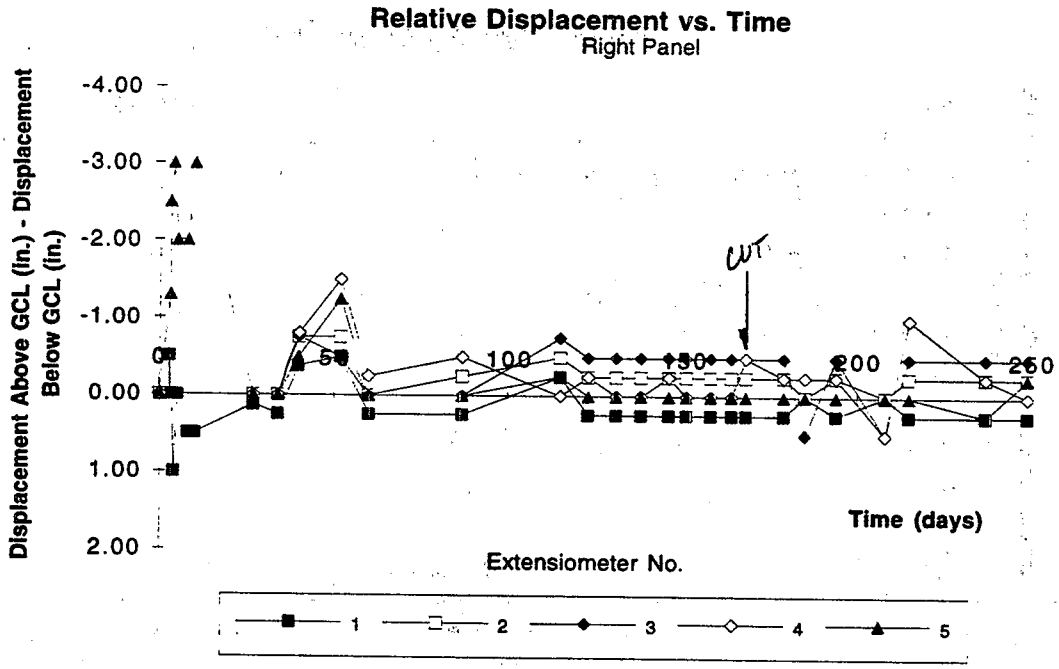

Displacement Above GCL - Displacement Below GCL

PLOT J — Bentomat - Granular Drainage - 2:1 Slope

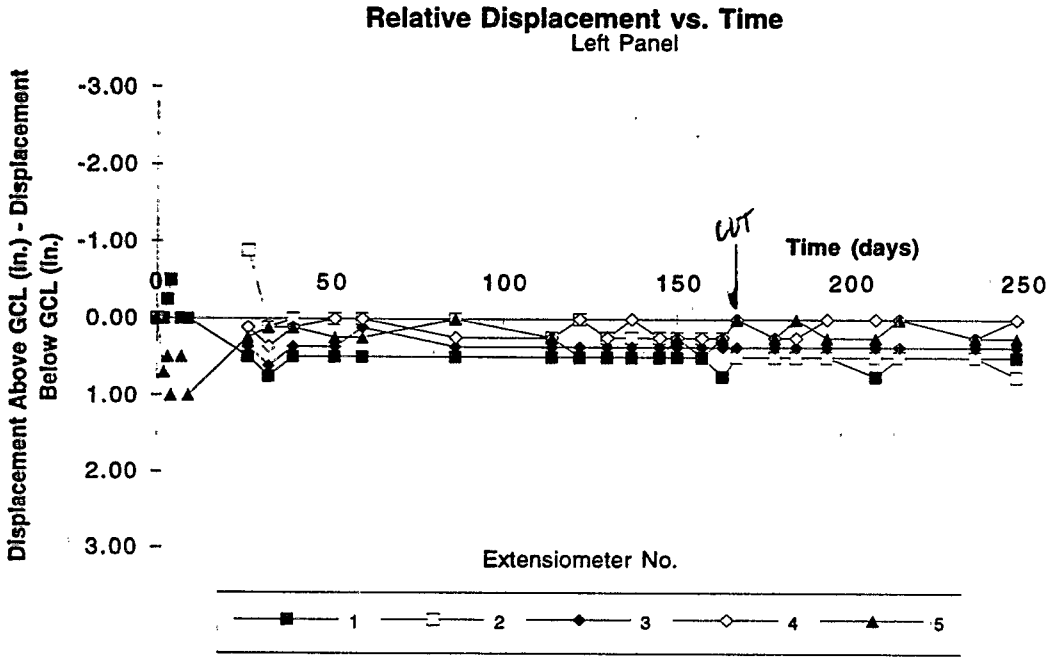

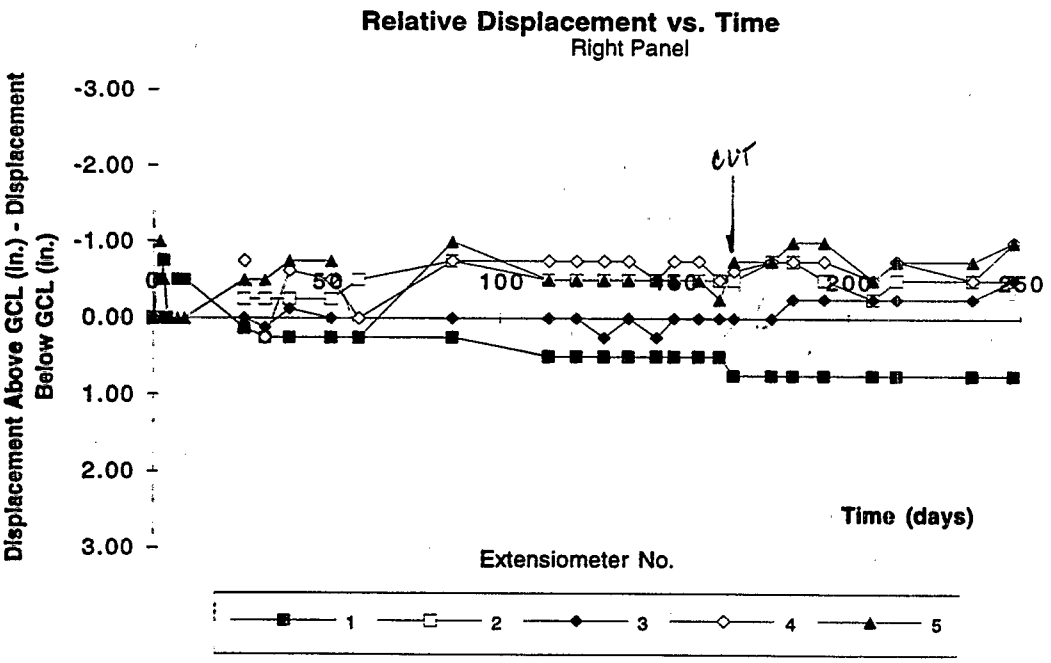

Displacement Above GCL - Displacement Below GCL

PLOT K — Claymax - Granular Drainage - 2:1 Slope

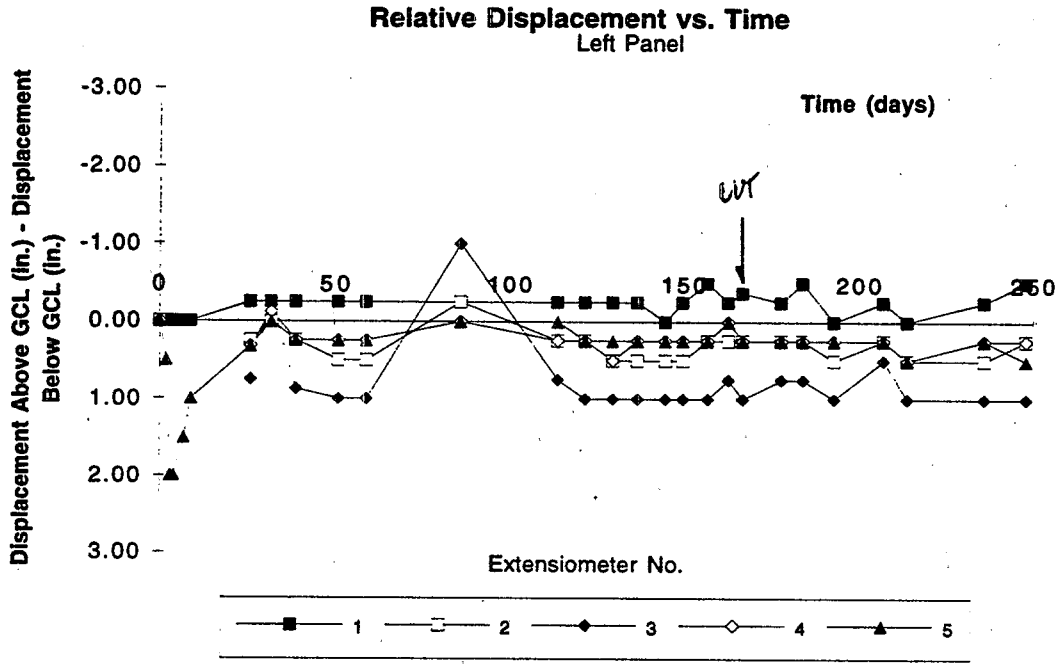

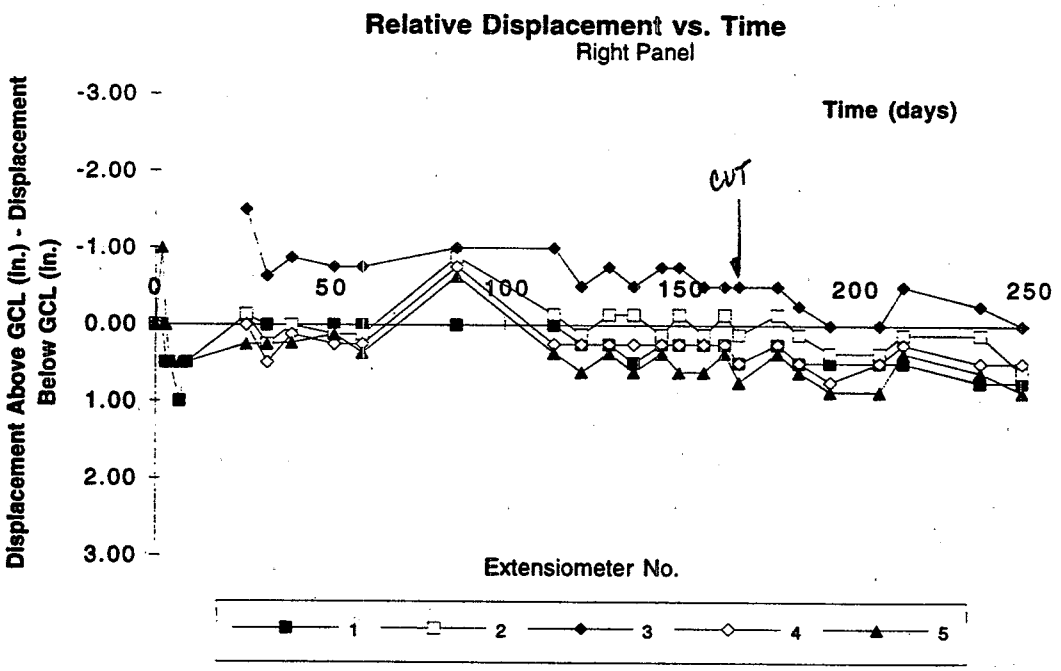

Displacement Above GCL - Displacement Below GCL

PLOT L — Bentofix I - Granular Drainage - 2:1 Slope

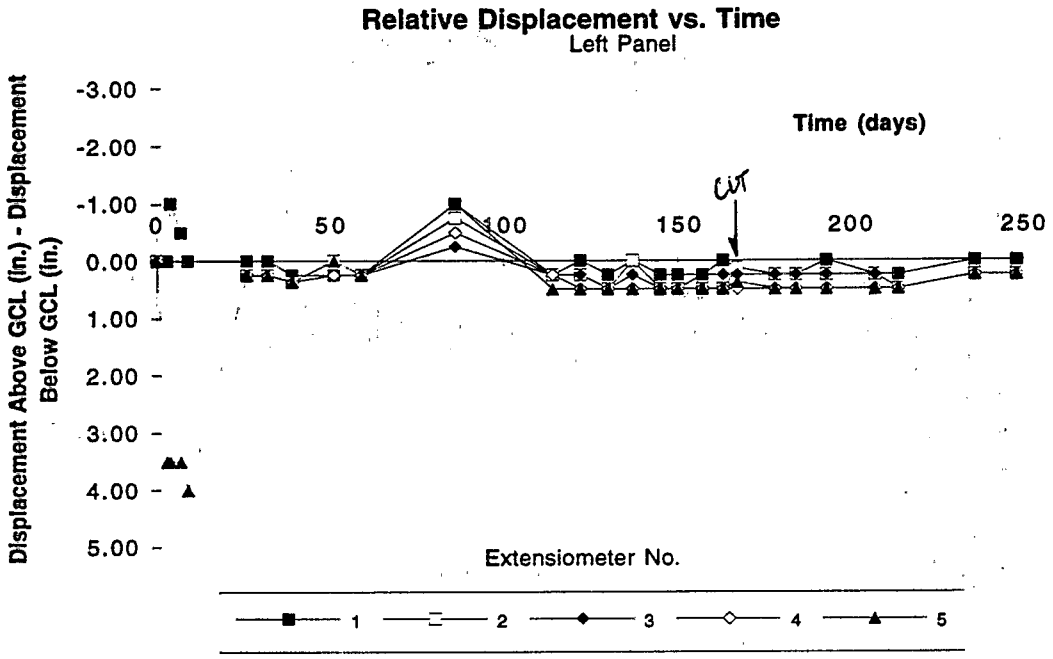

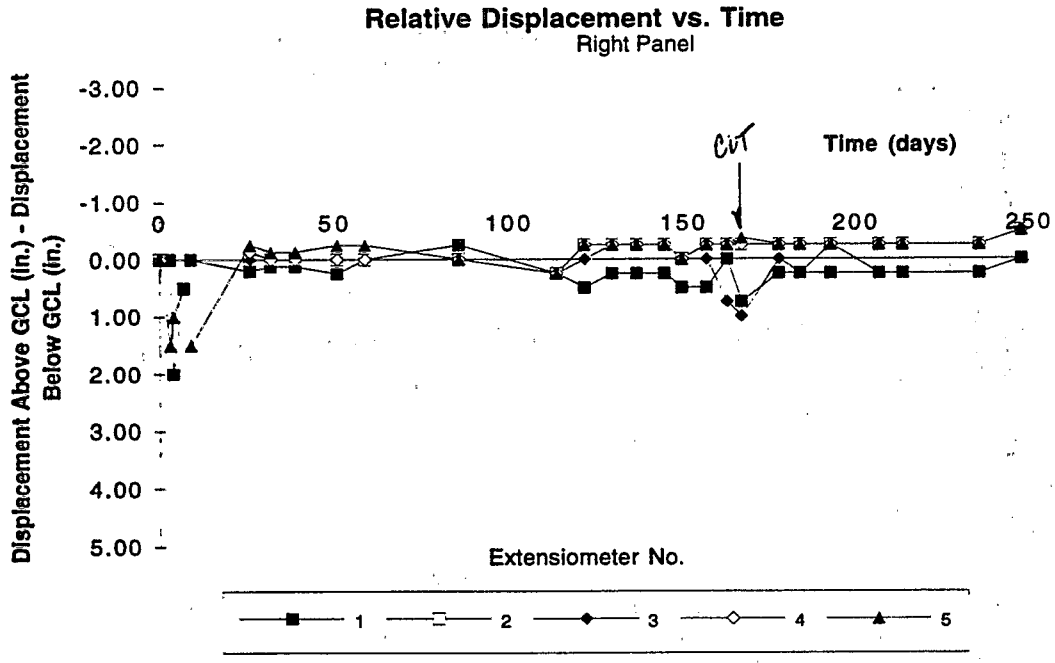

Displacement Above GCL - Displacement Below GCL

PLOT N — Bentofix II (NW up) - 2:1 Slope

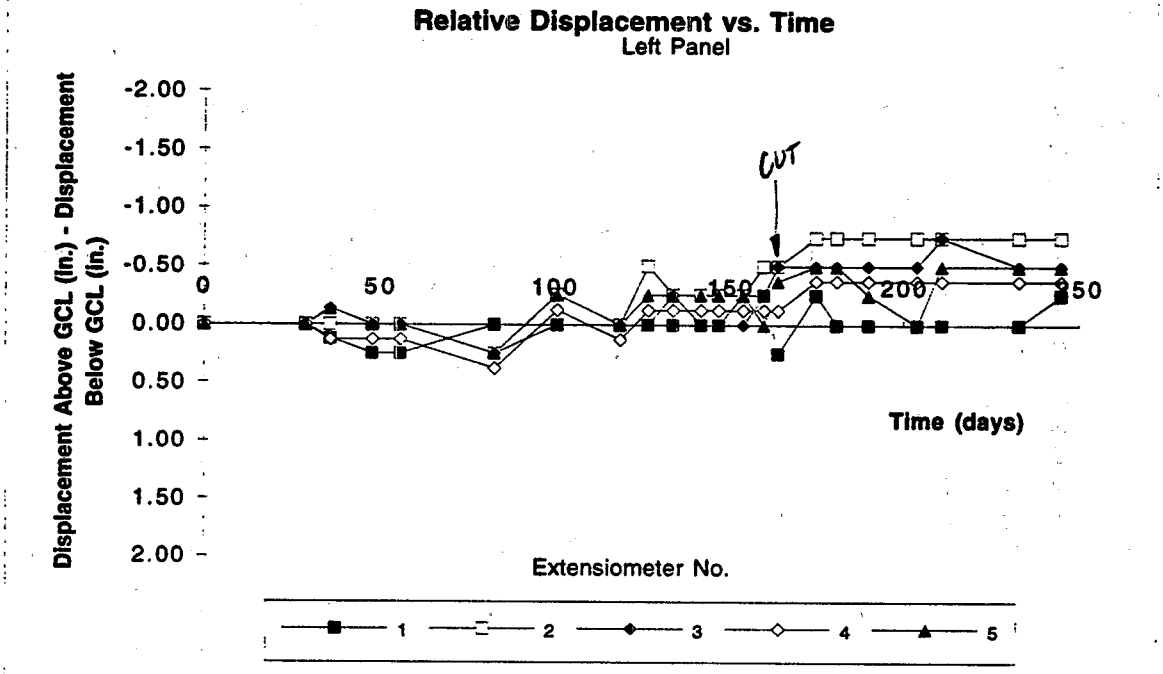

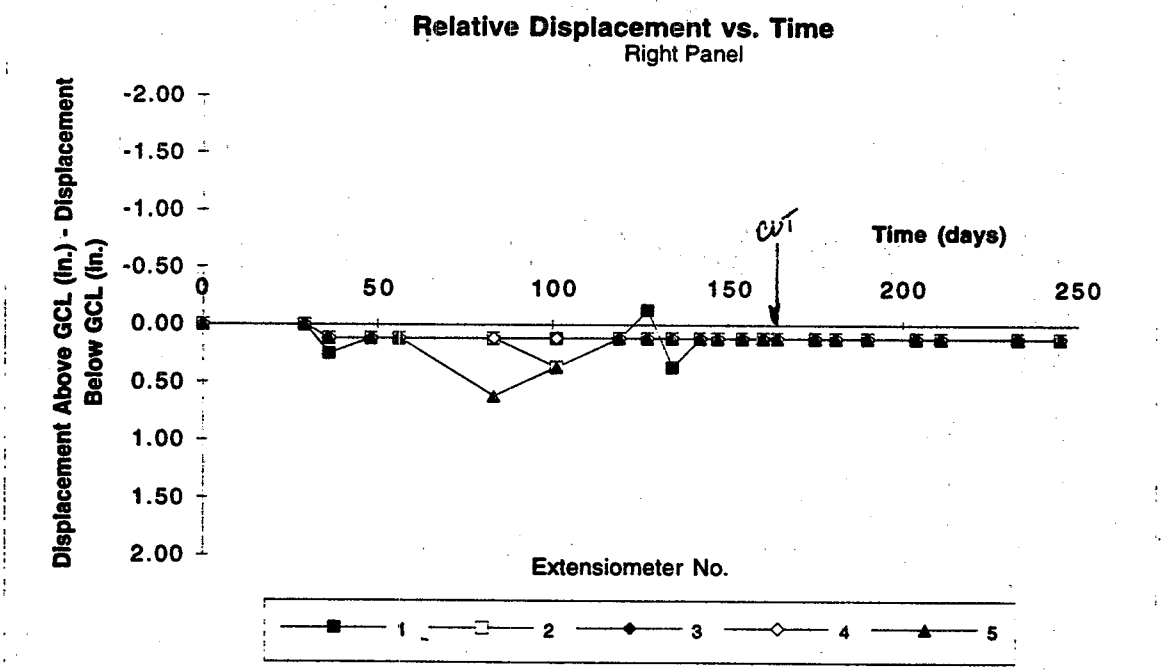

Appendix D

Moisture Instrument Readings in Test Plots

Moisture Readings vs. Time

Plot Location: Crest

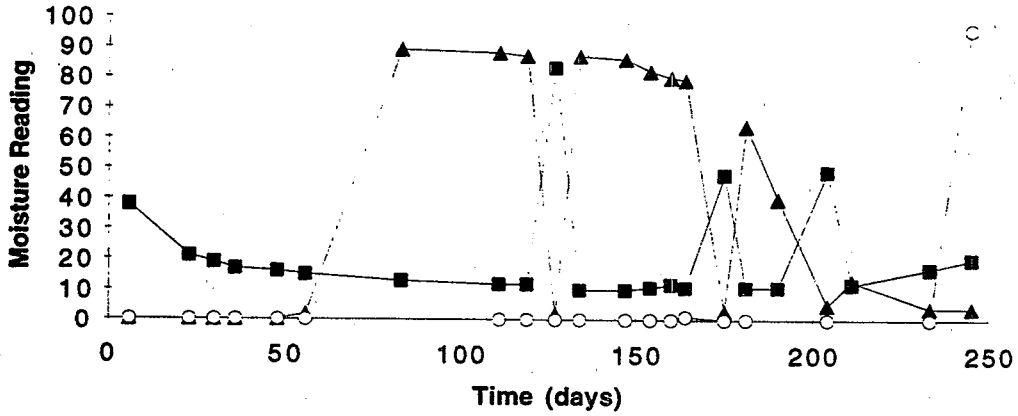

Plot Location: Middle

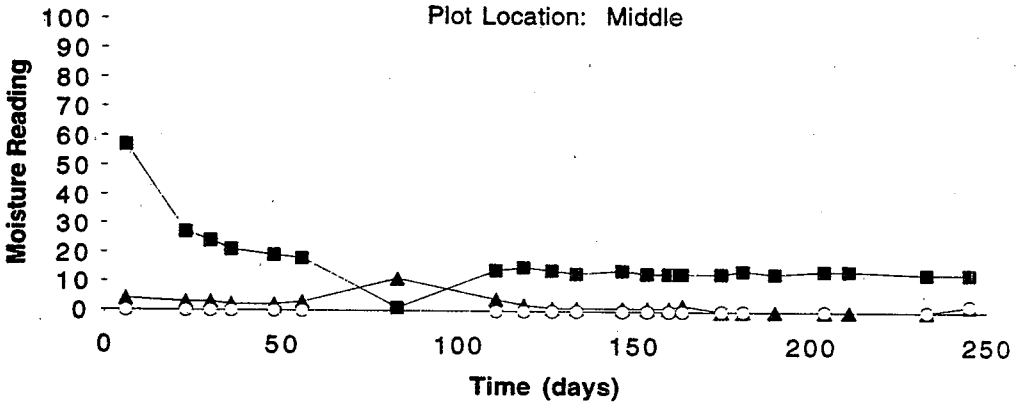

Plot Location: Toe

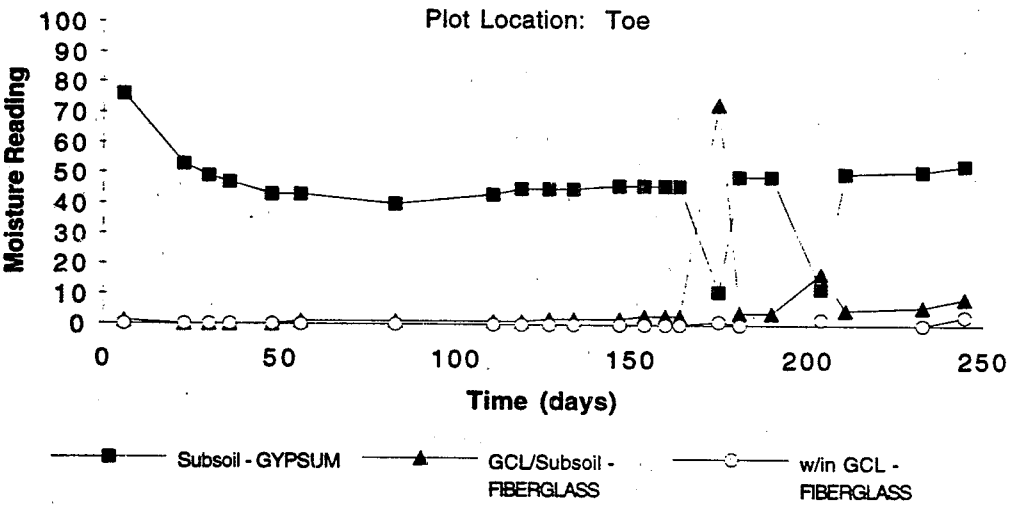

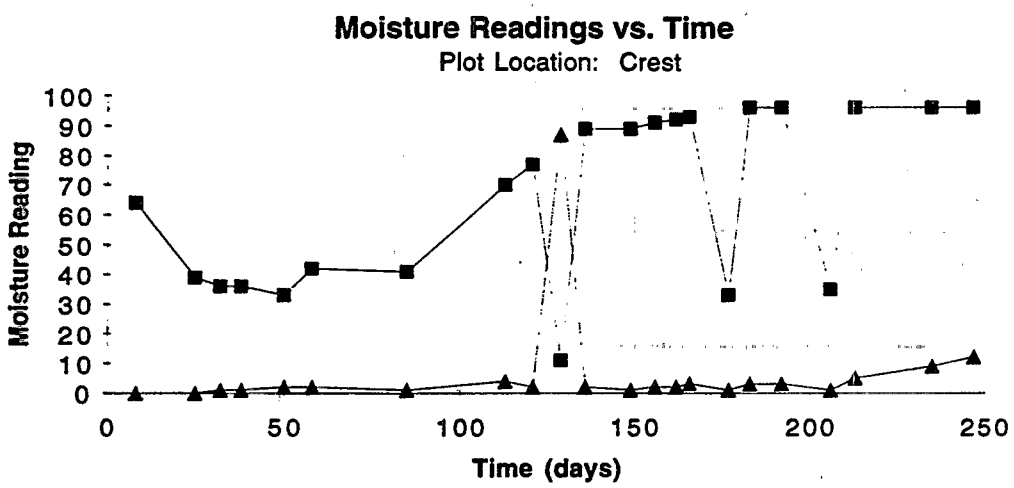
Moisture Readings vs. Time
Plot Location: Crest
Moisture Reading
100
90
80
70
60
50
40
30
20
10
0
0
50
100
150
200
250
Time (days)

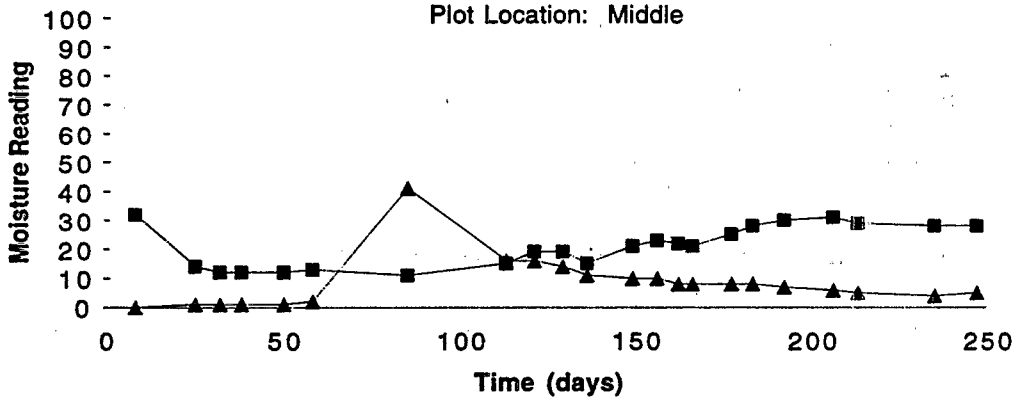
Plot Location: Middle
Moisture Reading
100
90
80
70
60
50
40
30
20
10
0
0
50
100
150
200
250
Time (days)

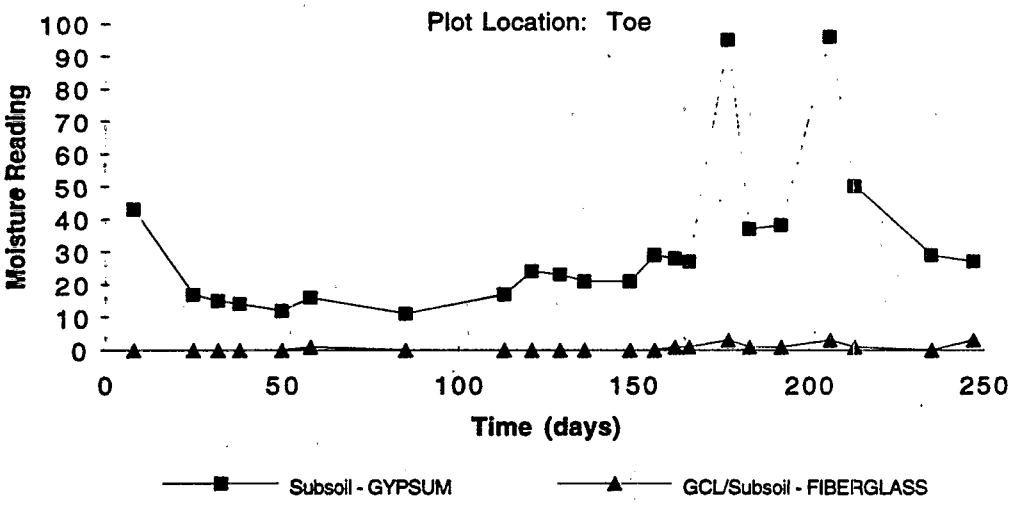
Plot Location: Toe
Moisture Reading
100
90
80
70
60
50
40
30
20
10
0
0
50
100
150
200
250
Time (days)
Subsoil - GYPSUM
GCL/Subsoil - FIBERGLASS

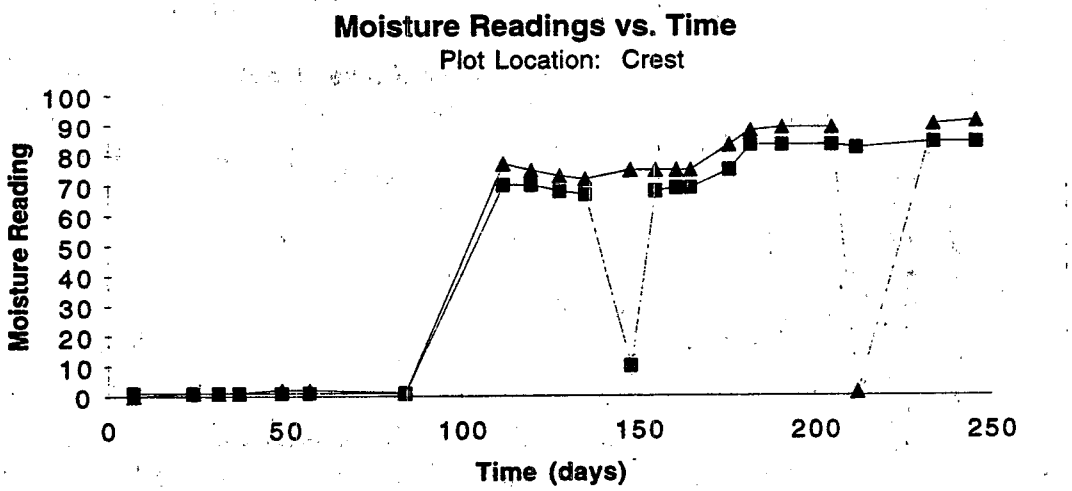
Moisture Readings vs. Time
Plot Location: Crest
Moisture Reading
100
90
80
70
60
50
40
30
20
10
0
0
50
100
150
200
250
Time (days)

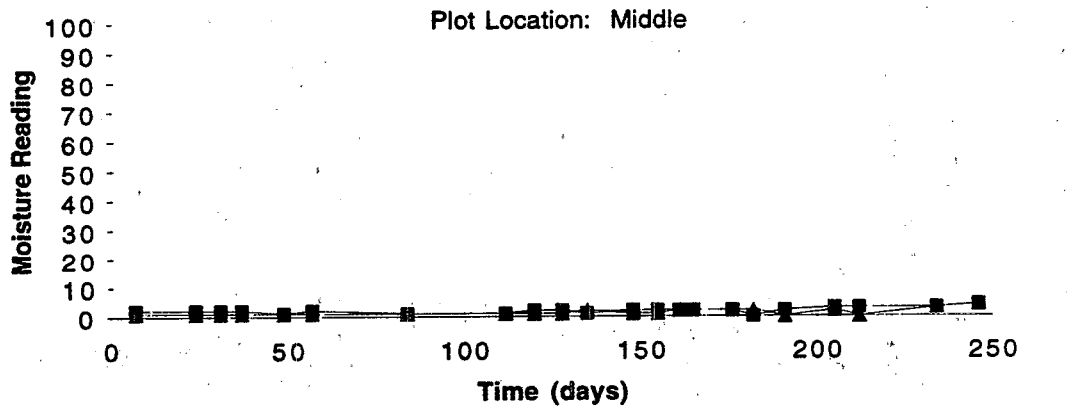
Plot Location: Middle
Moisture Reading
100
90
80
70
60
50
40
30
20
10
0
0
50
100
150
200
250
Time (days)

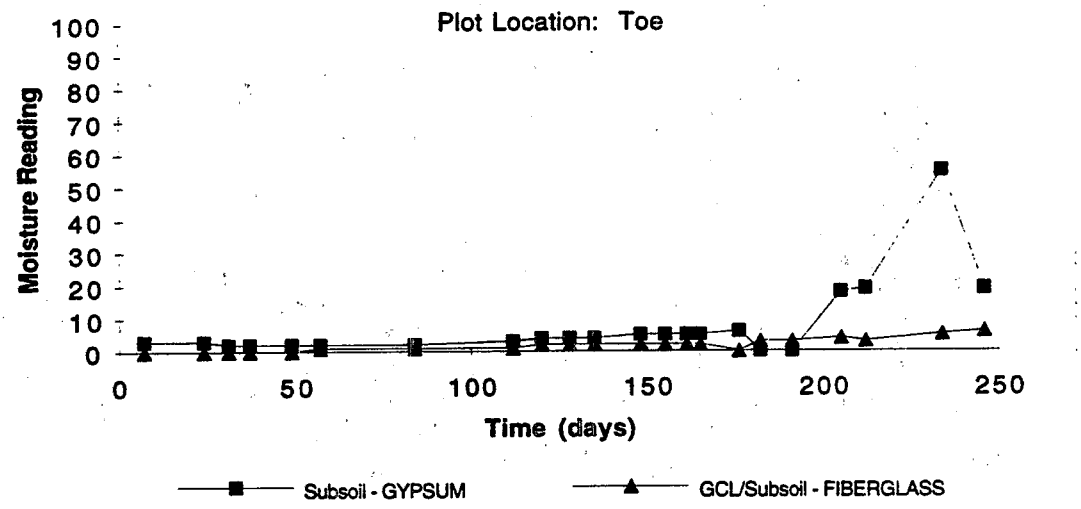
Plot Location: Toe
Moisture Reading
100
90
80
70
60
50
40
30
20
10
0
0
50
100
150
200
250
Time (days)
Subsoil - GYPSUM
GCL/Subsoil - FIBERGLASS

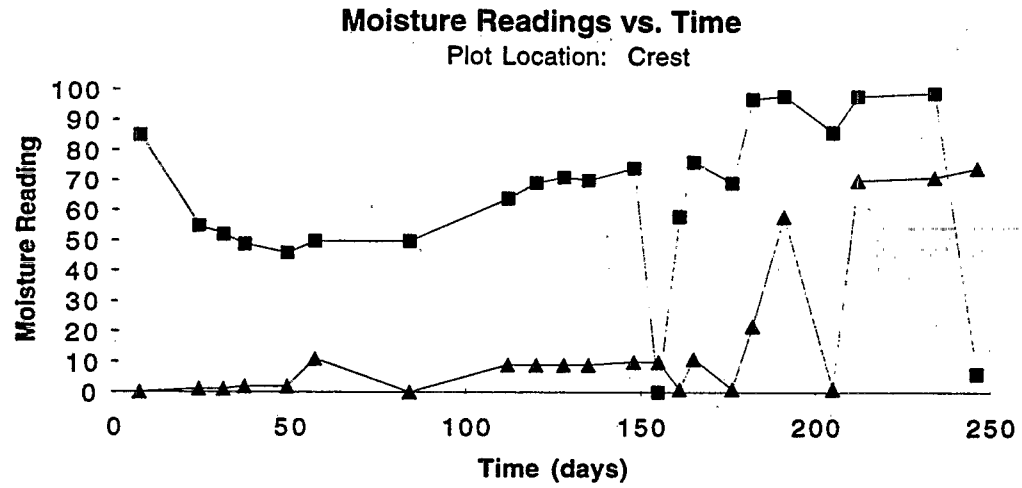
Moisture Readings vs. Time
Plot Location: Crest
Moisture Reading
100
90
80
70
60
50
40
30
20
10
0
0
50
100
150
200
250
Time (days)

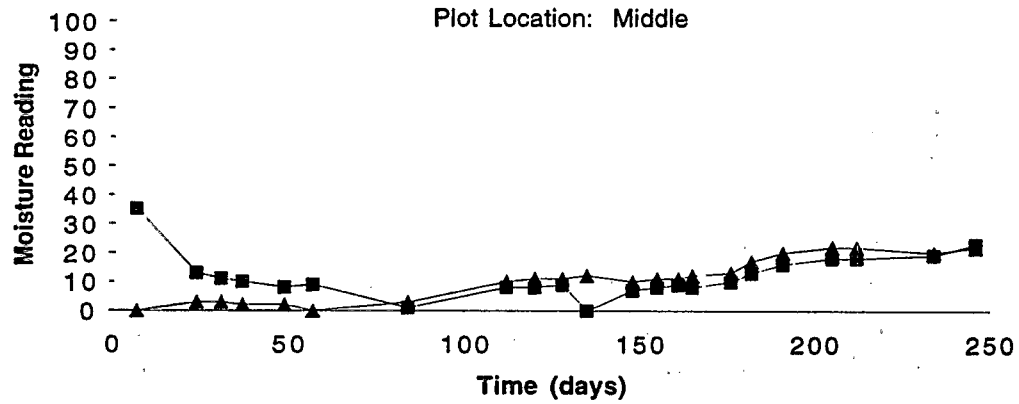
Plot Location: Middle
Moisture Reading
100
90
80
70
60
50
40
30
20
10
0
0
50
100
150
200
250
Time (days)

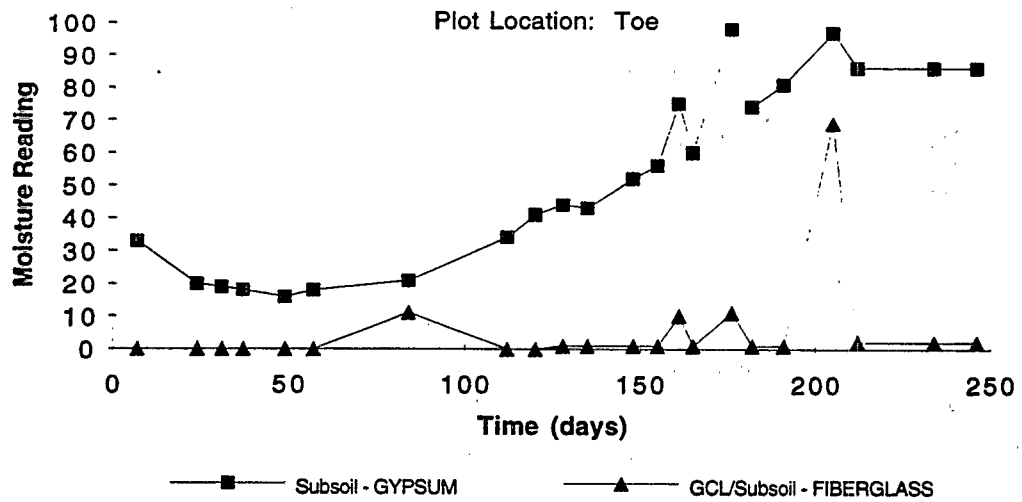
Plot Location: Toe
Moisture Reading
100
90
80
70
60
50
40
30
20
10
0
0
50
100
150
200
250
Time (days)
Subsoil - GYPSUM
GCL/Subsoil - FIBERGLASS

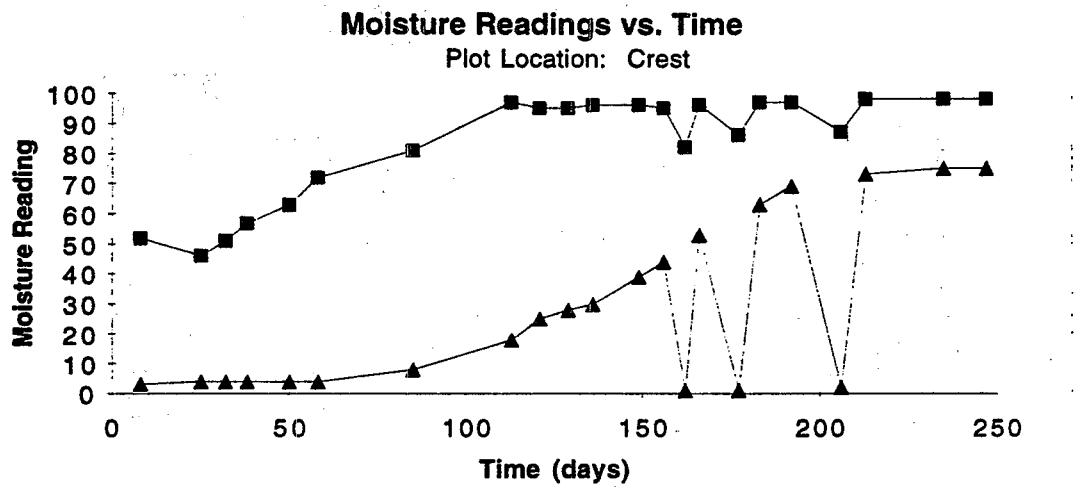
Moisture Readings vs. Time
Plot Location: Crest
Moisture Reading
100
90
80
70
60
50
40
30
20
10
0
0
50
100
150
200
250
Time (days)

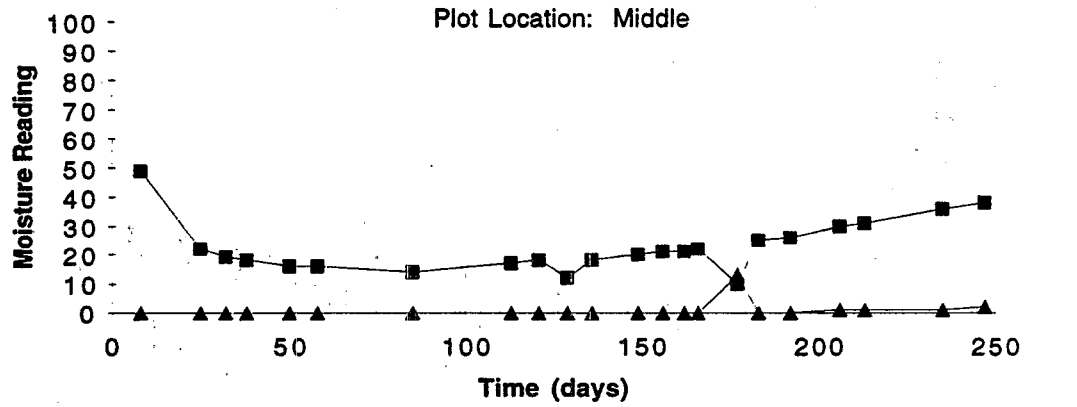
Plot Location: Middle
Moisture Reading
100
90
80
70
60
50
40
30
20
10
0
0
50
100
150
200
250
Time (days)

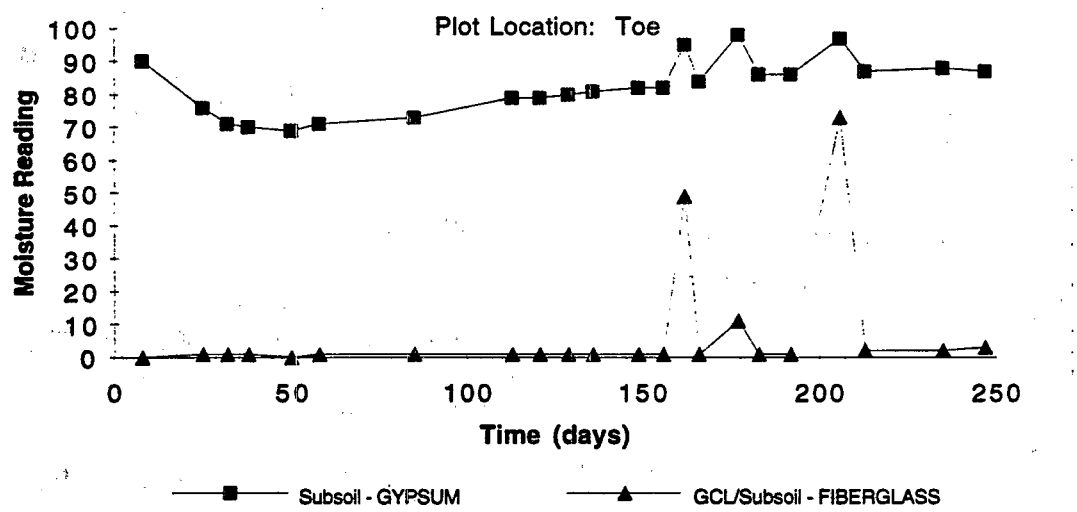
Plot Location: Toe
Moisture Reading
100
90
80
70
60
50
40
30
20
10
0
0
50
100
150
200
250
Time (days)
Subsoil - GYPSUM
GCL/Subsoil - FIBERGLASS

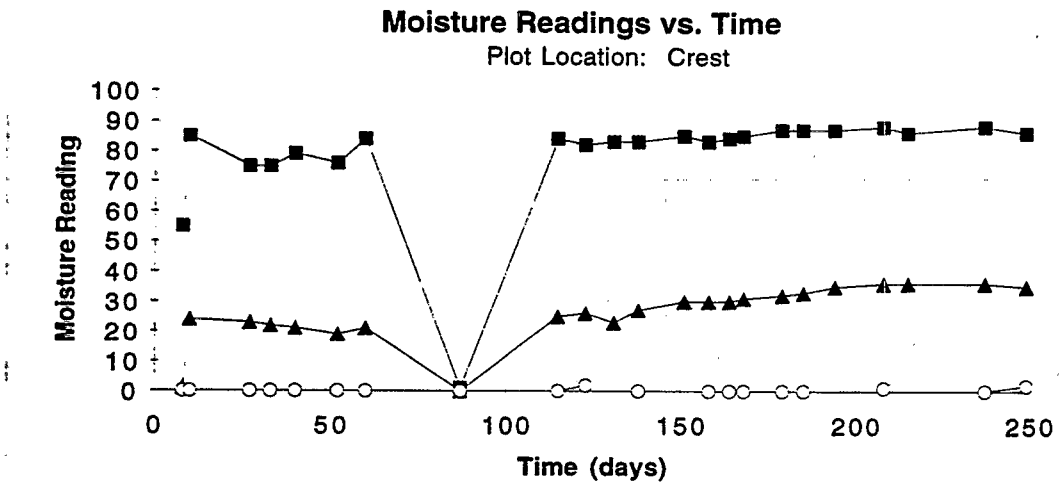
Moisture Readings vs. Time
Plot Location: Crest
Moisture Reading
100
90
80
70
60
50
40
30
20
10
0
0
50
100
150
200
250
Time (days)

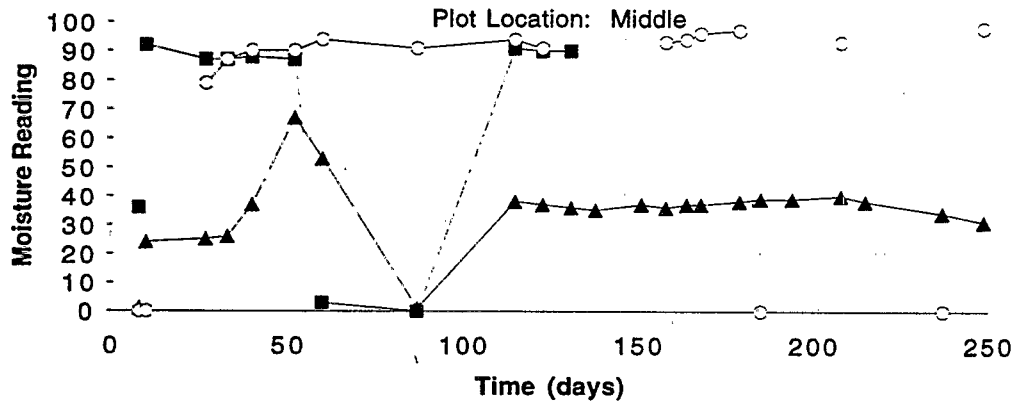
Plot Location: Middle
Moisture Reading
100
90
80
70
60
50
40
30
20
10
0
0
50
100
150
200
250
Time (days)

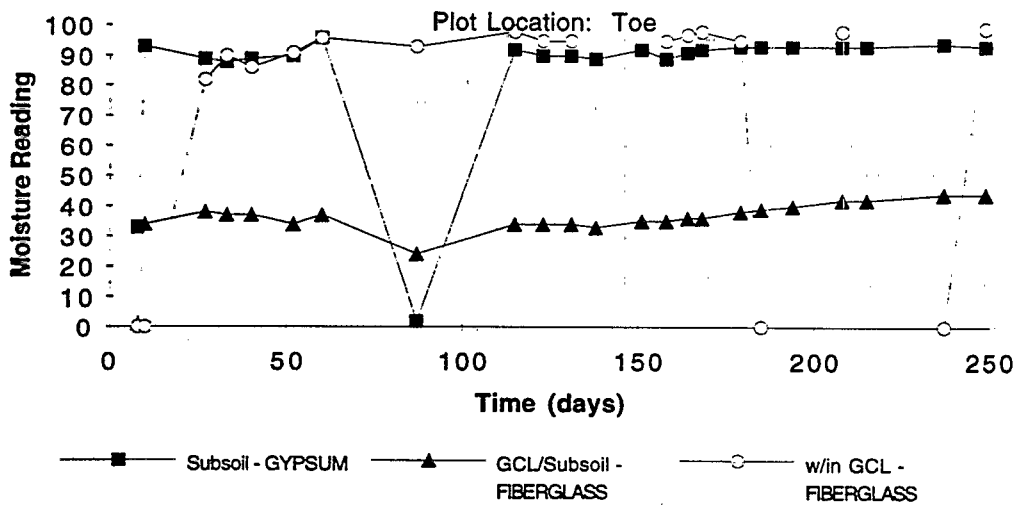
Plot Location: Toe
Moisture Reading
100
90
80
70
60
50
40
30
20
10
0
0
50
100
150
200
250
Time (days)
Subsoil - GYPSUM
GCL/Subsoil - FIBERGLASS
w/in GCL - FIBERGLASS

Moisture Readings vs. Time

Plot Location: Crest

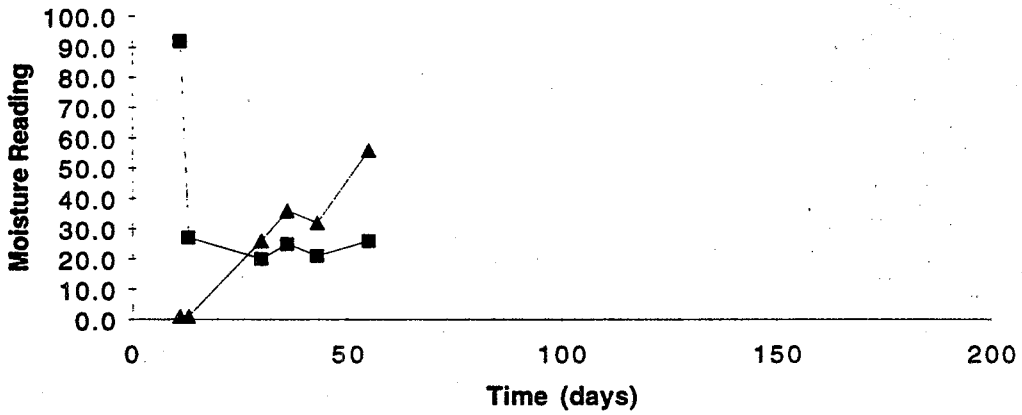

Plot Location: Middle

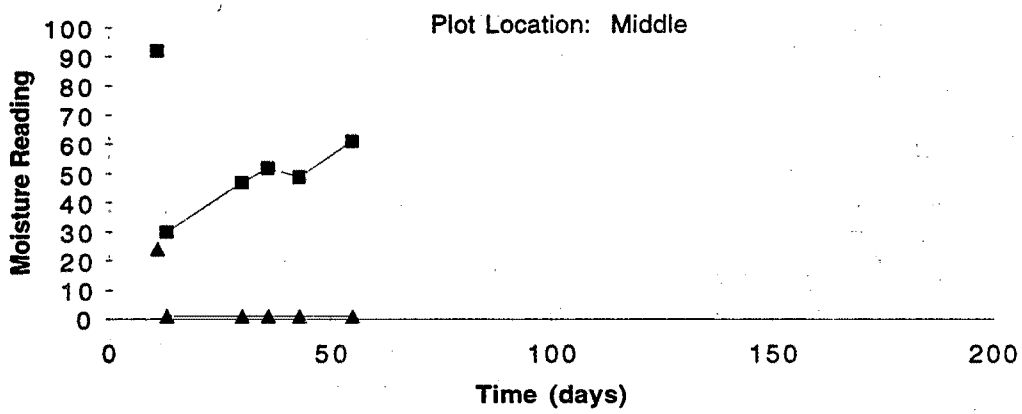

Plot Location: Toe

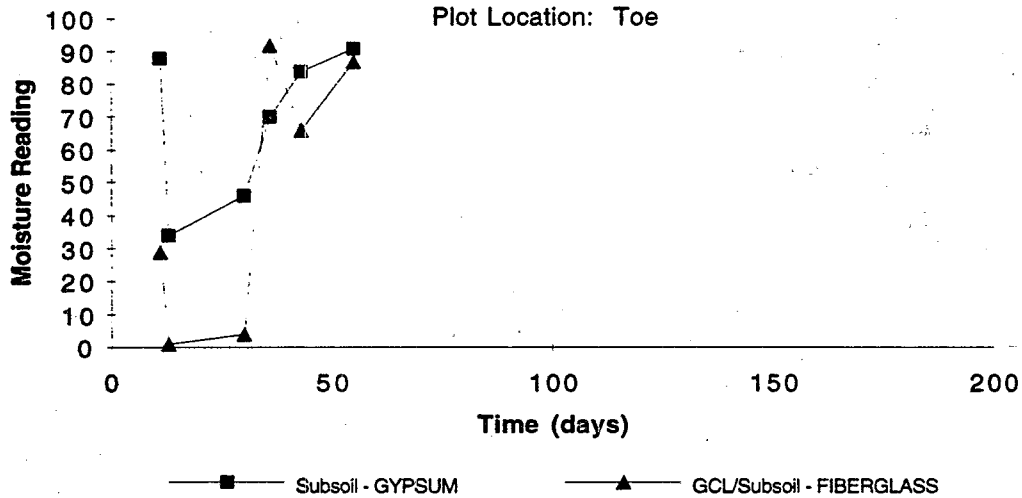

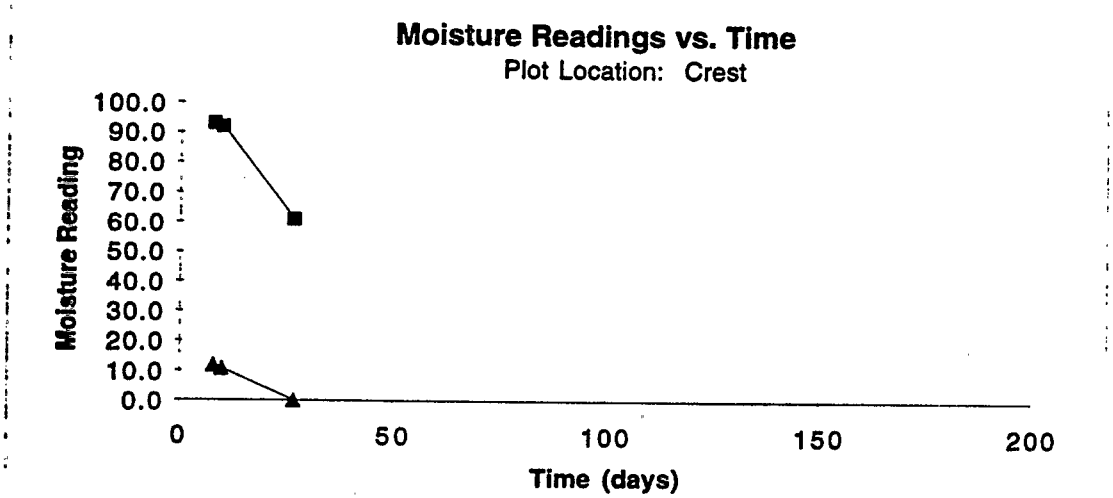
Moisture Readings vs. Time
Plot Location: Crest
Moisture Reading
100.0
90.0
80.0
70.0
60.0
50.0
40.0
30.0
20.0
10.0
0.0
0
50
100
150
200
Time (days)

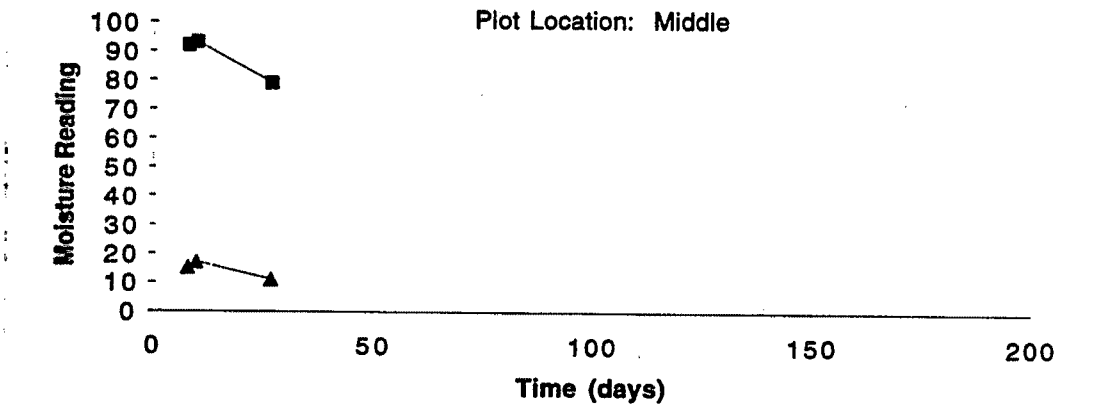
Plot Location: Middle
Moisture Reading
100
90
80
70
60
50
40
30
20
10
0
0
50
100
150
200
Time (days)

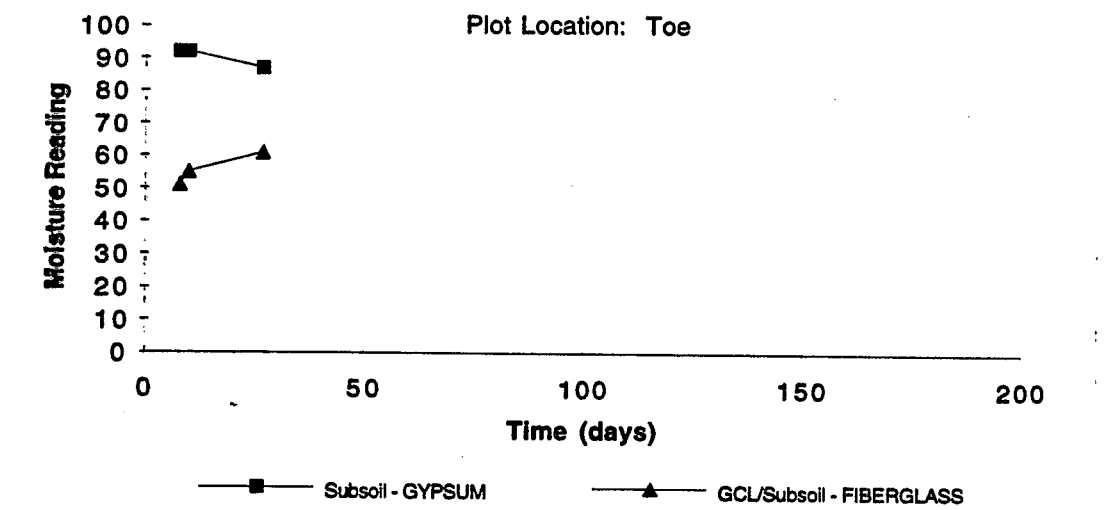
Plot Location: Toe
Moisture Reading
100
90
80
70
60
50
40
30
20
10
0
0
50
100
150
200
Time (days)
Subsoil - GYPSUM
GCL/Subsoil - FIBERGLASS

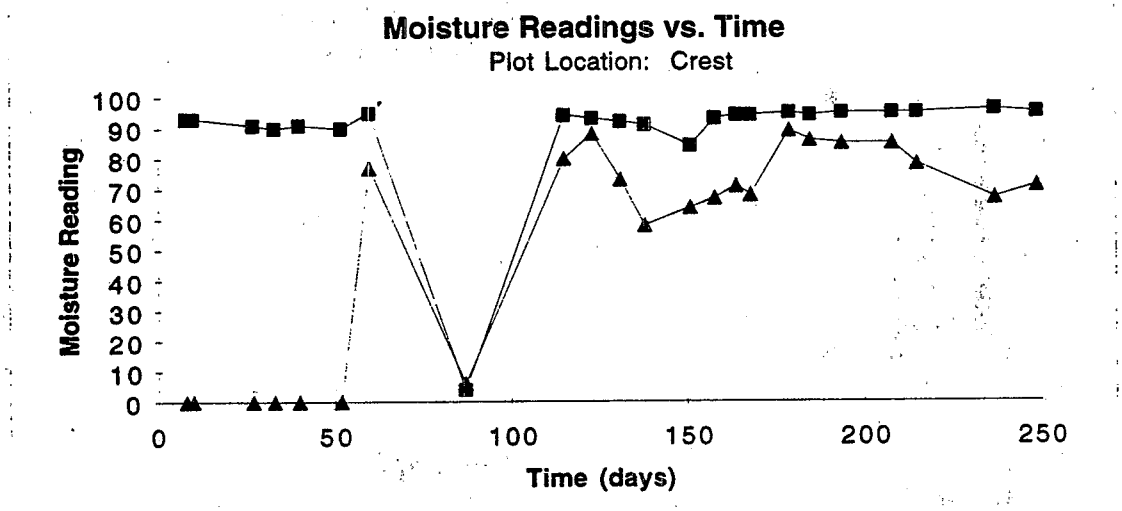
Moisture Readings vs. Time
Plot Location: Crest
Moisture Reading
100
90
80
70
60
50
40
30
20
10
0
0
50
100
150
200
250
Time (days)

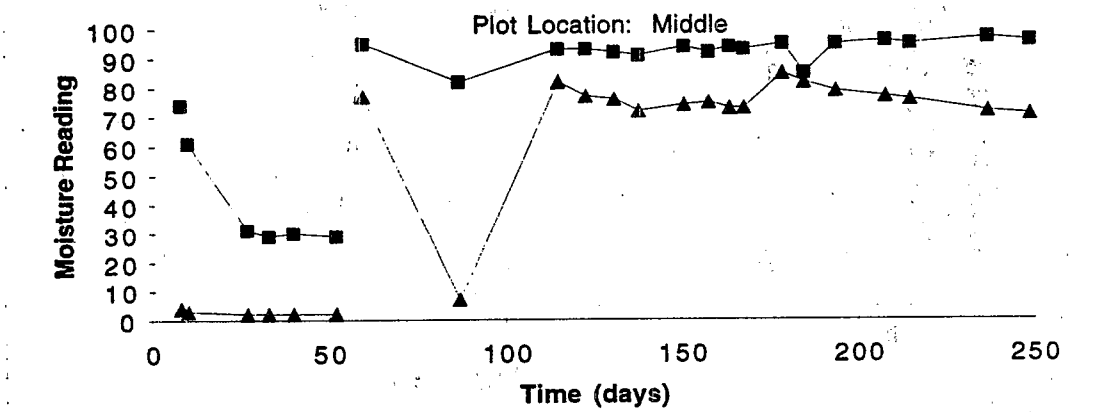
Plot Location: Middle
Moisture Reading
100
90
80
70
60
50
40
30
20
10
0
0
50
100
150
200
250
Time (days)

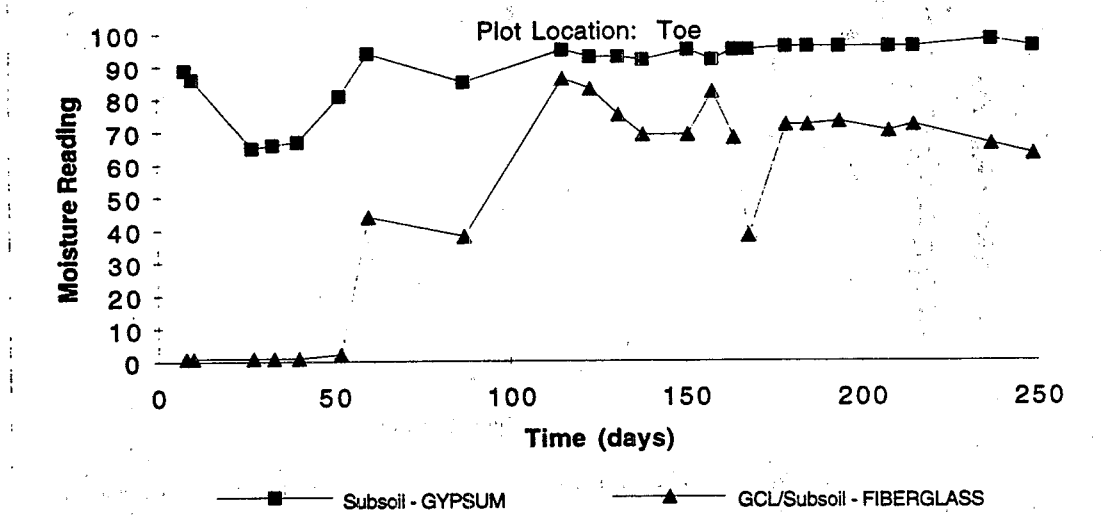
Plot Location: Toe
Moisture Reading
100
90
80
70
60
50
40
30
20
10
0
0
50
100
150
200
250
Time (days)
Subsoil - GYPSUM
GCL/Subsoil - FIBERGLASS

PLOT J Bentomat - Granular Drainage - 2:1 Slope

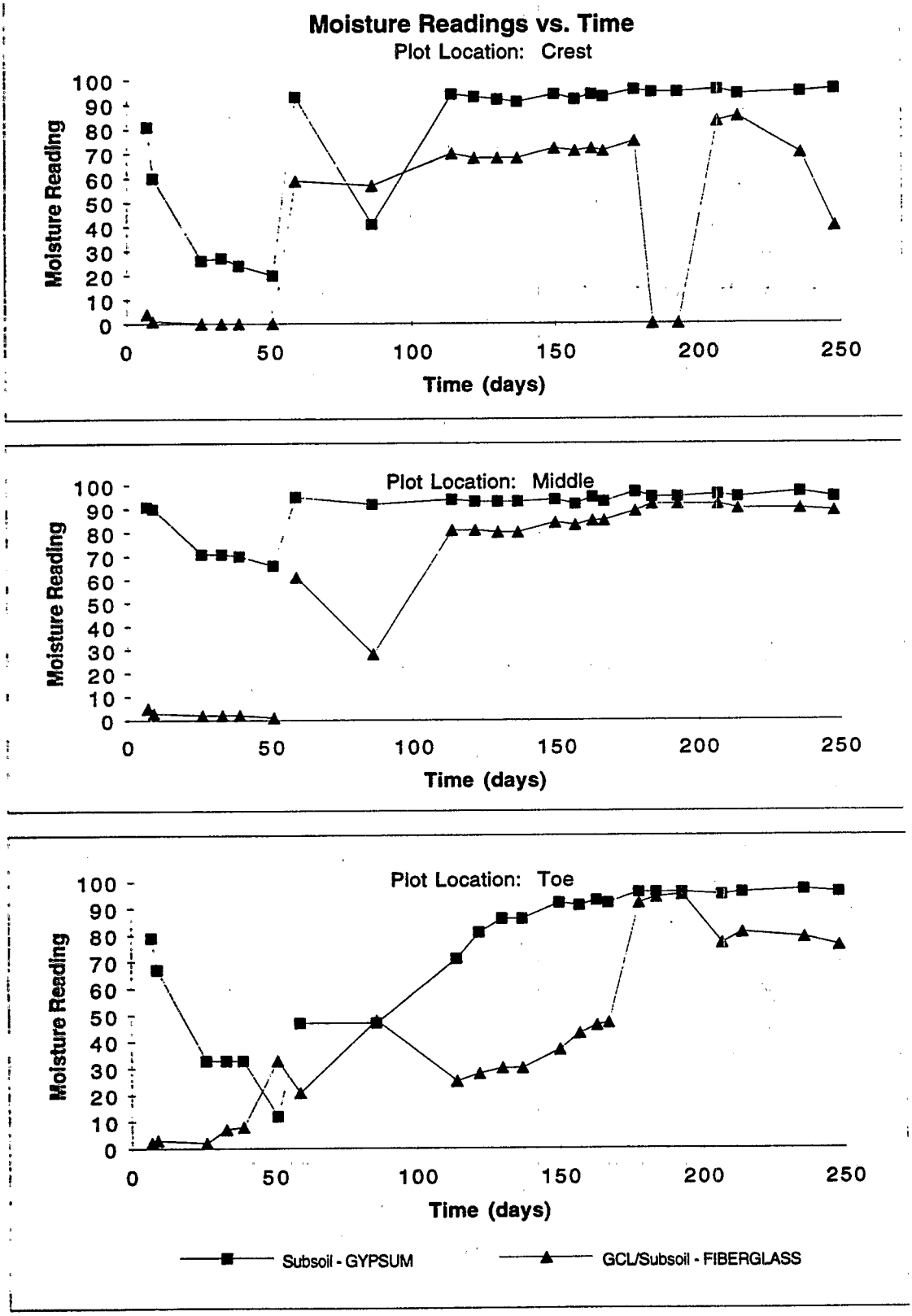

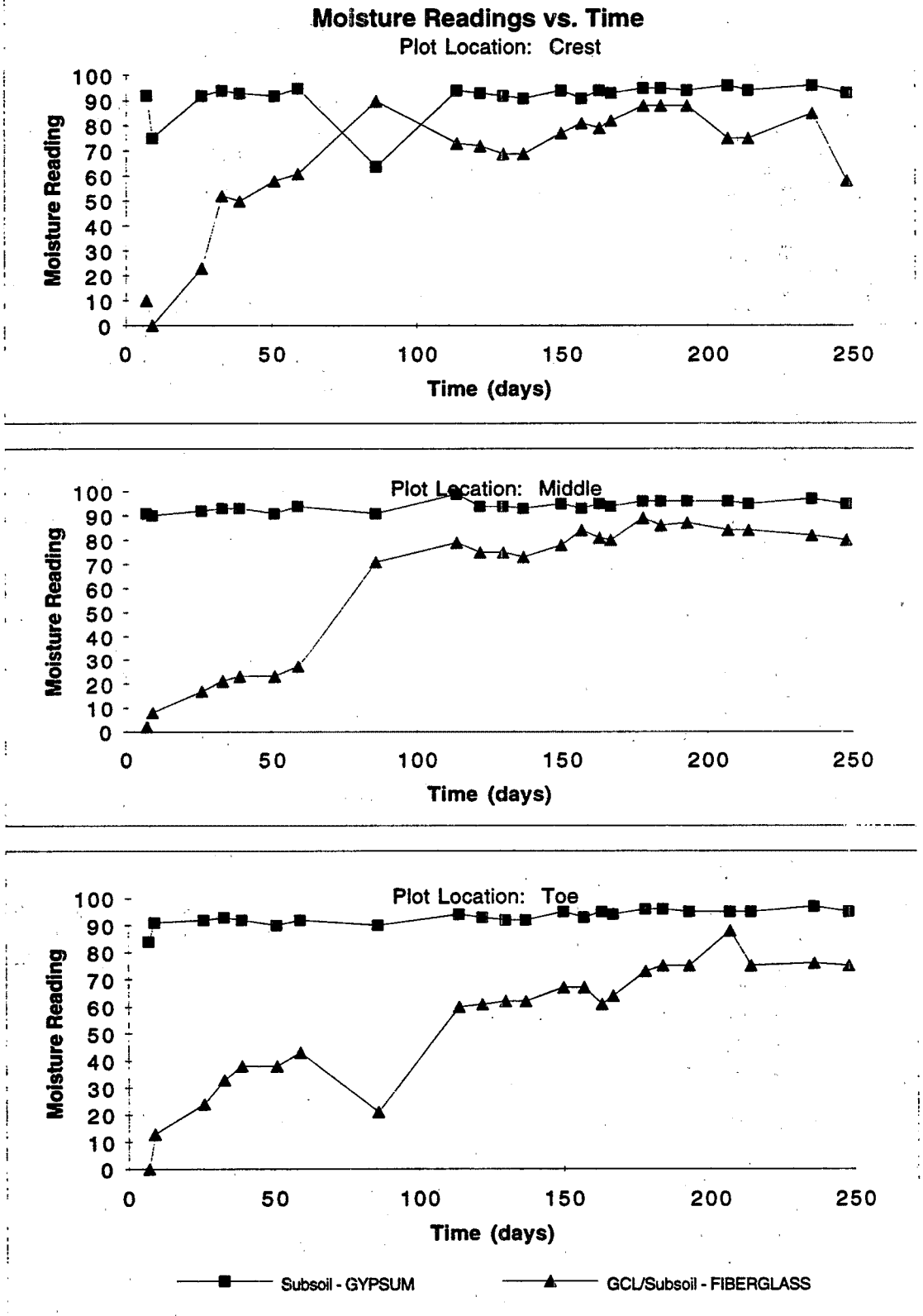
Moisture Readings vs. Time
Plot Location: Crest
Moisture Reading
Time (days)
Plot Location: Middle
Moisture Reading
Time (days)
Plot Location: Toe
Moisture Reading
Time (days)
Subsoil - GYPSUM
GCL/Subsoil - FIBERGLASS

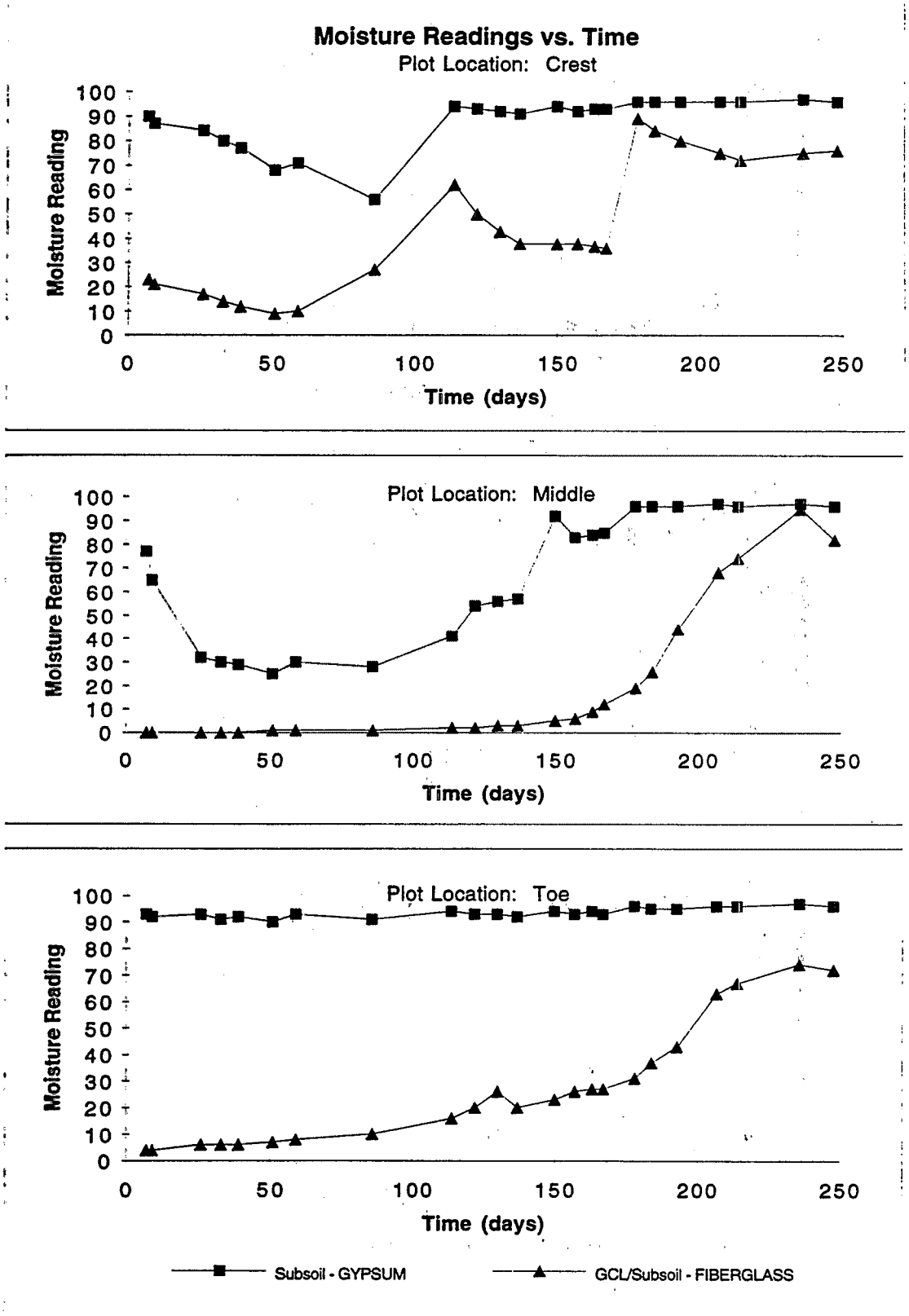
Moisture Readings vs. Time
Plot Location: Crest
Moisture Reading
Time (days)
Plot Location: Middle
Moisture Reading
Time (days)
Plot Location: Toe
Moisture Reading
Time (days)
Subsoil - GYPSUM
GCL/Subsoil - FIBERGLASS

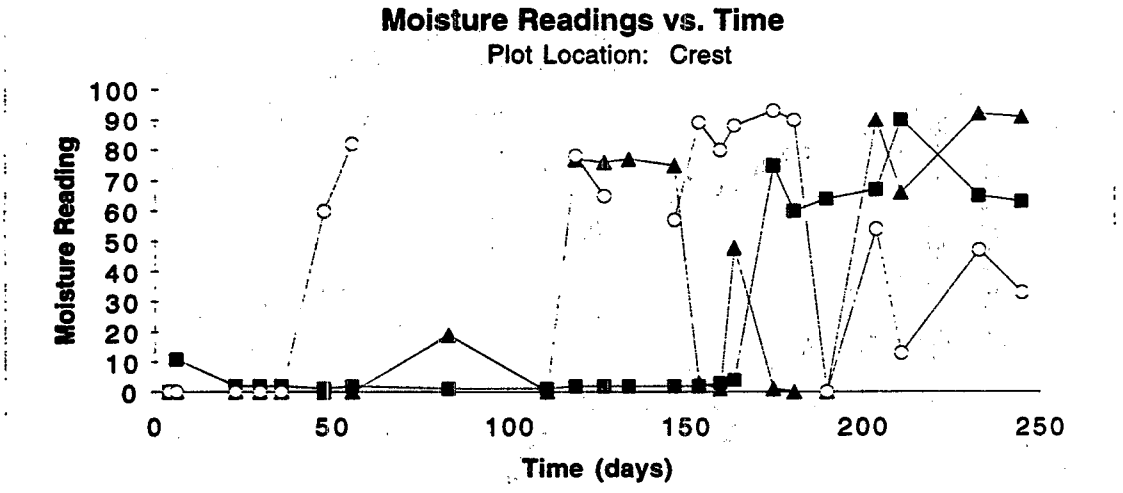
Moisture Readings vs. Time
Plot Location: Crest
Moisture Reading
100
90
80
70
60
50
40
30
20
10
0
0
50
100
150
200
250
Time (days)

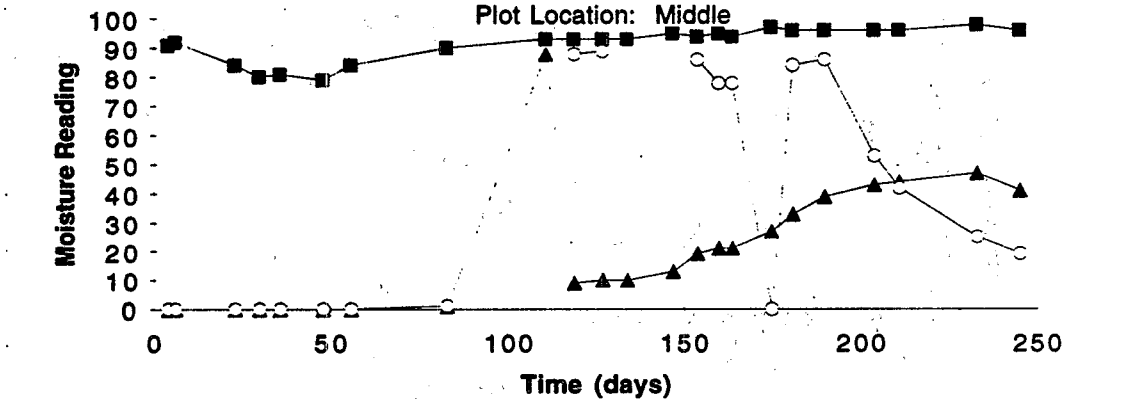
Plot Location: Middle
Moisture Reading
100
90
80
70
60
50
40
30
20
10
0
0
50
100
150
200
250
Time (days)

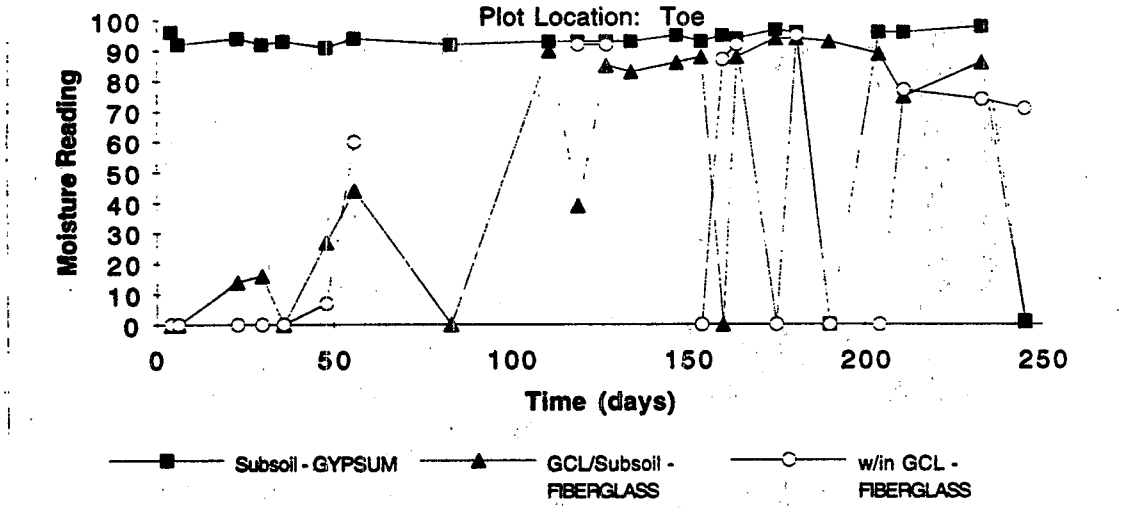
Plot Location: Toe
Moisture Reading
100
90
80
70
60
50
40
30
20
10
0
0
50
100
150
200
250
Time (days)
Subsoil - GYPSUM
GCL/Subsoil - FIBERGLASS
w/in GCL - FIBERGLASS

PLOT P Gundseal (bentonite up) - 2:1 Slope

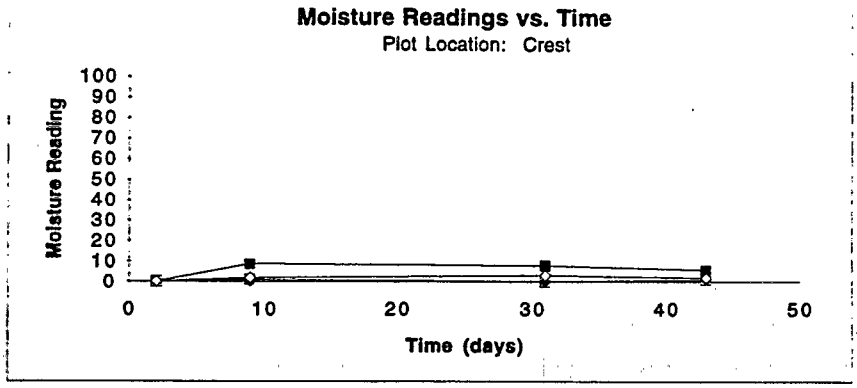

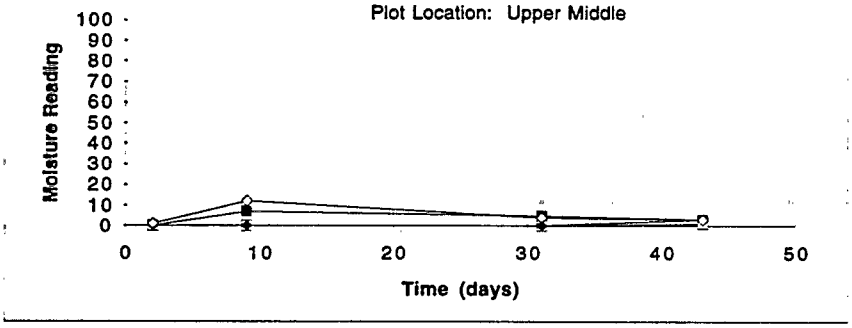

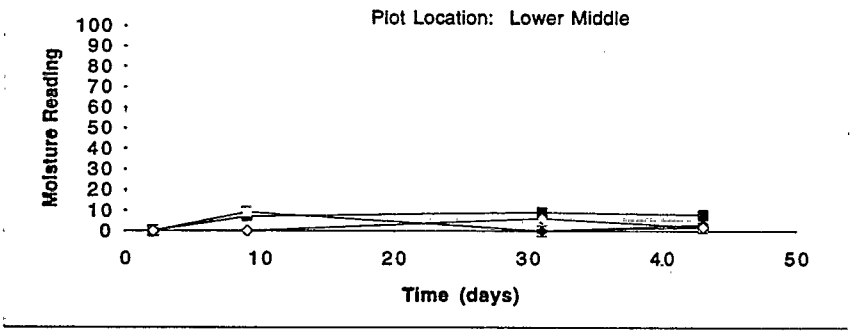

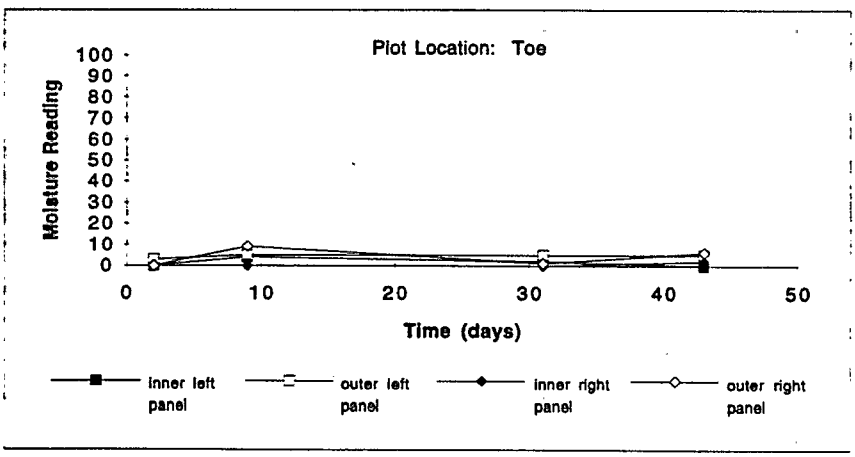

Appendix E

Results of Interface Shear Tests Performed at Drexel University's Geosynthetic Research Institute

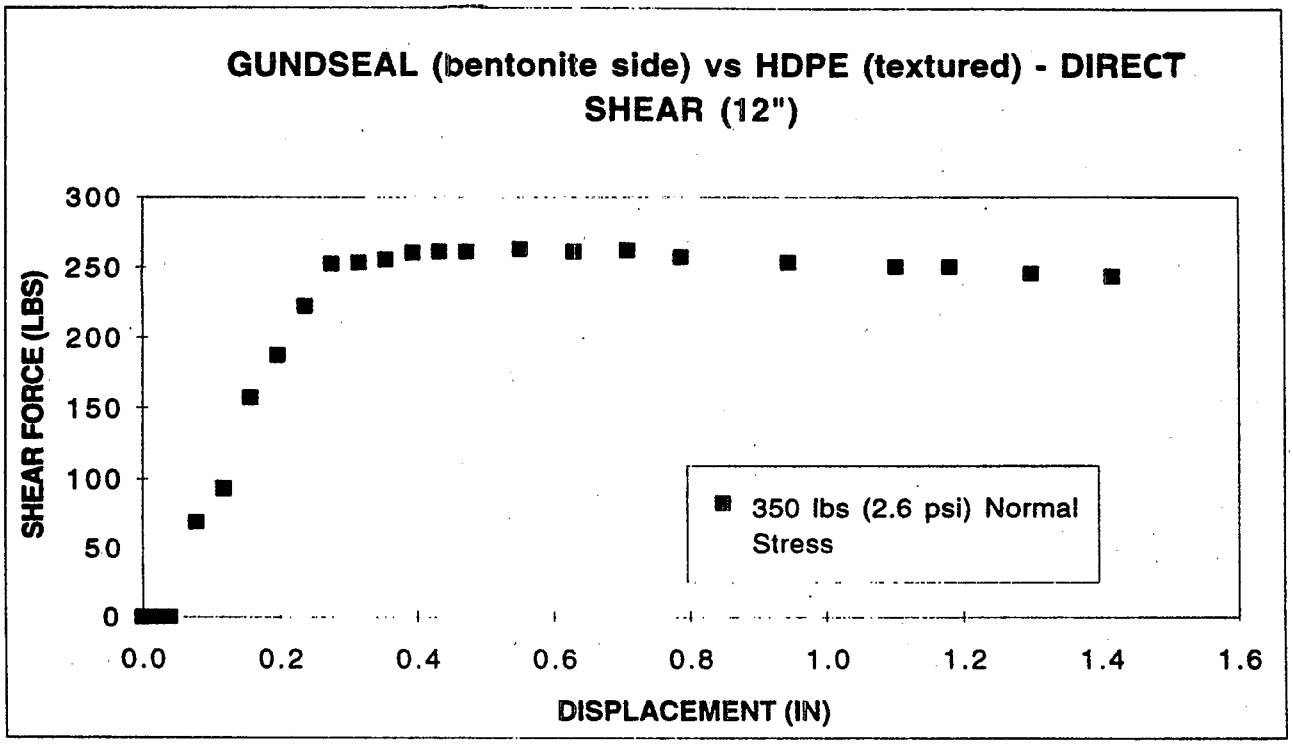
GUNDSEAL (bentonite side) vs HDPE (textured) - DIRECT SHEAR (12")
SHEAR FORCE (LBS)
300
250
200
150
100
50
0
0.0
0.2
0.4
0.6
0.8
1.0
1.2
1.4
1.6
DISPLACEMENT (IN)
350 lbs (2.6 psi) Normal Stress

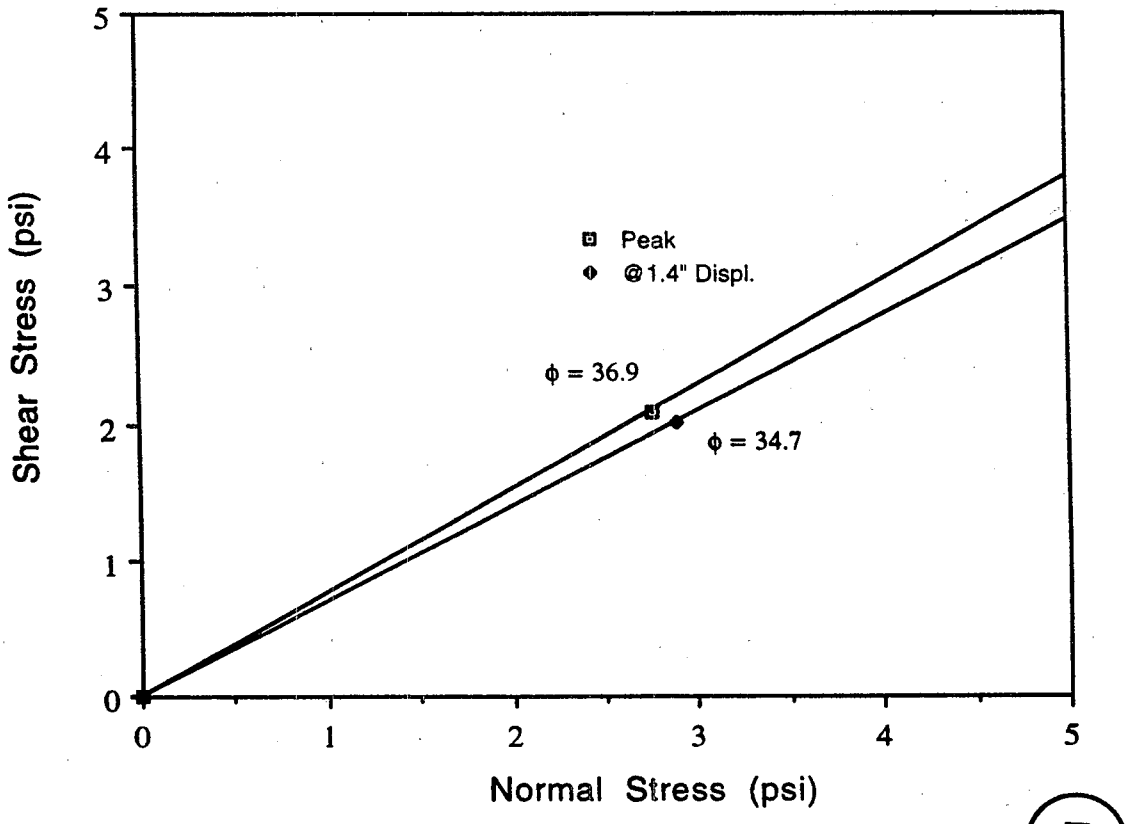
Shear Stress (psi)
5
4
3
2
1
0
0
1
2
3
4
5
Normal Stress (psi)
Peak
@1.4" Displ.
ϕ = 36.9
ϕ = 34.7

F

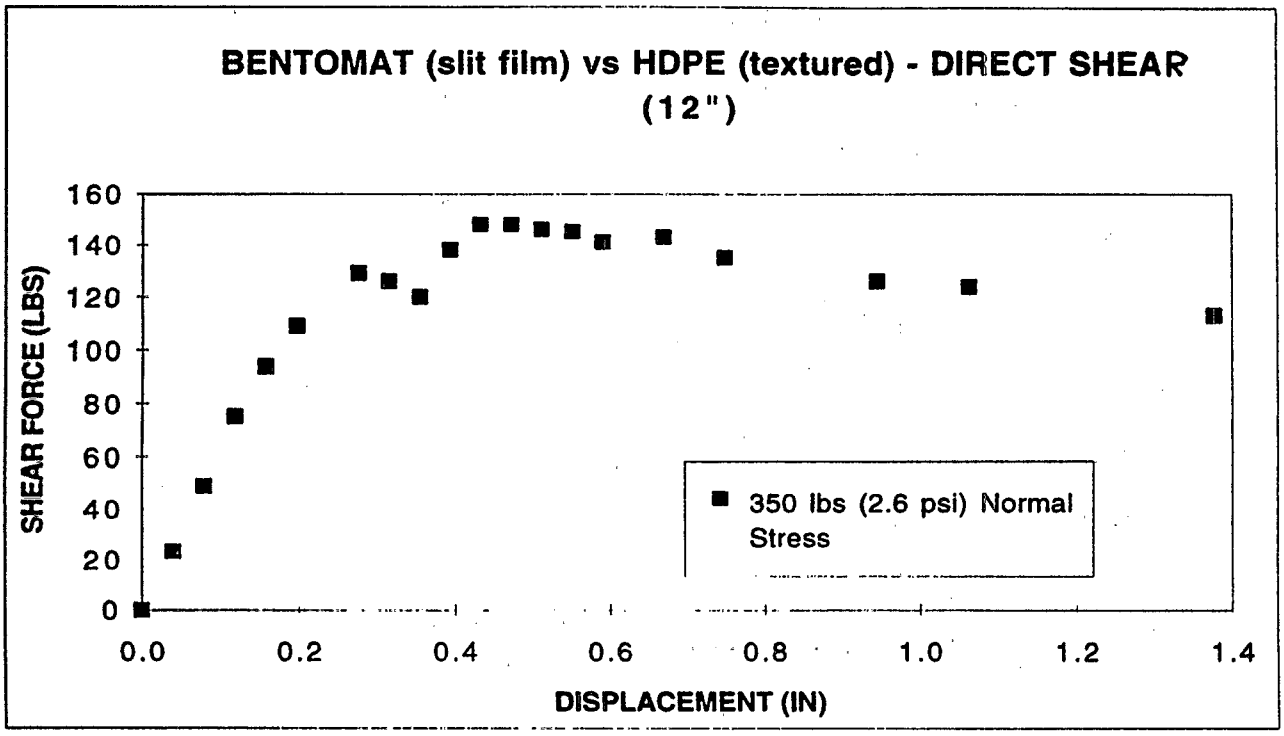
BENTOMAT (slit film) vs HDPE (textured) - DIRECT SHEAR
(12")
SHEAR FORCE (LBS)
160
140
120
100
80
60
40
20
0
0.0
0.2
0.4
0.6
0.8
1.0
1.2
1.4
DISPLACEMENT (IN)
350 lbs (2.6 psi) Normal Stress

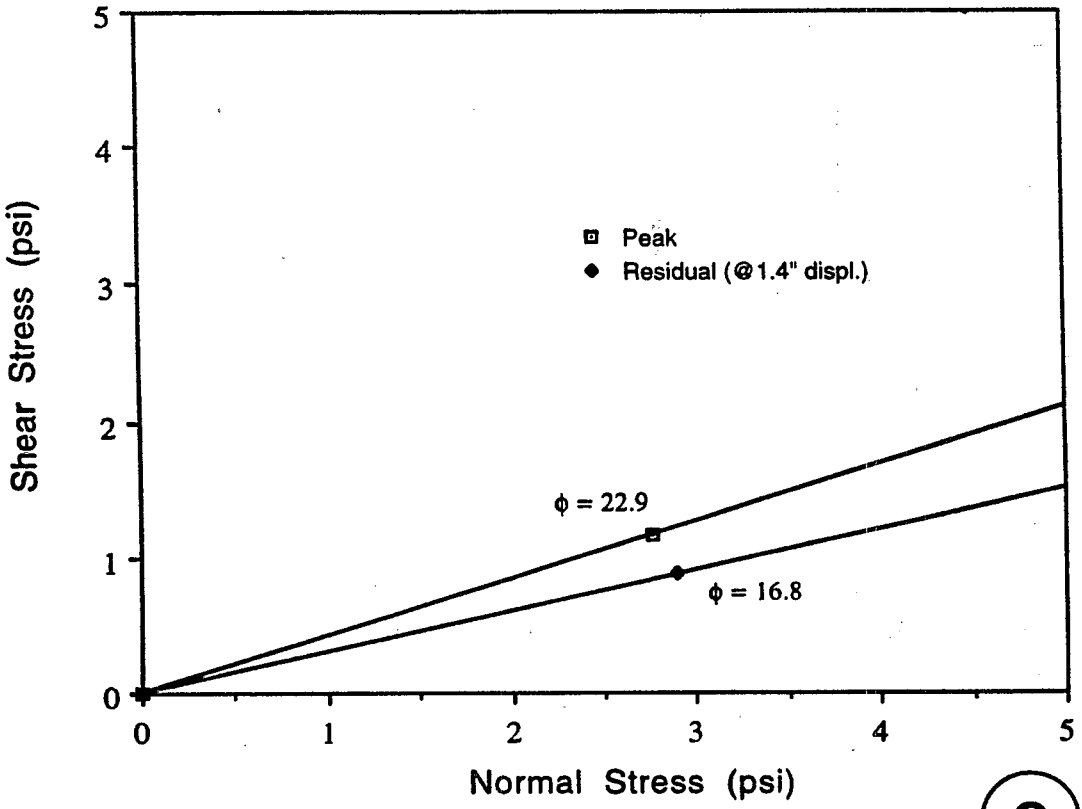
Shear Stress (psi)
5
4
3
2
1
0
0
1
2
3
4
5
Normal Stress (psi)
Peak
Residual (@1.4" displ.)
ϕ = 22.9
ϕ = 16.8

G

slid 1/12/95

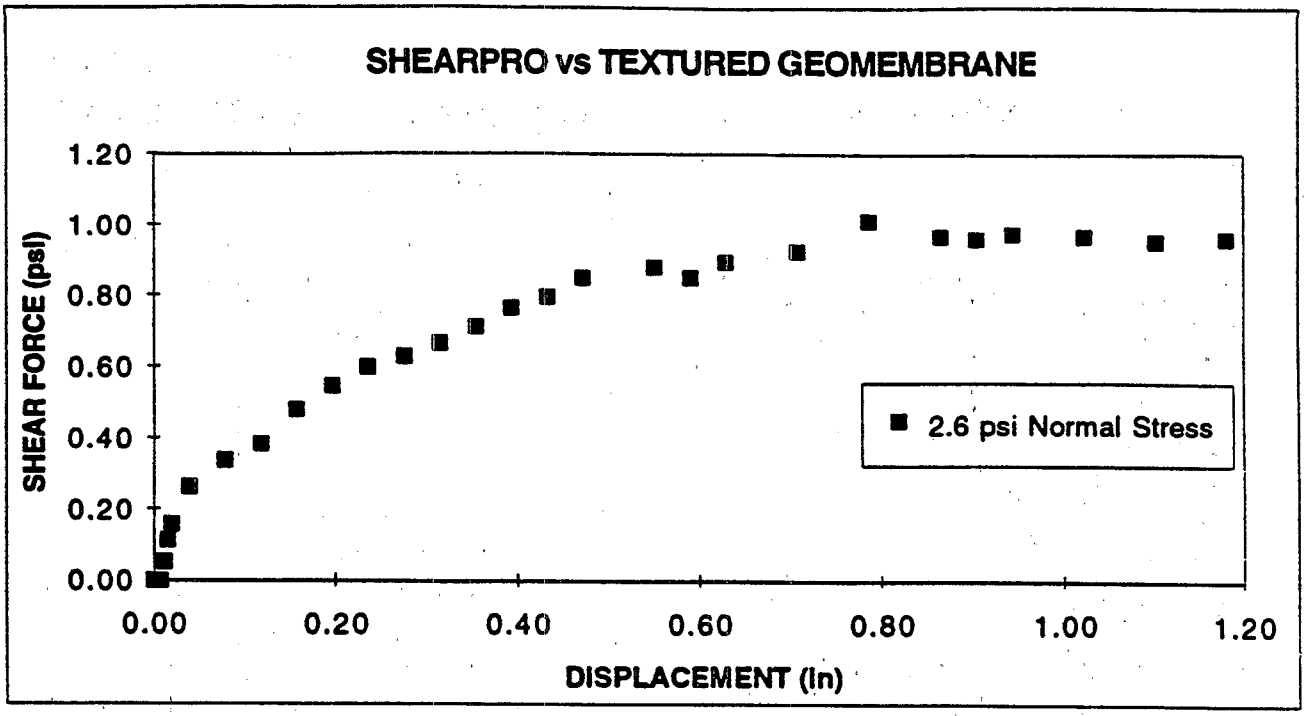

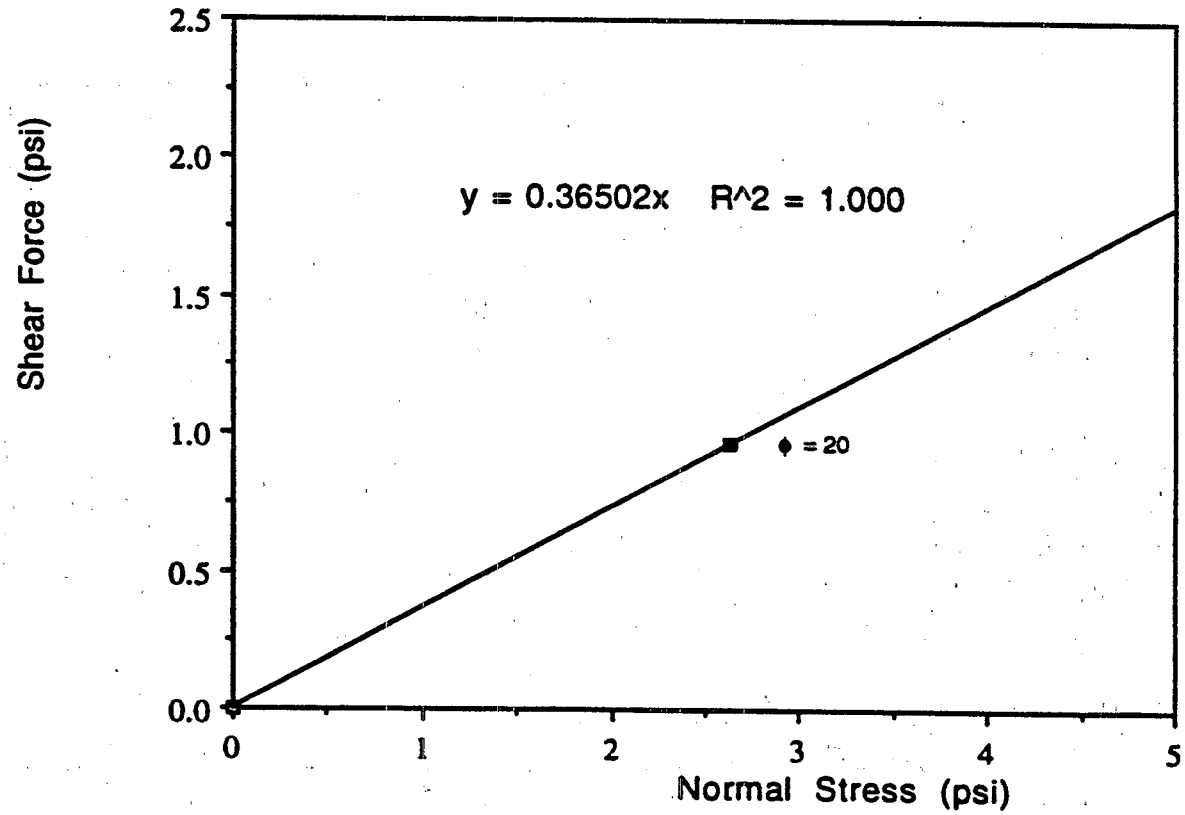

H

slid 12/10/95

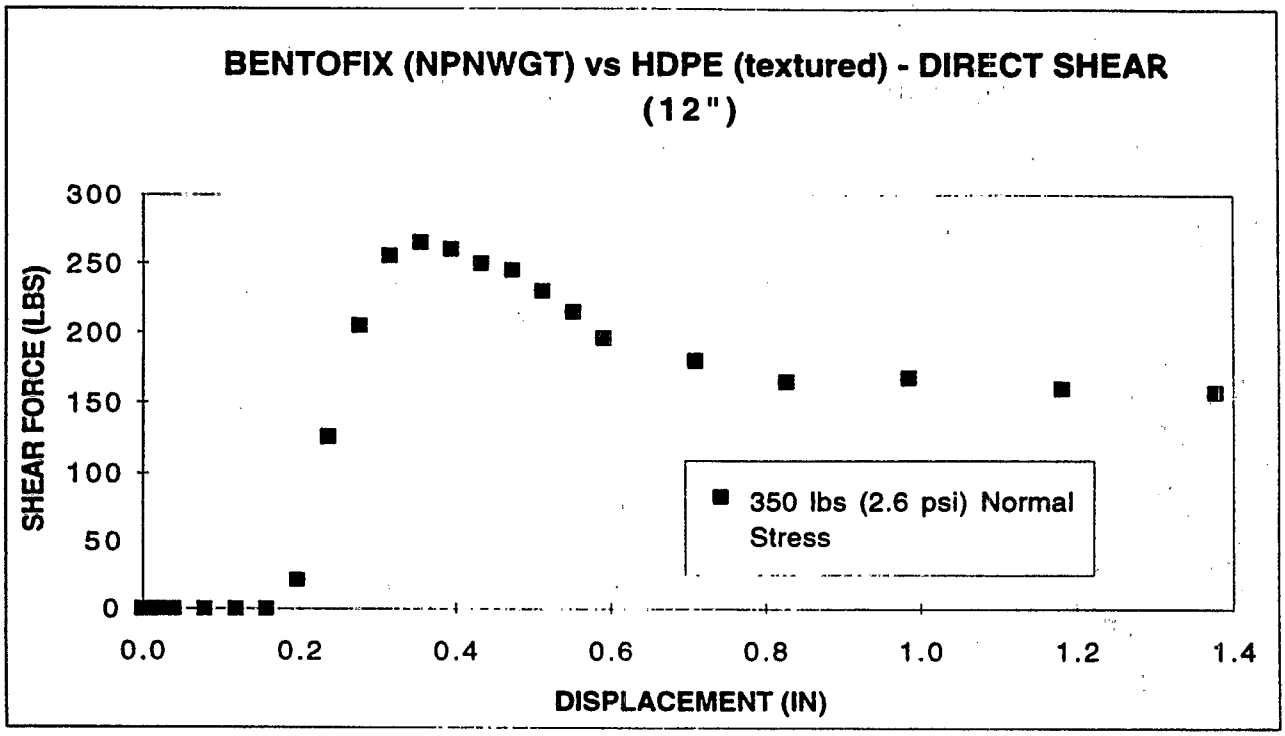
BENTOFIX (NPNWGT) vs HDPE (textured) - DIRECT SHEAR
(12")
SHEAR FORCE (LBS)
300
250
200
150
100
50
0
0.0
0.2
0.4
0.6
0.8
1.0
1.2
1.4
DISPLACEMENT (IN)
350 lbs (2.6 psi) Normal Stress

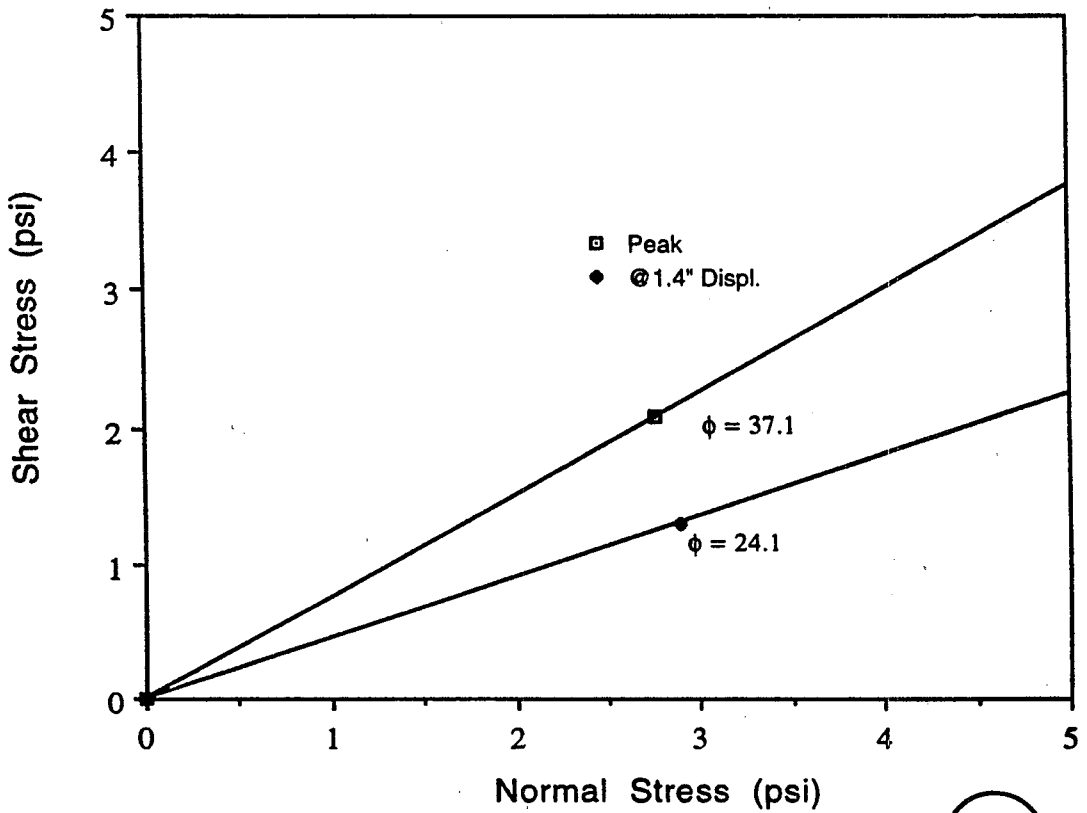
Shear Stress (psi)
5
4
3
2
1
0
0
1
2
3
4
5
Normal Stress (psi)
Peak
@1.4" Displ.
ϕ = 37.1
ϕ = 24.1

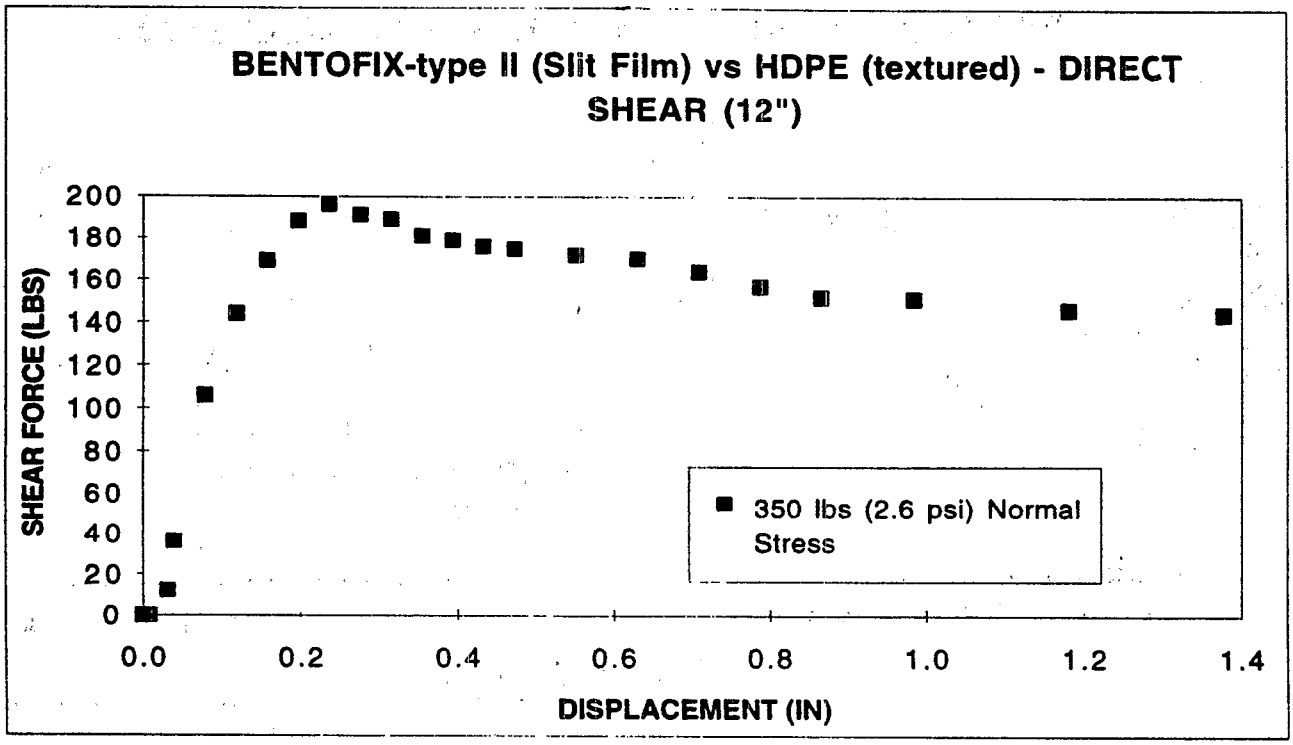
BENTOFIX-type II (Slit Film) vs HDPE (textured) - DIRECT SHEAR (12")
SHEAR FORCE (LBS)
200
180
160
140
120
100
80
60
40
20
0
0.0
0.2
0.4
0.6
0.8
1.0
1.2
1.4
DISPLACEMENT (IN)
350 lbs (2.6 psi) Normal Stress

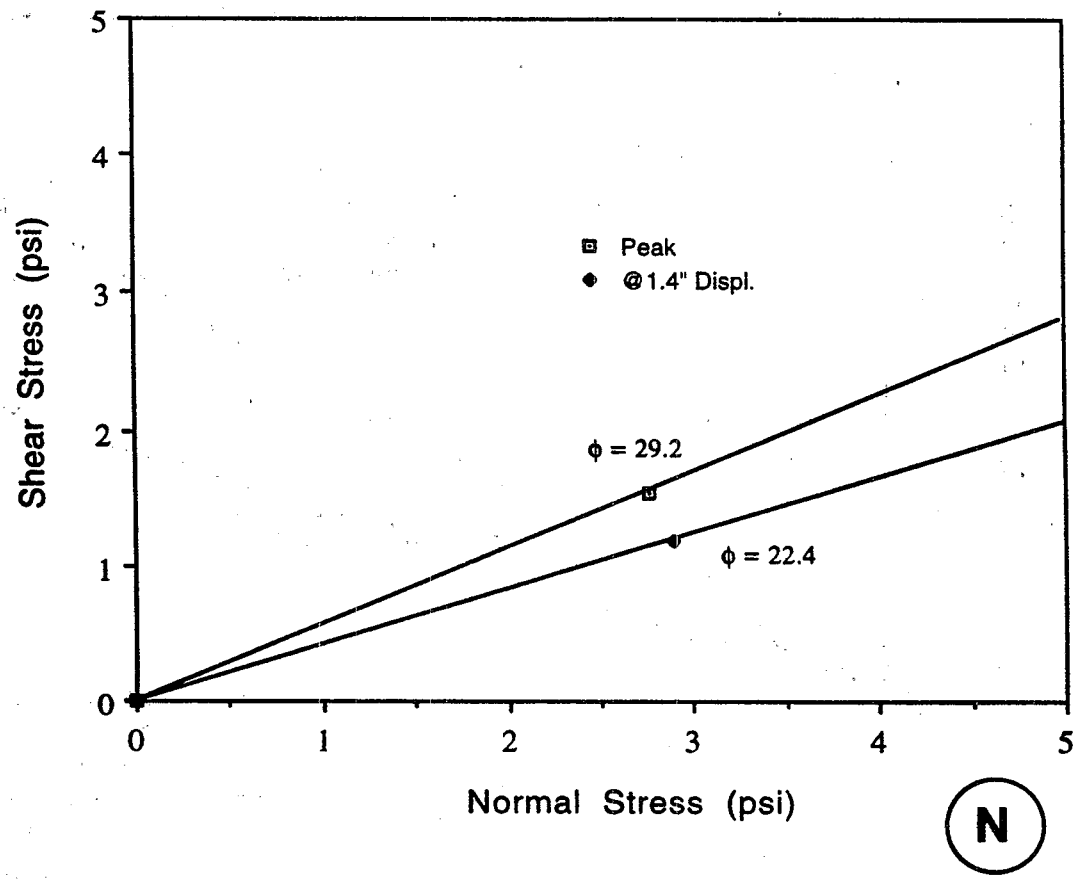
Shear Stress (psi)
5
4
3
2
1
0
0
1
2
3
4
5
Normal Stress (psi)
Peak
@1.4" Displ.
ϕ = 29.2
ϕ = 22.4
N

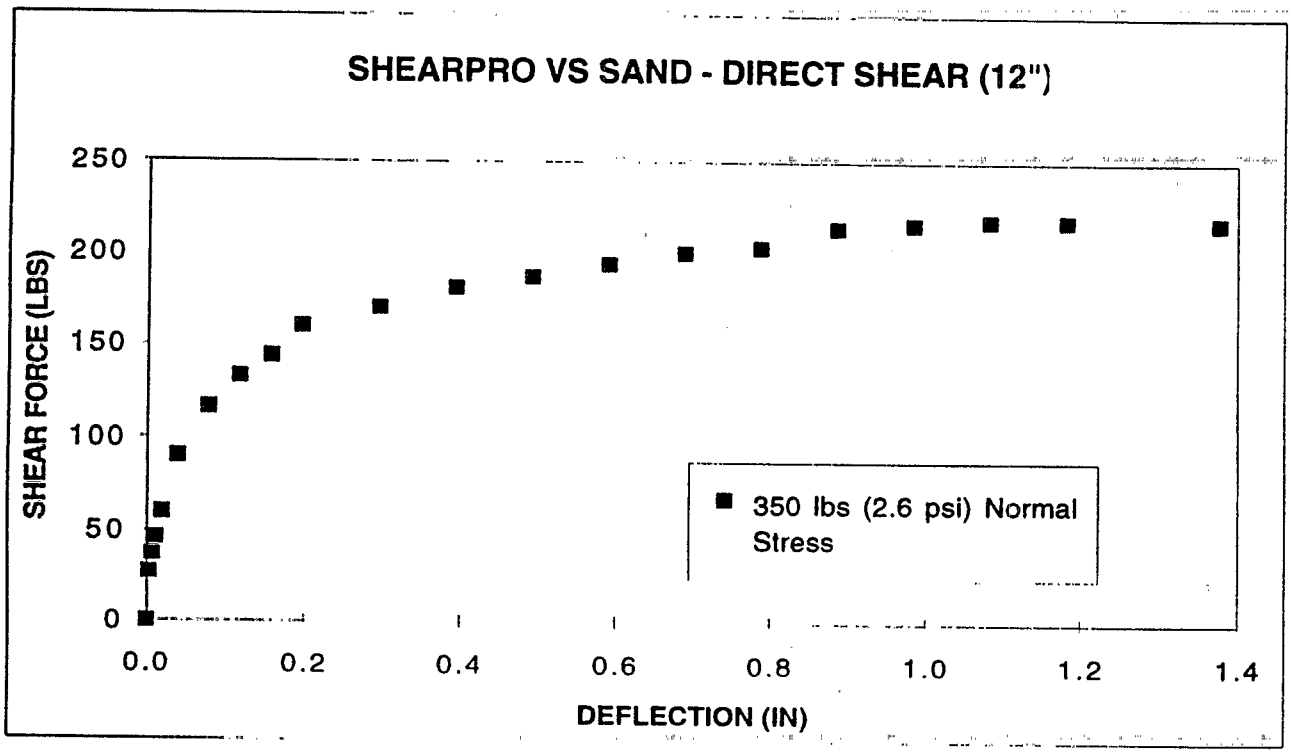
SHEARPRO VS SAND - DIRECT SHEAR (12")
SHEAR FORCE (LBS)
250
200
150
100
50
0
0.0
0.2
0.4
0.6
0.8
1.0
1.2
1.4
DEFLECTION (IN)
350 lbs (2.6 psi) Normal Stress

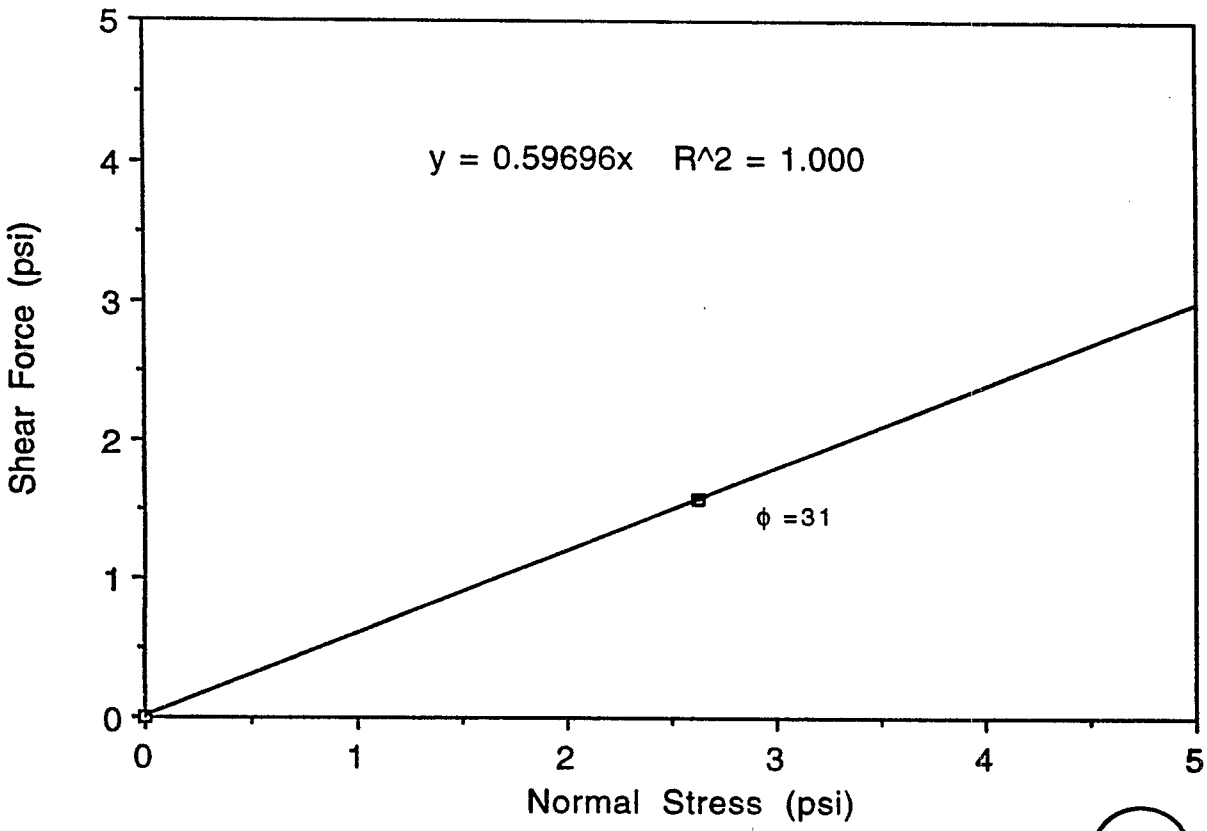
y = 0.59696x R^2 = 1.000
Shear Force (psi)
5
4
3
2
1
0
0
1
2
3
4
5
Normal Stress (psi)
ϕ =31

K

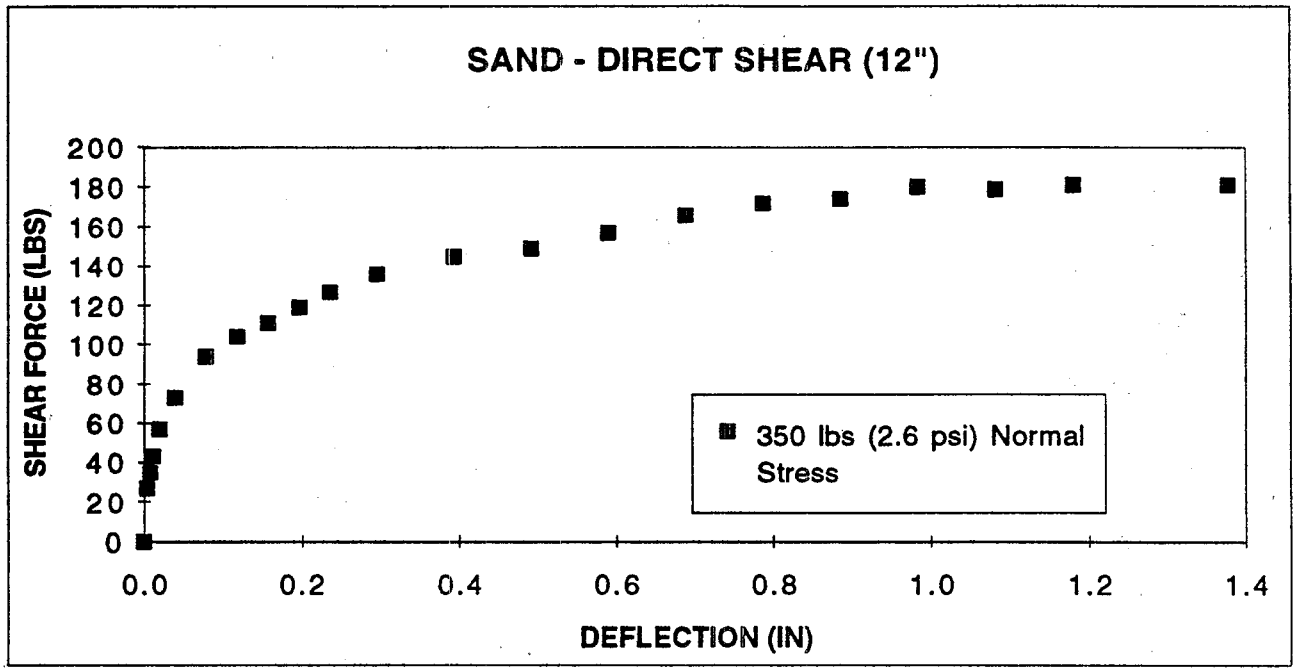
SAND - DIRECT SHEAR (12")
SHEAR FORCE (LBS)
200
180
160
140
120
100
80
60
40
20
0
0.0
0.2
0.4
0.6
0.8
1.0
1.2
1.4
DEFLECTION (IN)
350 lbs (2.6 psi) Normal Stress

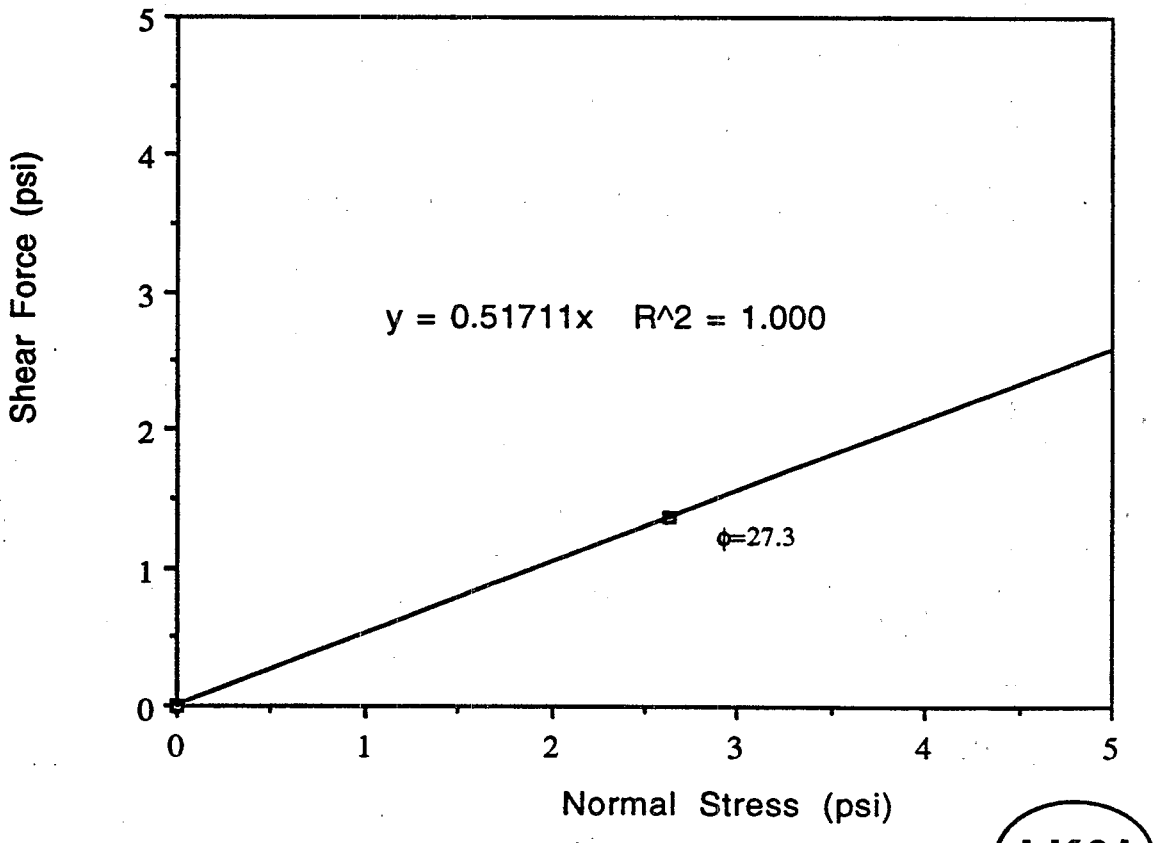
Shear Force (psi)
5
4
3
2
1
0
y = 0.51711x R^2 = 1.000
ϕ=27.3
0
1
2
3
4
5
Normal Stress (psi)

J,K&L

Appendix F

Evaluation of Various Aspects of GCL Performance, Prepared by GeoSyntec Consultants

EVALUATION OF VARIOUS ASPECTS OF GCL PERFORMANCE

by

R. Bonaparte[1], M.A. Othman[1], N.R. Rad[1], R.H. Swan[1],
and D.L. Vander Linde[1]

INTRODUCTION

The purpose of this paper is to briefly present the results of various activities that have recently been undertaken by the authors on the subject of geosynthetic clay liner (GCL) testing and performance evaluation. The subjects that are addressed are:

- field hydraulic performance of composite liners containing GCLs;
- drained shear strength of hydrated GCLs at high normal stress;
- interface shear strength between unhydrated GCLs and textured geomembranes at high normal stress;
- hydration of GCLs adjacent to soil layers; and
- causes of failure of a landfill cover system containing a GCL.

FIELD PERFORMANCE OF COMPOSITE LINERS CONTAINING GCLs

Sources of Flow in LDS of Double-Liner System

A double liner system consists of top and bottom liners with a leakage detection system (LDS) between the two liners. If the double-liner system is used in a landfill, it will also contain a leachate collection and removal system (LCRS) above the top liner. As part of an ongoing research investigation for the United States Environmental Protection Agency (USEPA), the authors have collected data

[1]GeoSyntec Consultants, 1100 Lake Hearn Drive, Atlanta, Georgia 30342

on the rates of liquid flow into the sumps of LCRSs and LDSs for a wide variety of double-lined waste management units located throughout the United States. Comparison of the rates of flow into the LCRS and LDS of a unit can be used to quantify the performance of the top liner (in terms of the ability to impede advective transport of liquid through the liner). In essence, the LDS serves as a large lysimeter (i.e., collection pan) below the top liner.

To make the evaluation, consideration must be given to the potential sources of liquid in the LDS. Gross et al. [1990] described the potential sources of LDS flow, which are (Figure 1): (i) leakage through the top liner; (ii) drainage of water (mostly rainwater) that infiltrates the leakage detection layer during construction but does not drain to the LDS sump until after start of facility operation ("construction water"); (iii) water expelled from the LDS layer as a result of compression under the weight of the waste ("compression water"); (iv) water expelled from any clay component of the top liner as a result of clay consolidation under the weight of the waste ("consolidation water"); and (v) for a waste management unit with its base located below the water table, groundwater infiltration through the bottom liner ("infiltration water").

Gross et al. [1990] and Bonaparte and Gross [1990] presented the following five-step approach for evaluating the sources of LDS liquid at a specific waste management unit.

- Identify the potential sources of flow for the unit based on double-liner system design, climatic and hydrogeologic setting, and unit operating history.
- Calculate flow rates from each potential source.
- Calculate the time frame for flow from each potential source.
- Evaluate the potential sources of flow by comparing measured flow rates to calculated flow rates at specific points in time.
- Compare LCRS and LDS chemical constituent data to further establish the likely source(s) of liquid.

Bonaparte and Gross [1990, 1993] used this five-step approach to evaluate the sources of LDS flow for 93 waste management units. Under a contract to the USEPA Risk Reduction Research Laboratory, the authors are currently performing this evaluation using new data from the facilities in the Bonaparte and Gross studies, as well as data from a significant number of additional waste management units not included in the original studies. Preliminary results for waste management units with composite top liners containing GCLs are presented below.

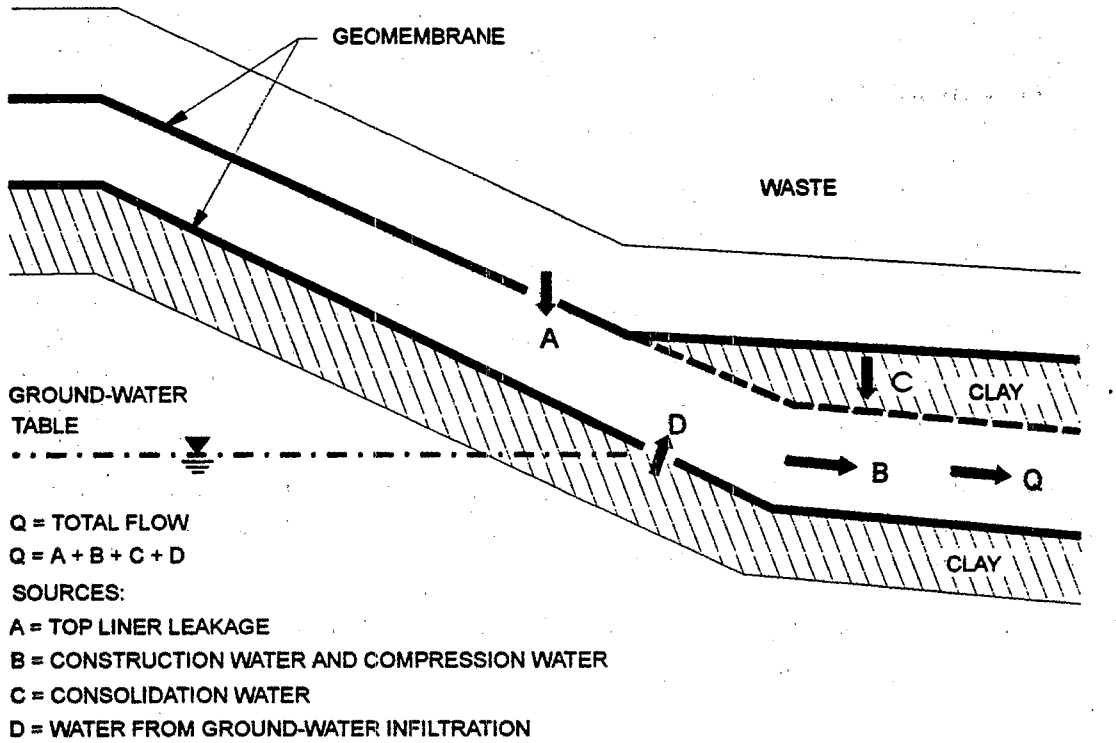

Figure 1. Sources of flow from leak detection layers.

LCRS and LDS Flow Data

Flow rate data have been collected for 26 waste management units containing composite top liners consisting of a geomembrane overlying a GCL. The 26 units are located at six different landfill sites. Descriptions of the components of the liner systems used at these facilities are presented in Table 1 and flow rate data for the LCRSs and LDSs in the units are presented in Table 2. Average daily flow rates were calculated for both systems on a monthly basis by dividing the total amount of liquid extracted from the system during the month by the number of days in the month and the area of the waste management unit. Flow rates are reported in units of liter/hectare/day (lphd). The volume of flow used in the calculation was typically obtained from the landfill operator, with flow measurements most often measured using accumulating flow meters. The reported flow volumes should be considered approximate.

Table 1. Description of landfill liner system components.

Landfill Identification	LCRS		Composite Top Liner		LDS		Bottom Liner		
	Material	Thickness (mm)	HDPE Geomembrane Thickness (mm)	GCL Thickness (mm)	Material	Thickness (mm)	HDPE Geomembrane Thickness (mm)	Layer 2	
								Material	Thickness (mm)
A	Sand	600	1.5	13	Sand	300	1.5	Clay	200
B	Sand	600	2.0	13	Sand	450	2.0	Clay	300
C	Sand	450	1.5	13	Sand	300	1.5	GCL	13
D	Sand	600	1.5	13	GT/GN[1]	5	1.5	N/A	N/A
E	Sand	600	1.5	13	GT/GN	5	1.5	Clay	900
F	GN	5	1.5	13	GT/GN	5	1.0	GCL	13

Notes: [1] GT= Geotextile, GN= Geonet.
[2] All material thicknesses are nominal values.

Table 2. Summary of flow data for the LCRS and LDS of units with composite top liners containing GCLs.

Cell No.	Cell Area	End of Cell Const.	Start of Waste Placem.	End of Final Closure	Initial Period of Operation[1]					Active Period of Operation[2]					Post Closure Period[3]				
					Time Period	LCRS Flow[4]		LDS Flow		Time Period	LCRS Flow		LDS Flow		Time Period	LCRS Flow		LDS Flow	
						Avg.	Peak	Avg.	Peak		Avg.	Peak	Avg.	Peak		Avg.	Peak	Avg.	Peak
	(hectare)	(month-year)	(month-year)	(month-year)	(months)	(lphd)	(lphd)	(lphd)	(lphd)	(months)	(lphd)	(lphd)	(lphd)	(lphd)	(months)	(lphd)	(lphd)	(lphd)	(lphd)
A1	2.0	7-88	7-88	2-91	1-2	16,718	19,738	0.0	0.0	3-32	561	2,384	0.0	0.0	33-83	65	103	0.0	0.0
A2	2.0	7-88	7-88	2-91	1-5	15,521	58,671	15.0	44.9	6-32	281	570	1.9	20.6	33-83	178	421	0.0	0.0
A3	1.7	8-88	9-88	4-93	1-5	3,366	7,985	34.6	150.5	6-56	290	1,075	3.7	46.8	57-81	206	458	0.9	9.4
A4	1.7	8-88	9-88	4-93	1-12	2,534	12,688	101.0	860.2	13-56	75	187	0.9	13.1	57-81	47	84	0.0	0.0
A5	2.8	9-88	10-88		1-11	1,384	3,394	37.4	91.6	12-80	56	187	1.9	37.4					
A6	3.9	11-88	12-88		1-9	3,759	7,171	53.3	92.6	10-80	168	655	0.0	0.0					
A7	2.6	1-89	2-89		1-10	5,376	12,155	33.7	46.8	11-76	234	851	1.9	9.4					
A8	3.8	7-89	7-89		1-14	4,881	21,038	47.7	188.9	15-71	439	1,384	0.0	0.0					
A9	3.3	12-89	12-89		1-9	1,047	3,478	0.9	7.5	10-65	37	159	0.0	0.0					
A10	3.9	2-90	7-90		1-7	2,786	13,698	0.0	0.0	8-59	374	645	0.0	0.0					
A11	3.0	2-90	2-90		1-16	4,675	14,586	0.0	0.0	17-64	150	337	0.0	0.0					
A12	4.0	10-90	10-90		1-18	2,945	8,836	0.0	0.0	19-56	655	1,505	0.0	0.0					
A13	3.0	1-91	1-91		1-32	3,740	14,343	0.0	0.0	33-53	281	486	0.0	0.0					
A14	2.8	4-91	4-91		1-11	2,777	6,582	0.0	0.0	12-38	281	449	0.0	0.0					
A15	2.8	5-92	5-92		1-12	5,573	11,809	0.0	0.0	13-37	299	561	0.0	0.0					
A16	4.5	1-93	1-93		1-22	4,675	17,756	0.0	0.0	23-29	206	393	0.0	0.0					
B1	3.6	5-93	8-93		1-10	3,273	12,155	177.7	822.8	11-17	393	1,403	2.8	15.0					
C1	2.4	4-93	5-93		1-12	6,358	20,570	130.9	523.6										
C2	2.4	7-93	8-93		1-10	3,553	7,480	289.9	514.3										
D1	4.0	12-90	2-91		1-23			11.2	24.3	24-47			0.9	3.7					
D2	2.4	12-92	1-93		1-24	4,208	11,688	0.9	14.0										
D3	2.8	12-92	1-93		1-13	3,179	8,228	0.0	0.0	14-24	187	309	0.0	0.9					
E1	3.8	9-92	12-92		3-23	3,890		1.9	22.4										
F1	1.3	7-94	10-94		1-9	6,330	12,052	0.0	0.0										
F2	1.0	7-94	8-94		1-11	9,967	21,729	4.7											
F3	1.0	7-94	8-94		1-11	11,248	31,313	11.2											

Notes:

[1] "Initial Period of Operation" represents period after waste placement has started and only a few lifts of waste and daily cover have been placed in the cell (i.e., no intermediate cover).

[2] "Active Period of Operation" represents period when waste thickness in cell is significant and/or an effective intermediate cover is placed on the waste.

[3] "Post Closure Period" represents period after final cover system has been placed on the entire cell.

[4] Flow rates are given in liter/hectare/day.

Figure 2 shows LCRS and LDS average daily flow rate data for a municipal solid waste management unit, located in Pennsylvania, that was active for 56 months. Subsequently, a final cover system containing a geomembrane was placed over the entire unit. Flow data for the 56-month operational period and a 25-month post closure period were obtained and analyzed. As Figure 2 shows, flow rates in both systems were highest immediately after the start of waste placement and thereafter decreased with time. During the first twelve months of operation, the average rate of flow into the LCRS sump decreased from 12,700 to 180 lphd. After that time, the LCRS flow rate stabilized and during the following 44 months, the rate of flow into the LCRS sump varied between 10 and 170 lphd. After final closure, the flow rate decreased even further, to between 10 and 80 lphd.

As illustrated in Figure 2, waste management unit development can be divided into three distinct periods. During the first period, herein referred to as the "initial period of operation", LCRS flow rates may be relatively high. High flows during this period are attributed to the occurrence of rainfall into a unit that initially contains little waste. To the extent rainfall occurs during this period, it will find its way rapidly into the LCRS. Obviously, the amount of LCRS flow during this period is highly dependent on climate. A lag exists between the time liquid first enters the LCRS and when it flows into the LCRS sump. The magnitude of the lag is largely dependent on the hydraulic characteristics (i.e., the length and slope of the LCRS and the hydraulic conductivity of the LCRS drainage material). Most available data indicate a decreasing LCRS flow rate with time during the initial period of operation. During the second period, referred to herein as the "active period of operation", the rate of flow into the LCRS continues to decreases and eventually stabilizes. This occurs as the amount of waste in the unit increases and as daily and intermediate layers of cover soil are placed. This trend in flow rates is also dependent on the type of waste but is likely representative of the trends observed at most new landfills, excluding those that accept sludges or other high moisture content wastes. During the "post closure period", the final cover system further reduces infiltration of rainwater into the waste, resulting in a further reduction in LCRS flow. Final covers containing geomembranes can, if functioning properly, virtually eliminate rainwater infiltration.

LDS flow rates for the waste management unit in Figure 2 were highest (860 lphd) at the beginning of operations and decreased in the following few months, becoming very low (i.e., less than 10 lphd) within approximately 15 months after the start of unit operation. The decrease in LDS flow with time is expected because: (i) flow rates in the LCRS during this time period decreased, and therefore, the potential for leakage through the top liner also decreased; (ii) most construction water initially present in the LDS flowed to the LDS sump in the first few weeks to months of unit operation; and (iii) the volume of compression and consolidation water for this waste management unit should be very small.

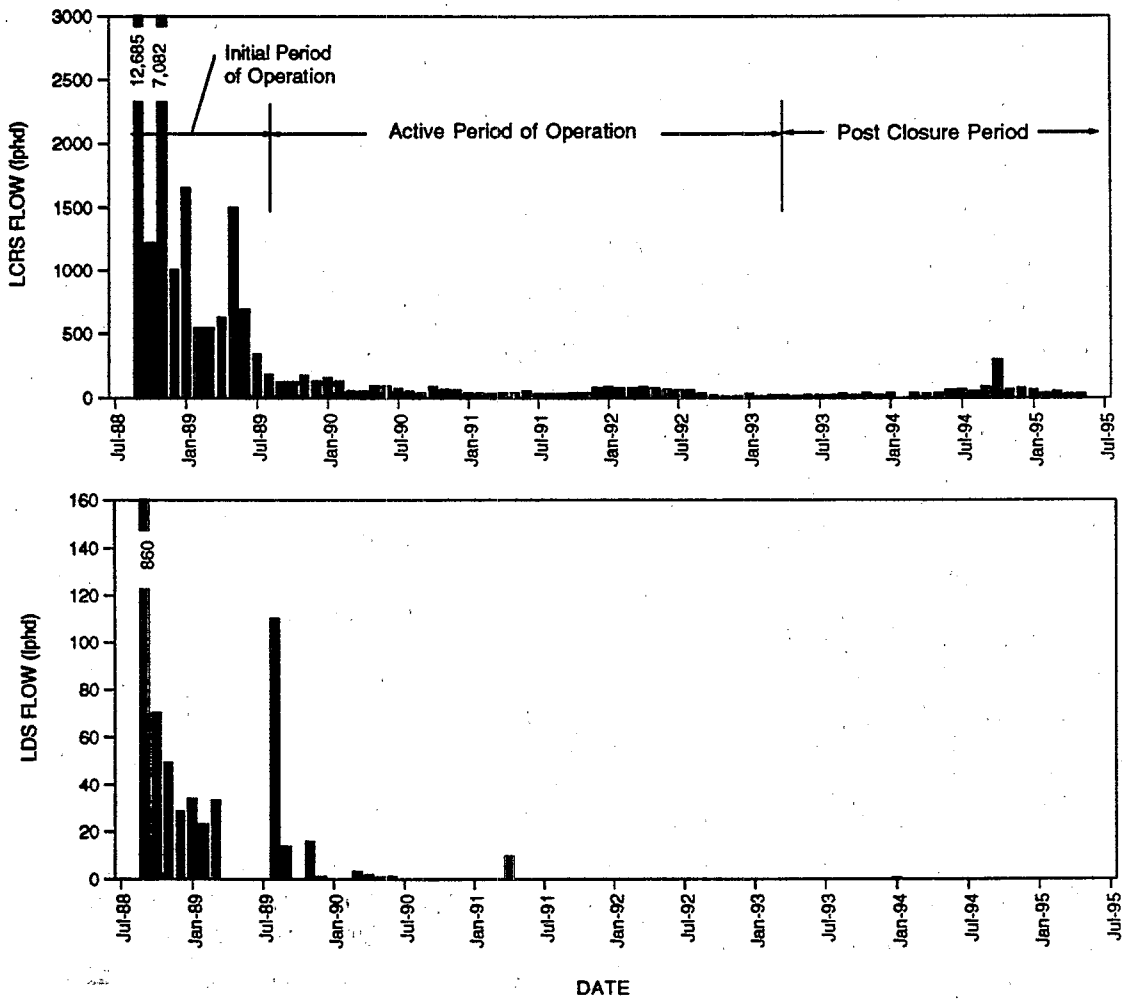

Figure 2. LCRS and LDS flow rates at a modern MSW landfill in Pennsylvania.

Table 2 summarizes LCRS and LDS flow data for the 26 waste management units containing GCLs in their composite top liners. Average and peak flow rates are reported for the three time periods described above. Table 2 shows that between the initial and active periods of operation, LCRS flow rates decreased one to two orders of magnitude and LDS flow rates decreased one to three orders of magnitude. Reported peak LCRS flow rates were up to 5 times the average, while peak LDS flow rates were up to 20 times the average. Table 3 presents the mean values of average and peak flows for the database.

Table 3. Mean values of flow for the data in Table 2 (Note: m = mean value; σ = standard deviation; values are in liter/hectare/day).

LCRS	Number of Units	Average Flow Rate		Peak Flow Rate	
		m	σ	m	σ
Initial Period of Operation	25	5,350	3,968	14,964	11,342
Active Period of Operation	18	276	165	752	590
Post-Closure Period	4	124	-	266	-

LDS	Number of Units	Average Flow Rate		Peak Flow Rate	
		m	σ	m	σ
Initial Period of Operation	26	36.6	68.5	141.8	259.9
Active Period of Operation	19	0.7	1.1	7.7	13.7
Post-Closure Period	4	0.2	-	2.3	-

Top Liner Hydraulic Efficiency

Table 4 summarizes calculated "apparent" efficiencies for the composite top liners of the 26 waste management units presented in Table 2. Liner apparent efficiency, AE, is calculated using the following equation:

$$AE\ (\%) = (1 - \text{LDS Flow Rate} / \text{LCRS Flow Rate}) \times 100 \qquad \text{(Equation 1)}$$

Table 4. "Apparent" efficiencies of composite liners containing GCLs[1].

Cells with Sand LDS				Cells with GT/GN LDS	
Cell No.	Initial Period of Operation (%)	Active Period of Operation (%)	Post-Closure Period (%)	Cell No.	Initial Period of Operation (%)
A1	100.00	100.00	100.00	D1	99.98
A2	99.90	99.33	100.00	D2	100.00
A3	98.97	98.71	99.55	E1	99.95
A4	96.01	98.75	100.00	F1	100.00
A5	97.23	97.50		F2	99.95
A6	98.58	100.00		F3	99.90
A7	99.37	99.20			
A8	99.02	100.00			
A9	99.91	100.00			
A10	100.00	100.00			
A11	100.00	100.00			
A12	100.00	100.00			
A13	100.00	100.00			
A14	100.00	100.00			
A15	100.00	100.00			
A16	100.00	100.00			
B1	94.57	99.29			
C1	97.94				
C2	91.84				
Number	19	17	4	Number	6
Range	91.84 - 100.00	97.5 - 100.00	99.55 - 100.00	Range	99.90 - 100.00
Mean	98.60	99.58	99.89	Mean	99.96
Median	99.90	100.00	100.00	Median	99.97

Notes: [1] Apparent Efficiency = (1 - LDS Flow / LCRS Flow) x 100 %

This liner efficiency is referred to as "apparent" because, as described above, flow into the LDS sump may be attributed to sources other than top liner leakage (Figure 1). If the only source of flow into the LDS sump is top liner leakage, then Equation 1 provides the "true" liner efficiency. Liner efficiency provides a measure of the effectiveness of a particular liner in limiting or preventing advective transport across the liner.

Table 4 presents calculated AE values for waste management units with sand LDSs (Landfills A, B, and C). For these units, the apparent efficiency is lowest during the initial period of operation (AE_m = 98.6 percent; where AE_m = mean apparent efficiency) and increases significantly thereafter (AE_m = 99.58 percent during the active period of operation and AE_m = 99.96 percent during the post closure period). The lower AE_m during the initial period of operation can be attributed to LDS flow from construction water. For units A, B, and C, calculated AE values during the active period of operation and the post-closure period may provide a reasonably accurate indication of true liner efficiency for the conditions at these units during the monitoring periods. It should be noted, however, that the true efficiency of a liner is not constant but rather a function of the hydraulic head in the LCRS and size of the area over which LCRS flow is occurring (the area is larger at high flow rates compared to low flow rates).

Table 4 also presents calculated AE values for waste management units with geonet LDSs (Landfills D, E, and F). The available data are limited to the initial period of unit operation. As shown in Table 4, AE_m for the six units with geonet LDSs is 99.96 percent. This value is much higher than the AE_m of liners of cells with sand LDSs for the same facility operational period (i.e., 98.60 percent). This higher efficiency can be attributed to the differences in liquid storage capacity and hydraulic transmissivity between sand and geonet drainage materials. A granular drainage layer can store a much larger volume of construction water and releases this water more slowly during the initial period of operation than does a geonet drainage layer. This suggests that, during the initial period of operation, the main source of flow in a sand LDS underlying a composite top liner containing a GCL is construction water.

Conclusions on Field Performance of Composite Liners Containing GCLs

From Table 2, LDS flows attributable to top liner leakage very from 0 to 50 lphd, with most values being less than about 2 lphd. These flow rates are very low. The data shown in Table 4 suggest that the true hydraulic efficiency of a composite liner incorporating a GCL may be greater than 99.90 percent. A liner with this efficiency, when appropriately used as part of an overall liner system, can provide a very high degree of liquid containment capability.

SHEAR STRENGTH OF HYDRATED GCLs

Overview

For a recent project, the authors were concerned with the long-term drained shear strength of hydrated GCLs at normal stresses in the range of 240 to 720 kPa. Drained shear strengths are applicable to long-term design and the range of considered normal stresses is applicable to conditions in a liner system at the base of a landfill. A testing program to evaluate the long-term drained shear strength of GCLs was undertaken and this program is ongoing. To develop interim values for preliminary design, the authors reviewed and analyzed available data from the technical literature on the consolidated-drained (CD) shear strength of GCLs. The findings of this review are presented below.

Required Deformation Rates to Achieve CD Conditions

To achieve consolidated drained (CD) test conditions, direct shear tests must be carried out at a very slow rate of shear displacement. The required displacement rate can be estimated using the well-known time-to-failure equation specified in American Society of Testing and Materials (ASTM) standard test method D 3080:

$$t_f = 50\ t_{50} \qquad \text{(Equation 2)}$$

where: t_f = total elapsed time to failure(s); and t_{50} = time required for the test specimen to achieve 50 percent primary consolidation under the specified normal stress, or increment(s) thereof. Using t_f from consolidation tests and an estimated failure displacement δ_t, the required shear displacement rate, d_r, can be calculated using the equation:

$$d_r = \delta_t / t_f \qquad \text{(Equation 3)}$$

Shan [1993] performed one-dimensional consolidation tests on the GCL products Claymax®, Gundseal®, Bentomat®, and Bentofix®. He evaluated t_f values for each product. The results of his evaluation are provided in Figure 3. With reference to this figure, at normal stresses in the range of 240 to 720 kPa, t_f values are in the range of about 100 to 400 hours. If it is assumed that a displacement of 25 mm is needed to achieve peak shear stress conditions, a required shear displacement rate of 0.05 to 0.25 mm/s is calculated. Only test results conducted at shear displacement rates that satisfy Equations 2 and 3 and the data from Shan [1993] should be considered to represent CD conditions. Test results at faster rates will yield lower shear strengths as a result of positive pore pressure development during the shearing phase of the test.

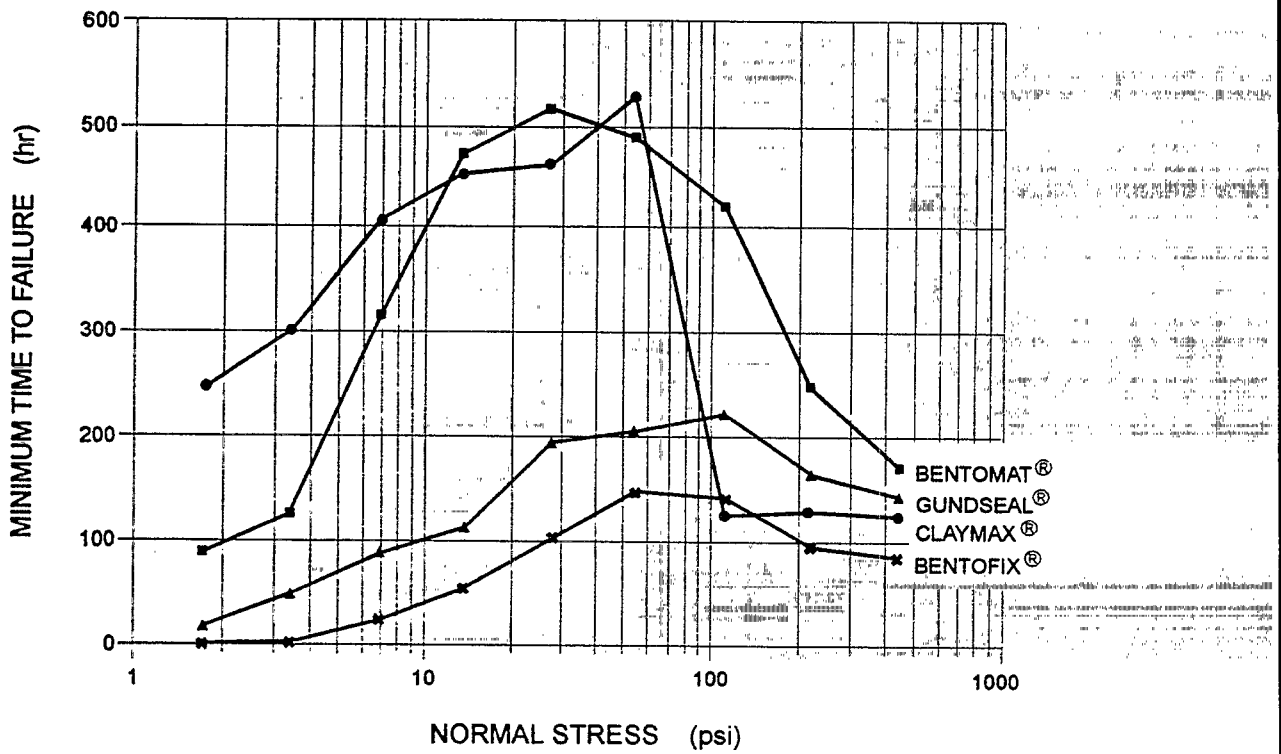

Figure 3. Relationship between time to failure of GCLs in direct shear tests and normal stress (from Shan, 1993; Note: 1 psi = 6.9 kPa).

It is noted that direct shear tests on GCLs are often performed in general accordance with the standard test method ASTM D 5321 ("*Determining the Coefficient of Soil and Geosynthetic or Geosynthetic and Geosynthetic Friction by the Direct Shear Method*"). This method provides the following guidelines for selecting shear displacement rates for tests involving soils:

> "*11.6 Apply the shear force using a constant rate of displacement that is slow enough to dissipate soil pore pressures, as described in Method D 3080 (Note 9). If excess pore pressures are not anticipated, and in the absence of a material specification, apply the shear force at a rate of 1 mm/min (0.04 in./min).*"

The foregoing requirement calls for performing direct shear tests involving soils at a shear displacement rate in conformance with ASTM D 3080 if pore pressures are anticipated. For the soil component of GCLs (i.e., sodium montmorillonite), significant pore pressures will certainly be generated if the GCL is sheared at rates faster than those satisfying Equations 2 and 3. Interestingly, however, most test data available in the published literature were generated at the default shear displacement rate of 0.017 mm/s. Data generated at the default shear displacement rate are considered to reflect "undrained" or "partially-drained," and not "fully-drained," conditions.

Review of Available Information for Unreinforced GCLs

For purposes of shear strength characterization, two different categories of GCL can be considered: GCLs that do not contain internal reinforcement (hereafter referred to as unreinforced GCLs) and those that do (hereafter referred to as reinforced GCLs). Published information relevant to the CD shear strengths of unreinforced GCLs is very limited. The available information is summarized below.

- Daniel and Shan [1991] and Shan and Daniel [1991] reported CD direct shear test results for the GCL product Claymax®. Tests were performed using 60-mm diameter specimens and a shear deformation rate of 5 x 10^{-6} mm/s. Test results have been interpreted herein in terms of "peak (p)" and "large-displacement (ld)" normalized shear strengths. Peak displacements in these tests were 0.5 to 5 mm with the largest displacement corresponding to the lowest normal stress; the reported "ld" shear strengths correspond to shear displacements of approximately 6 to 9 mm. Results from the tests are as follows:

σ_n (kPa)	$(\tau/\sigma_n)_p$	ϕ_p	$(\tau/\sigma_n)_{ld}$	ϕ_{ld}
34	0.236	13.3°	0.236	13.3°
69	0.238	13.4°	0.209	11.8°
100	0.194	11.0°	0.165	9.4°
140	0.178	10.1°	0.137	7.8°

where: σ_n = normal stress on the shear plane at failure (kPa); τ = shear stress on the shear plane at failure (kPa); and ϕ = secant friction angle (dimensionless), calculated as the inverse tangent of τ/σ_n. It is noted that ϕ should also be interpreted as a measure of normalized shear strength and not as a "true" indication of internal friction. This data interpretation is illustrated in Figures 4 and 5.

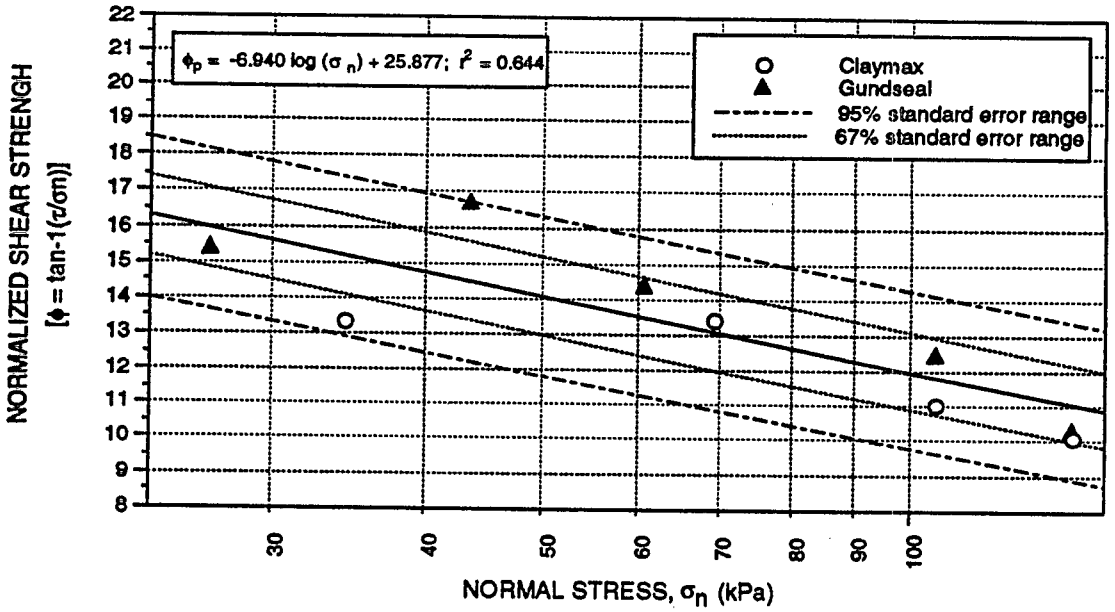

Figure 4. Log-linear regression analysis for peak CD conditions.

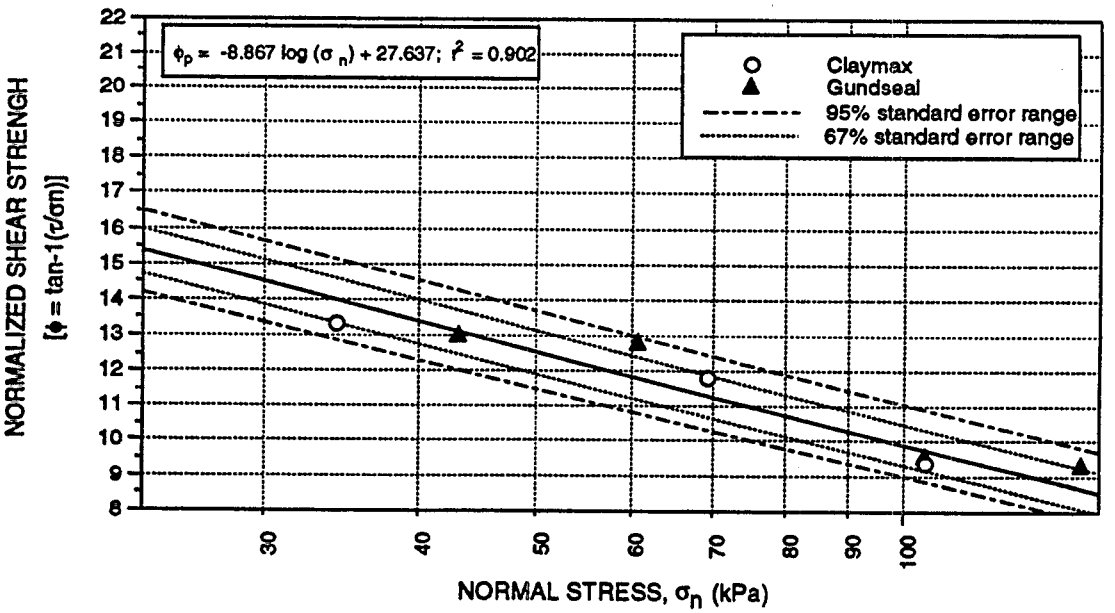

Figure 5. Log-linear regression analysis for large-displacement CD conditions.

- Daniel and Shan [1991], Daniel et al. [1993], and Shan [1993] reported direct shear CD test results for the GCL product Gundseal®. Tests were performed using 60-mm diameter specimens and a shear deformation rate of 5 x 10^{-6} mm/s. Test results have been interpreted herein in terms of peak and large-displacement normalized shear strengths. Typical peak displacements in these tests were 2 to 4 mm with the largest displacement corresponding to the lowest normal stress; the reported "ld" shear strengths correspond to shear displacements of approximately 9 to 12 mm. Results from the tests are as follows:

σ_n (kPa)	$(\tau/\sigma_n)_p$	ϕ_p	$(\tau/\sigma_n)_{ld}$	ϕ_{ld}
27	0.275	15.4°	-	-
44	0.300	16.7°	0.231	13.0°
61	0.256	14.4°	0.227	12.8°
100	0.223	12.6°	0.169	9.6°
140	0.181	10.3°	0.164	9.3°

The direct shear test results from Daniel and Shan are plotted in Figures 4 and 5 for "peak" and "large displacement" shearing conditions, respectively. Regression equations were developed to describe the test results. It is interesting to note the lesser amount of scatter in the results for the large-displacement shearing conditions compared to the peak shearing conditions.

The test results in Figures 4 and 5 only cover the stress range between 24 and 144 kPa. Even at these relatively low normal stresses, GCL CD shear strengths exhibit significant normal stress dependency. A basis is needed for extrapolating this stress dependency to higher normal stress. This basis was derived from published information from the soil mechanics literature on the shear strength of sodium montmorillonite. This information is summarized below.

- Mesri and Olson [1970] and Olson [1974] reported the results of constant rate-of-strain CD and consolidated-undrained (with pore pressure measurement) triaxial compression tests on homionic sodium montmorillonite consolidated from a slurry (Figure 6); approximate effective-stress normalized shear strengths and secant friction angles derived from the tests are as follows:

σ_n (kPa)	(τ/σ_n)	ϕ
72	0.21	12°
170	0.14	8°
340	0.10	6°
530	0.07	4°

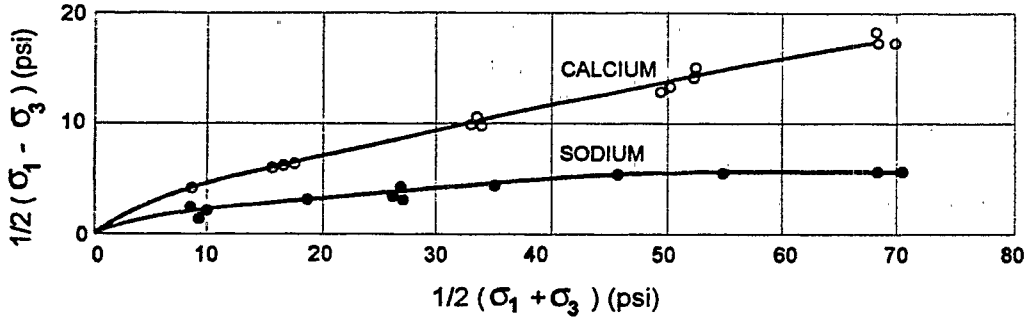

Figure 6. Effective-stress failure envelopes for calcium and sodium montmorillonite from CD and CU triaxial tests (from Mesri and Olson, 1970; Note: 1 psi = 6.9 kPa).

- Mitchell [1993] presented residual shear strength data for montmorillonite from Kenney [1967] and Chattopadhyay [1972]. Inspection of the residual shear strength data shown in Figure 7 reveals several significant points:

  - the residual friction angle exhibits significant stress dependency over a wide range of normal stress; stated differently the residual failure envelope is curved over a wide range of normal stress;

  - there may exist a normal stress above which the residual friction angle is independent of normal stress; based on Figure 7, this normal stress may be on the order of 480 kPa for sodium montmorillonite; and

  - the residual friction angle of montmorillonite is dependent on the dominant exchangeable cation and the soil pore chemistry; the smallest measured residual friction angle given in Figure 7 is 3° for homionic sodium montmorillonite in distilled water.

The GCL regression lines from Figures 4 and 5 are plotted along with the Mesri and Olson [1970] data in Figure 8. Reasonable agreement is observed between the Mesri and Olson data and the extrapolated regression lines for the unreinforced GCL. Also shown on this figure are the residual shear strengths for sodium montmorillonite developed by Kenney [1967] and Chattopadhyay [1972] as reported by Mitchell [1993]. These latter results further support the extrapolations presented in Figure 8.

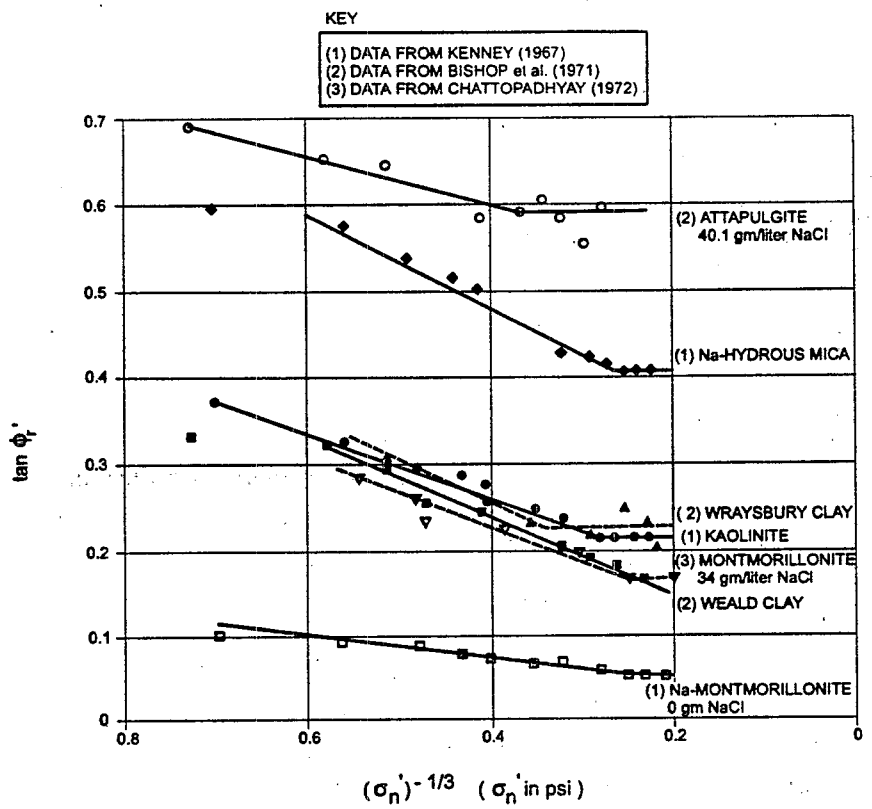

Figure 7. Residual effective-stress friction angles for clay minerals (from Mitchell, 1993; Note: 1 psi = 6.9 kPa).

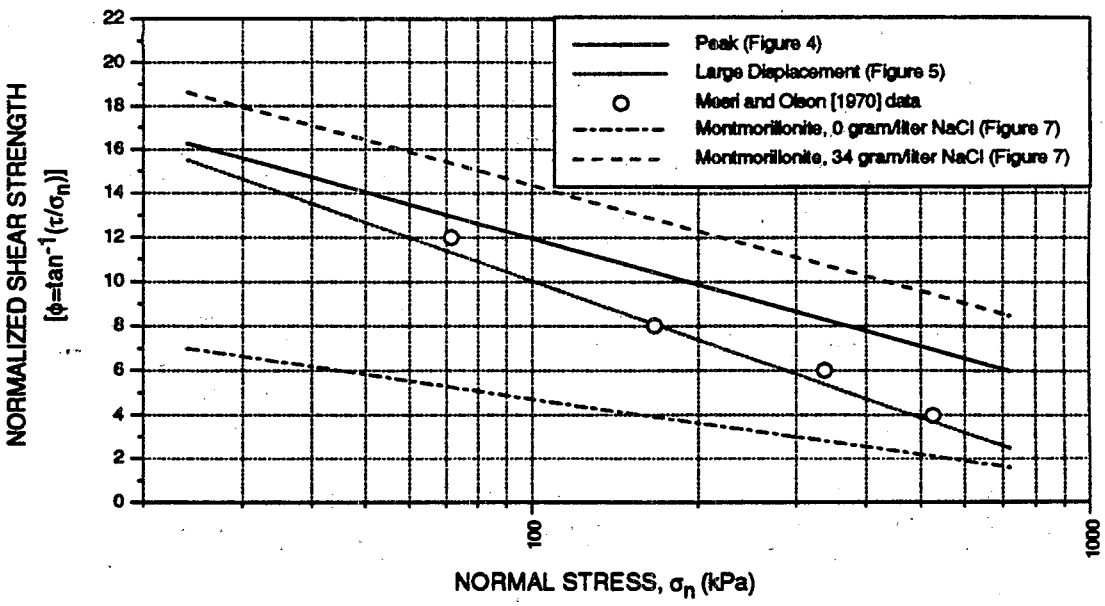

Figure 8. Comparison on montmorillonite shear strength data and GCL log-linear regression lines.

Review of Available Information for Reinforced GCLs

The authors were unable to find any information in the published technical literature on the CD shear strengths of reinforced GCLs at high normal stress. A few CD tests performed at low normal stress have been reported by Daniel and Shan [1991] for the product Bentomat®. These results cannot be extrapolated to higher normal stress, however, due to the current limited understanding of the effect of reinforcing fibers on the shear displacement-shear resistance-normal stress relationship for this type of material.

The authors have performed a limited number of consolidated-quick (CQ) direct shear tests on reinforced GCLs at normal stresses in the range of interest. Quick tests were performed at a displacement rate of 0.016 mm/s. While not "truly undrained" due to the lack of boundary drainage control in the direct shear test, the specimens in these tests will only undergo very limited pore pressure dissipation during the shear phase of the test due to the high rate of shear displacement. Due to these pore pressures, CQ tests at a given consolidation stress will result in lower GCL shear strengths than obtained from true CD tests at the same normal stress. CQ tests may therefore be considered to provide a lower bound of the CD shear strength of reinforced GCLs.

The results of the CQ direct shear tests on reinforced GCLs indicate relatively high peak shear strengths followed by a significant degree of shear softening (i.e., post peak decrease in shearing resistance). A typical test result is illustrated in Figure 9. Normalized peak and large displacement shear strengths, and the ratio of the two (ψ) for a normal stress of 480 kPa are given below:

	ϕ_p	ϕ_{ld}	τ_{ld}/τ_p
Bentomat®	29°	10°(↓)	0.32
Bentofix®	31°	16°(↓)	0.48
Claymax® 500SP	13°	6°(↓)	0.45

In the above table the downward arrow (↓) indicates that the GCL shearing resistance was decreasing at the end of the test (i.e., at a shear displacement of 40 to 50 mm). The ψ values reported above are low, generally in the range of 0.3 to 0.5. In contrast, ψ values for the CD direct shear tests on unreinforced GCLs were higher, typically in the range of 0.7 to 1.0. The ϕ_{ld} values reported above are somewhat larger than those obtained for the unreinforced GCLs. However, as noted above, observation of the shear force-displacement plots for the tests indicates that the shear stresses applied to the sample were decreasing at the ends of the tests, which typically occurred at a displacement of 40 to 50 mm. This observation, coupled with observations of the tested samples, that the GCL reinforcing fibers and stitching were still partially intact at the time the test was terminated, suggests that residual CD and CQ shear strengths of reinforced

GCLs may not be much larger than those of unreinforced GCLs. Clearly, testing is required to establish the large-displacement, high normal stress behavior of these materials, and to identify differences in product behavior based on differences in montmorillonite properties and reinforcing characteristics.

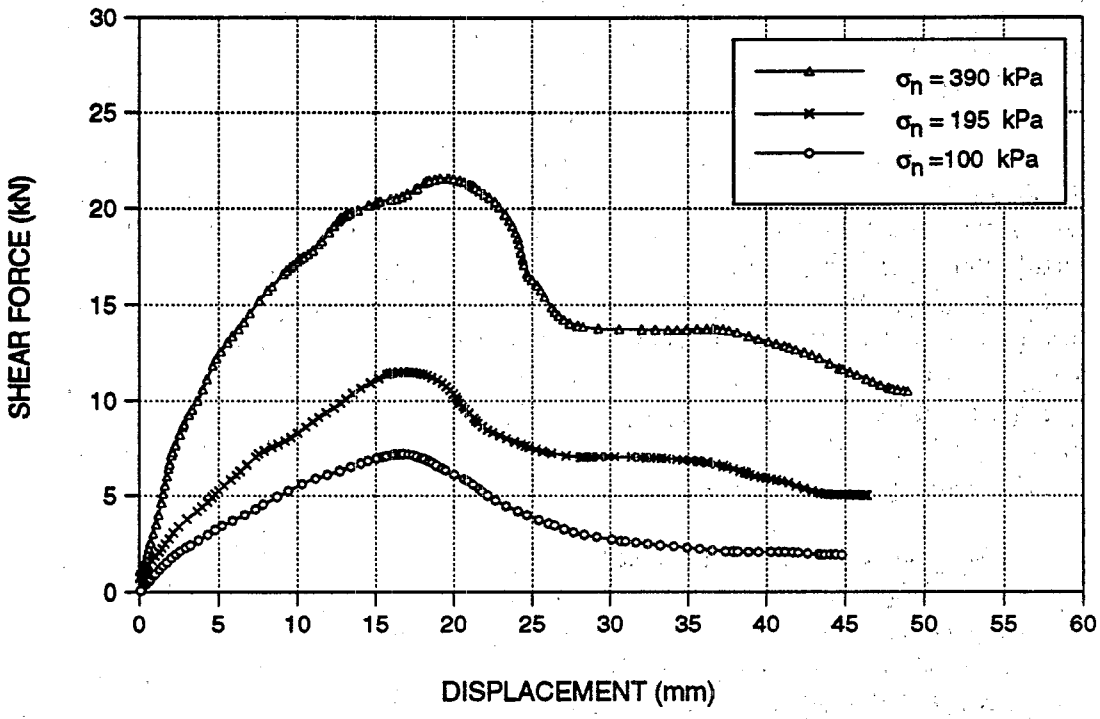

Figure 9. Results of CQ direct shear tests on reinforced Bentofix GCL.

Interim Design Values

Unreinforced GCLs: Based on the information presented in Figure 8, the authors used the following interim guidelines for performing liner system stability analyses for long-term drained conditions, for potential slip surfaces that involve internal shearing of unreinforced GCLs. These guidelines further assume that the GCL will hydrate through adsorption of water from an adjacent subgrade soil layer.

- Slope stability analyses are performed using: (i) peak internal GCL shear strengths and a minimum slope-stability factor of safety of 1.5; and (ii) large-displacement internal GCL shear strengths and a minimum slope-stability factor of safety of 1.15.

- Using the regression equation presented in Figure 4, peak normalized shear strengths are:

σ_n (kPa)	$(\tau/\sigma_n)_p$	ϕ_p
96	0.214	12.1°
240	0.157	8.9°
480	0.114	6.5°
720	0.106	6.1°

- Using the regression equation presented in Figure 5, large-displacement normalized shear strengths are:

σ_n (kPa)	$(\tau/\sigma_n)_{ld}$	ϕ_{ld}
96	0.178	10.1°
240	0.116	6.6°
480	0.070	4.0°
720	0.052	3.0°

For the large displacement strengths, a minimum friction angle cutoff of 3° was assumed based on the test results reported by Mitchell [1993], presented in Figure 7.

The normalized shear strengths given above are relatively low, and their use may be viewed by some as overconservative. This view should be tempered with the realization that the large-displacement GCL shear strengths reported in the technical literature do not represent true residual minimums (due to the limited displacement of the direct shear apparatus) and no allowance has been made for the possible effects of drained creep of the GCL under working stress conditions. Furthermore, the available CD direct shear test results for unreinforced GCLs correlate well with the triaxial compression test results for sodium montmorillonite from Mesri and Olson [1970] and Olson [1974] (Figure 6). Finally, it is noted that the foregoing approach, which utilizes a smaller slope stability factor of safety with the large displacement shear strengths than the factor of safety used with the peak shear strengths, is similar to the approaches advocated by Byrne [1994] and Stark and Poeppel [1994].

Reinforced GCLs: Recognizing the lack of data on the CD strength of reinforced GCLs at high normal stress, the complex behavior and high degree of shear-softening exhibited by these products, the authors utilized the same factors of safety and GCL long-term shear strengths for reinforced GCLs as for unreinforced GCLs. It is recognized that this assumption is conservative. However, given the limitations with respect to the available reinforced GCL test data (e.g., the technical literature does not contain any "true" CD direct shear test

results for reinforced GCLs at high normal stress) and the other factors discussed above, the authors believe the assumption was prudent.

SHEAR STRENGTH OF GCL-GEOMEMBRANE INTERFACES

Direct Shear Testing Program

For a project located in the desert of southeastern California, the authors performed 14 interface direct shear tests on unhydrated GCL-textured HDPE geomembrane interfaces. The tests were performed in a 300 mm x 300 mm shear box following procedures in general accordance with ASTM D 5321. Three different GCLs were tested. The geomembrane used in the tests was from a single roll of material and samples were selected based on visual observation of a consistent degree of texturing. The tests were carried out in a manner that allowed shearing either at the GCL interface or internally within the GCL bentonite layer. Tests were carried out at normal stresses ranging between approximately 350 and 1,920 kPa. Sliding in the tests consistently occurred at the interface and not within the GCL. Thus, the test results correlate to interface failures and at the same time provide conservative lower bound unhydrated shear strengths for the tested GCLs under the project testing conditions.

Typical test results are presented in Figure 10 and summarized in Table 5. The tests correspond to two shearing rates, namely 0.016 mm/s and 0.0007 mm/s. Interface friction angles obtained from the tests at the slower shearing rate are 1° to 2° lower than interface friction angles obtained from tests at the higher shearing rate. The test results also reveal an interface shear strength stress-dependency with secant interface friction angles 5° to 10° lower at 1,920 kPa than at 350 kPa. The interfaces exhibited only minor amounts of shear softening (typically less than 1 to 2°) at test displacements of up to about 50 mm.

Comment on Results

The foregoing interface direct shear test results illustrate the ranges of shear strengths obtained and several of the factors that affect this strength including normal stress, displacement rate, and magnitude of displacement.

The authors note that they have observed relatively wide variances in the degree of texturing of geomembranes, even from a given manufacturer. The degree of texturing significantly influences the interface shear strength. Thus, the strength values reported above should not be considered appropriate for design. Interface shear strengths for design should be established on a project-specific basis and construction-phase quality control testing should be used to establish that materials delivered to the construction site can achieve the interface strengths established during design.

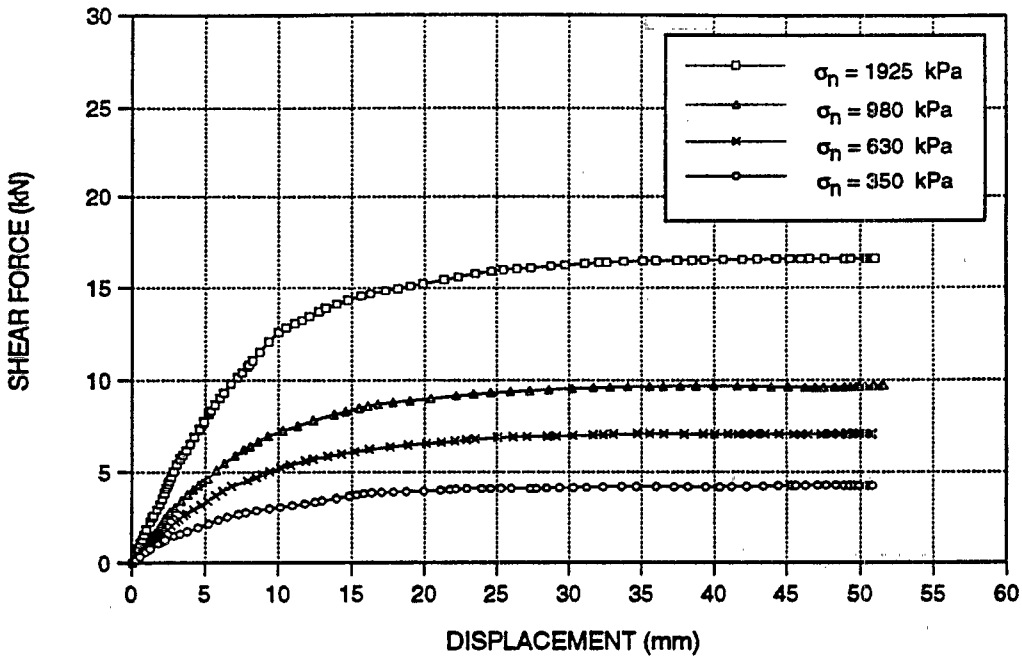

Figure 10. Results of direct shear tests on unhydrated Bentofix GCL-textured HDPE geomembrane interface.

HYDRATION OF GCLs ADJACENT TO SOIL LAYERS

Overview of Testing Program

The authors conducted an extensive laboratory testing program to evaluate the potential for hydration of GCLs placed against a compacted subgrade soil layer. Hydration tests were performed on three different GCL products to evaluate the effects of: (i) test duration (i.e., hydration time); (ii) soil initial water content; (iii) thickness of soil layer; and (iv) overburden pressure. Three commercially-available GCL products, namely, Claymax®, Bentomat®, and Bentofix® were used in the testing program. The soil used in the testing program was obtained from the USEPA GCL Field Test Site at the ELDA-RDF facility in Cincinnati, Ohio. This material is classified as low plasticity clay (CL) based on the Unified Soil Classification System (USCS). Tests were performed on two different soil samples and consistent results were obtained between samples. The results reported herein were obtained from tests on a sample with 99 percent of the soil passing the U.S. No. 200 standard sieve and 33 percent smaller than 2 μm (clay fraction). The liquid limit of the soil is 41 and the plasticity index is 19. The soil has an optimum moisture content (OMC) of 20 percent and a maximum dry unit weight of 16.7 kN/m^3 based on the standard Proctor compaction method (ASTM D 698).

Table 5. Direct shear test results of textured 80-mil HDPE geomembrane/unhydrated GCL interfaces[1].

Test Number	Type of GCL	Normal Stress (kPa)	Displacement Rate (mm/s)	Large Displacement Secant Friction Angle[2] (ϕ_{ld}°)
1	Bentomat GCL (nonwoven side)	350	0.016	24°
2	Bentomat GCL (nonwoven side)	620	0.016	24°
3	Bentomat GCL (nonwoven side)	960	0.016	23°
4	Bentomat GCL (nonwoven side)	960	0.0007	22°
5	Bentomat GCL (nonwoven side)	1,920	0.016	19°
6	Bentomat GCL (nonwoven side)	1,920	0.0007	17°
7	Bentofix GCL (nonwoven side)	350	0.016	28°
8	Bentofix GCL (nonwoven side)	620	0.016	26°
9	Bentofix GCL (nonwoven side)	960	0.016	23°
10	Bentofix GCL (nonwoven side)	1,920	0.016	21°
11	Gundseal GCL (bentonite granules side)	350	0.016	34°
12	Gundseal GCL (bentonite granules side)	620	0.016	29°
13	Gundseal GCL (bentonite granules side)	960	0.016	27°
14	Gundseal GCL (bentonite granules side)	1,920	0.016	24°

Notes: (1) The tests were performed using unhydrated GCLs and in a manner that allowed shearing at the geomembrane/GCL interface, as well as within the GCL bentonite layer.
(2) Final displacements in the tests were in the range of 25 to 50 mm.

Testing Apparatus and Procedure

Figure 11 shows the apparatus specially designed to conduct the GCL hydration tests. The apparatus consists of a polypropylene mold 75 mm in diameter and 150 mm in height. A geomembrane/GCL/soil composite specimen is placed in the mold and covered with two layers of a thin vapor barrier. A loading platen is placed on the specimen for application of overburden pressure.

To process the soil, it was first passed through a U.S. No. 4 standard sieve. The soil was then moisture conditioned to achieve the desired moisture content. The moist soil was placed in the mold in a loose condition and statically compressed to 50-mm thick lifts. The soil was compacted to a dry unit weight equal to approximately 90 percent of the maximum dry unit weight based on the standard Proctor method (ASTM D 698). Two soil lifts were used giving a total thickness of 100 mm. The GCL and geomembrane specimens were carefully trimmed from the same sheets. The initial moisture content of the GCL was measured by taking a small sample from the same GCL sheet and measuring its weight before and after oven drying. The initial moisture content of the GCLs varied between 15 and 20 percent.

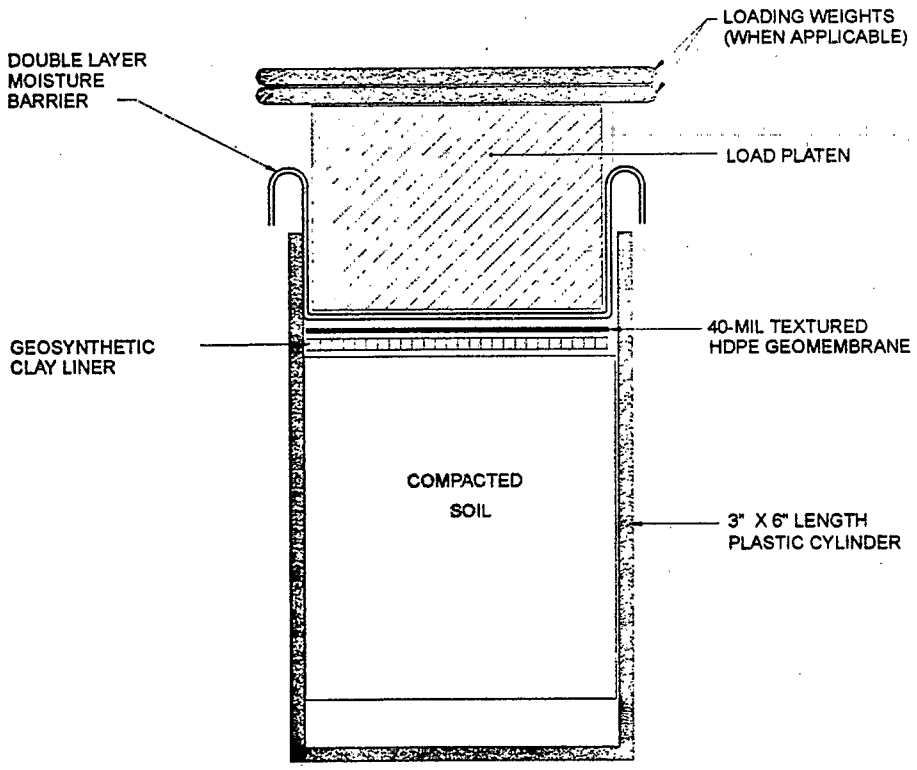

Figure 11. Simplified diagram of GCL hydration test set-up.

The GCL and geomembrane were placed on the soil and covered with the vapor barrier. The side of the GCL placed against the soil was woven in the case of Claymax® and nonwoven for Bentomat® and Bentofix®. Overburden pressure of 10 kPa was applied on the composite specimen utilizing standard weights which were placed on the loading platen. The entire apparatus was then placed in a temperature and humidity controlled room for the desired hydration time period. At the end of the hydration period, the test specimen was removed and the water content of the GCL and soil were measured. The final moisture content of the GCL was measured by weighing the entire GCL specimen before and after oven drying. The final moisture content of the soil was measured as the average water content of three samples obtained from the top, middle, and bottom of the soil specimen.

Testing Conditions and Results

As previously described, test conditions were varied to evaluate the effects of several factors on the hydration of GCLs. To evaluate the effect of test duration, tests were performed where the GCL was in contact with the soil for 5, 25, and 75 days. Soil specimens were compacted to initial moisture contents equal to OMC, 4 percentage points dry of OMC, and 4 percentage points wet of OMC to evaluate the effect of soil initial moisture content on GCL hydration.

Figures 12, 13, and 14 present the results of the hydration tests for the GCL products Claymax®, Bentomat®, and Bentofix®, respectively. These figures show that the moisture content of all three GCLs increased significantly as a result of contact with compacted subgrade soil. The increase in GCL water content was significant after only five days of hydration. With increasing time, GCL water content continued to increase at a decreasing rate. For most tests, GCL water content reached a maximum value after about 25 days of soil contact and for some of the tests water content continued to increase even after 75 days of hydration. It is interesting to note that all three GCL products showed relatively similar behavior. Increases in water content were comparable for the three GCL products despite differences in GCL fabric (i.e., woven vs. nonwoven) and types of bentonite clay used to manufacture the GCLs.

Figures 12, 13, and 14 illustrate the influence of soil subgrade initial moisture content on the hydration of GCLs. From these figures, it is evident that the moisture content of the GCL for any particular hydration time increases as the initial moisture content of the soil increases. These figures also show that a small increase in soil initial moisture content can have a significant impact on GCL moisture content. For example, after 75 days of hydration, the moisture content of Claymax® was approximately 16 percent higher when the initial moisture content of the soil was equal to OMC than when it was 4 percentage points drier than OMC. This behavior is expected because more water is available in the soil for the GCL to hydrate.

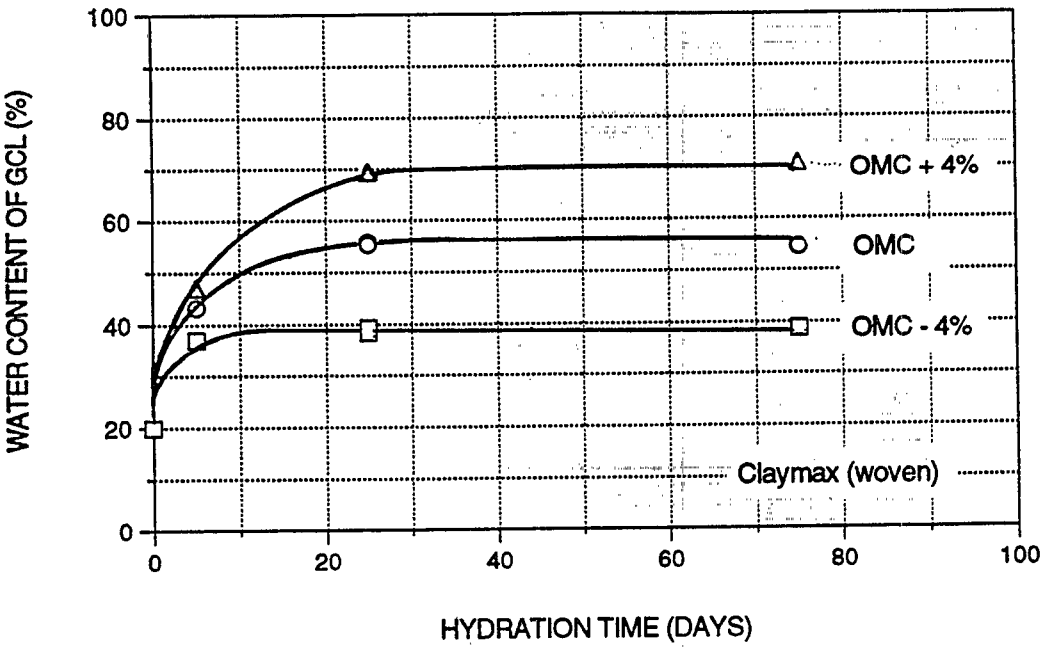

Figure 12. Increase in GCL moisture content due to contact with compacted subgrade soil: Claymax® with woven geotextile against soil.

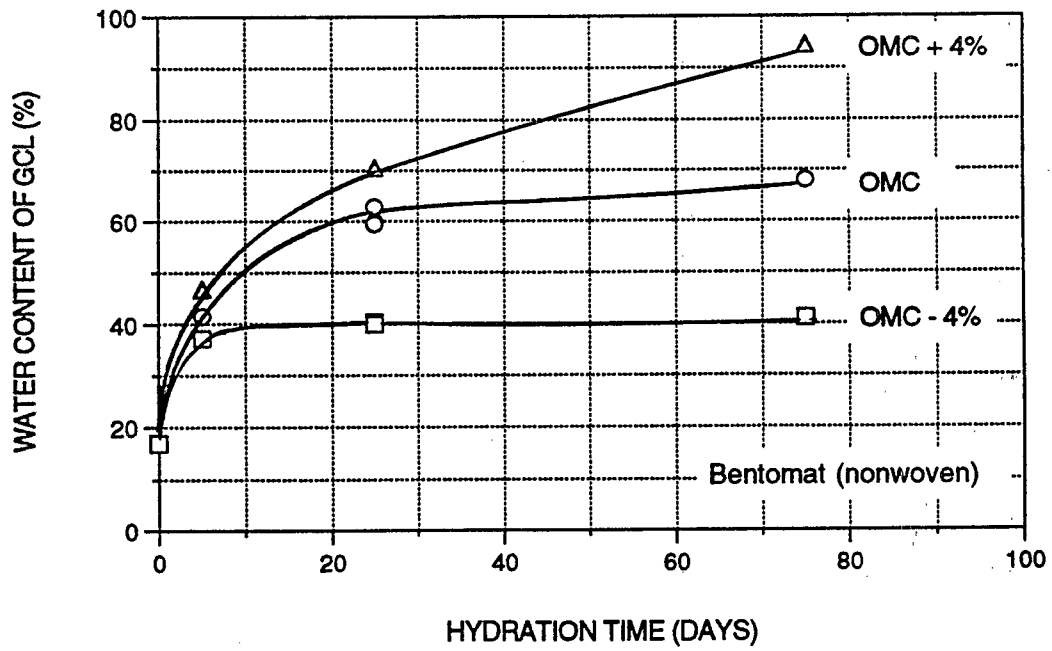

Figure 13. Increase in GCL moisture content due to contact with compacted subgrade soil: Bentomat® with nonwoven geotextile against soil.

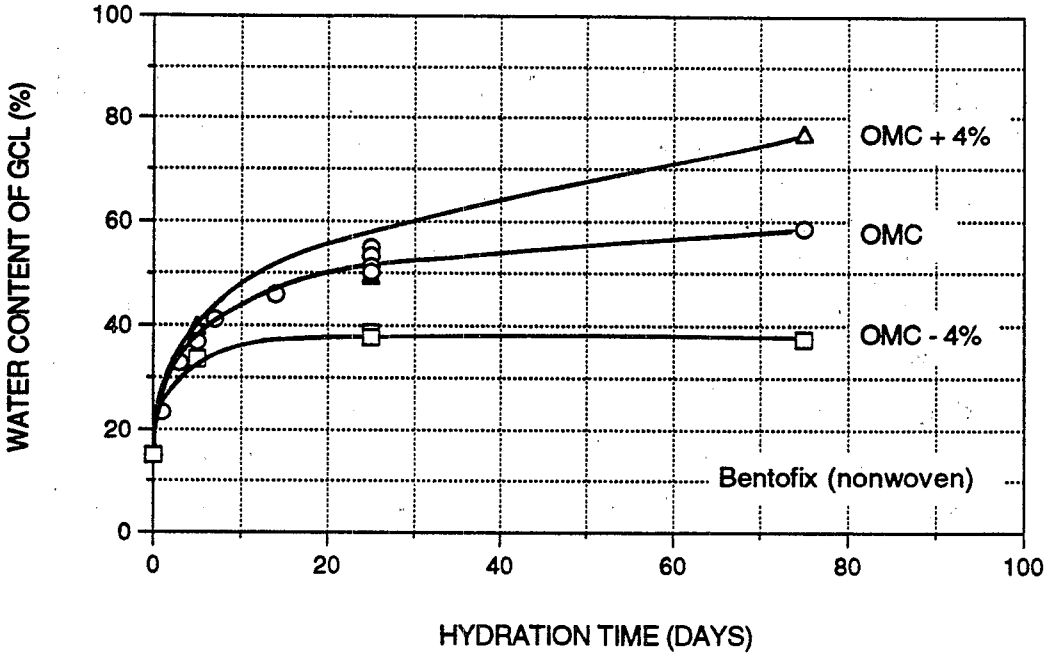

Figure 14. Increase in GCL moisture content due to contact with compacted subgrade soil: Bentofix® with nonwoven geotextile against soil.

The examination of the curves shown in Figures 12, 13, and 14 shows that the time required for the GCL to reach its final moisture content is less in the case of a dry soil than in the case of a wet soil. At the lowest soil initial moisture content tested, GCL moisture content ceased to increase after about 5 to 25 days. At the highest initial moisture content tested, the Bentomat® and Bentofix® GCLs continued to increase in moisture content after 75 days of hydration.

To evaluate the effect of soil layer thickness, specimens were prepared using 50, 100, 150, and 200 mm of soil thickness. Soil initial moisture content was 20 percent and dry unit weight was 14.9 kN/m^3 for all specimens. Figure 15 shows the results of hydration tests for the Bentofix® GCL after 25 days of hydration. The GCL moisture content increased with the increase of the soil layer thickness. However, it appears that only a small change in moisture content increase occurs for thicknesses greater than 100 mm.

The effect of overburden pressure on GCL hydration is illustrated in Figure 16 for the Bentofix® GCL. As shown in this figure, overburden pressure in the range of 5 to 390 kPa did not significantly affect the rate of GCL hydration during the 25-day test duration.

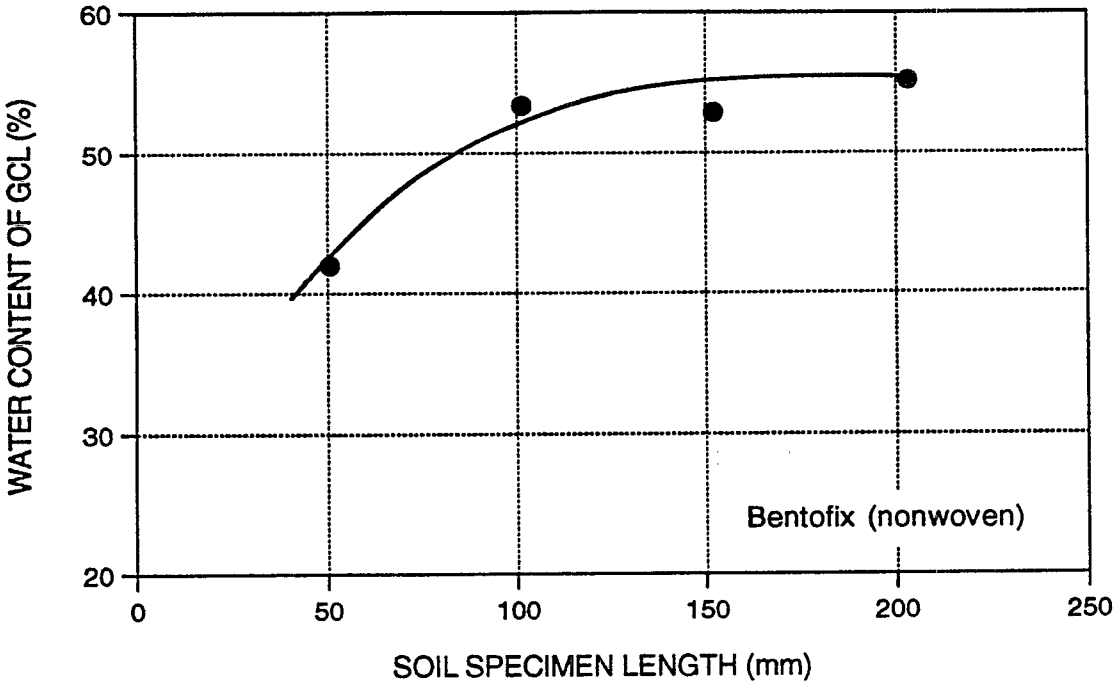

Figure 15. Influence of subgrade soil layer thickness on GCL moisture content.

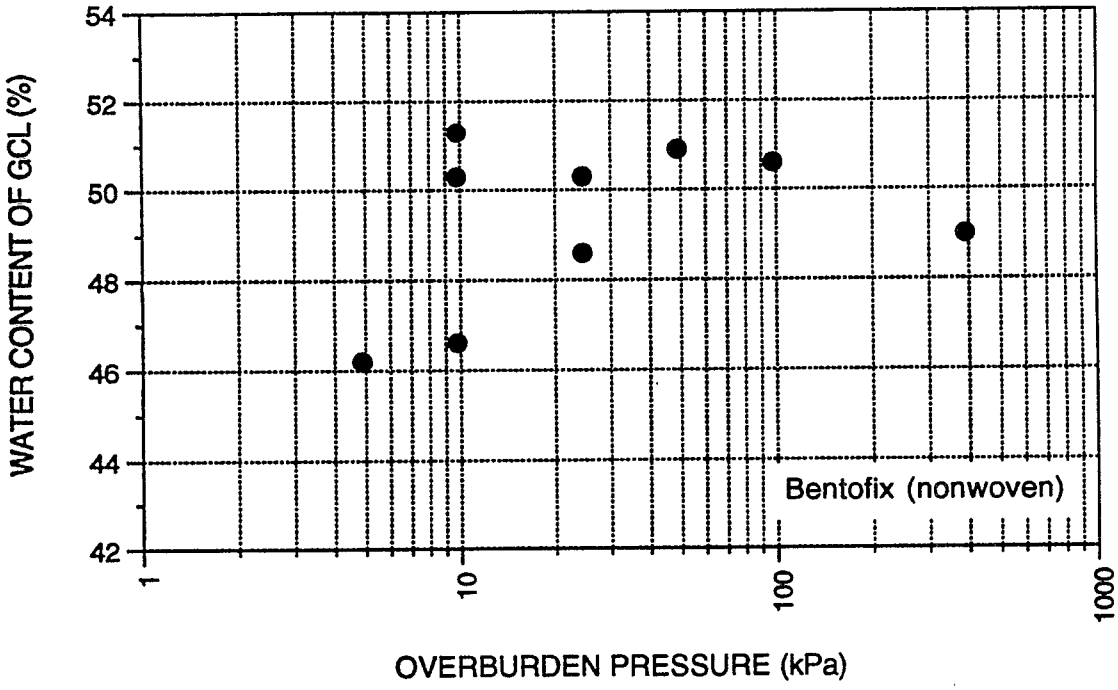

Figure 16. Influence of overburden pressure on the increase in GCL moisture content.

Summary

From the testing program results described above, the following can be concluded:

- GCLs will hydrate when placed in contact with subgrade soils compacted within the range of moisture contents typically found in earthwork construction specifications; this conclusion is consistent with data provided by Daniel et al. [1993]; even for the driest soil (compacted 4 percentage points dry of OMC), GCL moisture contents consistently increased from an initial value in the range of 15 to 20 percent up to about 40 percent within a 100-day period; it should thus be anticipated that GCLs placed even against relatively dry compacted subgrades will undergo substantial hydration;

- given that Daniel et al. [1993] have shown that long-term GCL shear strengths are insensitive to water content for water contents above about 50 percent, stability analyses involving GCLs placed in contact with compacted subgrade soils should be based on hydrated GCL shear strengths;

- significant increases in GCL moisture contents may occur within a few days of GCL contact with a moist soil; the rate of GCL hydration is initially highest and then decreases with increasing time;

- within the range of conditions tested a higher soil moisture content results in a higher GCL moisture content;

- larger soil layer thickness results in a larger increase in GCL moisture content, however, for soil layer thicknesses greater than 100 mm only insignificant increases were observed with increasing soil layer thickness;

- overburden pressure within the range tested (i.e., 5 to 390 kPa) did not influence the hydration process; and

- differences between GCL products tested (i.e., type of bentonite clay and fabric) did not seem to significantly affect the test results.

FAILURE OF LANDFILL COVER SYSTEM CONTAINING A GCL

Description of Cover System

The authors recently investigated the failure of a cover system for a municipal solid waste landfill near Atlanta, Georgia. The failure is described in more detail by Vander Linde et al. [1995]. The cover system was constructed in the fall of 1994 on 3H:1V (horizontal:vertical) side slopes to a maximum height above surrounding ground of approximately 18 m. The cover system consisted of, from top to bottom:

- 300-mm thick layer of final cover soil which is classified as silty sand containing approximately 40 percent fines based on ASTM D 2487, and which has a hydraulic conductivity in the range of 10^{-4} to 10^{-3} cm/s;
- stitch-bonded reinforced GCL; and
- 150- to 300-mm thick layer of intermediate cover soil which served as a foundation for the overlying final cover components.

Failure of System

During the winter of 1995, the cover system experienced several episodes of downslope movement. The first major episode occurred approximately one month after the completion of construction; the movement occurred after a three-day period in which 58 mm of rain fell at the site. The next major episode occurred six weeks later, after two days of inclement weather generated about 41 mm of rainfall at the site. Total downslope movements exceeded 1 m at some locations. The observed failure mechanism was sliding of the final cover soil on top of the GCL.

Analysis of Failure

The episodes of downslope movement both followed periods of extended rainfall at the site. A slope stability back-analysis of the cover system was performed which accounted for the influence of rainfall-induced seepage forces on cover system factor of safety against downslope sliding. The back-analysis involved two steps:

- estimating seepage forces within the cover soil using several different calculation methods and parameter values; and
- calculating the resulting slope stability factors of safety for the range of estimated seepage forces.

The evaluation of seepage forces involved calculating the water build-up (i.e., hydraulic head) within the final cover soil on top of the GCL. Head was calculated using a methodology developed by Giroud and Houlihan [1995] and checked using the United States Environmental Protection Agency (USEPA) Hydrologic Evaluation of Landfill Performance (HELP) computer program Version 3.03 [USEPA, 1994a, 1994b]. The values of head calculated using these approaches ranged from 150 mm to the full thickness of the cover soil layer, 300 mm.

Calculations to obtain slope stability factors of safety were performed using the equations presented by Giroud et al. [1995a, 1995b]. An important input to the equations is the shear strength of the interface between the cover soil and GCL. Tests to evaluate the shear strength of this interface had not been carried out as part of the original design. For the back-analysis of the failure, a range of friction angles (20° to 26°) was considered for the cover soil-GCL interface; this range likely brackets the actual interface strength and includes the value of 24° originally assumed by the design engineer. Calculations were performed and the following results were obtained:

Interface Friction Angle (degrees)	Factor of Safety (FS) vs. Hydraulic Head		
	0 mm	100 mm	200 mm
20°	1.09	0.84	0.60
24°	1.35	1.04	0.73
26°	1.47	1.13	0.80

These calculation results demonstrate the significant impact of seepage forces on the stability of the final cover soil. Even with the largest assumed interface strength, only 140 mm of head buildup is required to decrease the slope stability factor of safety to less than 1.0. Interface shear strength tests performed after the completion of the back analyses resulted in peak and large-displacement secant friction angles for the GCL-cover soil interface, at the applicable normal stress, of 23° and 21°, respectively.

Summary

The primary factor contributing to the observed final cover soil movements was the build-up of seepage forces in the final cover soil during periods of heavy rain. Seepage forces were not accounted for in the design. If seepage forces had been accounted for, the potential for instability likely would have been identified during preparation of the design. The development of seepage forces in cover soils is typically minimized by the inclusion of a drainage layer above the low-permeability barrier component of the cover (in this case, the GCL). A secondary factor contributing to the movements was a final cover soil-GCL interface shear strength lower than assumed in the design. An interface friction

angle of 24° was assumed by the design engineer, based on information provided by the GCL manufacturer. The actual project-specific interface shear strength was closer to 21°. This result highlights the fact that actual interface strengths can only be assessed by project-specific testing; such testing was not performed for the project.

ACKNOWLEDGEMENTS

The authors would like to thank Mr. Robert R. Landreth and Mr. David A. Carson of the U.S. Environmental Protection Agency, Risk Reduction Research Laboratory for their support in the evaluation of double-liner system performance.

REFERENCES

Bonaparte, R. and Gross, B.A., "Field Behavior of Double-Liner Systems" *Proceedings of the Symposium on Waste Containment Systems, ASCE Geotechnical Special Publication No. 26*, San Francisco, CA, 1990, pp. 52-83.

Bonaparte, R. and Gross, B.A., "LDCRS Flow from Double-Lined Landfills and Surface Impoundments", *EPA/600/SR-93/070*, U.S. Environmental Protection Agency, Risk Reduction Research Laboratory, Cincinnati, OH, 1993, 65 p.

Byrne, J., "Design Issues with Strain-Softening Interfaces in Landfill Liners", *Proceedings, Waste Tech '94*, National Waste Management Association, Charleston, SC, Jan 1994, 26 p.

Chattopadhyay, P.K., "*Residual Shear Strength of Pure Clay Minerals*", Ph.D. Dissertation, University of Alberta, Edmonton, Canada, 1972.

Daniel, D.E. and Shan, H-Y., "*Results of Direct Shear Tests on Hydrated Bentonitic Blankets*", University of Texas, Geotechnical Engineering Center, 1991, 13 p.

Daniel, D.E., Shan, H-Y., and Anderson, J.D., "Effects of Partial Wetting on the Performance of the Bentonite Component of a Geosynthetic Clay Liner, *Proceedings, Geosynthetics '93 Conference*, Vol. 3, Vancouver, Feb 1993, pp. 1483-1496.

Giroud, J.P. and Houlihan, M.F., "Design of Leachate Collection Layers", *Proceedings of the Fifth International Landfill Symposium*, Vol. 2, Sardinia, Oct 1995, pp. 613-640.

Giroud, J.P., Williams, N.D., and Pelte, T., "Stability of Geosynthetic-Soil Layered Systems on Slopes", *Geosynthetics International*, Vol. 2, No. 6, 1995a, pp. 1115-1148.

Giroud, J.P., Bachus, R.C., and Bonaparte, R., "Influence of Water Flow on the Stability of Geosynthetic-Soil Layered Systems on Slopes", *Geosynthetics International*, Vol. 2, No. 6, 1995b, pp. 1149-1180.

Gross, B.A., Bonaparte, R., and Giroud, J.P., "Evaluation of Flow from Landfill Leakage Detection Layers", *Proceedings of the Fourth International Conference on Geotextiles*, Vol. 2, The Hague, Jun 1990, pp. 481-486.

Kenney, T.C., "The Influence of Mineralogic Composition on the Residual Shear Strength of Natural Soils", *Proceedings of the Oslo Geotechnical Conference on the Shear Strength Properties of Natural Soils and Rocks*, Vol. 1, 1967, pp. 123-129.

Mesri, G. and Olson, R.E., "Shear Strength of Montmorillonite", *Geotechnique*, Vol. 20, No. 3, 1970, pp. 261-270.

Mitchell, J.K., "*Fundamentals of Soil Behavior*", 2nd Edition, John Wiley & Sons, Inc., New York, NY, 1993, 437 p.

Olson, R.E., "Shearing Strengths of Kaolinite, Illite, and Montmorillonite", *Journal of the Geotechnical Engineering Division*, ASCE, Vol. 100, No. GT11, 1974, pp. 1215-1229.

Shan, H-Y, "*Stability of Final Covers Placed on Slopes Containing Geosynthetic Clay Liners*", Ph.D. Dissertation, University of Texas, Austin, TX, 1993, 296 p.

Shan, H-Y. and Daniel, D.E., "Results of Laboratory Tests on a Geotextile/Bentonite Liner Material", Vol. 2, *Proceedings, Geosynthetics '91 Conference*, Atlanta, GA, Feb 1991, pp. 517-535.

Stark, T.D. and Poeppel, A.R., "Landfill Liner Interface Strengths from Torsional-Ring-Shear Tests", *Journal of Geotechnical Engineering*, ASCE, Vol. 120, No. 3, 1994, pp. 597-615.

USEPA, "*The Hydrologic Evaluation of Landfill Performance (HELP) Model, User's Guide for Version 3*", EPA/600/R-94/168a, U.S. Environmental Protection Agency, Washington D.C., December 1994a.

USEPA, "*The Hydrologic Evaluation of Landfill Performance (HELP) Model, Engineering Documentation for Version 3*", EPA/600/R-94/168b, U.S. Environmental Protection Agency, Washington D.C., December 1994b.

Vander Linde, D.L., Luettich, S.M., and Bonaparte, R., "Lessons Learned for Failures of a Landfill Cover System", *Geosynthetics: Lessons Learned from Failures*, J.P. Giroud and K.L. Soderman, Eds., International Geosynthetics Society, 1995, in press.

Appendix G

Summary of Bentomat Direct Shear Data, Prepared by CETCO

SUMMARY OF BENTOMAT DIRECT SHEAR TEST DATA

Lab[1]	Report Date	Interface Tested[2]	Normal Stresses (psi)	Bentomat Moisture[3]	Shear Rate (in/min)	Peak Friction Angle (deg)	Residual Friction Angle (deg)	Apparent Cohesion (psf)	Comments
J & L	05-30-90	NW/Sand	1 - 2 - 3	Hydrated	0.02	35	Not determined	10	
		NW/Sand	1 - 2 - 3	Dry	0.02	28	"	85	
		NW/Clay	1 - 2 - 3	Hydrated	0.02	41	"	77	
		NW/Clay	1 - 2 - 3	Dry	0.02	32	"	105	
STS	09-11-90	NW/40-mil Text. HDPE	35 - 52 - 70	Dry	0.2	18	Not determined	0	
		NW/80-mil Text. HDPE	35 - 52 - 70	Dry	0.2	37	"	0	
		W/80-mil Text. HDPE	35 - 52 - 70	Dry	0.2	24	"	0	
J & L	11-06-90	NW/Sandy soil	2 - 3.5 - 5	Dry	0.02	23	Not determined	119	
GRI	04-18-91	Internal	.5 - 1 - 5 - 10 - 20	Dry	0.035	42	Not determined	288	
		Internal	.1 - .5 - 1 - 5 - 10	Hydrated	0.035	37	"	115	
		Internal	.1 - .5 - 1 - 5 - 10	Hydrated	0.035	39	"	173	Hydrated in leachate
STS	05-28-91	NW/40-mil Text. HDPE	35 - 52 - 70	Hydrated	0.2	20	Not determined	0	
		W/80-mil Text. HDPE	35 - 52 - 70	Hydrated	0.2	19	"	0	
UTA	08-12-91	Internal	6 - 9 - 14 - 19	Hydrated	0.000131	26	Not determined	619	
J & L	09-09-91	W/Soil cover	0.6 - 1.25 - 1.88	Hydrated	0.035	22.5	20.5	55	
		W/Geonet	0.6 - 1.25 - 1.88	Hydrated	0.035	17	16	64	
		NW/2B Stone	0.6 - 1.25 - 1.88	Hydrated	0.035	53	52	10	
TRI	05-06-92	W/60-mil text. VLDPE	2 - 8 - 14	Hydrated	0.04	22	Not determined	113	Limited hydration
		W/60-mil sm. VLDPE	2 - 8 - 14	Hydrated	0.04	15	"	77	"
TRI	11-12-92	W/40-mil text. LLDPE	3.5 - 7 - 14	Hydrated	0.2	25	16.5	230	
TRI	03-16-93	W/Saturated soil	1 - 2 - 3	Hydrated	0.04	24	Not determined	100	Bentomat HS
		W/Dry soil	1 - 2 - 3	Hydrated	0.04	20	"	153	"
		NW/Drainage geocomp.	1 - 2 - 3	Dry	0.04	17	"	20	"

SUMMARY OF BENTOMAT DIRECT SHEAR TEST DATA (Continued)

Lab[1]	Report Date	Interface Tested[2]	Normal Stresses (psi)	Bentomat Moisture[3]	Shear Rate (in/min)	Peak Friction Angle (deg)	Residual Friction Angle (deg)	Apparent Cohesion (psf)	Comments
GA	09-04-92	W/60-mil sm. HDPE	0.5 - 1 - 2 - 4 - 10	Hydrated	0.02	8	7	0	
		W/60-mil text. HDPE	0.5 - 1 - 2 - 4 - 10	Hydrated	0.02	28	28 / 6	29	bi-modal residual
		W/Drainage geocomp.	0.5 - 1 - 2 - 4 - 10	Hydrated	0.02	21	19	0	
		Internal	0.5 - 1 - 2 - 4 - 10	Hydrated	0.0025	27	8	43	
TRI	05-07-93	W/80-mil text HDPE	40 - 60 - 80	Dry	0.04	18	9	100	text. fail at 80 psi
TRI	07-01-93	W/30-mil sm. PVC	1 - 3 - 5	Hydrated	0.04	13	Not determined	81	
		W/30-mil sm. PVC	1 - 3 - 5	Dry	0.04	24.5	"	48	
GSC	09-28-93	Internal	0.35 - 1 - 2 - 3.5	Dry	0.04	57	Not determined	370	
		Internal	0.5 - 1 - 2 - 4 - 10	Hydrated	0.04	59	"	265	
STS	10-01-93	W/80-mil text. HDPE	35 - 52 - 70	Hydrated	0.04	9	5	1,000	
GSC	02-02-94	Internal	14 - 70 - 142	Hydrated	0.04	24	7	515	
CGC	05-06-94	NW/Compacted soil	20 - 40 - 80	Dry	0.04	11.5	Not determined	1,110	
		W/60-mil sm. HDPE	20 - 40 - 80	Dry	0.04	12.5	"	0	
GSC	07-15-94	Internal	0.35 - 1 - 2 - 3.5	Hydrated	0.04	59	31	271	cross machine dir.
CETCO	07-19-94	W/80-mil text. HDPE	3 - 5 - 8	Hydrated	0.04	19	14	176	
MEI	08-04-94	W/40-mil text. VLDPE	1.5 - 2.5 - 3.5	Hydrated	0.04	18	14	13	
CETCO	08-20-94	W/80-mil text. HDPE	30 - 40 - 50	Hydrated	0.04	21.3	Not determined	210	
GSC	11-28-94	W/60-mil text. HDPE	7.5 - 15 - 30	Hydrated	0.04	18	17	175	Diff. membrane
		W/60-mil text. HDPE	7.5 - 15 - 30	Hydrated	0.04	16	12	345	manufacturers
ATT	11-30-94	W/80-mil sm. HDPE	30 - 60 - 90	Hydrated	0.04	11	10	16	
GSC	12-16-94	W/60-mil text. HDPE	1 -3 - 6 - (15)	Hydrated	0.04	25 (19)	10	100	(lower δ at 15 psi)

SUMMARY OF BENTOMAT DIRECT SHEAR TEST DATA (Continued)

Lab[1]	Report Date	Interface Tested[2]	Normal Stresses (psi)	Bentomat Moisture[3]	Shear Rate (in/min)	Peak Friction Angle (deg)	Residual Friction Angle (deg)	Apparent Cohesion (psf)	Comments
CETCO	03-24-95	NW/60-mil Text. HDPE	2 - 4 - 6	Hydrated	0.04	38	35	0	Hydrated 14 days
CETCO	04-05-95	W/Drainage composite	2 - 4 - 6	Hydrated	0.04	12	not applicable	193	brittle interface
AGP	07-12-95	NW/Reinforcing woven	2 - 4 - 5.5	Hydrated	0.04	12	11	12	
		W/80-mil Text. HDPE	14 - 28 - 69 - 104	Hydrated	0.04	18	8	192	
		W/80-mil Text. HDPE	14 - 28 - 69 - 104	Dry	0.04	30	14	0	

Notes:

[1] J & L = J & L Testing Company, Inc., Canonsburg, PA (3-inch Wykeham Farrance direct shear device)
STS = STS Consultants Ltd., Northbrook, IL (12-inch shear box)
GRI = Geosynthetic Research Institute, Drexel University, Philadelphia, PA (Wykeham Farrance device)
UTA = University of Texas at Austin, Civil Engineering Laboratory (2.4-inch direct shear box)
TRI = TRI Environmental, Inc., Austin, Texas (12-inch direct shear box)
GA = Golder Associates, Denver, Colorado (12-inch direct shear box)
GSC = GeoSyntec Consultants, Atlanta, Georgia (12-inch direct shear box)
CGC = Cumberland Geotechnical Consultants, Carlisle, PA (12-inch direct shear box)
MEI = Miller Engineering, Manchester, NH (12-inch direct shear box)
CETCO = CETCO, Arlington Heights, IL (12-inch direct shear box)
ATT = Advanced Terra Testing, Lakewood, CO (12-inch direct shear box)
AGP = AGP Laboratories, Inc., Arlington, TX (12-inch direct shear box)

[2] NW = Non-woven geotextile of Bentomat.
W = Woven geotextile of Bentomat.
Internal = Failure forced within the Bentomat (between the geotextiles).

[3] "Dry" = specimen was tested in the as-received moisture state, which is typically 15 percent.
"Hydrated" = specimen was hydrated prior to testing, *although the actual hydration methods and durations vary.*
All hydrated apecimens were hydrated with distilled or tap water, unless otherwise noted.

COLLOID ENVIRONMENTAL TECHNOLOGIES COMPANY
DIRECT SHEAR TESTING

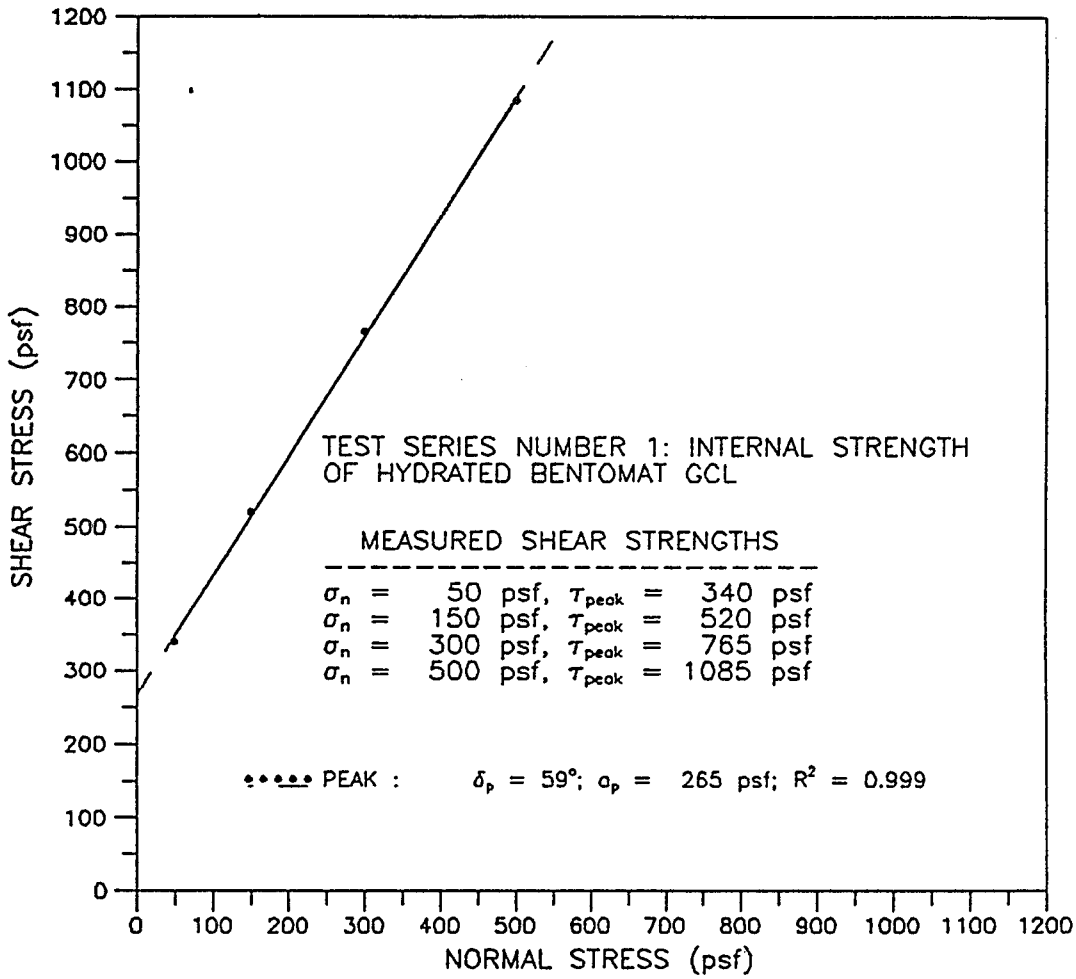

NOTE: The reported value of adhesion may not be the true adhesion of the GCL specimen, and caution should be exercised in using this adhesion value for applications involving normal stresses outside the range of stresses covered by the test.

DATE TESTED: 20 AUGUST 1993

GEOSYNTEC CONSULTANTS
GEOMECHANICS AND ENVIRONMENTAL LABORATORY

FIGURE NO.	1-2
PROJECT NO.	GL3419
DOCUMENT NO.	GEL93291
PAGE NO.	

COLLOID ENVIRONMENTAL TECHNOLOGIES COMPANY
DIRECT SHEAR TESTING

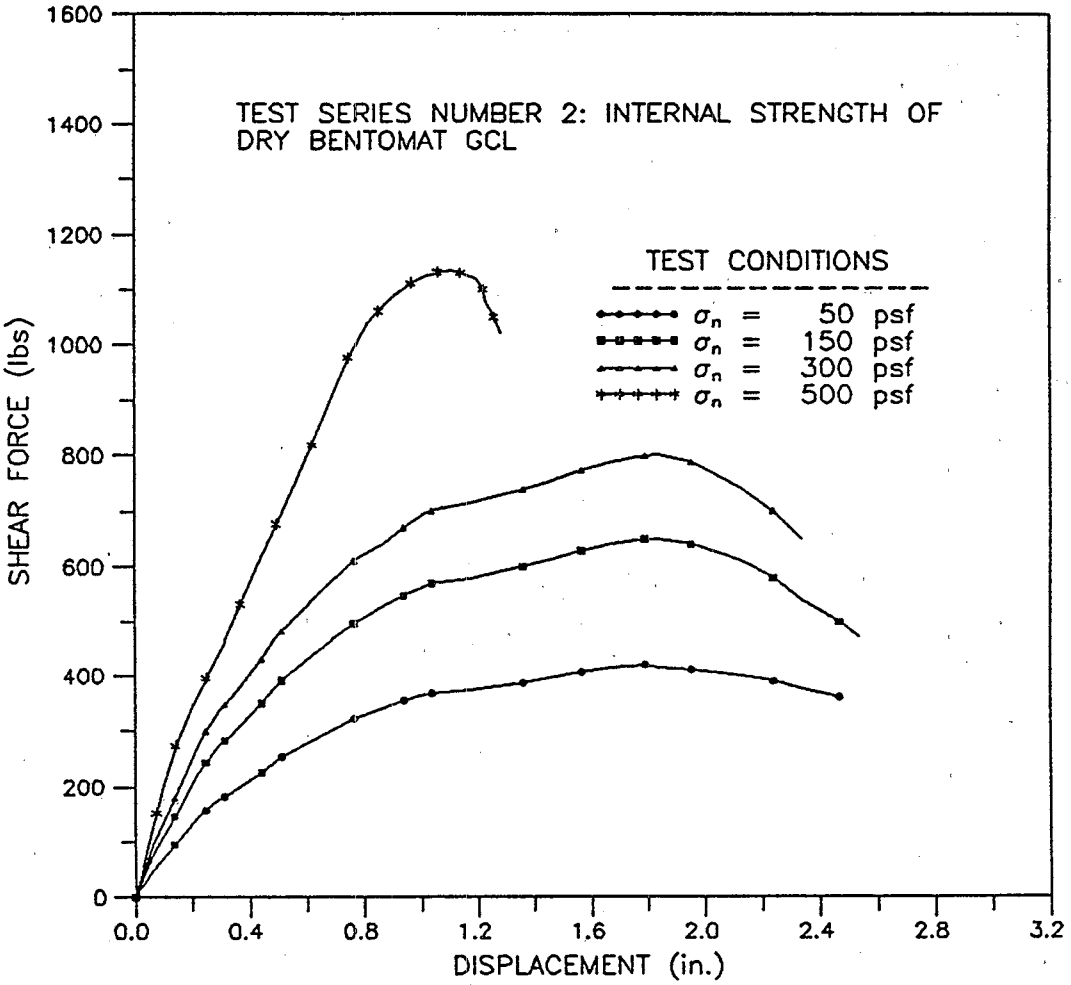

NOTE: The shear box size was 12 in. by 12 in.(300 mm by 300 mm), and the contact area remained constant throughout the entire test.

DATE TESTED: 19 AUGUST 1993

GEOSYNTEC CONSULTANTS
GEOMECHANICS AND ENVIRONMENTAL LABORATORY

FIGURE NO.	1–3
PROJECT NO.	GL3419
DOCUMENT NO.	GEL93291
PAGE NO.	

COLLOID ENVIRONMENTAL TECHNOLOGIES COMPANY
DIRECT SHEAR TESTING

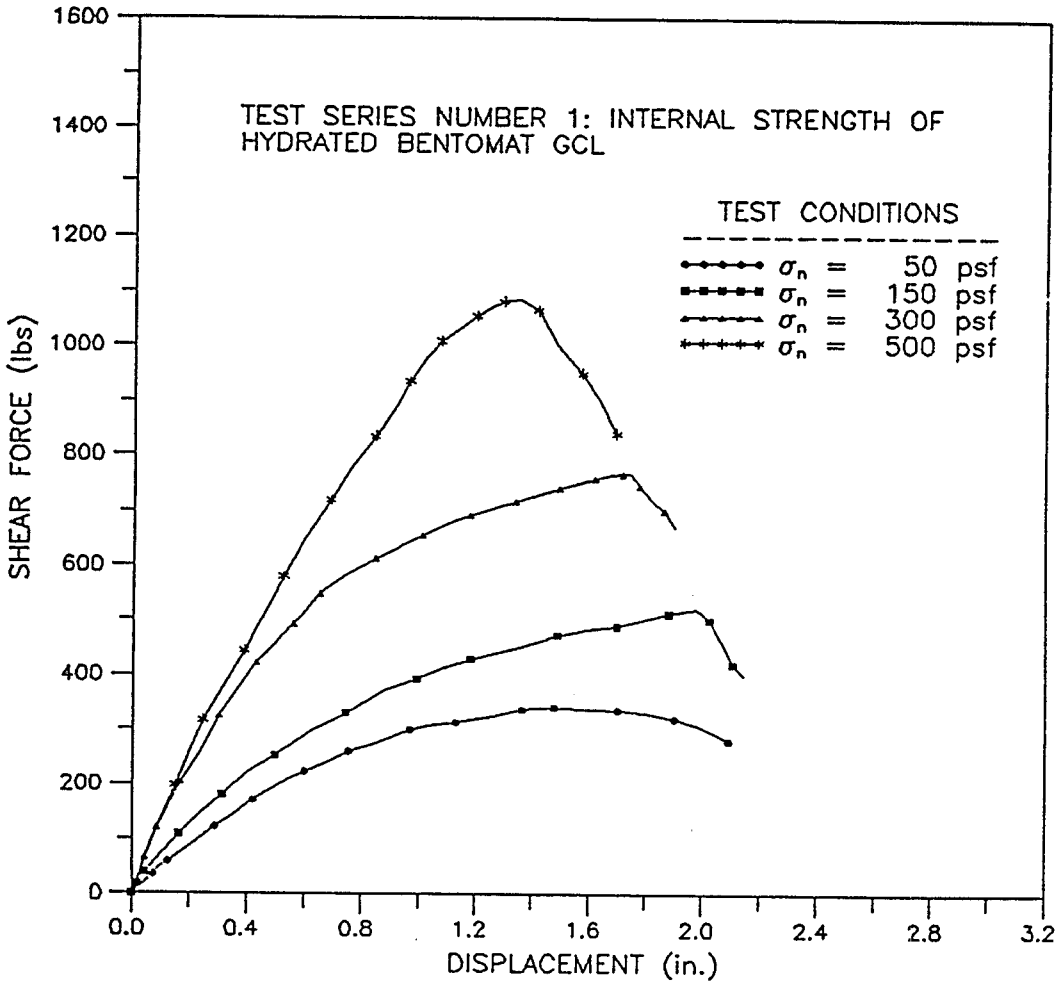

NOTE: The shear box size was 12 in. by 12 in.(300 mm by 300 mm), and the contact area remained constant throughout the entire test.

DATE TESTED: 20 AUGUST 1993

GEOSYNTEC CONSULTANTS
GEOMECHANICS AND ENVIRONMENTAL LABORATORY

FIGURE NO.	1-1
PROJECT NO.	GL3419
DOCUMENT NO.	GEL93291
PAGE NO.	

ATTACHMENT 1

DIRECT SHEAR TEST RESULTS

COLLOID ENVIRONMENTAL TECHNOLOGIES COMPANY
DIRECT SHEAR TESTING

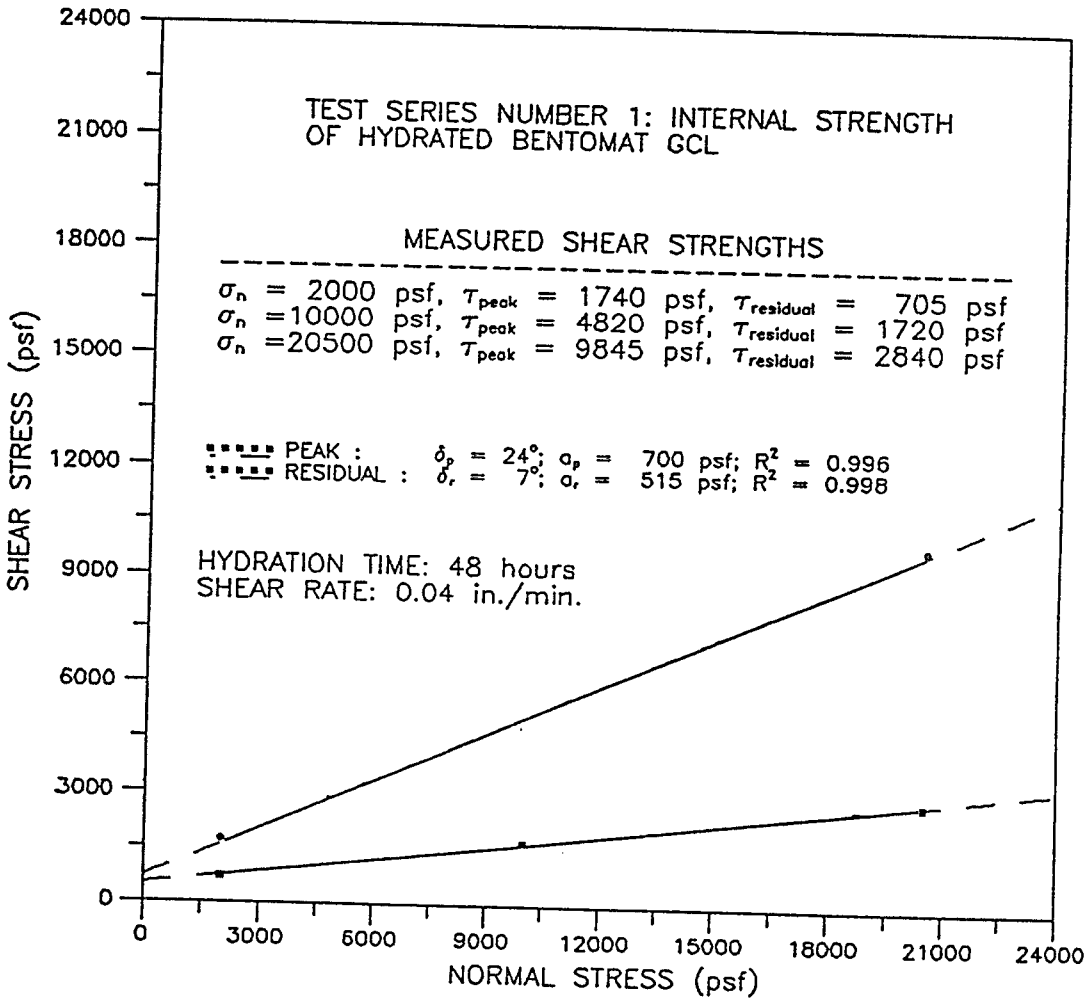

NOTE: The reported value of adhesion may not be the true adhesion of the GCL specimen, and caution should be exercised in using this adhesion value for applications involving normal stresses outside the range of stresses covered by the test series.

DATE TESTED: 10 TO 17 JANUARY 1994

GeoSyntec Consultants
GEOMECHANICS AND ENVIRONMENTAL LABORATORY

FIGURE NO.	1-2
PROJECT NO.	GL3529
DOCUMENT NO.	GEI94024
PAGE NO.	

COLLOID ENVIRONMENTAL TECHNOLOGIES COMPANY
DIRECT SHEAR TESTING

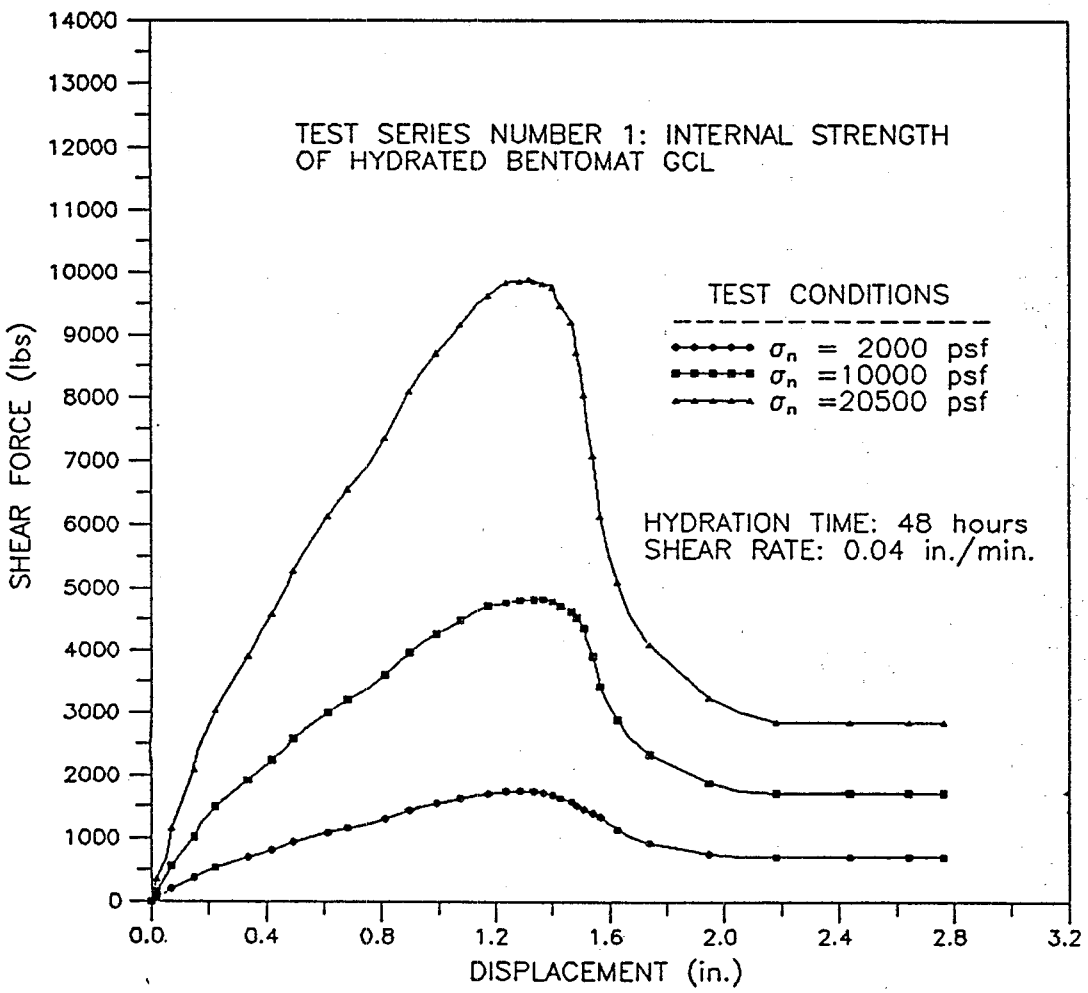

NOTE: The shear box size was 12 in. by 12 in.(300 mm by 300 mm), and the contact area remained constant throughout the entire test.

DATE TESTED: 10 TO 17 JANUARY 1994

GeoSyntec Consultants
GEOMECHANICS AND ENVIRONMENTAL LABORATORY

FIGURE NO.	1-1
PROJECT NO.	GI 3529
DOCUMENT NO.	GEI 94024
PAGE NO.	

TABLE 4

DIRECT SHEAR TEST RESULTS
MEASURED TOTAL STRESS SHEAR STRENGTH PARAMETERS
COLLOID ENVIRONMENTAL TECHNOLOGIES COMPANY

Test Series Number	Test Specimen[1]	Normal[2] Stress (psf)	Peak Strength[3]			Residual Strength (3)		
			Friction Angle	Adhesion (psf)	R^2	Friction Angle	Adhesion (psf)	R^2
1	Internal Strength of Hydrated Bentomat GCL	2,000 to 20,500	24°	700	0.996	7°	515	0.998

Notes: (1) For the test series, the GCL specimen was hydrated in tap water for 48 hours under each applied normal stress prior to shearing.

(2) Test specimens were sheared immediately after application of normal stress used for shearing.

(3) The reported value of adhesion may not be the "true adhesion" of the GCL specimen and caution should be exercised in using this adhesion value for applications involving normal stresses outside the range of stresses covered by the test series. The value of R^2, the coefficient of correlation, provides an indication of how well the best-fit shear strength parameters match the test data.

COLLOID ENVIRONMENTAL TECHNOLOGIES COMPANY
CREEP SHEAR TESTING
SHEARING PHASE

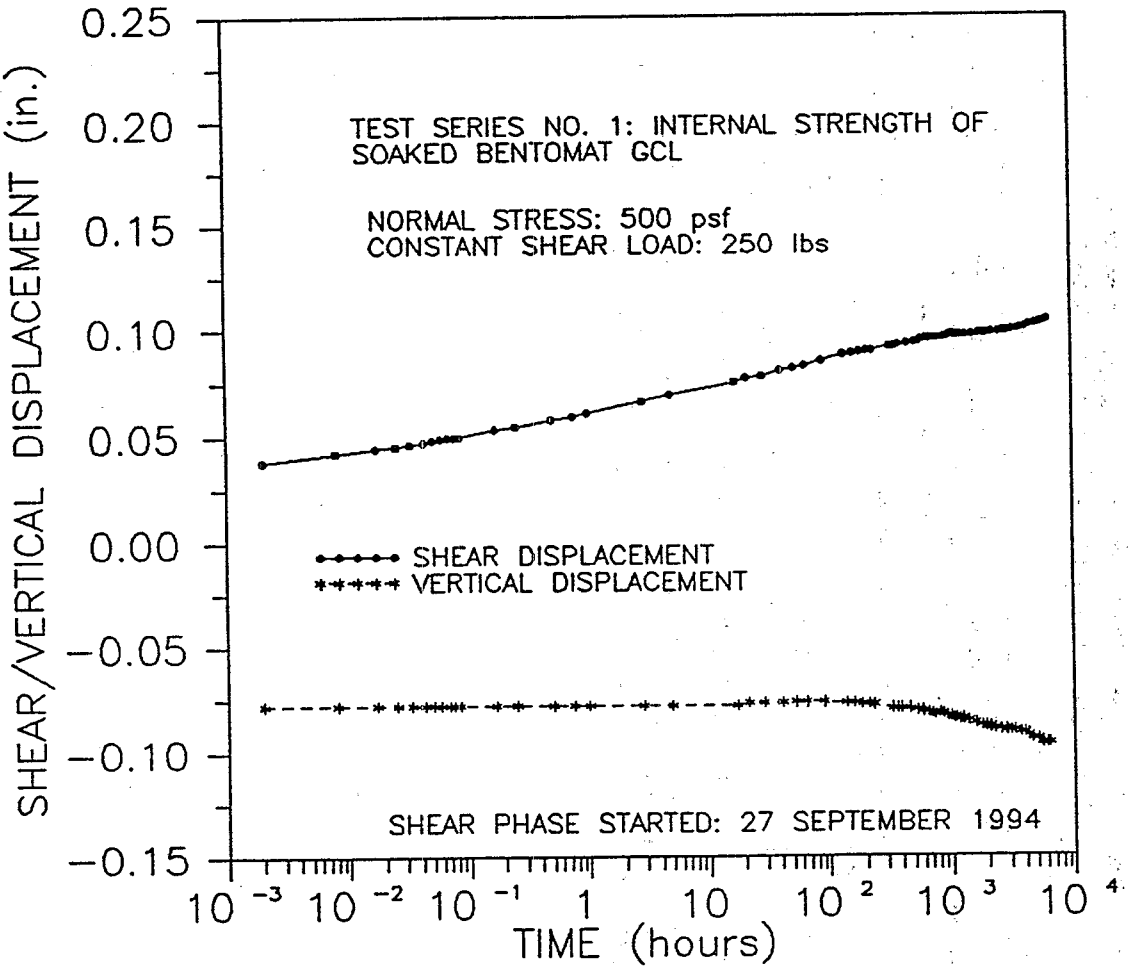

TESTING ATMOSPHERE: AIR MAINTAINED AND REGULARLY MONITORED AT A RELATIVE HUMIDITY OF 50 TO 72 PERCENT AND A TEMPERATURE OF 70 +/− 2 degF(21 +/− 1 degC).

DATE REPORTED: 16 JUNE 1995

GeoSyntec Consultants
GEOMECHANICS AND ENVIRONMENTAL LABORATORY

FIGURE NO.	
PROJECT NO.	GLI3545-02
DOCUMENT NO.	
PAGE NO.	

COLLOID ENVIRONMENTAL TECHNOLOGIES COMPANY
CREEP SHEAR TESTING
SHEARING PHASE

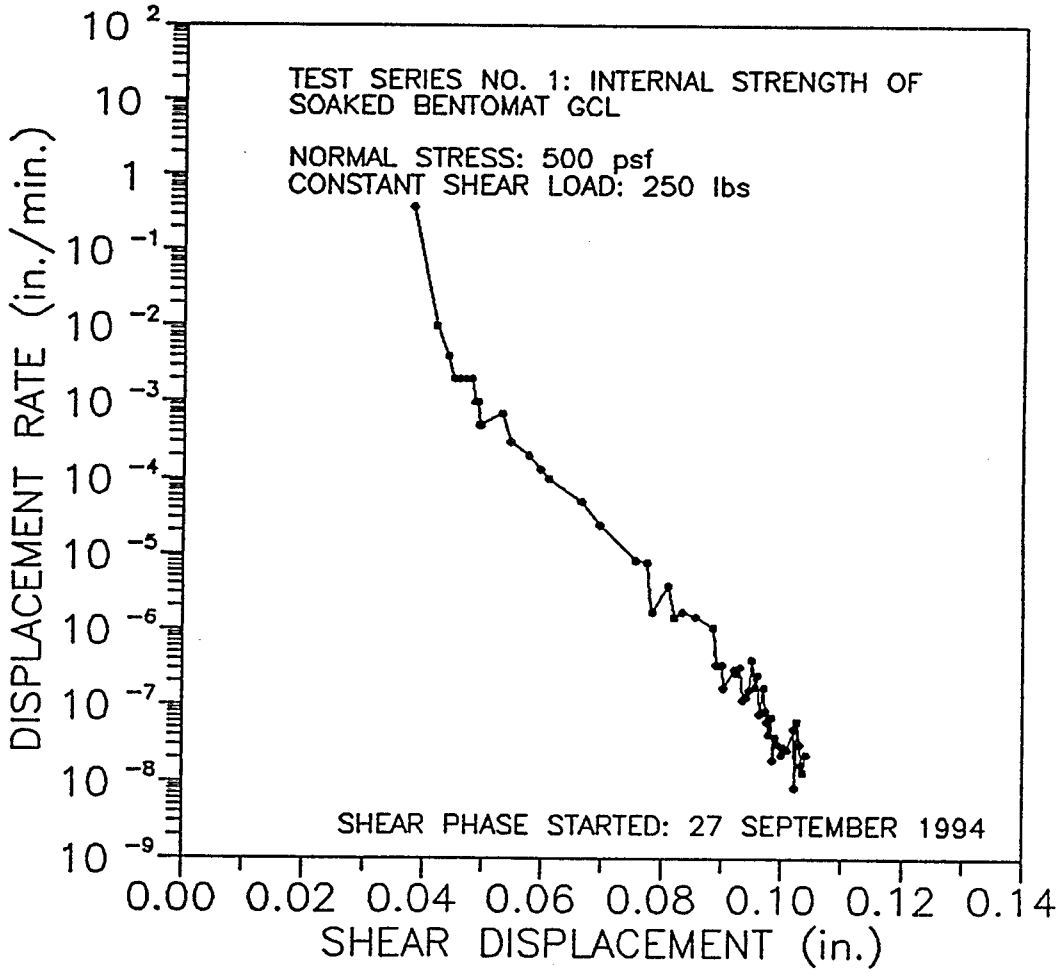

TESTING ATMOSPHERE: AIR MAINTAINED AND REGULARLY MONITORED AT A RELATIVE HUMIDITY OF 50 TO 72 PERCENT AND A TEMPERATURE OF 70 +/- 2 degF(21 +/- 1 degC).

DATE REPORTED: 16 JUNE 1995

GeoSyntec Consultants
GEOMECHANICS AND ENVIRONMENTAL LABORATORY

FIGURE NO.	
PROJECT NO.	GLI3545-02
DOCUMENT NO.	
PAGE NO.	

COLLOID ENVIRONMENTAL TECHNOLOGIES COMPANY
CREEP SHEAR TESTING
SHEARING PHASE – LOAD INCREMENT 3

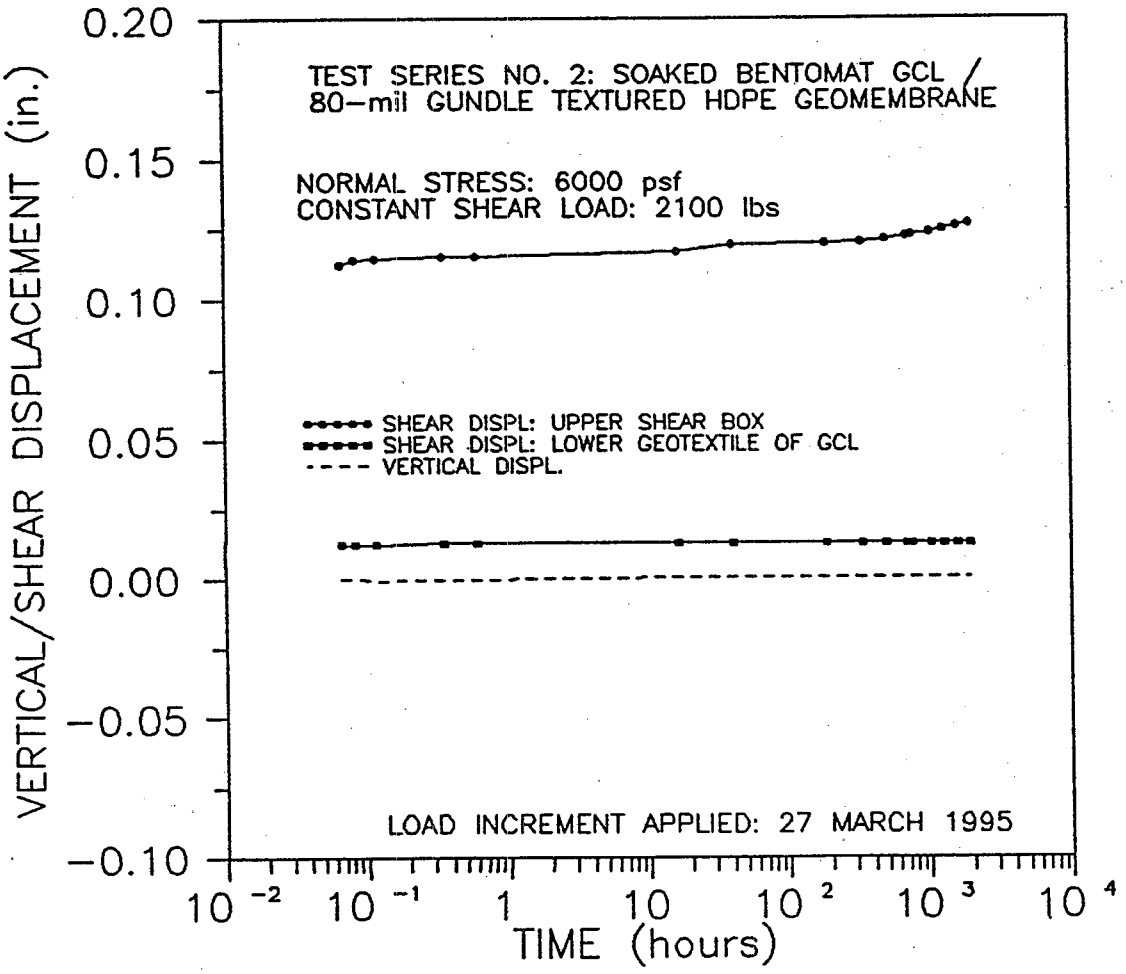

TESTING ATMOSPHERE: AIR MAINTAINED AND REGULARLY MONITORED AT A RELATIVE HUMIDITY OF 50 TO 72 PERCENT AND A TEMPERATURE OF 70 +/− 2 degF(21 +/− 1 degC).

DATE REPORTED: 16 JUNE 1995

GeoSyntec Consultants
GEOMECHANICS AND ENVIRONMENTAL LABORATORY

FIGURE NO.	
PROJECT NO.	GLI3545
DOCUMENT NO.	
PAGE NO.	

COLLOID ENVIRONMENTAL TECHNOLOGIES COMPANY
CREEP SHEAR TESTING
SHEARING PHASE – LOAD INCREMENT 3

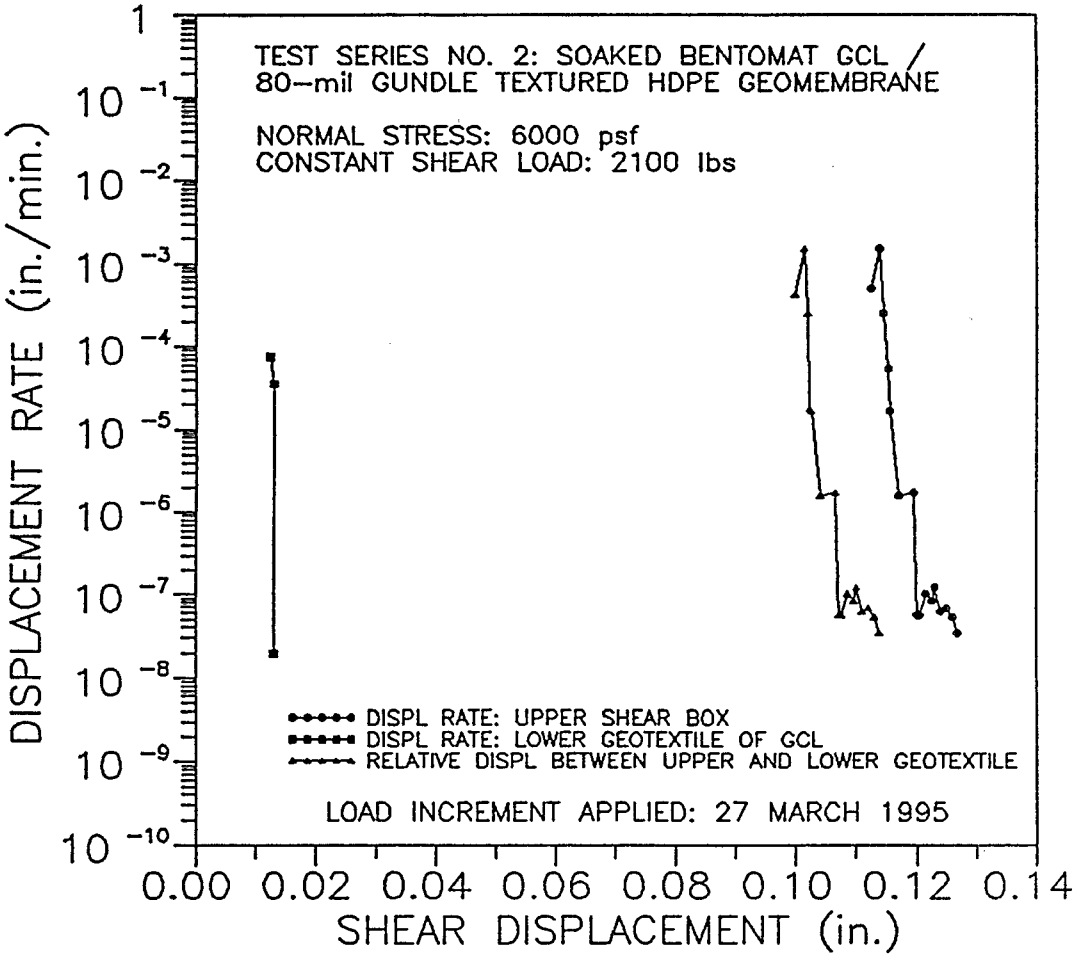

TESTING ATMOSPHERE: AIR MAINTAINED AND REGULARLY MONITORED AT A RELATIVE HUMIDITY OF 50 TO 72 PERCENT AND A TEMPERATURE OF 70 +/– 2 degF(21 +/– 1 degC).

DATE REPORTED: 16 JUNE 1995

GeoSyntec Consultants
GEOMECHANICS AND ENVIRONMENTAL LABORATORY

FIGURE NO.	
PROJECT NO.	GLI3545–02
DOCUMENT NO.	
PAGE NO.	

Appendix H

Summary of Bentofix Shear Test Results, Prepared by National Seal Co.

Internal Shear Strength

Bentofix NS Thermal Lock

NSC Job# 95033P;Normal Stresses = 720, 1440, & 2880 psf;Test Speed = 0.04 in/min

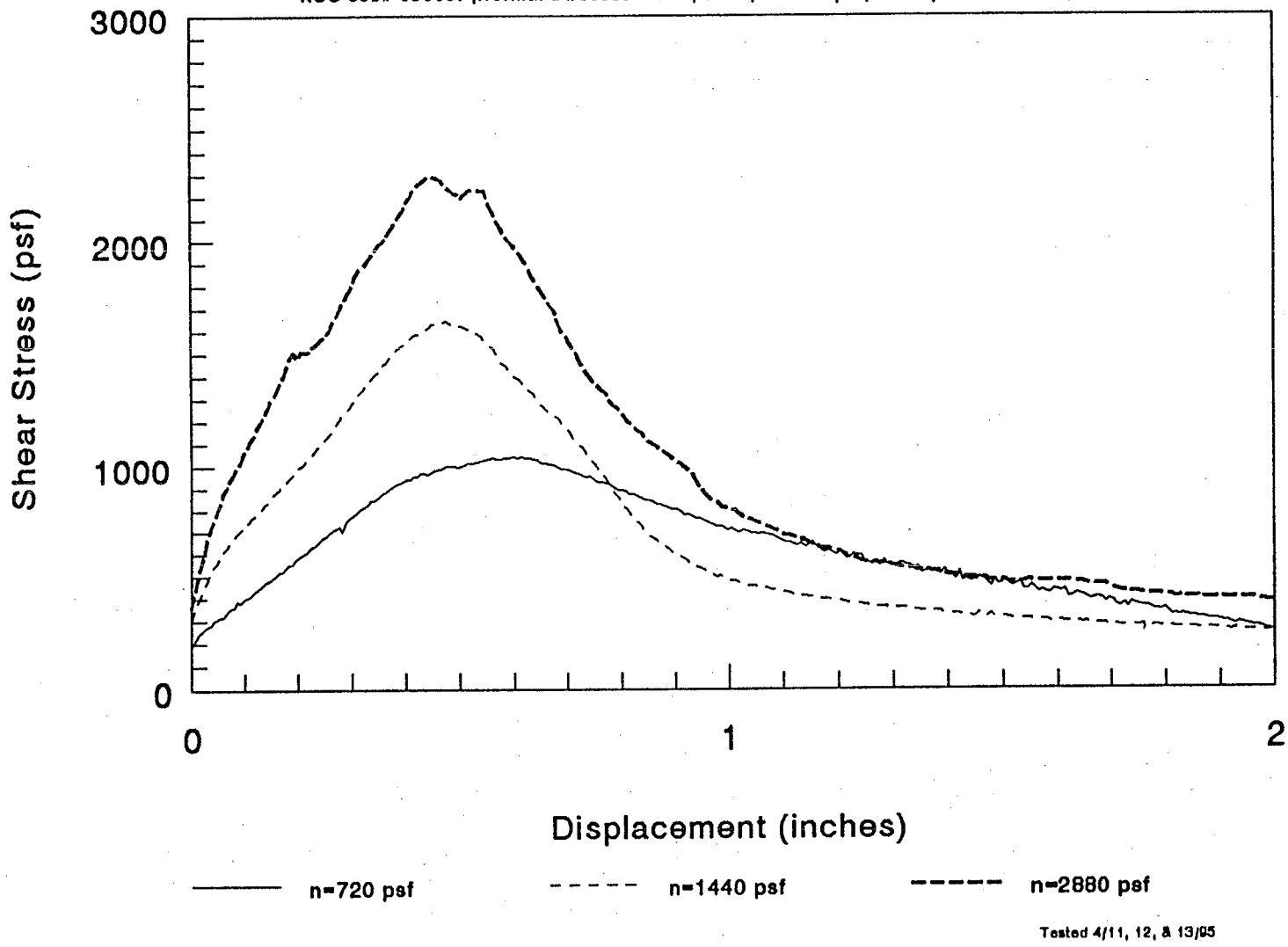

Tested 4/11, 12, & 13/95

Internal Shear Strength

Bentofix NS Thermal Lock

NSC Job# 95033P;Normal Stress = 720, 1440, & 2880 psf;Test Speed = 0.04 in/min

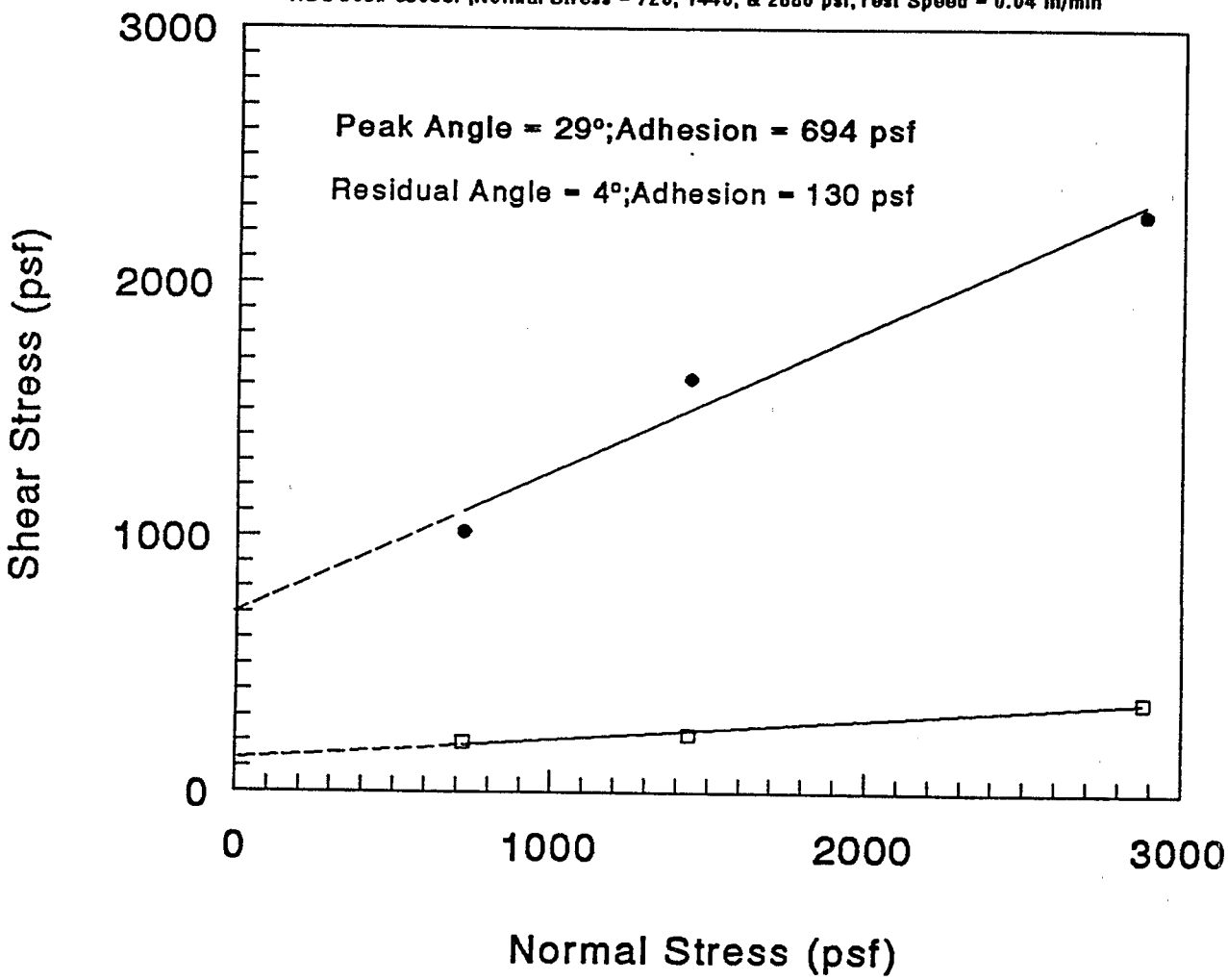

Test Area = 12" x 12"

Tested 4/11, 12 & 13/95

Internal Shear Strength

Bentofix NW, Thermal Lock

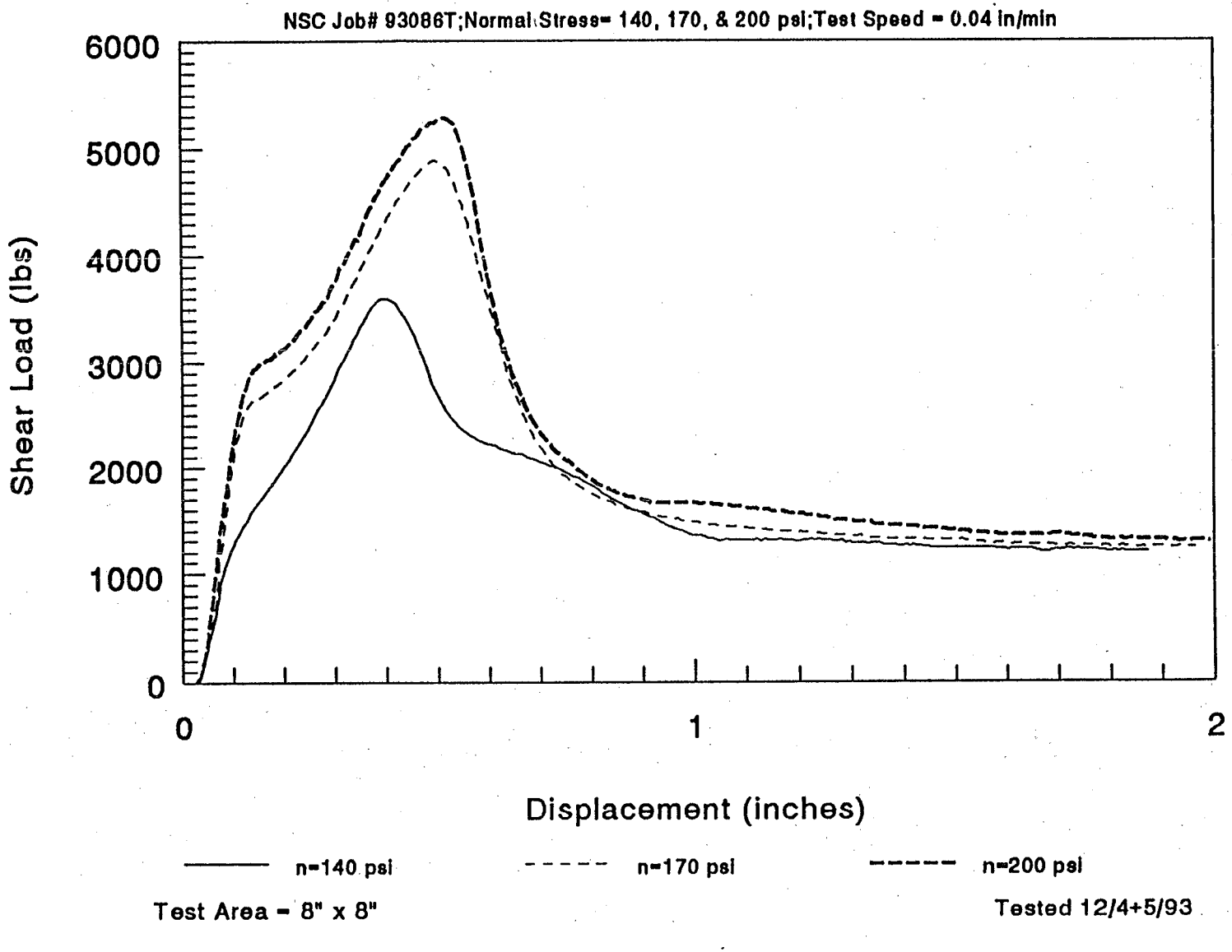

Internal Shear Strength

Bentofix NW Thermal Lock

NSC Job# 93086T;Normal Stress = 140, 170, & 200 psi;Test Speed = 0.04 in/min

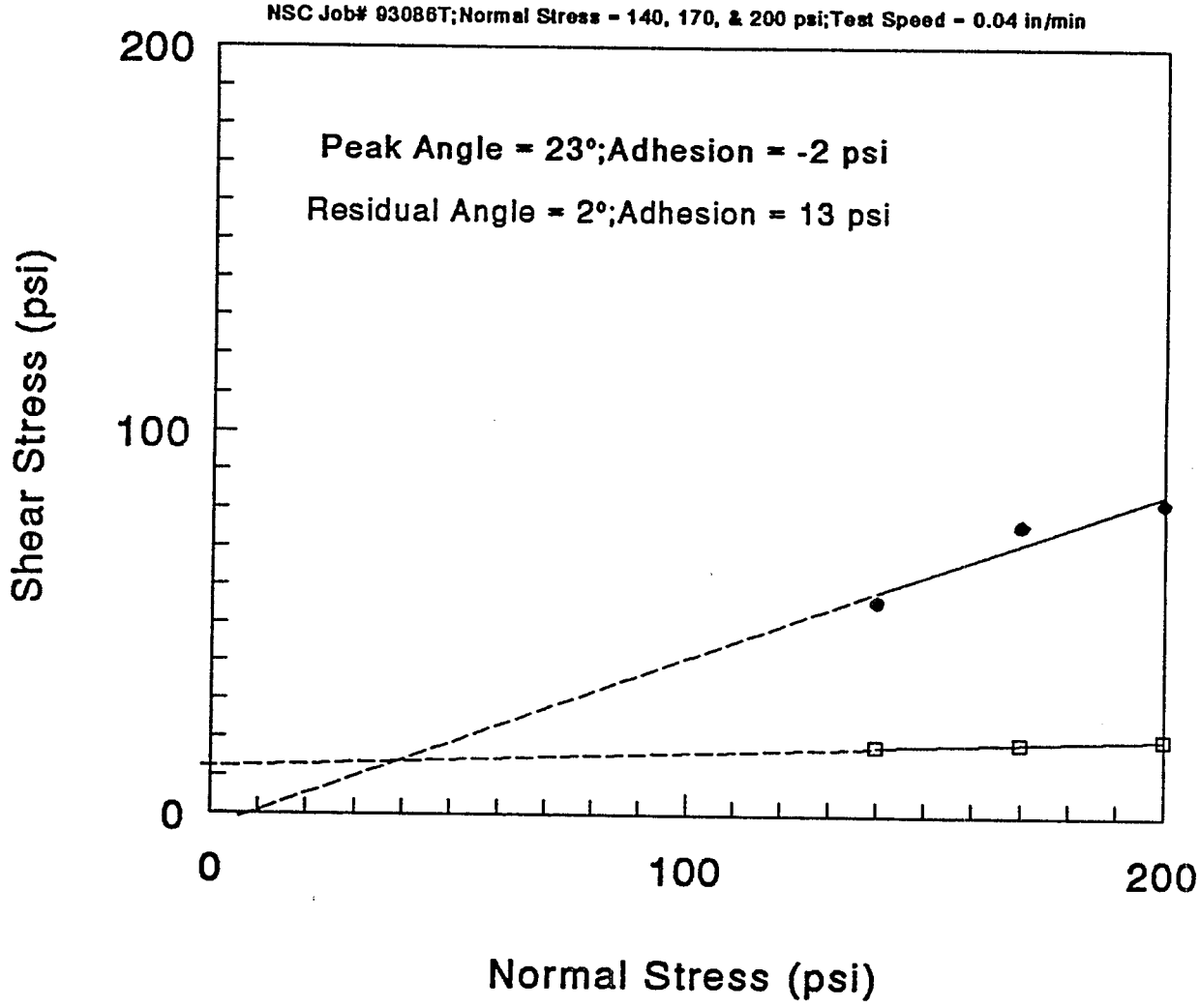

Test Area = 8" x 8"

Tested 12/4+5/93

NATIONAL SEAL COMPANY
CREEP SHEAR TESTING
SHEARING PHASE

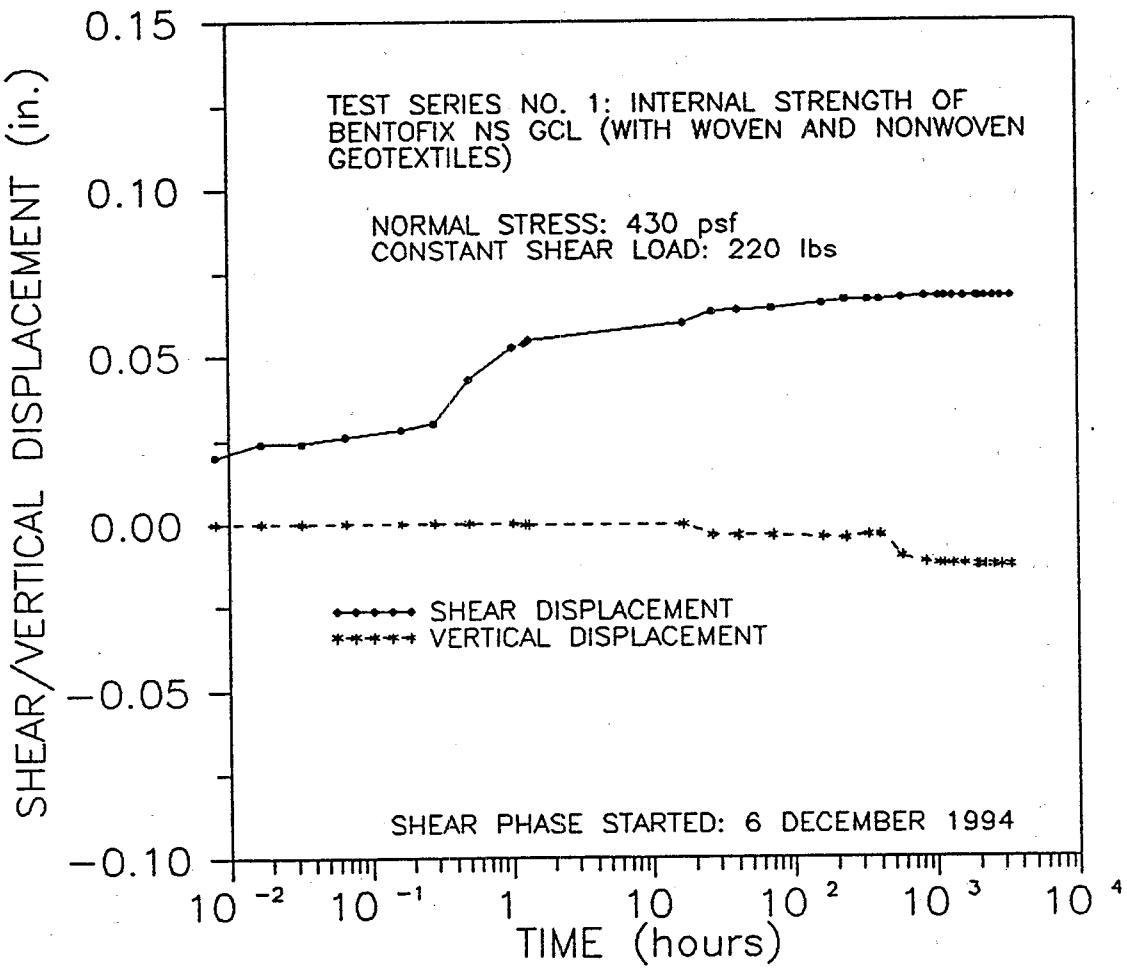

TESTING ATMOSPHERE: AIR MAINTAINED AND REGULARLY MONITORED AT A RELATIVE HUMIDITY OF 50 TO 72 PERCENT AND A TEMPERATURE OF 70 +/− 2 degF(21 +/− 1 degC).

DATE REPORTED: 28 APRIL 1995

GEOSYNTEC CONSULTANTS
GEOMECHANICS AND ENVIRONMENTAL LABORATORY

FIGURE NO.	
PROJECT NO.	GI13571-02
DOCUMENT NO.	
PAGE NO.	

NATIONAL SEAL COMPANY
CREEP SHEAR TESTING
SHEARING PHASE

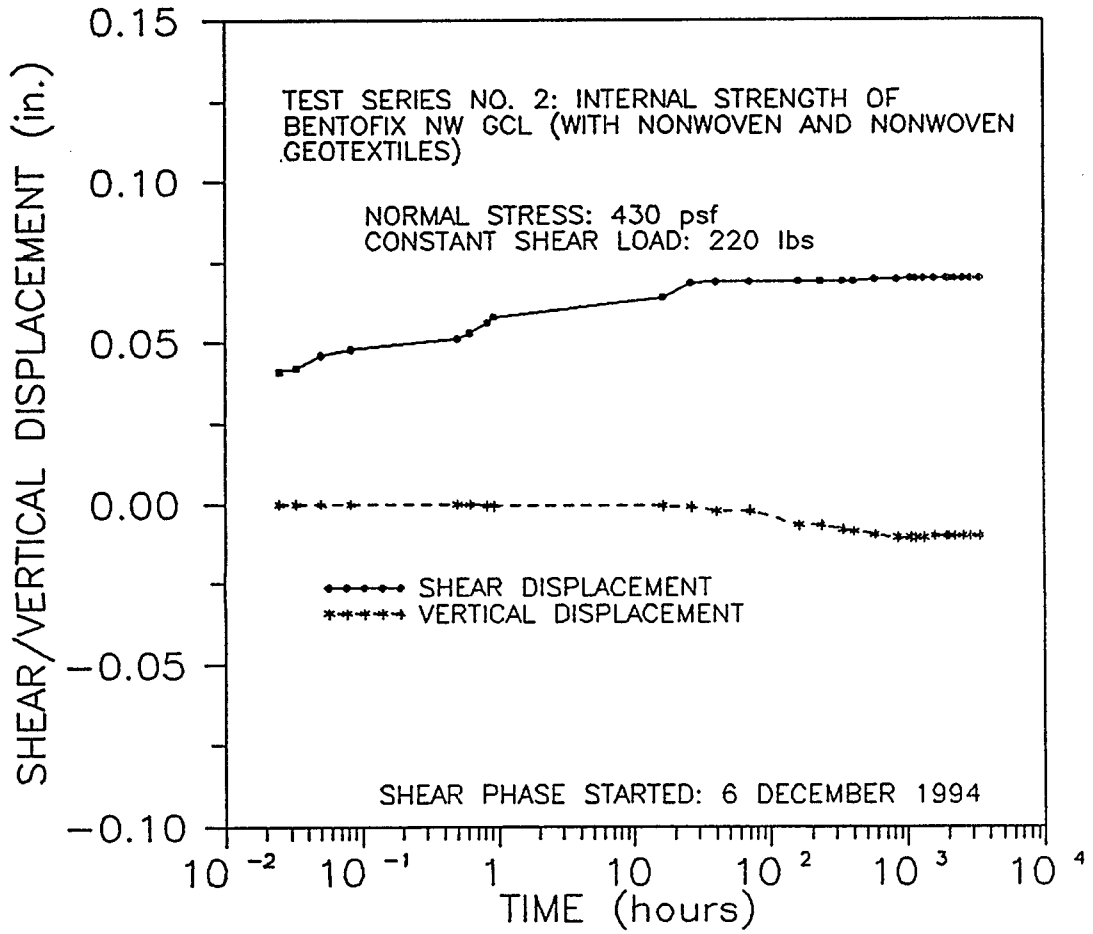

TESTING ATMOSPHERE: AIR MAINTAINED AND REGULARLY MONITORED AT A RELATIVE HUMIDITY OF 50 TO 72 PERCENT AND A TEMPERATURE OF 70 +/− 2 degF(21 +/− 1 degC).

DATE REPORTED: 28 APRIL 1995

GeoSyntec Consultants
GEOMECHANICS AND ENVIRONMENTAL LABORATORY

FIGURE NO.	
PROJECT NO.	GLI3571−02
DOCUMENT NO.	
PAGE NO.	

NATIONAL SEAL COMPANY
CREEP SHEAR TESTING
SHEARING PHASE I

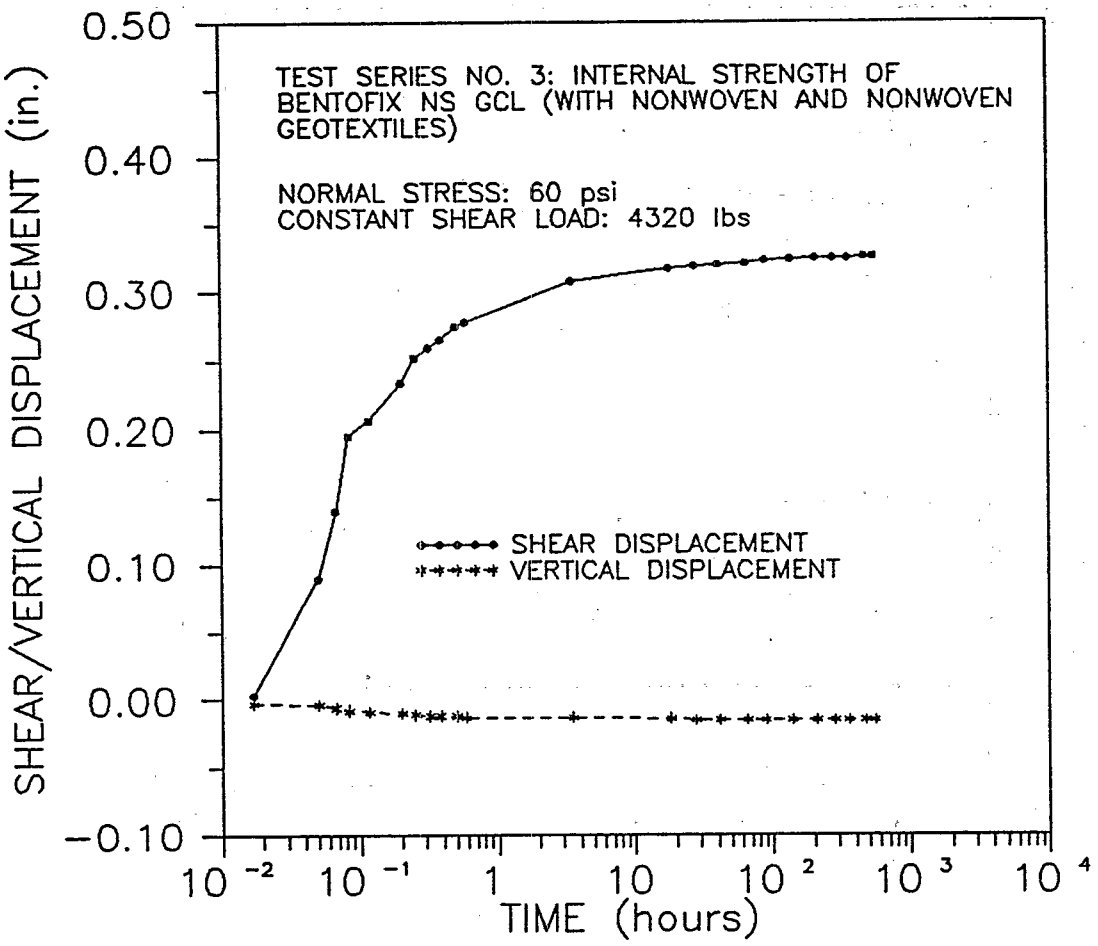

TESTING ATMOSPHERE: AIR MAINTAINED AND REGULARLY MONITORED AT A RELATIVE HUMIDITY OF 50 TO 72 PERCENT AND A TEMPERATURE OF 70 +/− 2 degF(21 +/− 1 degC).

DATE TESTED: 13 JUNE 1995 TO 7 JULY 1995

GEOSYNTEC CONSULTANTS
GEOMECHANICS AND ENVIRONMENTAL LABORATORY

FIGURE NO.	
PROJECT NO.	GLI3571-02
DOCUMENT NO.	
PAGE NO.	